SEDIMENT BUDGETING STUDIES FOR THE KOLLAM COAST

THESIS SUBMITTED TO THE

COCHIN UNIVERSITY OF SCIENCE AND TECHNOLOGY

IN PARTIAL FULFILLMENT OF THE REQUIREMENTS FOR THE AWARD OF THE DEGREE OF

DOCTOR OF PHILOSOPHY

IN

PHYSICAL OCEANOGRAPHY

UNDER THE FACULTY OF MARINE SCIENCES

by

K. RAJITH

CENTRE FOR EARTH SCIENCE STUDIES
THIRUVANANTHAPURAM

NOVEMBER 2006

CERTIFICATE

This is to certify that this thesis entitled "SEDIMENT BUDGETING STUDIES FOR THE KOLLAM COAST" is an authentic record of the research work carried out by Mr. K. Rajith (Reg. No. 2408), under my supervision and guidance, at the Marine Sciences Division, Centre for Earth Science Studies, Thiruvananthapuram, in partial fulfillment of the requirements for the Ph. D Degree of Cochin University of Science and Technology under the Faculty of Marine Sciences and no part thereof has been presented for the award of any degree in any University.

Thiruvananthapuram
24 November 2006

Dr. N. P. Kurian
(Research Guide)
Head, Marine Sciences Division
Centre for Earth Science Studies
Thiruvananthapuram –695 031

CONTENTS

1. INTRODUCTION

2.MATERIALS AND METHODS

3. WAVES

4.CURRENTS

5. BEACH PROCESSES

6. SEDIMENT BUDGET

CHAPTER 1

INTRODUCTION

1. INTRODUCTION

1.1 COASTAL ZONE

Coastal zones, encompassing the coastal planes and continental shelves, are regions that exhibit close interaction between the hydrosphere, lithosphere and atmosphere. These are highly dynamic and diverse ecosystems that are characterised by strong environmental and geological gradients. It consists of nearshore zone, gulfs, bays, inlets, creeks, tidal deltas, lagoons, coastal lakes, estuaries, coral reefs, shoals, tidal flats, mudflats, beaches, sand ridges, coastal dunes, mangroves, marshes, strand features, salt-affected land, rocks, cliffs, reclaimed land, deltaic plains and similar features. The developments attained through over exploitation of the resource of the coastal zone at the cost of the environmental quality would inadvertently destabilize the delicate balance between the biological, geological and meteorological component of the system. These resources have been plundered at an alarming rate contributing to the loss of functional integrity and reducing the capacity to retain material such as water, sediments and organic matter. While industrial developments, climatic modifications, sea level changes and changes in land use pattern affect the coastal zone globally, the direct use of coastal resources has local or regional impact.

The coastal region has been the centre of anthropogenic activity right from the pre-historic periods. The river valley civilisations of Egypt, Persia, India and China originated in the coast where the great rivers, the Nile, the Euphrates, the Tigris, the Indus and the Huango Ho met the oceans and flourished along the banks of these rivers. Human activity in the coastal region (e.g., agricultural production including fisheries, commercial activities including construction of buildings, ports and hotels, industrial activities including chemical processing industries, mineral exploitation and cultural activities) intervenes the natural processes active in this coastal system (an all inclusive term covering the region, the coastal processes and the human activities). The buffering capacity of the system absorbs the impact of human activity and maintains the system in a state of dynamic equilibrium. However, intense human activity may bring about appreciable imbalances in the system resulting in loss of this

equilibrium. Many a times, these changes bring about catastrophic effects on the current users of the system.

1.1.1 Glossary of the Coastal Zone

According to CEM (2002), coastal zone is "the transition zone where the land meets water, the region that is directly influenced by marine and lacustrine hydrodynamic processes. It extends offshore to the continental shelf break and onshore to the first major change in topography above the reach of major storm waves. On barrier coasts, it includes the bays and lagoons between the barrier and the mainland" (Fig. 1.1). The definition of a few of the zones in the coastal zone are (US Army, 1984 and 2002):

Backshore: That zone of the shore or beach lying between the foreshore and the coastline and acted upon by waves only during severe storms, especially when combined with exceptionally high water.

Bar: A submerged or emerged embankment of sand, gravel or other unconsolidated material built on the seafloor in shallow water by waves and currents.

Beach: The zone of unconsolidated material extending landward from the mean low water line to the place where there is a change in material or physiographic form as examples , the zone of permanent vegetation or a zone of dunes or a sea cliff.

Berm crest: The seaward limit of berm

Berm: A nearly horizontal part of the beach or backshore formed by the deposit of material by wave action.

Foreshore: The part of the shore lying between the crest of the seaward berm and the ordinary low water mark, that is ordinarily traversed by the uprush and backrush of the waves as the tides rise and fall.

Nearshore: The region seaward of the shore (from approximately the step at the base of the surf zone) extending offshore to the toe of the shoreface (Fig. 1.1). Nearshore is a general term used loosely by different authors to mean various areas of the coastal zone, ranging from the shoreline to the edge of the continental shelf.

Surf zone: The area between the outermost breaker and the limit of wave uprush.

Swash zone: The portion of the nearshore region in which the beach face is alternately covered by the uprush of the wave swash and exposed by the backwash.

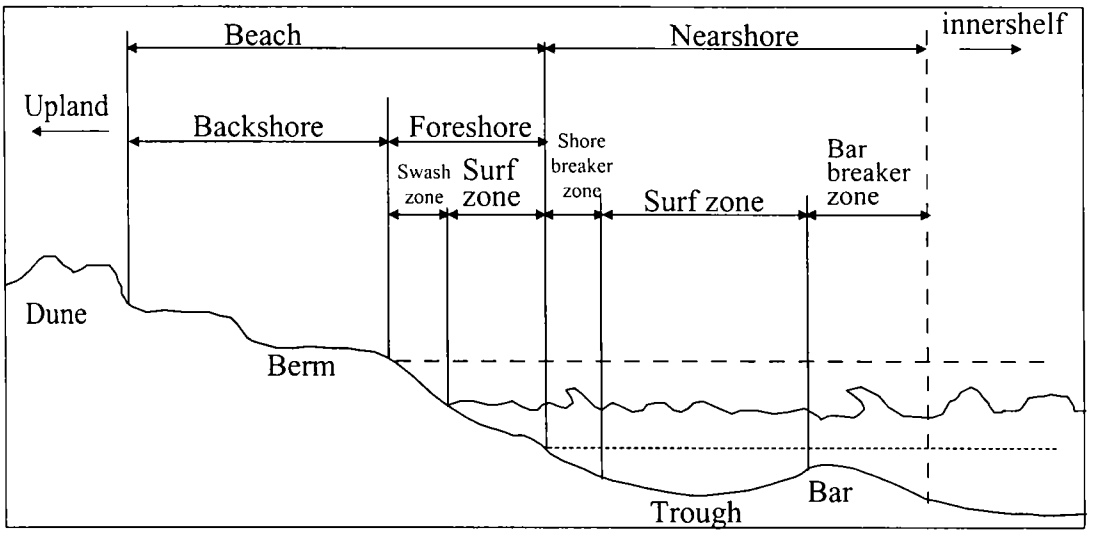

Fig. 1.1 A schematic diagram showing the different zones of the coast (US Army, 2002)

1.2 COASTAL PROCESSES

Driven by external forces, the fluid motion of the sea water manifests itself as coastal currents, tides and tidal currents, internal waves, surface waves, storm surges, tsunamis and others. Wind waves, storm surges and tsunamis bring powerful hydrodynamical forces to the shallow area of a coast. Once generated by atmospheric disturbances and submarine earthquakes, respectively, storm surges and tsunamis can release destructive effects on a coast. However, because of their infrequent occurrences, they are less important than wind waves from viewpoint of the coastal sedimentary processes. A description of a few of the important coastal processes is given in the sections below.

1.2.1 Waves

Waves are the principal source of input energy into the coastal zone. They comprise of the 'sea' generated locally and the swells propagated from other generating areas. In deep water, the water particle motion of waves is confined to the vicinity of the surface. As a consequence, the water particle velocity and pressure fluctuation are non-existent near the bottom. Therefore, neither bottom undulation nor bottom roughness appreciably affects wave motion in deep water. In shallow water, in

contrast, waves transform under the influence of the sloping bottom, bed characteristics, coastal structures, etc.

1.2.1.1 Wave transformation processes

The important shallow water wave transformation processes are shoaling, refraction, diffraction and reflection.

Shoaling: If waves are incident normal to the beach with straight and parallel bottom contours, change in the wave profile is caused solely by the change in water depth. This transformation is called shoaling.

Refraction: Variation in wave velocity occurs along the crest of a wave moving at an angle to underwater contours because that part of the wave in deeper water is moving faster than the part in shallower water. This variation causes the wave crest to bend toward alignment with the contours. This bending effect, called refraction, depends on the relation of water depth to wave length (Fig. 1.2). Refraction coupled with shoaling, determines the wave height in any particular water depth for a given set of incident deep water wave condition. Refraction therefore has significant influence on the wave height and distribution of wave energy along a coast. The change of direction of different parts of the wave results in convergence or divergence of wave energy, and materially affects the forces exerted by waves on structures.

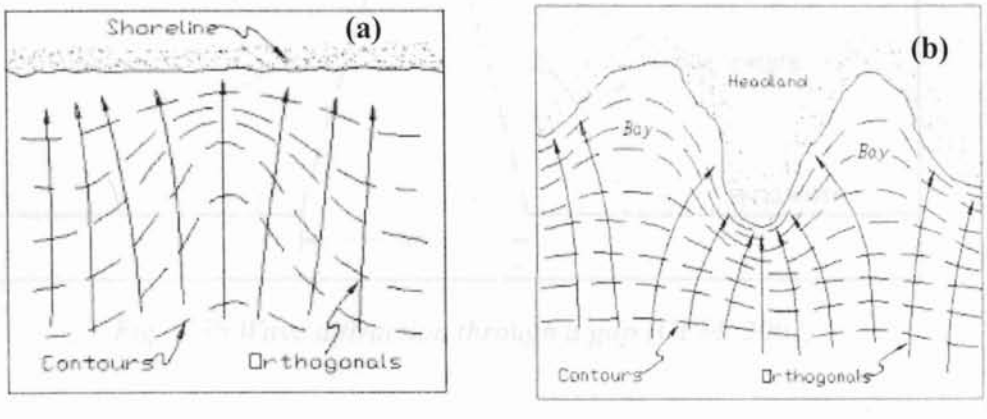

Fig. 1.2 Refraction of waves in the areas of (a) canyons (b) headland (CEM, 2002)

Diffraction: Diffraction of waves is a phenomenon in which energy is transferred laterally along a wave crest (Fig. 1.3 a and b). It is most noticeable where regular train of waves is interrupted by a barrier such as break water or an islet.

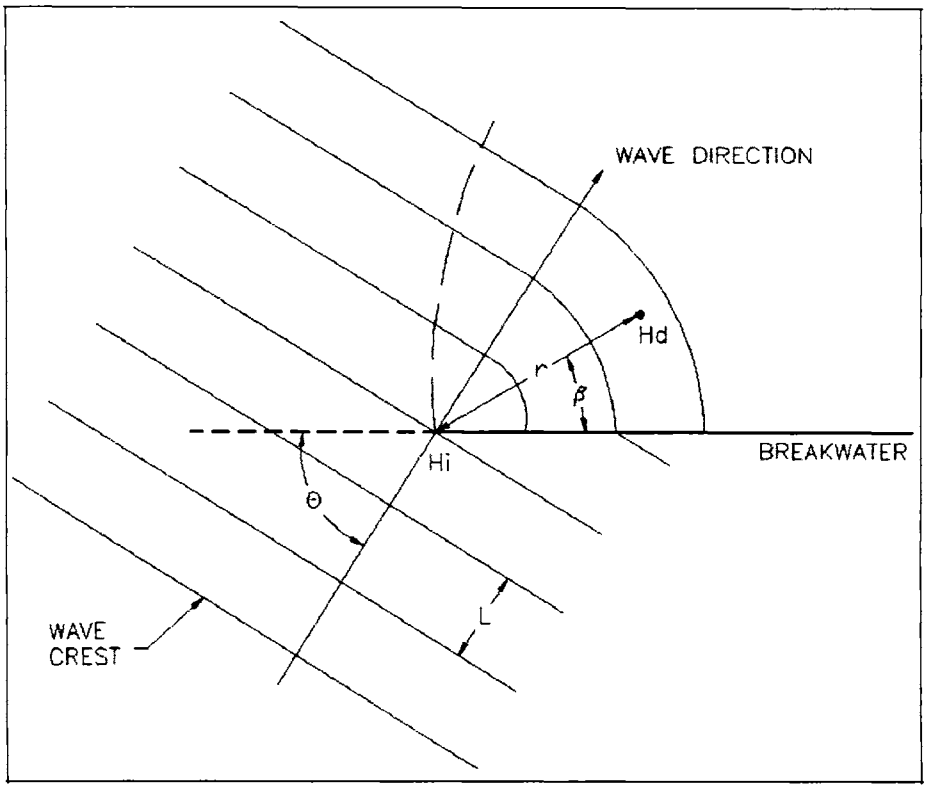

Fig. 1.3a Wave diffraction (CEM, 2002)

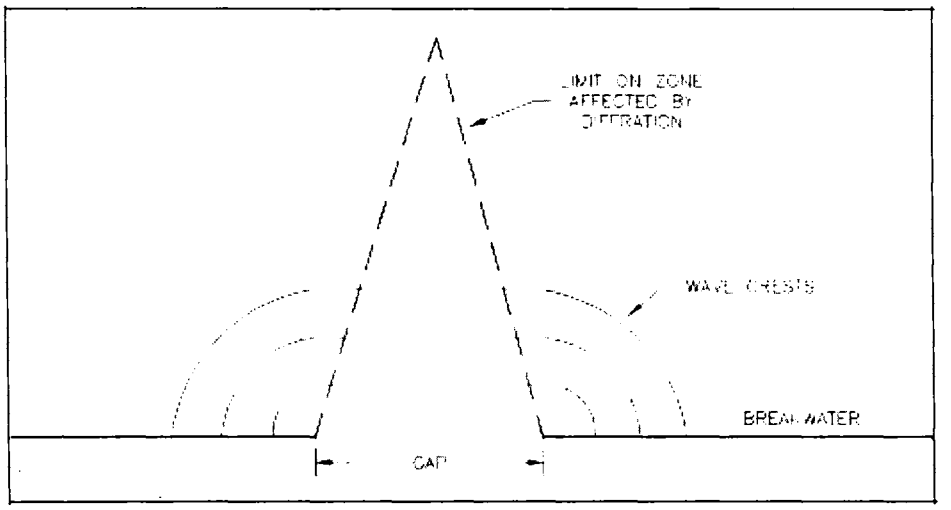

Fig. 1.3b Wave diffraction through a gap (CEM, 2002)

Reflection: Water waves may be either partially or totally reflected from both natural and manmade barriers. The degree of wave reflection is defined by the reflection coefficient $Cr = Hr/Hi$ where Hr and Hi are the reflected and incident wave heights, respectively (CEM, 2002). Wave reflection may often be an important consideration in the design of coastal structures, particularly for structures associated with

development of harbours. Reflection of waves implies a reflection of wave energy as opposed to energy dissipation (Fig. 1.4). Consequently, multiple reflection and absence of sufficient energy dissipation within harbour complex can result in a build up of energy which appears as wave agitation and surging in the harbour.

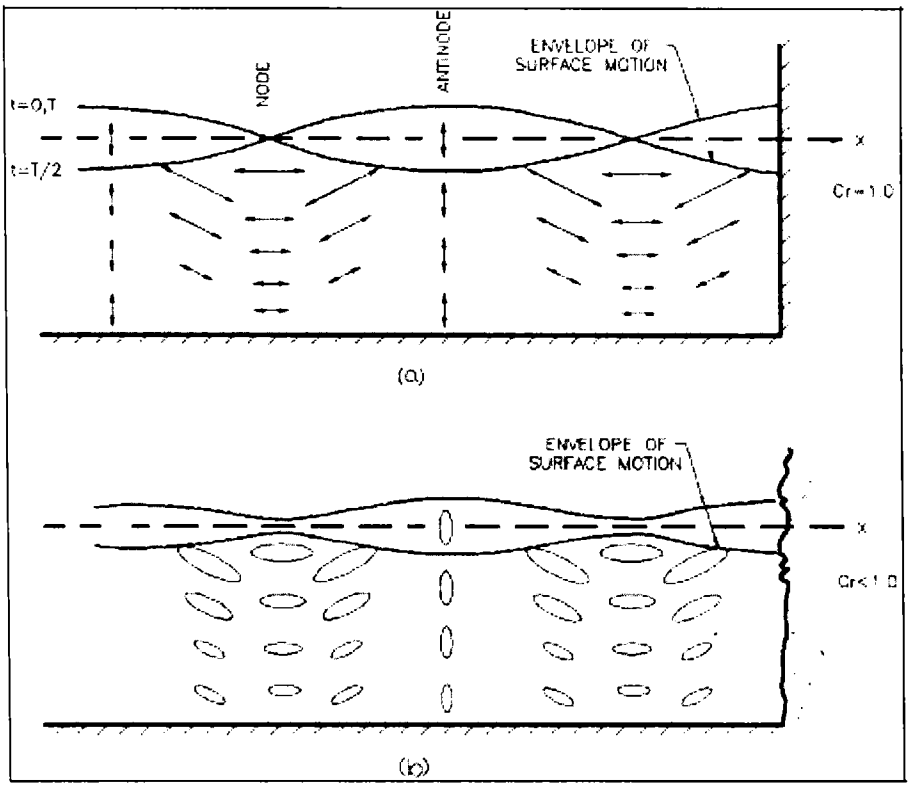

Fig. 1.4 Complete and partial reflection (CEM, 2002)

1.2.1.2 Shallow water wave breaking

Waves break when their height reaches a certain limiting value relative to their length or water depth. In the deep ocean, waves developed by wind will break when their steepness exceeds certain value. But, in the nearshore zone the wave breaking takes place on a slope as a result of decreasing water depth. It is near the breaking point where waves deform most rapidly. The waves normally continue to break as the water depth decreases, finally reaching the shoreline. The area between the breaking point and the shoreline is termed the surfzone where longshore currents/ nearshore cell circulation prevails as result of wave breaking. After breaking, the transformation of the broken waves depends largely on the bottom configuration in the surfzone. On a uniformly sloping beach, the waves will continue to break (Horikawa, 1988). On a

beach where the slope becomes milder after breaking, waves tend to stop breaking and recover the properties of an oscillatory wave. In either case, wave breaking induces secondary motion in the surf zone, particularly the turbulence and the currents. At the final stage of wave propagation to the shore, waves run up and down on the dry bed, a process called the swash oscillation (Horikawa, 1988). Some amount of the incident energy is reflected back, forming partial standing waves. The rest of the incident wave energy is dissipated in the swash zone.

1.2.2 Currents

Various currents exist in the coastal region such as coastal currents, tidal currents and wind and wave induced currents. A current that flows roughly parallel to a coast, outside the surf zone is called as coastal current. It comprises of tidal currents, wind driven currents, continental shelf currents and currents due to coastal-trapped waves. Coastal currents are more steady, but changes with season. Tidal currents are oscillatory and non-uniform, but of large scale both in time and space. Wave induced currents generated directly by the action of swell and wind waves are concentrated within or near the surfzone. A description of the different types of currents follow in the section blow.

1.2.2.1 Tidal currents

The astronomical forces of the moon and sun cause tides in the ocean which in turn create currents. The tidal currents vary from locality to locality, depending upon the character of the tide, the water depth and the configuration of the coast, but in any locality, they repeat themselves as regularly as the tides to which they are related. In open ocean, tidal currents usually are rotating due to the effect of the coriolis force (Fairbridge, 1966). In the northern hemisphere, tidal currents rotate clockwise. Tidal currents in the open sea are controlled by amphidromic systems. Tidal currents may be of the semidiurnal, diurnal, or mixed type, corresponding to a considerable degree to the type of tide at the place, but often with a stronger semidiurnal tendency. Tidal currents have periods and cycles similar to those of the tides, and are subject to similar variations, but flood and ebb of the current do not necessarily occur at the same times as the rise and fall of the tide. The speed at strength increases and

decreases during the 2 week period, month, and year along with the variations in the range of tide.

1.2.2.2 Wind-induced currents

When wind blows over a water surface, pure wind-driven currents are produced by transfer of momentum from wind to water at the air-sea interface and by friction between moving layers within the water. The direct effect of wind stress is confined to the layer beneath the surface called Ekman layer. It is observed that the ocean currents do not move directly downwind of prevailing wind but is controlled by the Coriolis effect, stratification of the ocean and ocean basin boundaries. Ekman assumed a uniform ocean without any boundaries and predicted that the magnitude and direction of motion of a layer of the water column were caused by stress from moving, overlying layer. As the wind blows across the sea surface, the upper most layer of the water begins to move. The current is deflected by the Coriolis effect. Thus, in northern hemisphere, the surface layer moves to the right of the wind. The moving surface layer imparts stress to the underlying layer, which in turn begins to move and is further deflected by the Coriolis effect. These layers are defined by density, which is controlled by temperature and salinity. Current velocities diminish with depth because of the friction between the layers. The Ekman layer extends from the surface to the depth at which this slow current occurs in the ocean. The progressive decrease in speed and change in direction as a function of depth is called the Ekman spiral. The overall motion of water is determined by integrating all individual currents and in the northern hemisphere, the direction is 90° to the right of prevailing wind (Corso and Joyce, 1995).

1.2.2.3 Wave-induced currents

Shepard and Inman (1950) introduced the term 'nearshore currents' to distinguish the nearshore current system from other currents. They defined the nearshore current system as composed of the currents associated directly with the action of waves. There are two wave induced current systems in the nearshore zone which dominate the water movements in addition to the to-and-fro motion produced by the waves

directly. These are: (1) a cell circulation system of rip currents and (2) longshore currents produced by an oblique wave approach to the shoreline (Fig. 1.5).

Longshore currents: Longshore currents flow parallel to the shoreline and are restricted mainly between zone of breaking and the shoreline. Most longshore currents are generated by the longshore component of motion in waves that obliquely approach the shoreline. Although, longshore currents generally have low speeds, they are important in littoral processes because they flow along the shore for extended period of time, transporting sediment set in motion by the breaking waves.

Rip currents: Rip currents are currents that flow perpendicular to the shoreline and are caused by water moving down slope (away from beach) as a result of wave setup (Fig. 1.5). Rip currents are fed by a system of longshore currents. The slow mass transport, the feeding longshore currents and the rip currents taken together form a cell circulation system in the nearshore zone. The rip currents of the circulation can be important in the cross-shore transport of sand, but there is minimal net displacement of beach sediments along the coast.

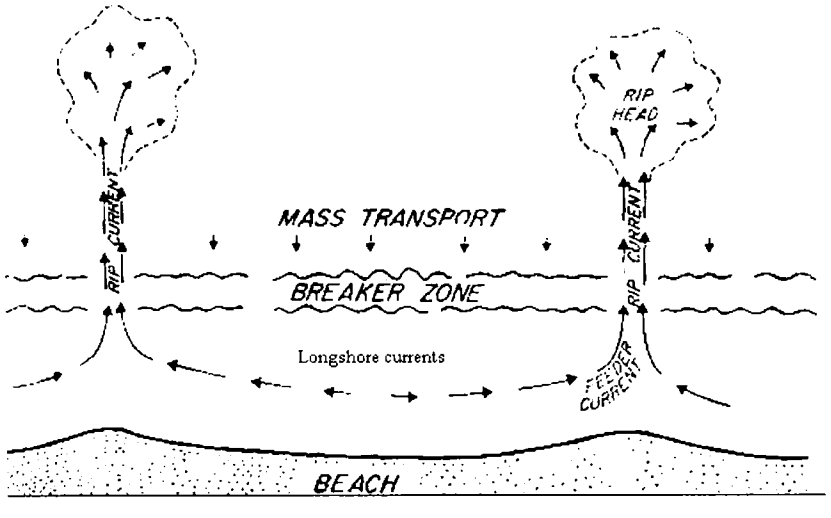

Fig. 1.5 Nearshore circulation systems (After Komar,1976)

1.2.3 Coastal Sediment Transport

Sediment transport occurring in the nearshore region may be divided into two in terms of direction: cross-shore and longshore. Cross- shore transport is mainly produced by the wave orbital motion and innershelf currents whereas longshore transport is primarily associated with wave- induced longshore currents.

In deep water the orbital motion is circular and does not touch the bottom. Consequently the bottom sediments are not disturbed. However, in shallow water ($d < L/2$) the orbital motion is elliptical and touches the bottom due to which the sediment entrainment process takes place. According to U.S. Army (1984), the threshold flow velocity for initiation of sediment motion by oscillatory flow is

$$U_m = (8\,(s-1)\,g d_{50})^{0.5} \tag{1.1}$$

where U_m is the peak fluid velocity at the sediment bed. s is the ratio of the sediment density (ρ_s) to fluid density (ρ), g is the acceleration due o gravity and d_{50} is the median sediment size.

A better physically relevant parameter with regard to wave forcing on bottom sediments is the Shields parameter which has been used by different authors (Graber et al., 1989; Komar, 1989). Shields parameter is defined as the ratio of the entraining force or tangential shear stress to the stabilising force of gravity acting on a sediment grain. It is very well proved experimentally that non-cohesive sediment will begin to move in steady, uni-directional flow when the Shields parameter exceeds a critical value which in turn depends on the sediment grain properties. Later Madsen and Grant (1975, 1976, and 1977) demonstrated that the Shields criterion for initiation of sediment movement is also valid for oscillatory motions associated with waves. The critical value of the Shields parameter for initiation of motion, following Madsen and Grant (1976) is given by

$$\psi_c = \frac{\tau_{bo}}{\rho(s-1)gd} \tag{1.2}$$

where τ_{bo} is the critical bottom boundary shear stress and d is the mean diameter of the sediment grains.

The influence of the wave motion on the sea bed can cause significant quantities of sediment to be suspended above the bed where it is then transported with nearly the horizontal component of the current velocity. Also, the bottom shear stress exerted by the waves and currents cause bed load transport of the sediments. The shear stress under combined waves and currents is an important parameter for the sediment

transport prediction. The transport of sediment as bed load is generally related to the skin friction component of the total shear stress at the bed. In a combined flow environment, current in the region above the wave boundary layer, i.e., the potential flow region for the wave, experiences a shear stress which depends not only on the physical bottom roughness but also on the wave boundary layer characteristics.

Sediment transport in the coastal waters takes place mainly as bed load and suspended load. The distinction between bedload and suspended load is certainly an idealization (Yalin, 1977) and there is no agreement about the relative importance of these transport components. A third mode is also identified as sheet flow transport under high energy conditions. An intermediate type between bed load and suspended load is also suggested by some authors.

1.2.3.1 Bed load Transport

Bed load transport is traditionally considered to be that portion of the transport that occurs by rolling and by saltation in a relatively thin layer close to the bed (Einstein, 1950). The transport occurs when the bed is practically flat with no sand ripples nor suspended sediment cloud. Sediment particles move along the bed surface, frequently impacting each other. Much of the difficulty in sediment transport estimations lies in determining the concentrations of suspended sediments and of bed load very close to the sea bed as, for sand in particular, most transport takes place close to the bed in the region of interaction between the wave boundary layer and that of the steady current (Smith, 1977; Grand and Madsen, 1979).

1.2.3.2 Suspended load Transport

Suspended sediments are particles (such as sand) that have been lifted off the seabed into suspension in the water column. The influence of the wave motion on the bed can cause this suspension effect above the bed, where it is then transported with nearly the horizontal component of the current velocity. Fine materials, silt and mud having low settling velocities can be lifted high into the water column by the turbulence within the flow field and significant transport of such material can occur well away from the bed. For coarser material such as sands, the height is restricted to the region close to

the bed. Accurate knowledge of the current velocity above the bed is clearly needed to calculate the suspended load transport. In nearshore coastal regions, the suspension of such particles is associated with wave-induced orbital currents (Green and Vincent, 1990; Osborne and Greenwood, 1992a&b; Aagaard and Greenwood, 1994) and the sea bed characteristics (Nielsen, 1986, 1992; Greenwood et al., 1990). Since the suspended sediment concentration is greatest near to the bed where the current profile is reduced the most under combined flow, it is obvious that the ability to account for the wave influence on the current velocity profile is critical to the successful modelling of the suspended load transport (Grant and Madsen, 1979).

1.2.3.3 Sheet flow

In the sheet flow condition the motion is intense enough so that the bottom boundary layer is fully turbulent, sand ripples are not present and sand moves in a very thin layer near the bottom. Ripples disappear at high bottom shear stresses. Sediment particles move as a layer in the sheet flow mode whereas only surface grains are in motion in the bed load mode. Sediment particles, which have started moving during positive flow under wave profile, are transported in the positive direction.

It is generally concluded that bedload is the more important component in alongshore sand transport within highly turbulent surf zones; on the other hand, the major component in the onshore-offshore sand transport under non-breaking waves is the suspended mode. The sheet flow condition prevails in high energy conditions such as in tropical winter cyclones. Nearly all sand transport over wave ripples occurs in the form of suspended load. That is, most of the moving grains are supported by drag forces from the surrounding fluid rather than by grain-grain interactions.

1.2.4 Sediment Transport and Beach Morphological Changes

Beaches are composed of unconsolidated material such as silt, sand, gravel or a mixture of these, and they undergo reversible (recoverable) change, erosion and accretion, in response to the external forces acting on them. Dynamics of sediment transport and the evolution process of the beaches are interesting fields of study for coastal engineering projects. Waves continuously arrive at the coast and the beach

form changes correspondingly. Changes in beach configuration result from spatial differences in the sediment transport rate.

Cross-shore sediment transport encompasses both offshore transport, such as occurs during storms, and onshore transport, which dominates during mild wave activity. Net cross-shore exchange of sediment may occur over long time periods and large areas, having implications for the regional shoreline evolution. During a typical year, the cross-shore net transport at the boundaries of the nearshore zone may be small, especially at the seaward end, but over decades or centuries the net contribution could be significant. Also, in the case of extreme events large net transport could take place over a short time period, having implications for the evolution of the nearshore topography at much longer time scales than the storm itself. However, there are also places where sediment might be lost from the nearshore to the shelf area. The long-term net sediment exchange between the nearshore and the shelf area is probably related to the general properties of the shelf, such as width, slope, and sediment availability. Relative change in sea level causes cross-shore exchange of sediment that occurs over long time periods because of the time scale of the forcing.

Longshore currents generated by waves approaching obliquely to the coast transport sediment along the shore. Tidal and wind-generated currents also contribute to this sediment transport, although it is the stirring by the breaking waves that mobilizes the sediment transported by longshore (and cross-shore) currents. Gradients in the longshore transport rate alter the shoreline, resulting in areas of erosion and accretion. The gradients and their characteristic scale determine the spatial extent of these areas. The mechanism causing the gradients in local transport may be related to, for example, structures (Fig. 1.6), engineering activities and the offshore bathymetry. Similarly, gradients in the regional transport may produce areas of accretion and erosion, leading to complex regional shoreline shapes upon which the local shoreline responds to transport gradients. Various types of controls can establish spatial gradients in the longshore sediment transport rate at the regional scale as, for example, offshore contours, shadowing by large landmasses and geological constraints such as headlands. Under certain conditions, equilibrium may be attained,

eliminating the gradients at the regional scale and leading to shoreline trends that are stable over longer time.

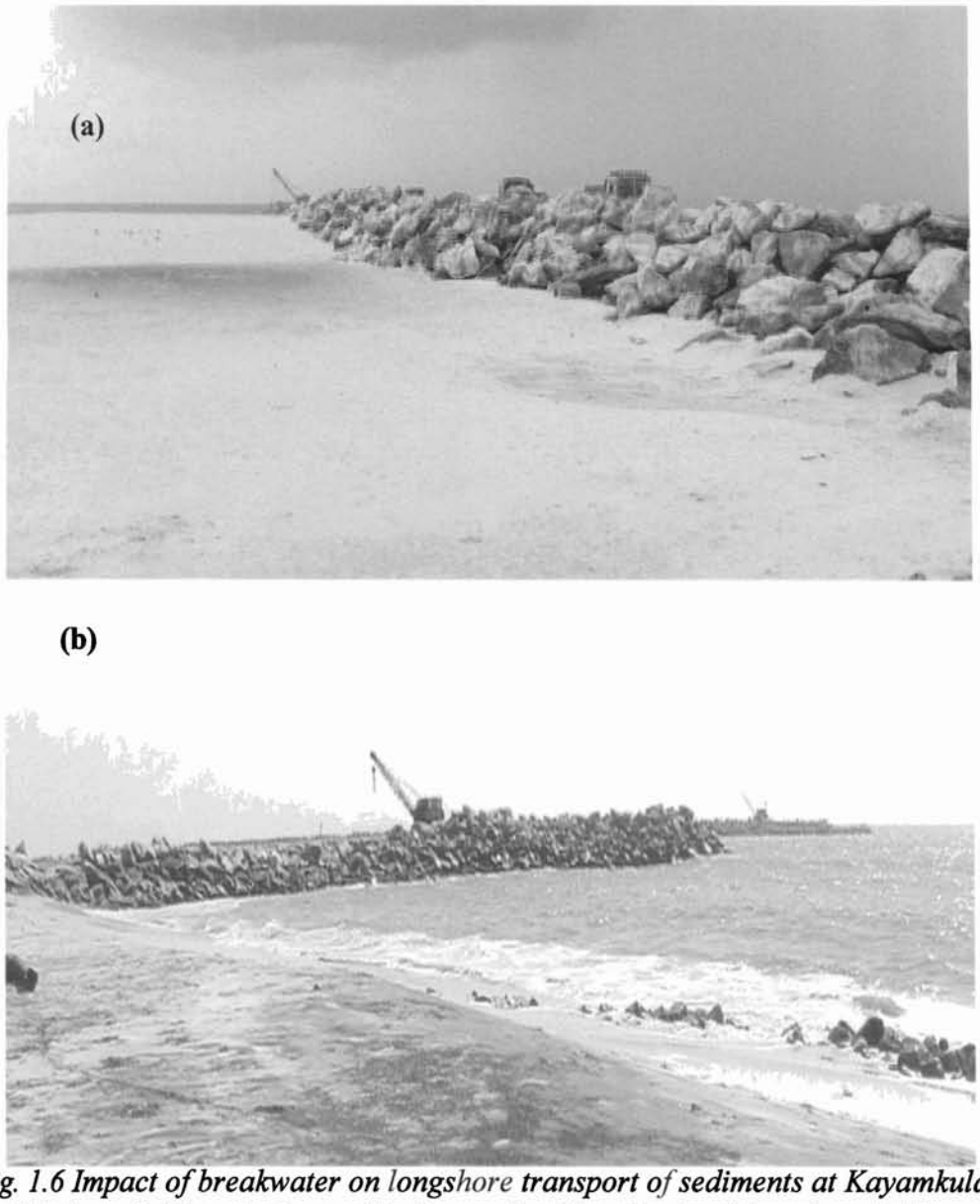

Fig. 1.6 Impact of breakwater on longshore transport of sediments at Kayamkulam inlet. Accreted beach observed in the south of breakwater (a) and eroded beach formed in the north (b)

1.3 SEDIMENT BUDGET

Sediment budgeting is the study process to understand the sediment sources, sinks, transport pathways and magnitudes for a selected region and within a defined period of time. For coastal regions, the sediment budget is a balance of volumes (or volume rate of change) for sediments entering (source) and leaving (sink) a selected region of the coast, and the resulting erosion or accretion in the coastal area under consideration

(Rosati, 2005). The sediment budget may be constructed to represent short-term conditions such as for a particular season of the year, to longer time periods representing a particular historical time period or existing conditions at the site. Sediment budgeting is an important tool to unravel the complex processes that take place in the coastal zone. Sediment budgeting involves making assessment of the sedimentary contributions (credits) and losses (debits), and equating these to the net gain or loss (sediment balance) in a given beach compartment or littoral cell. It is very difficult to quantify these sources and sinks. So any beach sediment budgeting studies include detailed collection of hydrodynamical and sedimentological data and also model studies to assess different sources and sinks. Model results are compared with historical conditions and used to predict the evolution of beach. Thus sediment budget can be used for two purposes; first to analyse the present situation, and second, using the present conditions, to predict the coastal changes either due to any constructions or due to natural conditions.

1.3.1 Sources

Any process that increases the quantity of sand in a selected area of the coast is known as source. There are two types of sources; point sources which add sand across a limited part of a control volume boundary and line sources which add sand across an extended segment of a control volume boundary. Source of materials can be varying from place to place and from time to time. Important sources identified are longshore transport into the area, onshore transport, river/estuary input, wind transport on to the beach, beach nourishment, sea cliff erosion, in-situ shell production and dune/ridge erosion (Hume et al., 1999) (Table 1.1).

1.3.1.1 Longshore transport

Longshore transport is an important source of sediment and is caused by longshore currents that flow parallel to the coast in the surf zone. Longshore currents are generated by the longshore component of motion in waves that obliquely approach the shoreline. The direction of longshore transport is related to the wave direction. Longshore current velocity is determined by two factors; angle between wave crest and the shoreline and breaker height. The longshore current velocity varies both

across the surf zone and in the longshore direction. The volume of longshore sediment transport depends on five parameters; the breaker height, wave period, breaker angle with local shoreline, alongshore current velocity and the surf zone width.

Table 1.1 The ledger of sediment budgets (adapted from Hume et al., 1999)

Credit	Debit
• Longshore transport into the area • Onshore transport • River/estuary input • Wind transport onto the beach • Beach nourishment • Sea cliff erosion • In-situ shell production • Dune/ridge erosion	• Longshore transport out of the area • Offshore transport • Estuary infilling • Wind transport away from the beach • Sand extraction • Deposition in canyons • Solution and abrasion • Dune/ridge formation

1.3.1.2 Onshore transport

Onshore transport of sediments can take place due to waves and currents. In low energy conditions, the sediments may be transported from the offshore to the beach by the wave orbital motion. Occasionally sediments may be eroded from unconsolidated offshore sources on the continental shelf and drift shoreward and on to the beach. This potential source of sediments is the most difficult to evaluate quantitatively. The presence of the source can sometimes be judged through an examination of the petrology of the shelf and beach sands. In the overall budget of sediments, the offshore source generally remains unknown. Sometimes it can be roughly estimated indirectly by drawing the balance between the known losses and gains and comparing this with the beach erosion (Komar, 1976). Numerical methods are being successfully put to use these days for estimation of onshore transport.

1.3.1.3 River / estuary input

River/estuary may be a source depending upon the characteristics of the hinterland. Elevation, the types of rock, density of vegetation and the climate are the important factors determining the sediment supply. Damming of rivers has severely affected input of sediments from rivers. There are two distinct approaches to estimate the sediment supplied to the beach by the river. The first involves empirical correlation between the sediment supply, the drainage area of the river basin and the effective annual precipitation. The second approach is that of estimating the sand transport from measurements of the river discharge or velocity, by using appropriate mathematical formulations.

1.3.1.4 Wind transport

Wind can influence the beach profile changes in two ways, directly by being a vehicle for transport of sand to and fro the beach and indirectly by influencing the hydrodynamic processes, which are the main vehicles of sediment transport in the nearshore environment. On beaches where a strong seasonal wind blows, sand transport by wind is an important mechanism contributing to beach changes. If the wind speed at certain elevation reaches a critical value, sand grains on a loose sand surface begin to move. Once movement begins, wind of the same or higher speed can move the sand grains and cause their flow continuously downwind. After the sand grain rises from the surface, it is acted on by the forces of gravity and force due to the wind (drag force), and when the force of gravity exceeds the drag force, the sand grain falls. In addition to this, direct effect of wind can cause onshore transport of sediments by influencing the hydrodynamic processes. Depending on the wind direction with respect to the shoreline, the wind can cause a seaward movement of the surface waters, which is compensated by a land ward near bottom current. With offshore winds, the advancing waves tend to be reduced in height by the head winds, so that the waves reaching the shore are of lower steepness, resulting in beach accretion.

1.3.1.5 Beach nourishment

Beach nourishment is the introduction of sediment onto a beach. It is a soft, eco-friendly beach protection measure. It involves importing of sand or gravel to replace the eroded sediment. Most of the sediments used for beach nourishment project are material dredged from harbour construction, harbour maintenance, channel deepening etc. Another low cost method is to collect sediment from offshore. But the major drawback of offshore sediment is that it contains high percentage of silt and clay. Sand bypassing, another method, involves transport of sediment from a wide beach to an eroding beach by mechanical ways. Before accepting the sediment material for nourishment, its similarity to the present sediments available in the beach, in size, grading and other chemical constituents is to be ensured. A good knowledge of local beach process is an essential prerequisite on beach nourishment. The beach nourishment does not stop erosion, but act as source of material for erosional forces. The advantage of beach nourishment includes the widening and restoration of the beach and the protection of structures behind the beach. There are different beach nourishment methods: (1) dune nourishment, (2) dry beach nourishment, (3) profile nourishment, (4) nearshore bar nourishment and (5) beach nourishment with sand retention devices.

1.3.1.6 Backshore and sea cliff erosion

Sea cliff erosion is an important source in some coastal areas. During storms, erosion of cliff occurs due to the hydrostatic pressure exerted by the waves. Rock type, orientations of rock formation, jointing and bedding pattern and wave exposure are the important factors that affect the sea cliff erosion by waves. In addition to wave action, ice wedging and rain-wash also contribute to sea cliff erosion. Cliff erosion rate can be determined by field surveys or by comparing aerial photos. Earlier, the principal source of sediment to any coast was rivers. River transported sediments were redistributed by the longshore currents. But due to human interferences such as construction of dams etc., such sources get reduced and the principal source becomes erosion of adjacent shore and sea cliffs. Backshore erosion is a significant source where older coastal deposits, which contain a large fraction of sand, get eroded.

1.3.1.7 Shell production

Shell and coral fragment are important source in some beaches. It is important especially in tropical beaches such as in Lakshadweep islands of India, southerly shorelines on the Atlantic, and Gulf coasts of the US and in Hawaii. Shell production is a slow process.

1.3.1.8 Dune/ridge erosion

Dunes are considered as natural beach protection systems. When wind blow is obstructed by any object, the sand grain, which it carries, gets deposited and the sediment gets accumulated resulting in the formation of dunes. Dune has two functions in a coastal environment; acts as a natural beach protection system and also as a source of sediments at the time of erosion. During storm conditions dunes will erode. This process of erosion is called scarping. During scarping sediment stored in the dune system get released to beach system. The sediment gets moved to offshore and form offshore bars during storm season. During fair weather, this sediment is brought back to shore to rebuild the dunes. So erosion of dunes acts as a major source in certain beaches.

1.3.2 Sinks

Processes that decrease the quantity of sand in a selected area of the coast are known as sinks. Just like source there are two types of sinks; point sinks and line sinks. The sinks also vary from place to place and time to time. Important sinks identified are longshore transport out of the area, offshore transport, estuary infilling, wind transport away from the beach, sand extraction (mining), deposition in canyons, solution and abrasion and dune/ridge formation.

1.3.2.1 Longshore transport out of the area

As already discussed in Section 1.3.1.1 wave induced longshore current is an important means of sediment transport in a coastal environment. Longshore transport out of the area also could be a significant component of the sediment budget.

1.3.2.2 Offshore transport

Transport to offshore, which is just the reverse process of onshore transport, is an important sink. Transport to the offshore is caused by storm waves, which erode beach sand and transport it offshore. This offshore transport is very much prevalent during monsoon season along the west coast of India. Onshore winds, which pile up surface waters on the shore causing seaward bottom return flow also is a contributing factor.

1.3.2.3 Estuary infilling

Estuaries can trap sediments making it a sink in the sediment budget. Flood tidal deltas formed within estuaries (Black and Baba, 2001) are composed of sediments from the nearshore. These sediments are a loss to the beach-nearshore system.

1.3.2.4 Wind transport away from the beach

As already discussed, wind induced transport of sediments is an important component of sediment budget. It is quite often seen that wind has major role as sink than source. When wind blows in onshore direction, it could lead to removal of sediments from beach to inland resulting in a net loss of sediment from beach unless it is backed by a hinterland sand dunes. Wind blowing in offshore direction also can cause loss of sediment to the beach.

1.3.2.5 Sand extraction

Removal of beach sediments has the opposite effect of beach nourishment, leading to undermine the buffering role of the beach and therefore promoting erosion. For this reason, the removal of beach sands is generally prohibited except in locations where beach placer deposits are available. The Chavara and Manavalakuruchi beach placer deposits are world famous and are being mined by virtue of their commercial and strategic importance.

1.3.2.6 Deposition in canyon

In certain areas like Pacific coasts, deep canyons act as a major sink of littoral sediments. In this area, the heads of the submarine canyons are in shallow water very near to the beach and therefore can intercept the beach sands.

1.3.2.7 Solution and abrasion

Solution and abrasion of sand reduces its grain size so that one would expect that it might become too fine to remain on the beach, and be carried off into deep water. However, from studies so far conducted, it is concluded that abrasion is insignificant. Similarly, the solubility of quartz in seawater is negligible and thus there is no loss of beach sand for this reason. However, the situation is different in beach sediments comprising of shell and coral debris.

1.3.2.8 Dune/ridge formation

Beach ridges consist of sand deposited by wave action. They can form as successive beach berms deposited on a seaward advancing shoreline. Grasses and other obstacles (eg. debris) on the beach ridge aids increase in width and height by accumulation of wind blown sand.

Dunes are composed of wind blown sand. Foredunes are deposited immediately behind sandy beaches. Strong onshore winds erode dry sand from steepening face of the beach. This wind blown sand is deposited towards the top of the beach and a foredune gradually forms. Foredunes also form where vegetation and other obstacles on the upper part of the beach cause deposition of windblown sand. During periods of shoreline advance, successive foredunes may develop to form a series of parallel dunes. Blowouts, parabolic dunes and mobile sandsheet complexes are initiated in foredune, parallel dune or beach ridge system, where strong onshore winds erode sand from unstable areas. During this season, the shoreline system responds to the low waves by transferring sand onshore and storing it in the subaerial beach and dune.

1.3.3 The Balance: Beach Erosion or Accretion

For a given littoral compartment (or cell) the total volume of sand added to the beach (credits) from various sources can be balanced against total losses (debits). If the losses are greater than the gains, then there will be a net deficit, which will be reflected as a decrease in the total volume of beach sediment: beach erosion will occur. Similarly, if the credits over weigh the debits, there is accretion to the beach. The lack of either erosion or accretion indicates a state of equilibrium between sources and sinks.

Thus sediment budgeting becomes a very valuable exercise to assess the erosion/accretion status of a beach and to identify the causative factors. This particularly should form a prerequisite in situations where commercial mining is going on or are proposed to be taken up. Since mining is a process by which sediments are lost to the beach-nearshore system, it is bound to have an impact on the equilibrium of the system. Mining of beach sand rich in placer deposits or other commercially important mineral is essential in view of their economic and strategic importance. However, sediment budgeting studies need to be undertaken in such situations to ensure that the damage to the sedimentary balance of the system is minimal and the mining goes on in a sustainable way.

1.4 BACKGROUND OF THE PRESENT INVESTIGATION

The Chavara coast of Kollam district, Kerala is world famous for its rich placer deposits. The heavy mineral content in the beach sand goes up to as high as 95%. Sand extraction by Indian Rare Earths Ltd (IREL) and its predecessor companies has been going on at various sites along the Chavara coast (Fig. 1.7) since 1930. Two sources contribute to the heavy mineral sand in-take by IREL at present: (i) the beach washing from the Vellanathuruthu and Kovilthottam mining sites of IREL and the collection by the local populace, mainly from the Kayamkulam inlet area and (ii) the dredging from the hinterland sites of IREL. The intake from the beach constituted a major share of the sand extraction by IREL.

The Chavara coast is also known for the occurrence of erosion. What is the role of mining on erosion along this coast? This has been a long pending question which was not answered due to lack of studies on beach-nearshore sedimentary dynamics of this coast. In fact many dwellers of this coast believe that erosion along this coast is caused due to mining and there have been occasional attempts to block the mining.

In this context, a workshop on "Sustainable Development of Heavy Mineral Resources of Chavara" was held in Chavara in October 1997 to draw up action programmes for scientific investigation. Pursuant to the decision in the workshop, a project "Heavy Mineral Budgeting and Management at Chavara" was undertaken by Centre for Earth Science Studies in May 1999 with financial support of the IREL. The present thesis emanates from the sediment budgeting studies carried out under that project.

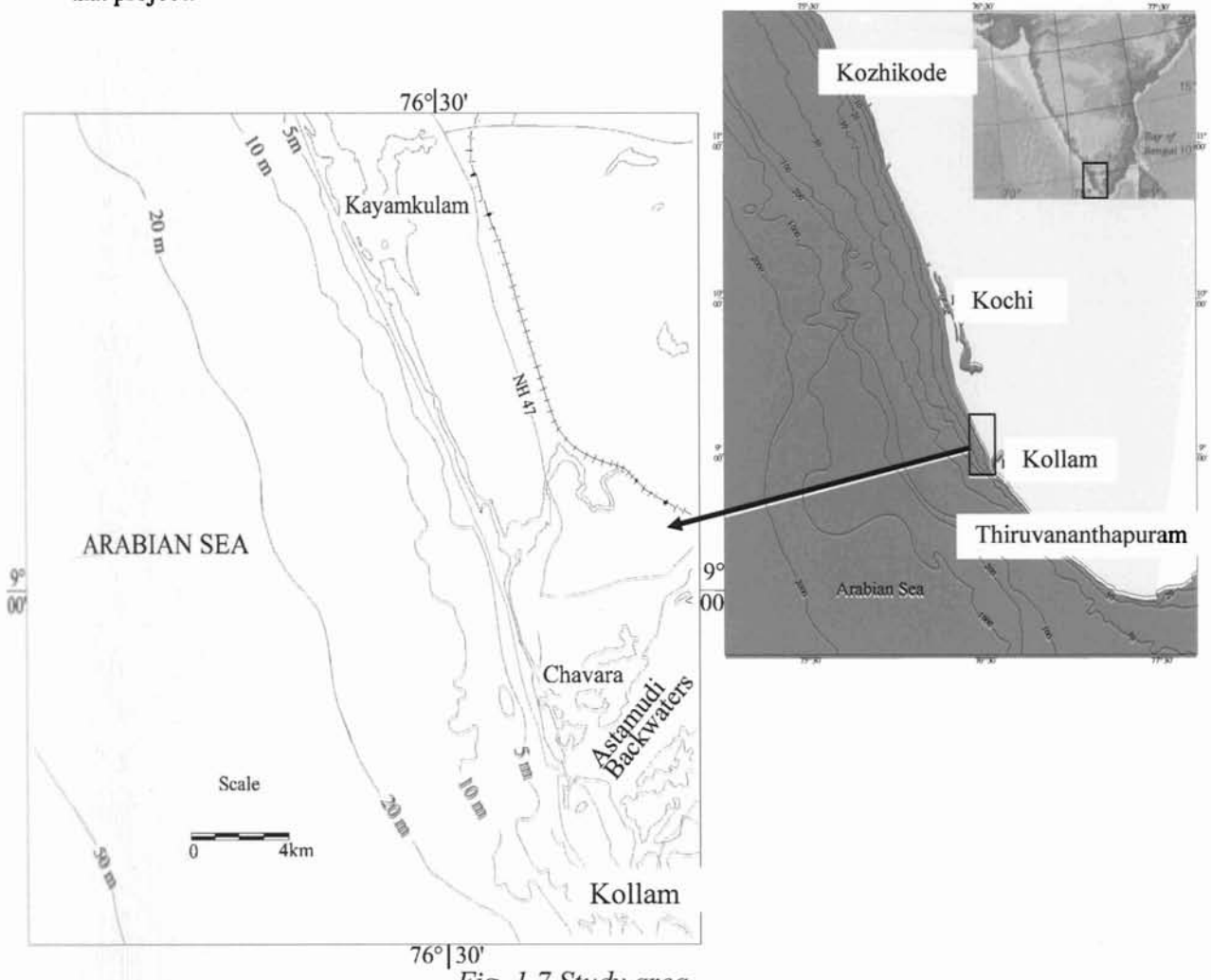

Fig. 1.7 Study area

1.5 AIMS AND OBJECTIVES

The investigation has been taken up with the following aim and objectives:

- Study the hydrodynamic processes and mechanism involved in the sediment movement along the Chavara coast
- Identify the different sources and sinks of beach sand along the coast
- Quantify the sediment input/output into/from the coast
- Assess the erosion/accretion scenario of the coast based on the study

1.6 STRUCTURE OF THE THESIS

The thesis has been presented in 7 chapters including this introductory chapter.

A description of the field experiment design, instruments used, deployment sites, instrument set-up, data analysis etc. are described in chapter 2. Chapter 3 deals with the wave characteristics of the Chavara coast. The wave climate and distributions of different wave parameters for the Chavara coast are presented based on the recorded data.

Recorded data on currents is very scanty for Indian coast. In chapter 4 the current regime of Chavara coast is described based on the extensive data collected during the study period. Distribution of current vectors including cross-shore and alongshore components and progressive vector plot for different periods are described in this chapter. The observed characteristics are discussed in relation to the causative factors such as wind, shelf circulation, etc.

Chapter 5 presents the beach processes along the Chavara coast. Characteristics of littoral environmental parameters such as breaker height, breaker period, breaker angle, breaker type, longshore current observed in the field are presented. Beach profiles and volume changes measured over the two years period are presented in this chapter. Nearshore profiles collected by operating SLED are also presented. The observed beach processes are discussed in terms of the meteorological and hydrodynamic parameters.

Chapter 6 deals with the sediment budgeting work. The numerical models used for the computation of sediment transport rates, the methodology followed and the results of the computations are presented. The sedimentary dynamics of the beach-innershelf system of this coast is discussed. The erosion/accretion scenario of the coast is discussed with reference to the sediment budget.

The summary and conclusions of the investigation are presented in chapter 7. Recommendations for future work are also given in this chapter.

CHAPTER 2

MATERIALS AND METHODS

2. MATERIALS AND METHODS

2.1 INTRODUCTION

The physical processes that occur in the nearshore region include wave transformation, nearshore currents, sediment transport and beach morphometric changes. Field studies, observational or experimental are indispensable tools to understand the actual processes. In the present study an extensive field measurement programme spanning over a period of 27 months was planned and implemented in the beach-innershelf region of Chavara. Apart from the measurements using equipments deployed in the nearshore and offshore regions, regular field programmes involving beach profile measurements, littoral environmental observations, etc. were also conducted. Such major efforts were essential to understand the beach-innershelf sedimentary processes and set up numerical models for sediment budgeting. One major difficulty in such data acquisition is the instrument failures under the unfavourable environmental conditions and the safety of the human resources employed. This chapter outlines the methods followed in the field measurements and data processing.

2.2 SITES OF FIELD MEASUREMENTS/ OBSERVATIONS

Three regions in the beach-nearshore-innershelf system (Fig. 2.1) were covered for sediment budgeting studies. The first region is around the 8 m isobath, chosen to separate the inner shelf from the nearshore zone. Given that this isobath is well within the "wave stirring" zone where sediment movement under waves is common, the net transfer of sediment across the 8 m isobath represents transfer to or from the coast, from or to the inner continental shelf.

The second key region is the zone of offshore bars that occur mostly in 2-5 m depth. Transfers between the bar and the beach are common worldwide, whereby, sediment is taken from the beach and deposited on the bar in storms, and then returned slowly by shoreward bar migration in narrow-band swell.

The third key region is the inter-tidal beach, where sand may be pushed up to the high tide line by swash, longshore currents and surf zone processes. Beach sediments are moved around and piled up by waves, but much of the movement could be an internal re-adjustment, rather than a net flux.

As a first step, the Vellenathuruthu-Pandarathuruthu sector midway in the coastline under study (Fig. 1.7) was chosen for the field measurements. A field station was setup in the area. Based on the bathymetric survey carried out in the region, the sites for offshore measurements were chosen. The first site, corresponding to the first region was chosen at a depth of 8m, about 1600m from the shore. This site is called the "offshore site". The second site corresponding to the second region was chosen at a depth of 5.5m, about 700m from the shore. This site is called the "nearshore site". A detailed programme of beach profiling was undertaken to examine the beach transitions and to measure volumes changes from the beach. An automated video camera was established in the beach to monitor the beach and littoral processes twice daily over 15 months. Finally, a series of offshore profiles were obtained using a Sliding Level Estimation Device (SLED) with a vertically-mounted staff in the breaker zone and echo sounding in the inshore to show the bar position and migration.

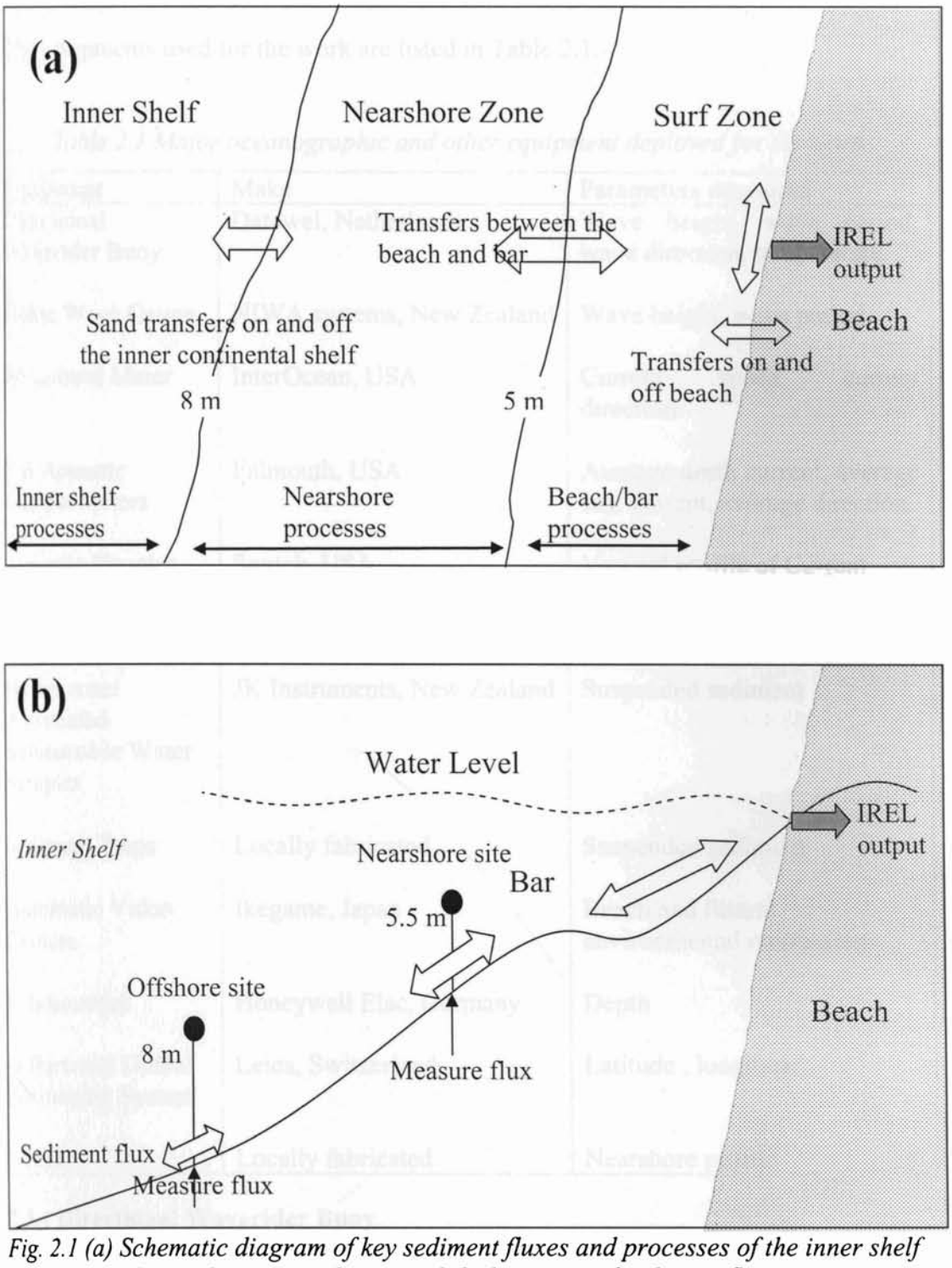

Fig. 2.1 (a) Schematic diagram of key sediment fluxes and processes of the inner shelf and nearshore coastal zone and (b) locations of sediment flux measurement

2.3 EQUIPMENTS USED FOR THE WORK

The equipments used for the work are listed in Table 2.1.

Table 2.1 Major oceanographic and other equipment deployed for the work

Equipment	Make	Parameters measured
Directional Waverider Buoy	Datawel, Netherlands	Wave height, wave period, wave direction, temperature
Dobie Wave Gauge	NIWA systems, New Zealand	Wave height, wave period,
S4 Current Meter	InterOcean, USA	Current speed, current direction
FSI Acoustic Current Meters	Falmouth, USA	Average north current, average east current, average direction
Acoustic Doppler Profiler	Sontek, USA	Vertical profile of Current speed and direction
Hydrocamel Automated Submersible Water Sampler	JK Instruments, New Zealand	Suspended sediment
Sediment Traps	Locally fabricated	Suspended sediment
Automatic Video Camera	Ikegame, Japan	Beach and littoral environmental monitoring
Echosounder	Honeywell Elac, Germany	Depth
Differential Global Positioning System	Leica, Switzerland	Latitude , longitude
SLED	Locally fabricated	Nearshore profile

2.3.1 Directional Waverider Buoy

The directional waverider buoy (M/s. Datawell, The Netherlands) is a spherical, 0.9 m- diameter buoy (Fig. 2.2) used to measure wave height, wave period, wave direction and sea surface temperature. It contains a heave-pitch-roll sensor (Hippy-

40), a three axis fluxgate compass, two fixed X and Y accelerometers and a temperature sensor.

The vertical acceleration is obtained by means of an accelerometer, placed on a gravity-stabilised platform. This platform is formed by a disk, which is suspended in the fluid within a plastic sphere placed at the bottom of the buoy. Two vertical coils are wound around the plastic sphere and one small horizontal coil is placed on the platform. By measuring the coupling between the fixed coils and the coil on the platform, the pitch and roll angles are determined. The result of the measurement gives the sign of the angles between the coil axis and the horizontal plane.

By means of fluxgate compass, the components of the earth's magnetic field in the direction of the x- and y-axis and the direction of z-axis are measured. By all these measurements the position of the buoy with respect to fixed co-ordinates (north, south and vertical) are completely determined. The direction measurement is based on the translation principle, which means that horizontal motions instead of wave slopes are measured. As a consequence the measurement is independent of buoy roll motions and therefore a relatively small spherical buoy can be used.

Fig. 2.2 Deployment of directional waverider buoy

The complete system consists of the directional waverider buoy, the wave direction receiver (WAREC) and personal computer with software for display and data storage. The signals from the buoy deployed in the sea were transmitted in 27.705 MHz which

was picked up by the antenna of the receiving station and processed by the WAREC and the computer. The buoy has a transmitter range up to 50 km.

2.3.2 Dobie Wave Gauge

Dobie wave gauge (Fig. 2.3) is a self-recording system based on a pressure sensor to measure waves and water level changes. The Dobie was mounted inside a cylindrical steel housing welded to a steel gate that provided a stable platform resistant to sinking into the sea floor. When waves are passing overhead the Dobie deployed at the seabed, the fluctuating pressure, associated with the rising and falling of water is recorded by the instrument. The fluctuations in pressure due to waves actually decrease in amplitude with depth below the mean water level (MWL) and the rate of decrease with depth depends on the wave period. Thus, pressure under long period waves can be readily felt, and measured at depth, but pressure fluctuations under short-period waves may not actually penetrate to the same depth.

Fig. 2.3 Dobie wave gauge

In order to convert the pressure sensed at depth by Dobie into wave statistics, the data were transformed *back up to the surface* using linear wave theory to account for the way the different pressure components of the wave train decay with the depth below the MWL.

The instrument once deployed could record data for a period of few weeks, depending on the recording interval and duration.

2.3.3 S4 Current Meter

An InterOcean S4 electromagnetic current meter (Fig. 2.4) was used to record near-bed water velocities, required for calibration of numerical models. The S4 is designed to measure true magnitude and direction of horizontal current motion in any water environment. Water flows through the electromagnetic field created by the instrument, produces a voltage (potential gradient), which is proportional to the magnitude of the water velocity past the sensor. This voltage is then sensed by the two pairs of titanium electrodes located symmetrically on the equator of the sensor.

A triangular marine grade stainless steel frame supported the S4 current meter 1 m above the sea bed. Sufficient weights were added to the 3 corners of the triangular frame to prevent any movement from the deployment site.

2.3.4 FSI Acoustic Current Meter

The two Dimensional Acoustic Current Meter (2D ACM) manufactured by Falmouth Scientific, Inc.(FSI), USA (Fig. 2.5) measures current velocity in two dimensions based on the acoustic principle. The 2D ACM can also interface with an optional CTD thereby providing conductivity, temperature and depth of installation. The ACM is powered from an internal alkaline battery pack. It has a standard 1-MB internal RAM. The ACM is small in size and low in weight and has a depth rating of 200 m. Two 2D ACM current meters among which one has the CTD facility were used for the work. Using 3D ACM97 software, the instrument was set up with the required on/off and averaging intervals. The instruments were deployed in the sea in a housing and the data stored in its internal flash memory, retrieved subsequently.

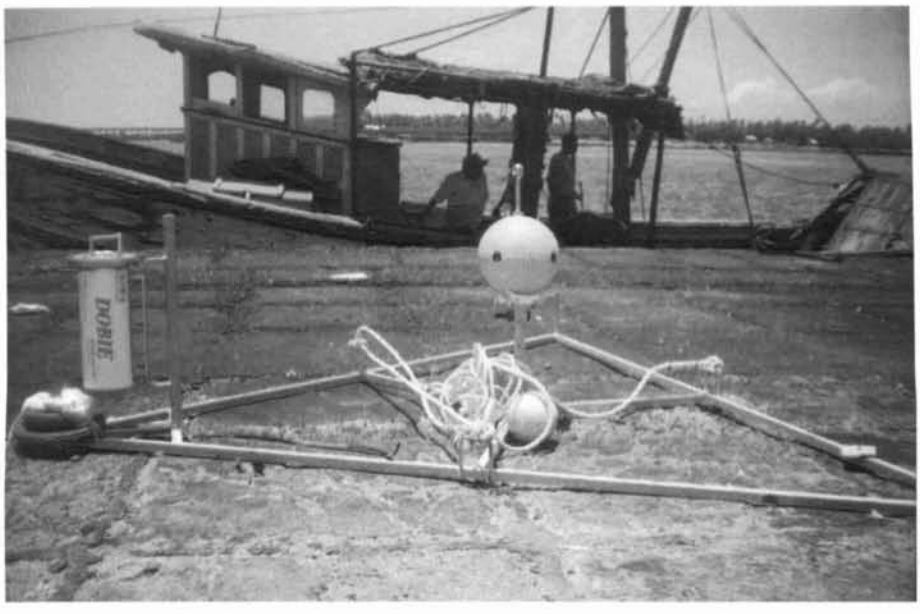

Fig. 2.4 S4 Current meter (spherical yellow colour) attached to stainless steel frame. The Dobie wave gauge is also seen attached to the same frame at one corner.

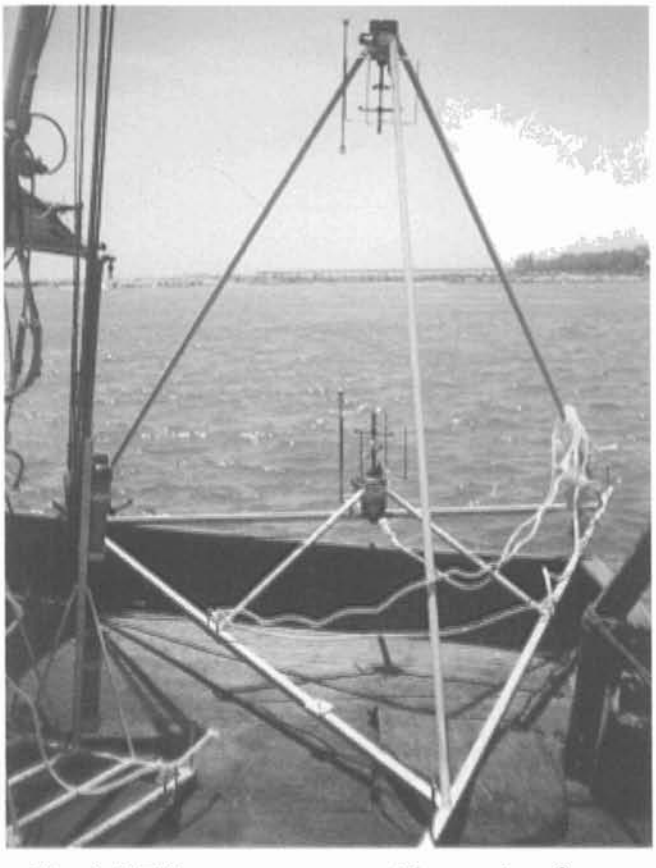

Fig. 2.5 FSI current meter with mooring frame

2.3.5 Acoustic Doppler Profiler

The Acoustic Doppler Profiler (ADP) measures current speed and direction by transmitting high-frequency bursts of sound though the water column. Particles in the water column scatter the sound back to the ADP, which listens for these echoes, records them as data, and labels the different depths from which they have returned. Motion of the particles in the water column (such as movement with the current) causes the echoes to change in frequency. The ADP (Fig. 2.6) measures this change, the Doppler shift, to determine current speed and direction at the different depths in the water column. The ADP can measure current velocities through the water column either looking vertically downwards or vertically upwards. The measurement was from a moving boat for synoptic current measurement of a large area or moored on the seabed.

All acoustic current profilers have a region immediately in front of the transducers where no measurements can be made, this is called the blanking region. The blanking distance over which the ADP could not measure for the present deployments was 0.4 m.

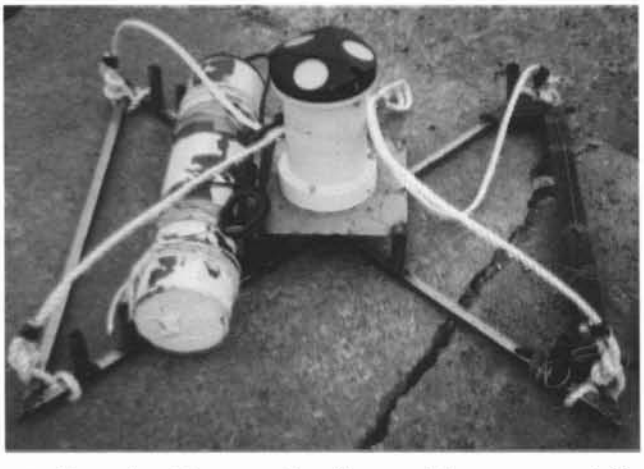

Fig. 2.6 Acoustic Doppler Current Profiler and battery pack fixed on a frame

The ADP used for the work was hired and hence only limited data required for circulation modeling was collected using the equipment.

2.3.6 Hydrocamel Automated Water Sampler

The Hydro Camel automated submersible water sampler (Fig. 2.7) is manufactured by JK Instruments, New Zealand. Automatic water sampling eliminates the high cost of manual collection and provides samples in all weather conditions and harsh locations. Constructed of stainless steel and modern plastics to eliminate corrosion, the instrument is easy to transport and deploy from a small boat. The Hydrocamel can be programmed with Windows-based software to take water samples at pre-selected intervals and quantity and store these in sample bags of 3 litres capacity. The water sampler used for the work had 20 ports and hence 20 water samples at the programmed intervals could be obtained in one deployment. The system flushes before every sample thus removing any of the remaining particles of the previous sample.

Fig. 2.7 Final verification of the HydroCamel water sampler before its deployment

The HydroCamel had its own purpose-built peristaltic pump and valve system to eliminate blockages and to operate in high suspended loads. The sampler used a 12 V rechargeable battery and can be deployed up to a depth of 40 m. The CamelTalk software provided by the firm enabled instrument programming of the required sampling regime.

2.3.7 Sediment Traps

The sediment trap (Fig. 2.8) is an instrument which, when deployed in the sea, will provide the quantum of suspended sediment load in the seawater over a period of time. The sediment trap for the present work was fabricated for the work, as per the design provided by Prof. Kerry Black. It was made of PVC pipe with a diameter of 9 cm and length 35 cm. The bottom end was closed using an end cap. Two types of sediment traps were used. Those placed in the bottom layers or in zones of high sedimentation have a nozzle or a reducer in the top to provide a reduced opening of 4 cm. This was to take care of the anticipated higher sediment load in the bottom layers that might result in overfilling. Further from the seabed where the suspended load is less, there is no need for a nozzle. The trap, which was kept very close to the bottom, was made in such a way that it can be kept in a horizontal position with an opening on its side using a connector. The sediment traps mounted on the sensor housing were open when deployed in the sea. Before retrieval the traps was closed by sending a diver to the depth of deployment.

Fig. 2.8 Sediment trap attached to the sensor housing

2.3.8 Automatic Video Camera

A video camera system (Fig. 2.9) was installed in the beach near the Field Station for monitoring of the beach and littoral zone. The camera used was the model ICD-703P

colour CCD camera manufactured by Ikegami Tsushinki Co. Ltd., Tokyo, Japan. It was installed on a vertically mounted coconut trunk at a height of about 9m from the mean sea level. The camera features high sensitivity and high picture quality. An internal RGB digital signal processor was introduced for video signal processing to give a stable, clear picture. By adopting the high sensitivity CCD with on-chip micro-lens as well as the low-noise high quality image processor, the camera could shoot under the minimum illumination of 3 lux. Effective backlight compensation is readily made through the auto iris lens.

Fig. 2.9 Video camera

The camera was also provided with the one push preset white balance control system and the manual adjustment mechanism. In view of the highly corrosive humid coastal environment, an all-weather housing with heater and blower was provided for the camera.

2.3.9 Echosounder

A Honeywell Elac-Nautik echosounder (Fig. 2.10) was used for depth measurement, and preparing the bathymetric map and data input for numerical modelling. The echo sounder used in the study was a portable shallow water echosounder capable of measuring up to a depth of 60m. It operates with a combined 35/200 kHz transducer as transmitting and receiving transducer. The transducer was mounted at the boat's

bottom or as portable version attached on the side of the boat/vessel. It can be operated at four depth ranges:0-18m, 15-33m, 30-48m and 45-63m with an accuracy of 0.25% of selected scale range. The echo sounder used analogue recording paper for recording the bottom echo. The analogue data could be read for the precise depths at different positions.

2.3.10 Differential Global Positioning System (DGPS)

GPS is a navigational aid, which is used to locate the position and altitude based on satellite positioning. The equipment used for position fixing initially was the Magellan

Fig. 2.10 Honeywell Elac-Nautik echosounder

GPS NAV 5000, manufactured by Magellan Systems Corporation, California. The NAV 5000 is generally capable of better than 100 meters horizontal accuracy in autonomous operation. It uses five channels working simultaneously to locate and collect data from the GPS satellites. The data received from the satellites were rapidly processed to compute current position, altitude, velocity and navigational data in less than one minute. Though it could compute the altitude it is not a reliable estimate. A Differential GPS- SR9400 (Fig. 2.11) with accuracy of the order of 1m was procured subsequently for the work. This was manufactured by Leica, Switzerland. It consists of two sets of receiver and controller, one as a base unit and the other as a rover unit. The real time surveying was made possible by using a radio modem, which links between the base and the rover.

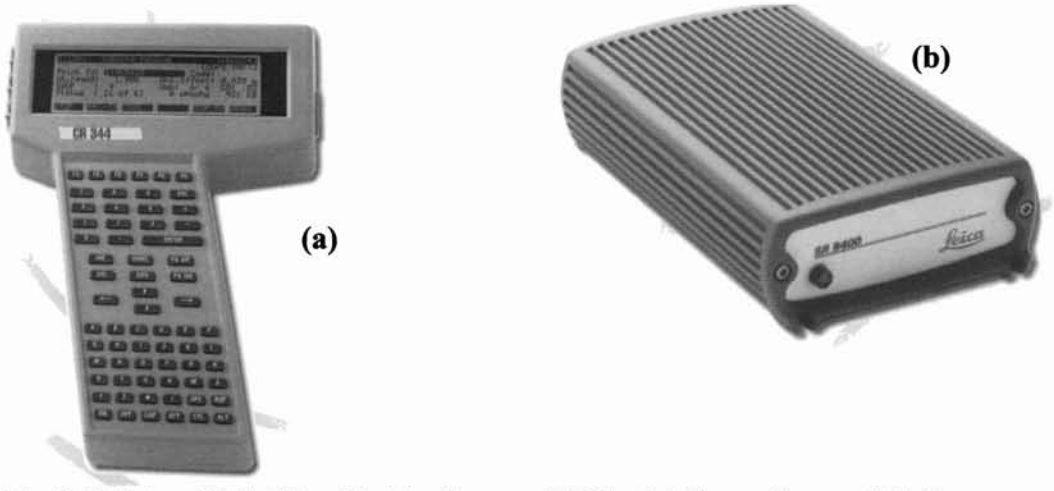

Fig. 2.11 Leica Global Positioning System (GPS): (a) Controller and (b) Sensor

2.3.11 SLED

A Sliding Level Estimation Device (SLED) was used for measuring the nearshore profile, the measurement of which was very difficult on account of the wave breaking in this zone. The SLED had a 6 m high graduated staff mounted vertically on its base (Fig. 2.12).

Fig 2.12 Sliding Level Estimation Device

In addition to the above, an anemograph of make Global Water, USA was also deployed for the work, but the data was erroneous for most of the time and hence could not be used for the work.

2.4 OFFSHORE INSTRUMENTATION AND ITS DEPLOYMENT

A schematic diagram showing the offshore instrumentation is given Fig. 2.13. Each equipment, except the waverider buoy, which was anchored, was fixed to sensor housings, fabricated locally. Marker floats were provided around the deployment sites to give warnings to the fishermen.

The instruments at the Offshore Site comprised of 2 FSI current meters, automated water sampler and sediment trap assembly (with 7 traps). The Nearshore site instrumentation comprised of a S4 current meter, Dobie wave gauge and another sediment trap assembly, with 4 traps. During the first spell of wave data collection, i.e., May-August 1999, a Directional Wave rider Buoy was used; afterwards till the end of the year 2000 Dobie Wave Gauge was used. For the deployments in 2001 both the current meters, S4 and FSI, were used for the measurement of the wave parameters since the wave gauges were not working properly. The current meter setup has been altered to suit the measurement of waves and currents simultaneously.

Before each installation, the instruments were set up as per the data requirements. Each time the equipment was hauled up the instruments were cleaned thoroughly and washed before connecting to the computer for data retrieval. The record of field deployments and data collected is given in Table 2.2

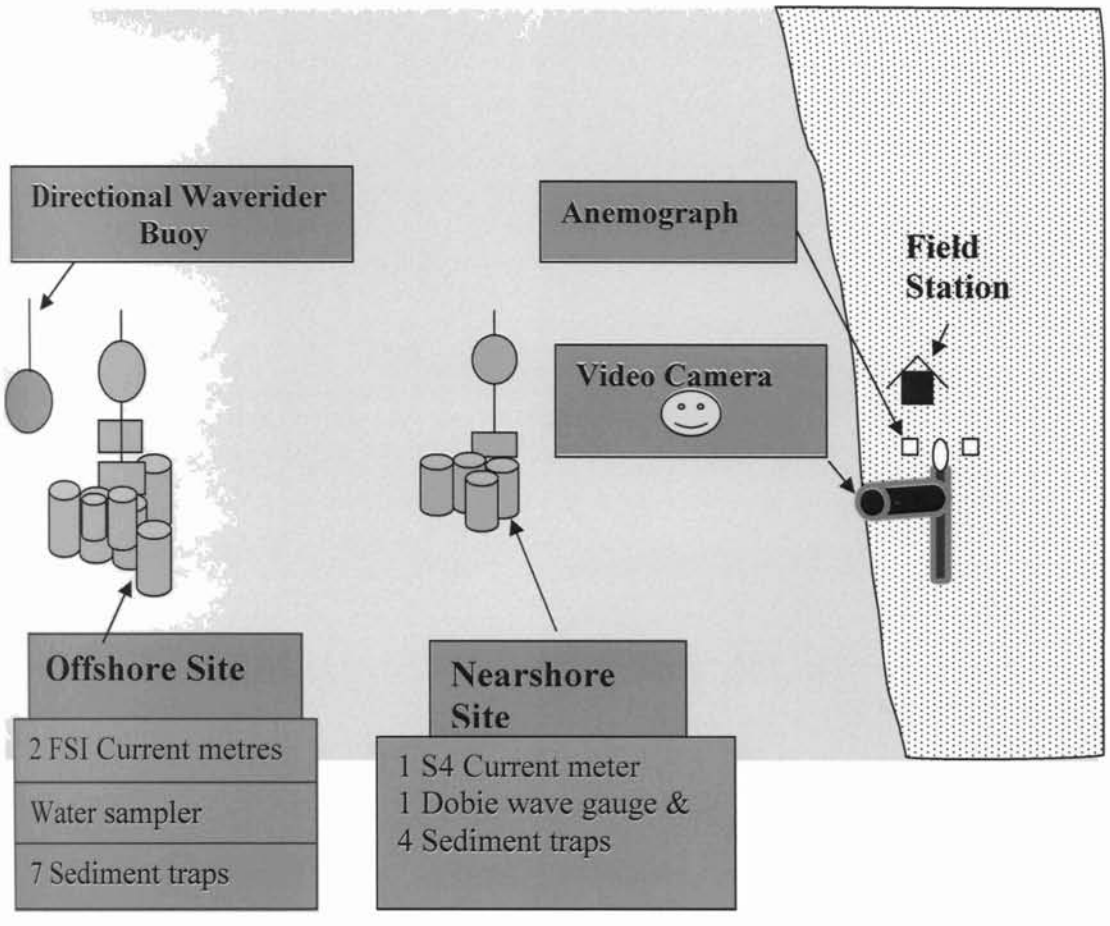

Fig. 2.13 Schematic diagram showing the offshore instrumentation and Field Station

Table 2.2 Record of offshore deployments of current meters and wave gauges and data collected

Period	S4	FSI	FSI CTD	Wave rider buoy	Dobie
7/5/99-23/5/99	Y	N	N	Y	N
25/06/99-13/08/99	Y	N	N	Y	N
22/08/99-5/9/1999	N	Y	Y	N	Y
28/09/99-28/10/99	Y	Y	N	N	Y
2/11/99-26/11/99	Y	Y	N	N	Y
7/3/00-7/4/00	Y	Y	N	N	Y
21/05/00 -14/6/00	Y	Y	N	N	Y
15/06/00-11/7/00	Y	N	N	N	Y
20/7/00-19/8/00	Y	Y	N	N	Y
27/10/00-27/11/00	Y	Y	Y	N	Y
25/04/01-16/05/01	Y	Y	Y	N	N
19/07/01-14/08/01	Y	Y	N	N	N

'Y' indicates data obtained and 'N' indicates data lost due to instrument damage, malfunctioning etc.

2.5 ANALYSIS OF HYDRODYNAMIC DATA

2.5.1 Wave Data

After wave data is collected, the analysis of that data is typically approached through both spectral analysis and statistical analysis (zero crossing analysis)

2.5.1.1 Spectral analysis

Spectral analysis, also referred to as harmonic analysis, provides a tool capable of generating information on the complicated mixture of waves produced by different storms. Spectral analysis is based on the mathematics of Fourier. The term 'wave energy spectrum' is derived from the concept that a random wave field is characterised by the superposition of a large number of linear progressive waves with different heights and periods. Generally the wave spectrum is presented as a plot of the component wave energies against wave frequencies. Spectral analysis describes the complete distributions of wave energies and frequencies (periods) than does statistical analysis. Spectral analysis works backward from the complexity of a wave climate to determine the simple components that combine to produce complex wave signals. For the present analysis the computer programme 'spdob' developed by Hameed (Unpublished) was used.

2.5.1.2 Statistical analysis

Statistical analysis provides basic information on the wave climate such as maximum wave height of the record, average wave height and root mean-square wave height. A generally accepted method applied to extract representative statistics from raw wave data is the zero crossing method. According to this method, waves are defined as the portion of a record between two successive zero up crossings. The wave height is taken as the difference between the maximum and minimum water level in a zero-crossing interval and the wave period is equal to the duration of a zero-crossing. The period is usually denoted by T_z. The average of the highest 1/3rd of the heights over the full measurement record is known as the significant wave height H_s.

The zero-crossing technique separates the time series into wave segments, recognized by the zero-crossings of the time series.

For the present work the statistical parameters are derived from the equations

Significant wave height ($H_{1/3}$) = $4\sqrt{m_0}$

Zero crossing period (T_z) = $\frac{m_0}{m_2}$

Spectral width parameter (ϵ) = $\sqrt{1-\frac{(m_1)^2}{m_2 m_0}}$

where m_0, m_1 and m_2 are spectral moments

2.5.2 Current

The current data are presented in two ways: (i) as time series and (ii) as progressive vectors. The latter show the accumulated progressive distance calculated by summing the current velocities over the duration of the measurement period and converting to a progressive distance by multiplying by the time interval between bursts. The progressive vector diagram is very useful as it shows the net movement of the water, and it is indicative of the net sediment movement. For the computation of progressive vector plots, the programme 'Tseries' developed by Richard Gorman, NIWA, New Zealand was used.

2.6 LITTORAL ENVIRONMENTAL OBSERVATIONS

2.6.1 Visual Observations

Littoral environmental observations such as breaker height, period and type and longshore current were also made at each beach profile station. Wave direction was measured using a brunton compass. The breaker height and period were estimated visually by averaging ten consecutive significant waves. The longshore current velocity and direction were measured by deploying neutrally buoyant float in the surf zone and measuring the distance travelled by the float in two minutes. Daily littoral

2.6.2 Video Camera

Visual analysis of video images for a period of one year from December 1999 to December 2000 has given a detailed picture of the temporal variation on a day-to-day scale of the different littoral environmental parameters pertaining to the area of coverage which was on the northern edge of the Vellanathuruthu mining site. The camera was connected to a programmable VCR and TV installed in the field station. The programmed VCR recorded the pictures two times in a day, 0800 hrs and 1600 hrs for two minutes. From these recordings littoral environmental parameters were derived by visually analysing the images.

2.7 BEACH AND NEARSHORE PROFILING

2.7.1 Beach Profiling

Beach-based field programmes were initiated in the present study along the Neendakara-Kayamkulam barrier beach soon after establishing the Field Station. A reconnaissance along the coast revealed that a major portion of the shoreline was fronted by sea wall with no frontal beach. Only at Kovilthotam and Vellanthurthu where beach washing is being carried out by IREL, an open beach is seen. These two sites have been chosen for fortnightly beach monitoring with close grid profiles at distances of 300 m. Thus a total of 11 stations numbered VMS 1-11 have been established at Vellenathuruthu and 5 stations numbered 1-5 established at Kovilthottam (Fig. 2.14). Beach stations (NK1-19) at 1-km interval covering the entire Neendakara - Kayamkulam sector were also established and monthly measurements carried out. The beach profile measurements were made using the standard level and staff method (Fig. 2.15).

The beach volume changes between successive measurement dates were calculated from the beach profile data using a computer programme by Shahul Hameed (unpublished). From this, beach volume changes per day were worked out.

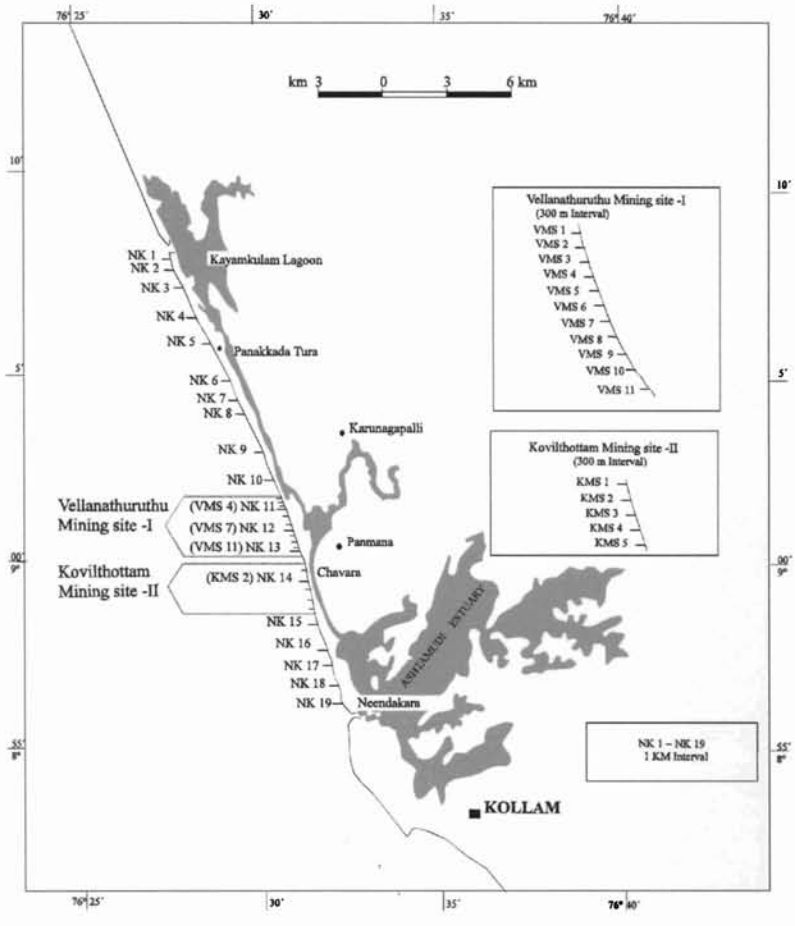

Fig. 2.14 Beach monitoring stations along the Neendakara-Kayamkulam coast

Fig. 2.15 Beach profile measurements

2.7.2 Nearshore Profiling

The nearshore profile measurement using SLED involved its transportation to the offshore first up to a depth of about 5 m and its positioning in the offshore, off the station at which profile measurement is required. Then it is pulled shorewards in the selected directions, taking care to stop at regular intervals to facilitate level measurement using a theodlite which is already positioned on the beach. Simultaneous to the SLED profiling of nearshore, (from 5m to shoreline) beach profiling (from backshore to shoreline) using dumpy level and staff and echosouding of the offshore (from 5 m to about 10m depth) were carried out. By combining the three profiles with necessary datum adjustments, cross-shore profiles of the innershelf were prepared.

2.8 SUMMARY

A comprehensive field measurement programme taking care of the data requirements for the investigation was meticulously planned and implemented. Wave and current data for different periods spanning over a period of more than 2 years were collected and analysed. Beach based field programmes were also implemented successfully. Close grid beach profiling was carried out at two sites while coarse grid profiling was carried out along the rest of the 22km coastline. For the first time in the country an automatic video camera was installed for monitoring the littoral processes. Bathymetric survey was carried out over a region extending 70 km along the coast encompassing the study area and extending out to 60m depth. In addition, seasonal bathymetric surveys were carried out in the inshore regions coupled with SLED measurements to study the seasonal changes in the nearshore profile. Considering the immensity of the task undertaken, particularly the offshore deployment/retrieval operations, it is felt that the data collection programme was a big success with only few cases of data misses due to instrument malfunctioning, vandalism by the fishermen, etc.

CHAPTER 3

WAVES

3. WAVES

3.1 INTRODUCTION

Waves, being the principal source of input energy in the coastal environment, play a significant role in sediment transport and beach evolution processes. Hence understanding the wave climate and its characteristics in the study area is essential. As already discussed in Chapter 2, a comprehensive measurement programme was planned and implemented. Waves were measured by deploying a directional wave rider buoy in the offshore site during the monsoon period of 1999 and Dobie wave gauge in the nearshore site for the period August 1999 to August 2001. The details of the instrumentation set up and deployments are already given in Chapter 2. An analysis of the extensive data set was undertaken and the results presented in this chapter. In addition, considering the importance of wind as an important forcing for the hydrodynamic processes, its characteristics also have been studied and presented in this chapter using data obtained from the India Meteorological Dept. (IMD) for Alleppey which is the closest located observatory of IMD.

3.2 LITERATURE REVIEW

In India the source for long-term information on ocean waves in the past was the record of ship's observations made by merchant vessels (Baba, 1988). The meteorological charts of Indian Ocean (H.M.S.O., 1949) and the Ocean Wave Statistics (Hogben and Lump, 1967) contain some information on deep-water wave climate over the Arabian sea. The ship based visual observations were reported by the IMD in the daily weather reports. The IMD data have been analysed by Srivastava and George (1976), Mukherjee and Sivaramakrishnan (1982a&b) and Thiruvengadathan (1984). The two important contributions that emerged from the ships observations were the Wave Statistics of the Arabian Sea prepared by Naval Physical and Oceanographic Laboratory using the data for 1960-1969 (NPOL, 1978) and the Swell Atlas for the Arabian Sea and Bay of Bengal by the National Institute of Oceanography using the data for the period 1968-1973 (NIO, 1982). The probability of monthly distribution of wave height, wave periods and wave direction based on 20

ears of ships observation data is presented in Table 3.1 (Kurian et al., 2002). Real time data on ocean waves started accruing with the deployment of wave recorders Diwan et al., 1985) at selected locations of the Indian coast, and from the records of the oceanographic research vessels (Sathe et al., 1979; Das et al., 1979). The southwest coast of India had not been adequately covered by any studies till 1980, except for stray observations made off Cochin (Srivastava et al., 1968) and Trivandrum (Swamy et al., 1979).

Table 3.1 Frequency of occurrence of different deep water wave components compiled from ships observation over a period of 20 years (Kurian et al., 2002)

Month	Probability of occurrence (%)	Height (m)	Period (s)	Direction from (°N)
January	5.8	1.5	6	270
February	5.2	2.0	6	270
	3.3	3.0	8	270
March	5.5	1.5	6	270
	3.3	1.0	6	202
April	6.7	0.5	12	202
	6.7	1.5	6	270
May	10.5	1.0	6	270
	15.8	1.0	6	180
June	4.9	2.0	6	270
	4.1	3.0	8	270
	3.4	4.5	8	270
July	2.4	1.5	6	247
	2	2.0	6	225
	6.1	2.0	6	270
	2.6	3.0	10	270
August	6.6	1.0	10	180
	3.3	0.5	10	270
September	4.3	2.0	6	270
	2.8	2.0	6	247
	2.0	1.5	6	225
October	5.7	1.5	6	270
	3.0	1.0	6	247
November	6.4	1.5	6	270
	2.8	1.5	6	247
	1.3	1.5	8	202
	1.3	1.0	10	247
	2.6	1.0	14	270
December	6.8	1.5	8	180
	7.3	1.0	6	270

Serious and concentrated efforts in the study of waves of Southwest coast of India were made by Centre for Earth Science Studies (Baba and Kurian, 1988) under the *Wave Project* and considerable data on deep water and shallow water waves were recorded. The most important aspects of these studies were the continuous and coincidental wave recording at 4 nearshore locations spread over the southwest coast of India for a period of 5 years. Studies utilising these data (Table 3.2) brought out the significant variations in wave intensity along the coast. Valiathura, near Trivandrum recorded the highest Hmax of 6.02m and H_s of 3.4m. A sharp decrease in nearshore wave intensity is seen at Alleppey and a further decrease is seen towards north. At Tellicherry, the maximum H_{max} and H_s are 2.58m and 1.60m respectively.

The spatial variations in wave intensity along the coast were studied by Kurian (1988) and Kurian and Baba (1987) and were attributed to the bottom dissipation processes which in turn are controlled by the bottom slope. The intensity variations are correlated very well with the bottom steepness which is maximum in Trivandrum and least in Tellicherry. The temporal and spatial variations observed in wave characterisitics (Table 3.2-3.4) clearly illustrate the need for generating site specific and season specific data for the coastal environments for various applications.

Table 3.2 Wave height distribution along Kerala coast

Locations	Tellichery (Harish, 1988)		Calicut (Kurian, 1988)		Alleppey (Hameed, 1988)		Valiathura (Thomas, 1988)	
	Rough	Fair	Rough	Fair	Rough	Fair	Rough	Fair
Max. Wave height	2.58	1.94	3.50	2.00	3.80	2.00	6.02	3.20
Significant wave height	1.60	1.20	2.25	1.00	3.00	1.40	3.40	2.20
H_s of 50% or more occurrence	0.80	0.30	0.80	0.50	0.95	0.52	2.50	1.50

Table 3.3 Distribution of zero crossing period along Kerala coast

Locations	Tellichery (Harish, 1988)		Calicut (Kurian, 1988)		Alleppey (Hameed, 1988)		Valiathura (Thomas, 1988)	
	Rough	Fair	Rough	Fair	Rough	Fair	Rough	Fair
Max Zero crossing period	17	18	16	16	20	21	12	18
Min Zero crossing period	7	7	6	5	6	6	6	6
Range of max.	8-9	12-13	8-9	9-10	8-9	9-10	9-10	10-11

Table 3.4 Distribution of wave direction along Kerala coast

Locations	Tellichery (Harish, 1988)		Calicut (Kurian, 1988)		Alleppey (Hameed, 1988)		Valiathura (Thomas, 1988)	
	Rough	Fair	Rough	Fair	Rough	Fair	Rough	Fair
Max direction	230	240	310	310	310	310	270	210
Min Direction	190	180	200	200	200	220	250	190
Range of max. occurrence	210-220	200-210	260-270	240-250	245-250	235-240	190-210	190-210

An year long measurement of deep water wave that have direct relevance to the Southwest coast of India were made off Kavaratti, Lakshadweep Island by Baba et al. (1992). They observed that the southerly-southwesterly waves are persistent in the Lakshadweep sea through out the year and the westerly waves dominate only when the monsoon is very intensive, i.e., in the rough season. The maximum wave height observed during the study period was 8.95 m in August followed by 8.24 m in July. The zero-crossing period (T_z) varied from 3.5 to 13.3s.

Muraleedharan et al. (1989) demonstrated the need to exercise caution while comparing the data from visual observations (over wider deep sea) and recorded waves (from shallow depths). Kurian (1989) proposed a model for predicting wave transformation in shallow waters. Numerical wave refraction study conducted by Sajeev et al. (1997) illustrated the variation in the distribution of wave heights spatially and temporally. The convergence and divergence of wave energy was found to induce non-uniform distribution of wave heights during the monsoon period.

The convergence/divergence pattern of wave energy based on wave refraction studies was illustrated for waves from different directions and of different periods by Jose (2000) and the significant interaction with local geomorphological features was brought out. Sanil Kumar et al. (2002) studied the nearshore wave characteristics off Nagapattinam coast. They compared the ratio of spectral energy at the first and second spectral peaks and found that energy at the second peak was more than 50% of that at first peak in 46% of the data collected and was attributed to the presence of sea and swell waves. Rajesh et al. (2005) reported on the observations on extreme

meteorological and oceanographic parameters in Indian seas. They observed a maximum of 13.93m of wave height during Orissa super cyclone in October 1999.

Thus the available literature gives a reasonably good picture about the wave characteristics of the seas around India. The wave climate in the Arabian Sea is dominated by the influence of the southwest monsoon when the maximum intensity is seen. The spatial variations in coastal wave climate point to the need for site specific measurements of waves.

3.3 MEASURED WIND AT ALLEPPEY

As already mentioned, no accurate wind data could be collected from the anemograph installed for the study at the Field Station. Hence wind data from the IMD observatory at Alleppey is used for the study. The polar plots of daily wind recorded at Alleppey during May 1999-October 2001, are presented in Fig. 3.1 for each month.

In the month of May'99, the winds are predominantly westerlies with a maximum speed of about 8 m/s. This was incidentally the month of onset of monsoon. In July, the winds are more scattered. This scattering is conspicuously absent in the month of August with the wind confined to the NW quadrant. In September the pattern is similar to July with a good scattering of the direction. The month of October is notable for high wind speeds up to 8 m/s from the westerly direction. During the months November and December the higher speed components are missing.

January 2000 is notable for the occurrence of the westerlies with speeds up to 5 m/s. In February, wind speed further increases up to 7m/s and the predominant direction is NW. In the month of March the distribution is more similar to February with speed up to 6 m/s. Unlike the months of January to March, more scattering is found from April onwards. However, the predominant direction is the northwesterly. In May wind speed increases up to 10m/s indicating the setting up of monsoon. However, higher wind speeds typical of monsoon are conspicuously absent in June. Wind speed increases in July in comparison with June. The wind speed further intensifies in August and the highest speed of 11 m/s in this month is seen from the SW quadrant.

Wind speed observed in this month is the maximum for the entire study period. During the period September-October, the wind direction is similar with August but the speed reduced considerably. The high wind speed recorded in October 1999 is not seen in October 2000, but is seen in November 2000 with a shift in the predominant direction to WNW. In December, wind speed reduces but the speed is in general higher when compared to December '99.

In the January-April period of 2001, the wind distribution is typical of the fair weather period with low speeds. The higher wind speeds recorded in earlier years are not seen in May 2001. As in the year 2000, the wind speed is not as high as is expected for the monsoon. The wind speed picks up in July with a predominant NW direction. The distribution of winds in August is different when compared to the previous year with the absence of the strong wind condition. However, in September and October, the distribution is more or less the same as in the previous year.

To sum up, the distribution of winds shows the characteristics typical of the different seasons. However, year-to-year variations in speed and direction are prevalent in each season. During fair weather period of November-April, the speeds are generally low with a good scattering. In the rough weather months of May-October, the speeds are higher with a focusing of the direction in the SW-NW quadrants. However, during the rough weather also, the easterlies which are generally weak when compared to the strong westerlies are prevalent. During the study period, encompassing a period of 2 ½ years, the highest wind speed of 11 m/s is recorded in August 2000.

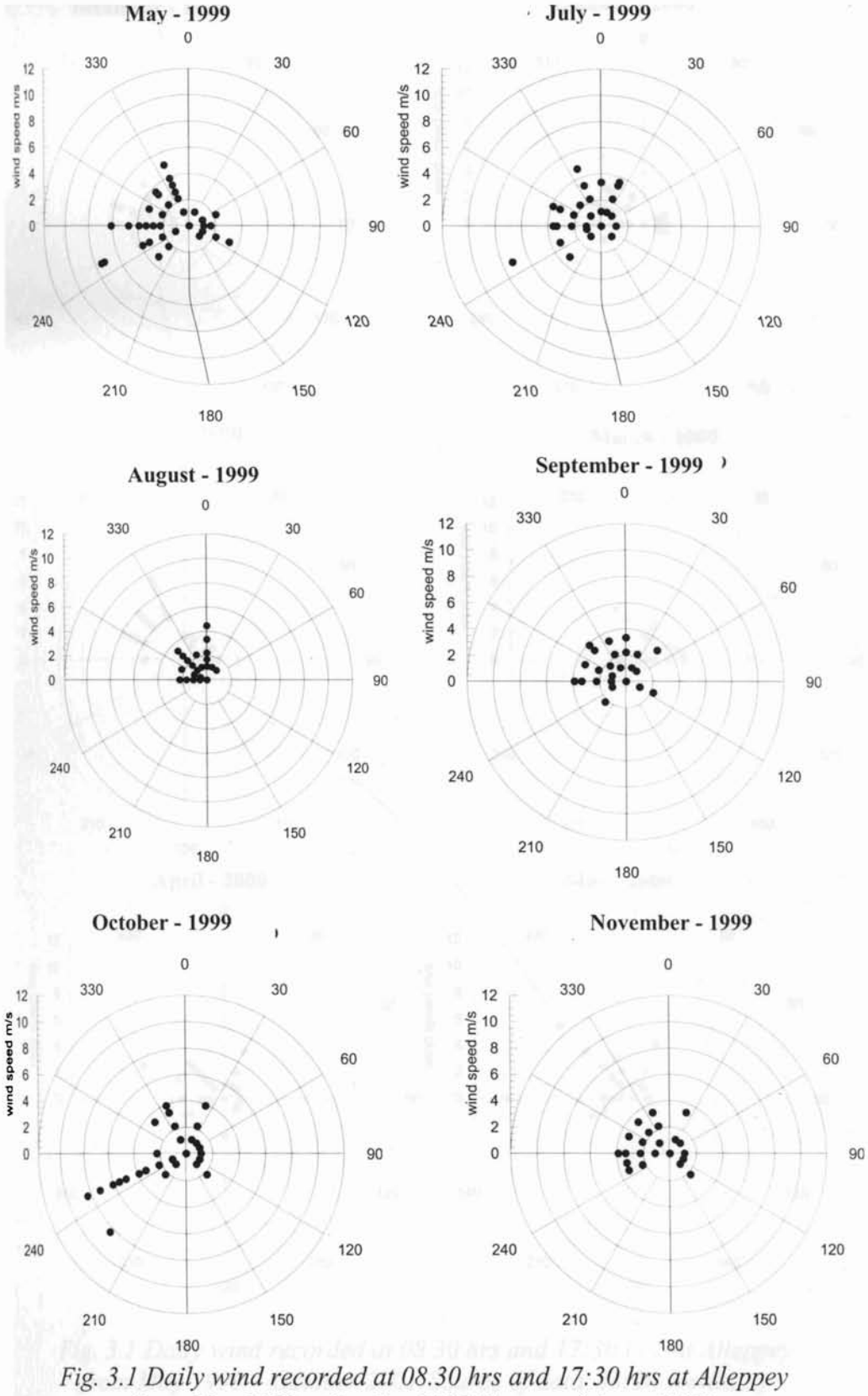

Fig. 3.1 Daily wind recorded at 08.30 hrs and 17:30 hrs at Alleppey from May 1999 – October 2001(Source of data: IMD)

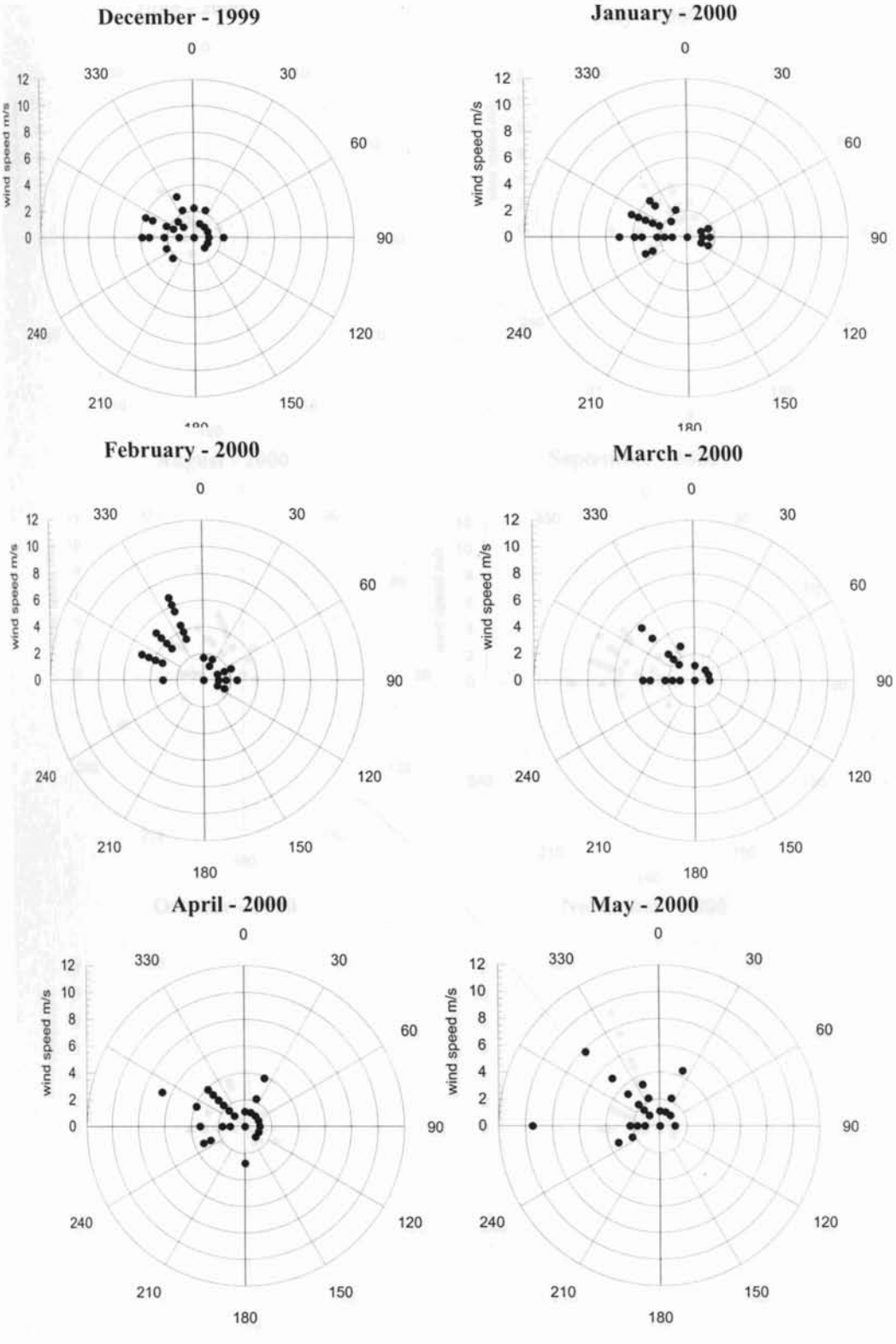

Fig. 3.1 Daily wind recorded at 08.30 hrs and 17:30 hrs at Alleppey from May 1999 – October 2001(Source of data: IMD) (contd...)

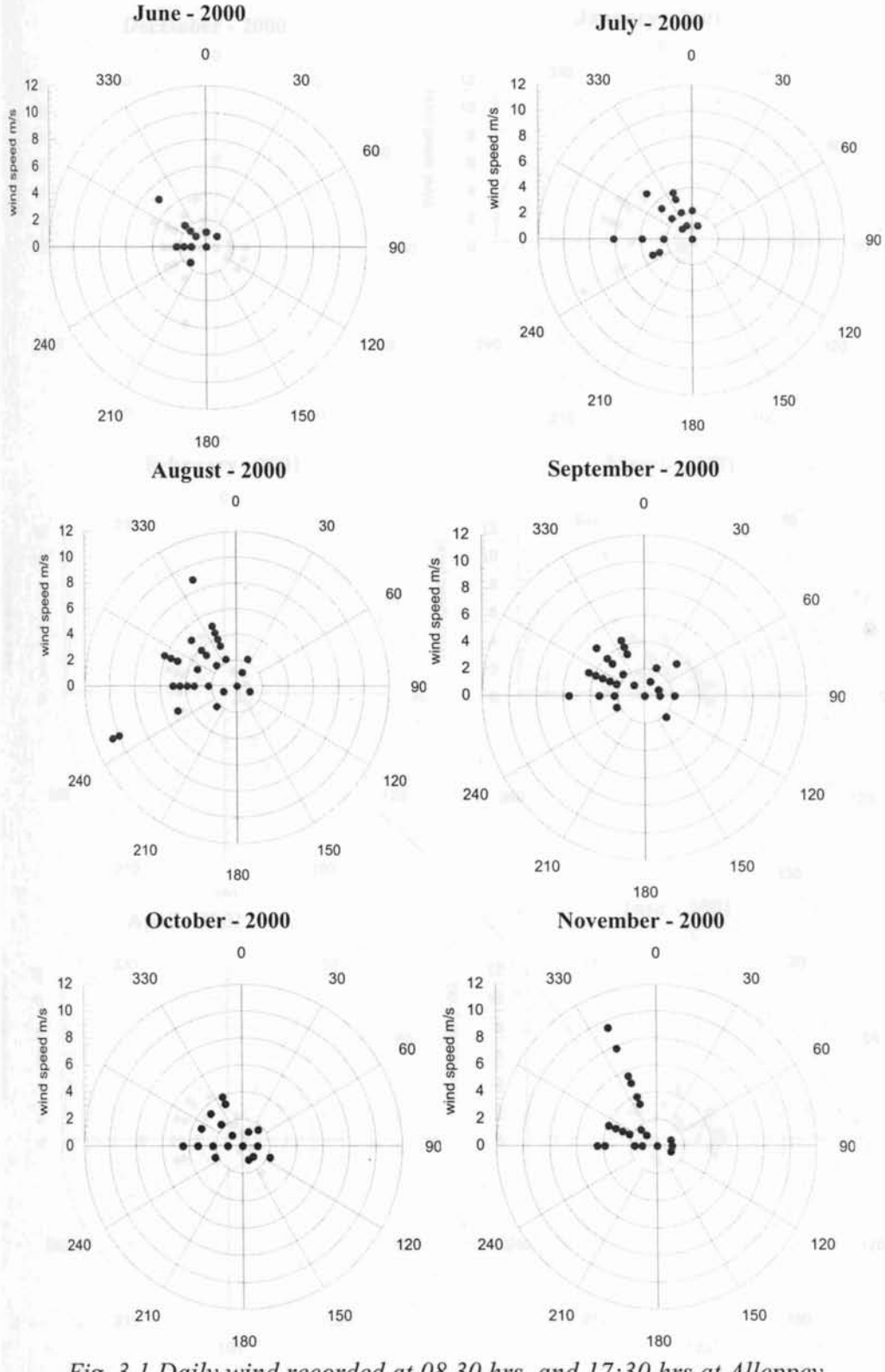

Fig. 3.1 Daily wind recorded at 08.30 hrs and 17:30 hrs at Alleppey from May 1999 – October 2001(Source of data: IMD) (contd...)

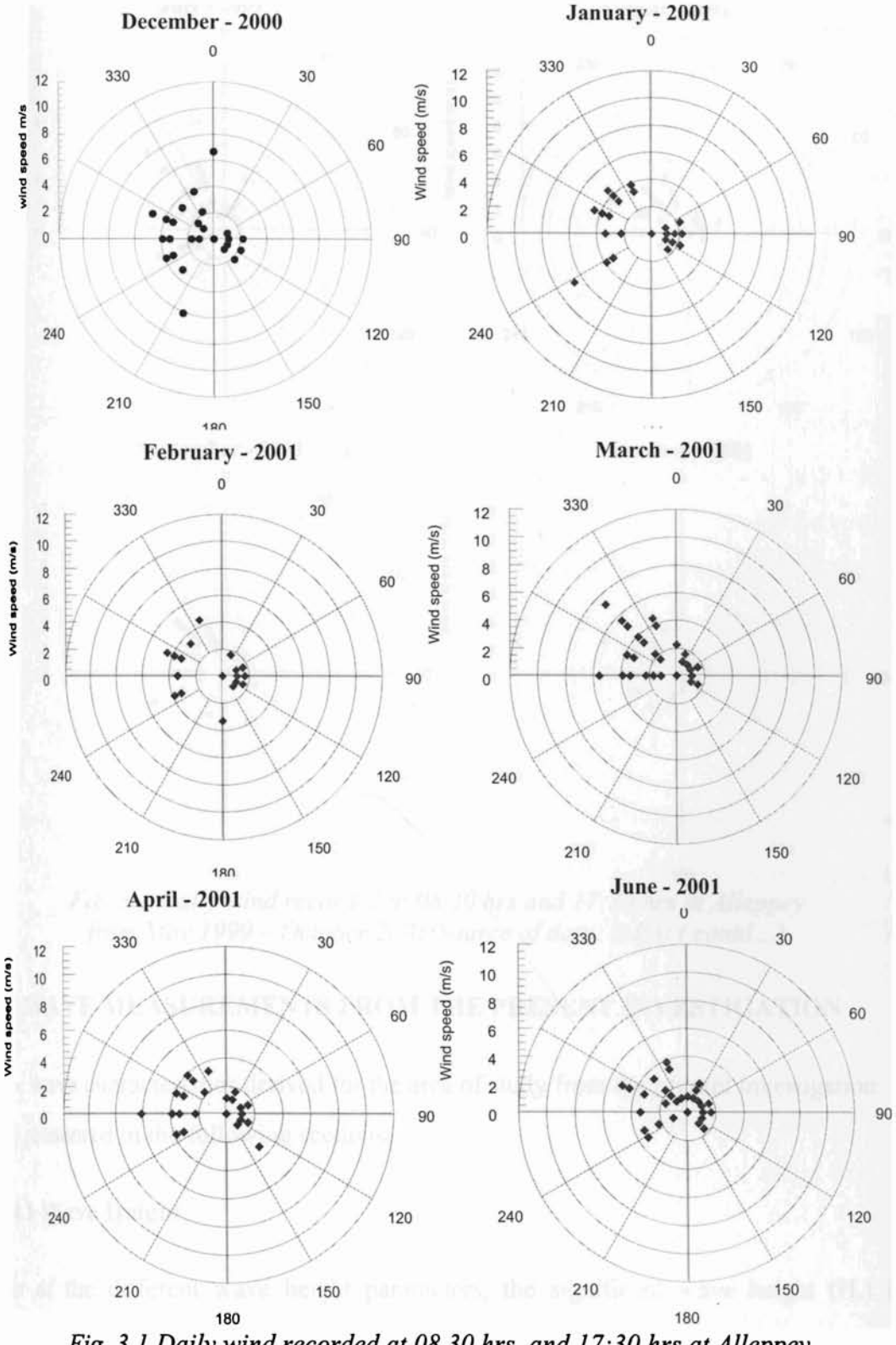

Fig. 3.1 Daily wind recorded at 08.30 hrs and 17:30 hrs at Alleppey from May 1999 – October 2001 (Source of data: IMD) (contd...)

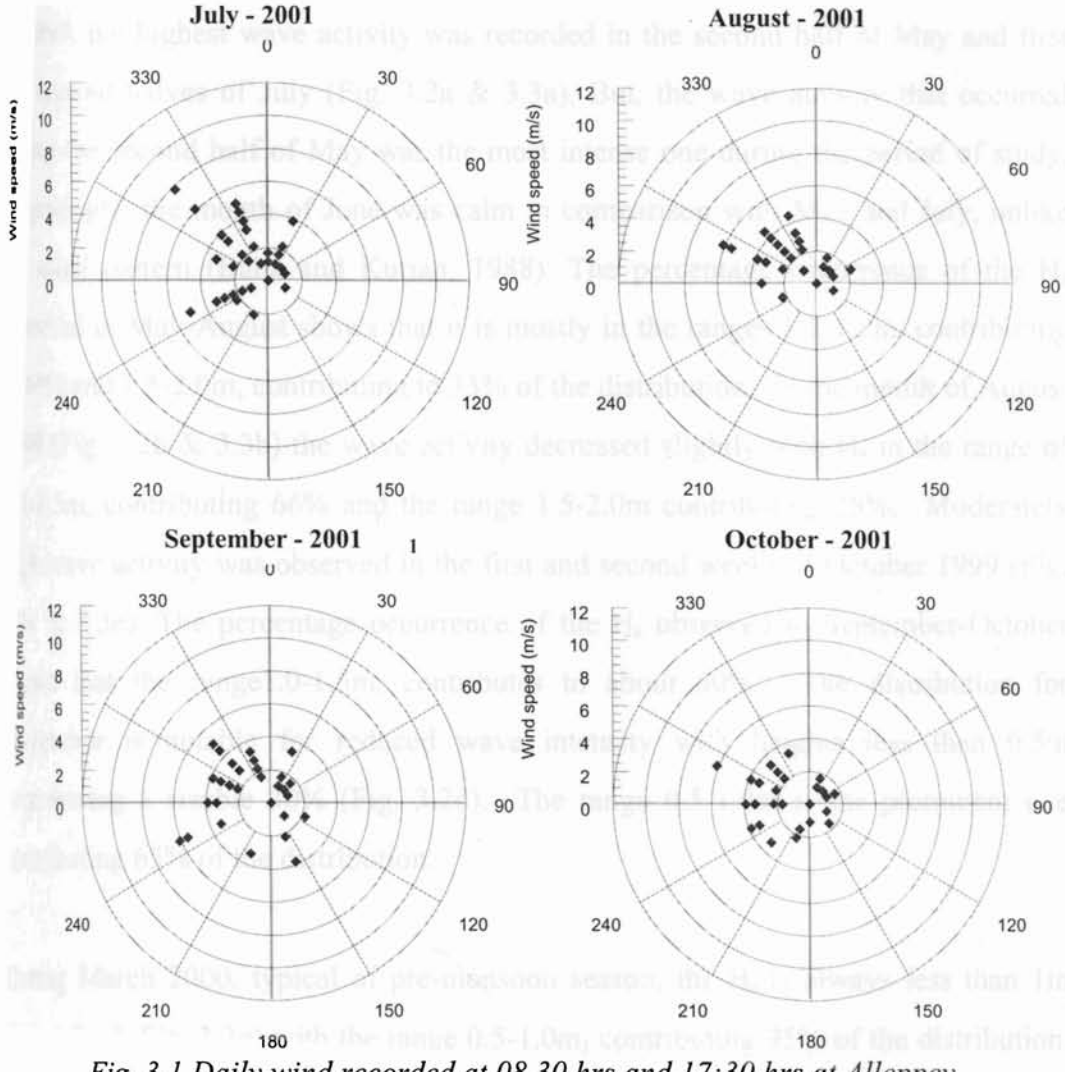

Fig. 3.1 Daily wind recorded at 08.30 hrs and 17:30 hrs at Alleppey from May 1999 – October 2001(Source of data: IMD) (contd...)

3.4 WAVE MEASUREMENTS FROM THE PRESENT INVESTIGATION

The wave characteristics derived for the area of study from the present investigation are presented in the following sections.

3.4.1 Wave Height

Out of the different wave height parameters, the significant wave height (H_s) is commonly used to represent wave heights. Hence the H_s is used here to present the wave height characteristics. The time series of H_s during the study period (May 1999 - August 2001) are presented in Fig. 3.2a-k. The frequency distribution of different heights is depicted in Fig. 3.3a-k.

In 1999, the highest wave activity was recorded in the second half of May and first and second halves of July (Fig. 3.2a & 3.3a). But, the wave activity that occurred during the second half of May was the most intense one during the period of study. Surprisingly, the month of June was calm in comparison with May and July, unlike the usual pattern (Baba and Kurian, 1988). The percentage occurrence of the H_s observed in May-August shows that it is mostly in the ranges 1.0-1.5m, contributing to 40% and 1.5-2.0m, contributing to 33% of the distribution. In the month of August 1999 (Fig. 3.2b & 3.3b) the wave activity decreased slightly with H_s in the range of 1.0-1.5m, contributing 66% and the range 1.5-2.0m contributing 25%. Moderately high wave activity was observed in the first and second weeks of October 1999 (Fig. 3.2c & 3.3c). The percentage occurrence of the H_s observed in September-October shows that the range1.0-1.5m, contributes to about 50%. The distribution for November is notable for reduced wave intensity with heights less than 0.5m contributing a sizable 30% (Fig. 3.2d). The range 0.5-1.0m is the prominent one contributing 65% of the distribution.

During March 2000, typical of pre-monsoon season, the H_s is always less than 1m (Fig. 3.2e & Fig. 3.3e) with the range 0.5-1.0m, contributing 95% of the distribution. There is a slight increase in the H_s values after the 10^{th} of March from around 0.55m to 0.8m. By May 2000 (Fig. 3.2f & Fig. 3.3f), the wave intensity increased significantly. During this month the H_s values are mostly above 1m and they ranged up to 1.8m. The H_s values are 1.0-1.4m high during the 3^{rd} week of May but it increased to 1.2-1.8m by the last week of May. The frequency distribution of the waves observed during this month shows the predominance of height ranges of 1.0-1.5m contributing 86%.

The June-August 2000 (Fig. 3.2g-h & 3.3g-h) is the roughest period of the year 2000 and the wave heights are the maximum during this period. But in comparison with the previous year, it is calmer. The wave heights occurring during June-July and July-August are in almost the same order of magnitudes, the ranges being 0.29-1.86m in

June-July and 0.33-1.87m in July-August. The H_s values are mostly between 0.5m and 1m till 28 June. Thereafter the heights increase and the H_s are in the range 1.1-1.86m till the middle of July. The H_s are in the range 0.33-0.86m during 20th July to 3rd August, but again increased to the range 1.00 – 1.87m till the middle of August. The frequency distributions during June-July and July-August have striking similarities. During June-July, the predominant values of H_s are in the range 0.5-1.0m which contributes to 40% of the distribution, followed by1.0-1.5m range contributing to 33%. During July-August 2000 the predominant values of H_s are in the range 0.5-1.0m constituting 44% followed by the range 1.0-1.5m contributing 30%.

October-November 2000 is characterised by waves of lower heights (Fig. 3.2i & 3.3i). The H_s occur in the height ranges of 0.39-1.18m with an average of 0.71m. The predominant values of H_s are in the range 0.5-1.0m which contribute to around 87% of the distribution.

In the year 2001 also, April-May is characterised by moderate heights typical of pre-monsoon with H_s in the range 0.3-1.2m (Fig. 3.2j & 3.3j). The frequency distribution shows the predominant class as 0.5-1.0m constituting 69%. This is followed by 0.0-0.5m with a percentage of occurrence of 30%.

The distribution during July-August 2001 is characteristic of the latter half of monsoon and is similar to the record in 1999 than 2000. The values of H_s ranged from 0.8 to 2.65m (Fig. 3.2k & Fig. 3.3k). The predominant values fall in the range 1.0-1.5m with percentage occurrence of 66% followed by the range 1.5-2.0m with an occurrence of 22%.

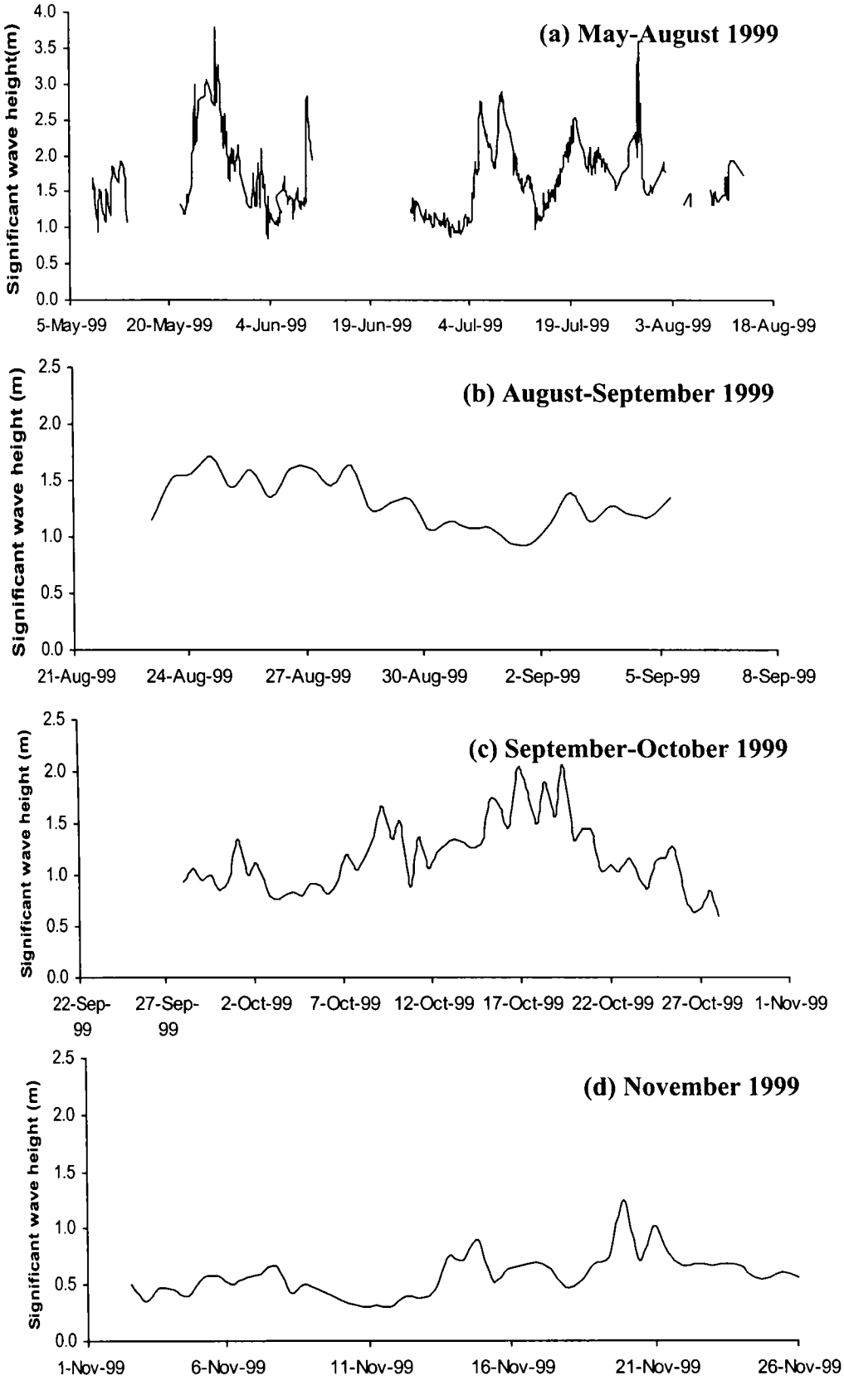

Fig. 3.2 Time series plot of significant wave heights measured during different measurement periods

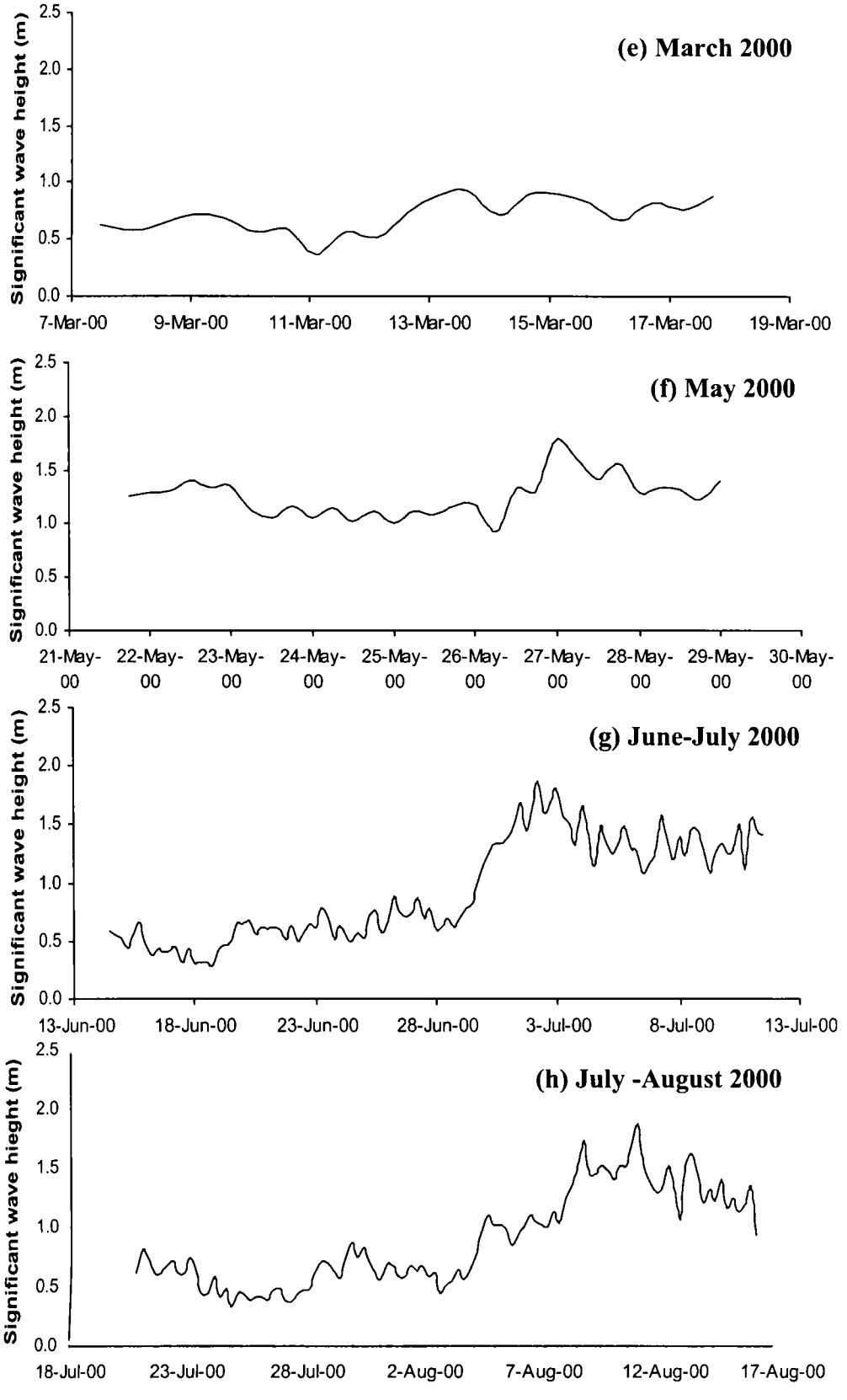

Fig. 3.2 Time series plot of significant wave heights measured during different measurement periods (contd...)

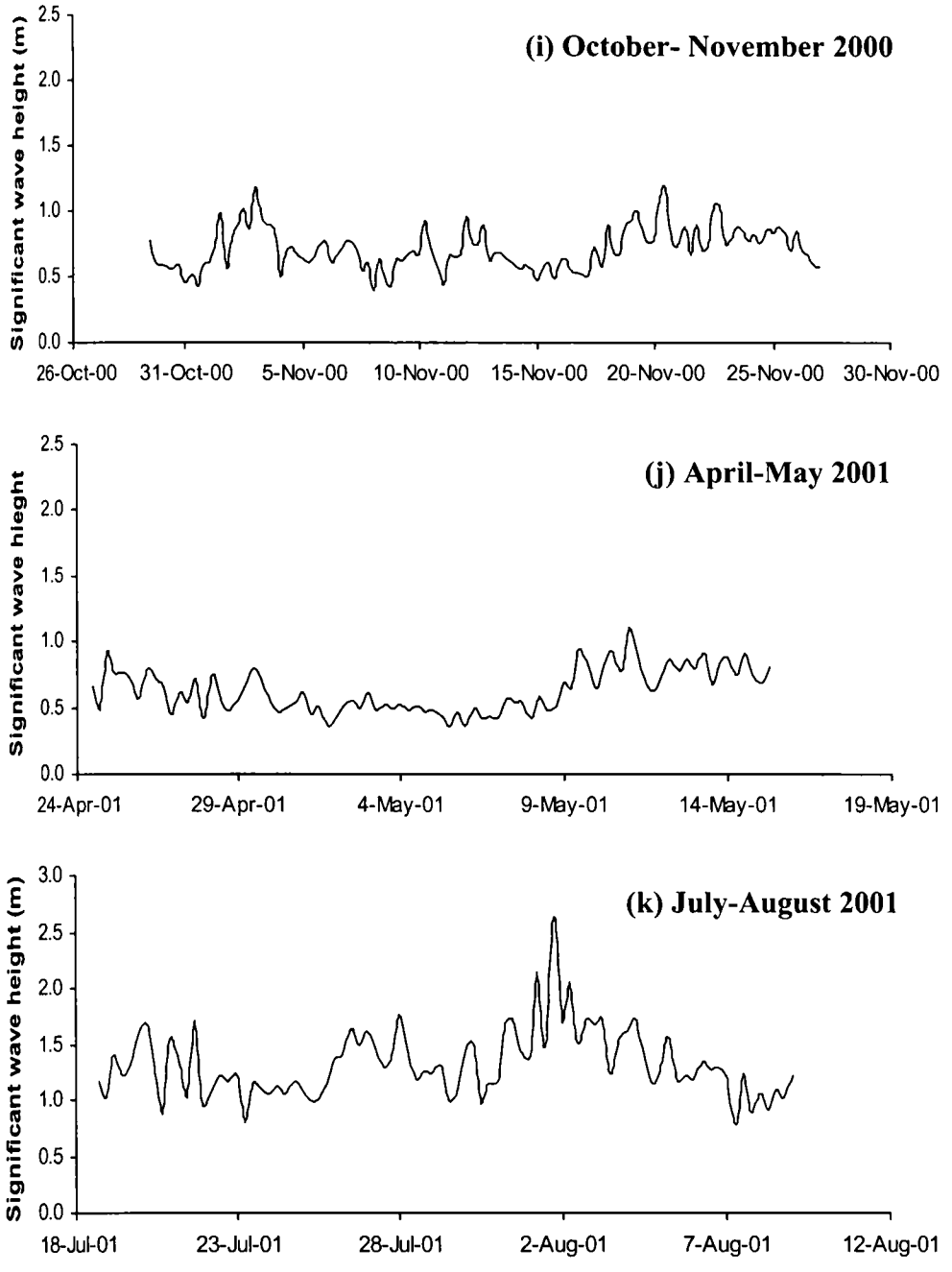

Fig. 3.2 Time series plot of significant wave heights measured during different measurement periods (contd...)

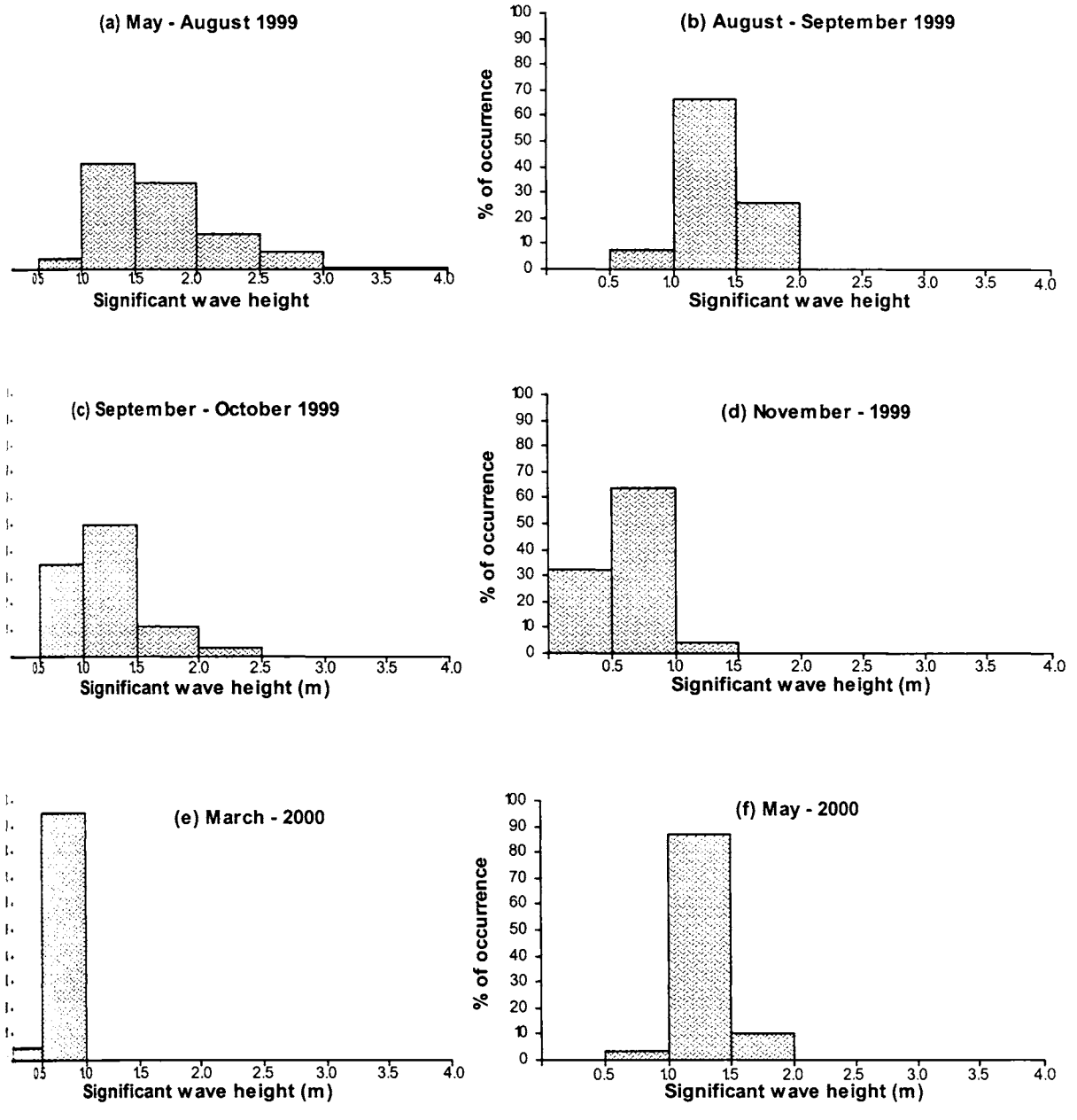

Fig. 3.3 Frequency of occurrence of H_s during different measurement periods

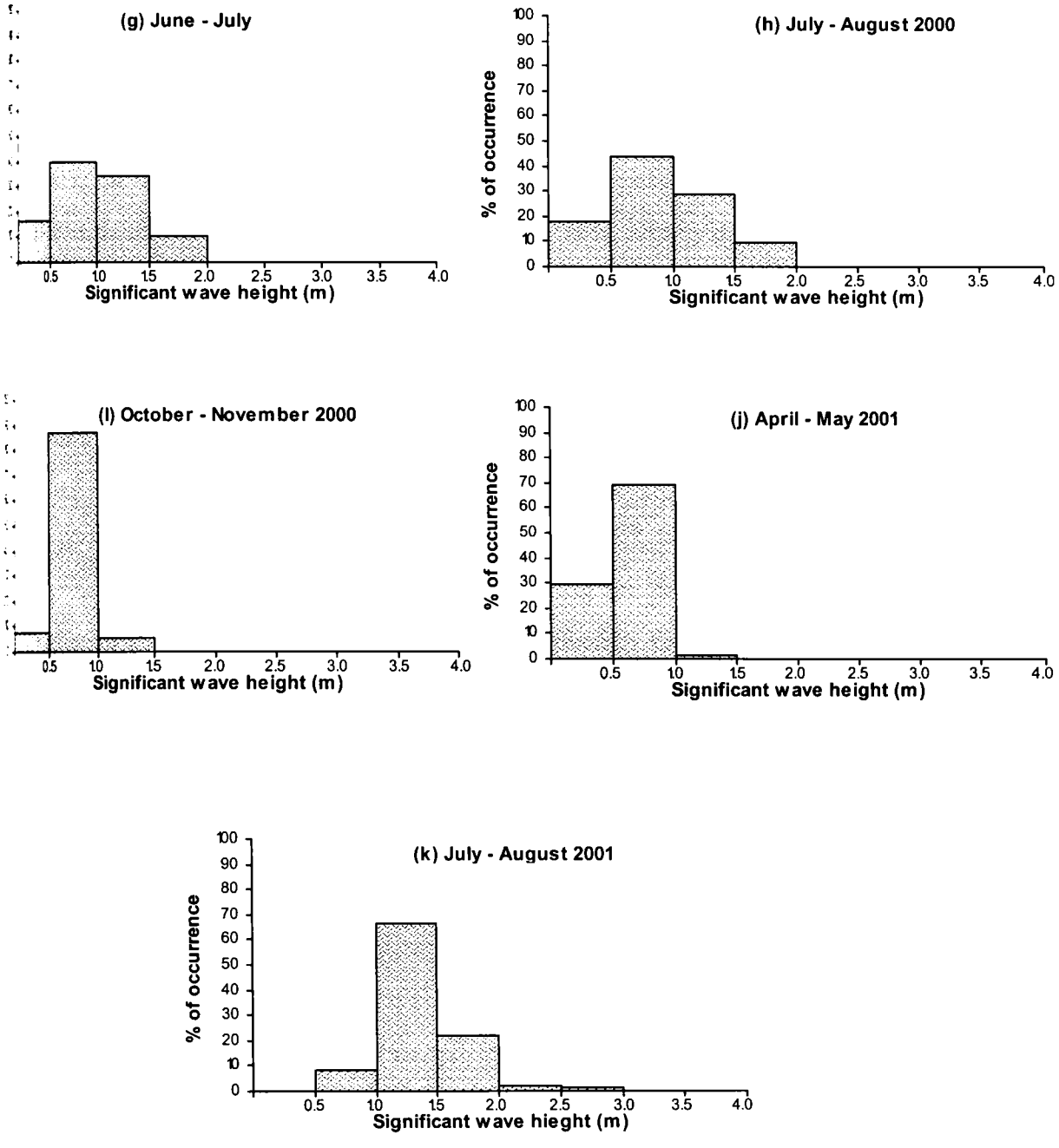

Fig. 3.3 Frequency of occurrence of H_s during different measurement periods (contd...)

3.4.2 Wave Period

The different wave period parameters generally referred to are the peak periods (T_p) which is the period corresponding to the maximum energy density in the wave spectrum, the zero-crossing period (T_z) which is the period of up-crossing/down-crossing the average zero position about which the crest and trough of the waves are calculated and the average period (T_{avg}). Out of these parameters the zero-crossing period (T_z) is the commonly used parameter to represent wave periods and hence it is used in this study to represent wave period. The characteristics of T_z are discussed here based on time series plots (Fig. 3.4 a-k) and frequency distribution analysis (Fig. 3.5 a-k).

The period May-August 1999 shows a narrow range of 5-10s with the mean T_z 7.2s (Fig. 3.4a & 3.5a). The predominant values of T_z are in the range 7-8s, which contributes to around 50% of the distribution, followed by the range 6-7s with 30% of contribution. The lowest periods are observed in the first week of June. Lower periods are seen in July associated with intense wave activity. In August-September, wave period slightly increased (Fig. 3.4b & 3.5b) and the range 7-8s contributes only 15% of the distribution while the range 8-9s contributes 66% of the distribution. During September-October, T_z further increased (Fig. 3.4c & 3.5c) and during this period 47% of distribution is in the range 7-8s and 23% is in 8-9s range. There is a further increase in the T_z during the post-monsoon month of November (Fig. 3.4d & 3.5d) with a wide range of 6.5-14s and an average value of 9.6s. The frequency distribution is characterised by the range 8-9s contributing 21%, 9-10s contributing 25% and the range 10-11s contributing 15% of the distribution.

During the month of March 2000 (Fig. 3.4e & 3.5e) T_z is reduced when compared to the post-monsoon with an average of 8.23s within the range 5.9-10.3s. The predominant values of T_z are in the ranges 8-9s and 7-8s. During May 2000 (the duration of record is only a week) the period distribution is very narrow in the range 7.0-8.7s with an average of 7.9s, typical of monsoon conditions (Fig. 3.4f & 3.5f).

56% of the distribution falls in the range 7-8s and the remaining 43% falls in the period range of 8-9s. Higher period waves occur in the first few days followed by the lower period waves.

The months of June-July and July-August 2000 also have lower periods with a narrow range of 7-9s (Fig. 3.4g-h & 3.5g-h). The second fortnight of June experienced occasional higher period waves. The percentage occurrence of the T_z observed during the two months of June-July and July-August is characteristic of monsoon conditions with the whole values packed in the range 7-9s, constituting more than 86% and 97% respectively of the distributions.

The waves that occurred during October-November 2000 (Fig. 3.4i & 3.5i) are generally of higher period, confined to the range of 8.4-12.0s with an average of 10.8s. The predominant wave periods are in the range 9-10s and 10-11s, which together constitute 74% of the distribution.

During the period April-May 2001 (Fig. 3.4j & 3.5j), the zero crossing period ranges from 6s to 15s. The higher periods, typical of pre-monsoon season are observed in the beginning and the end of the recording period. The occurrence of long period as well as short period waves result in the absence of any predominant peaks in the frequency distribution. July-August 2001 (Fig. 3.4k & 3.5k) shows the typical monsoon period distribution except for the first week of the recording period when long period waves are observed. As expected the frequency distribution for this period shows the peaks in the lower period side (8-11s).

ent

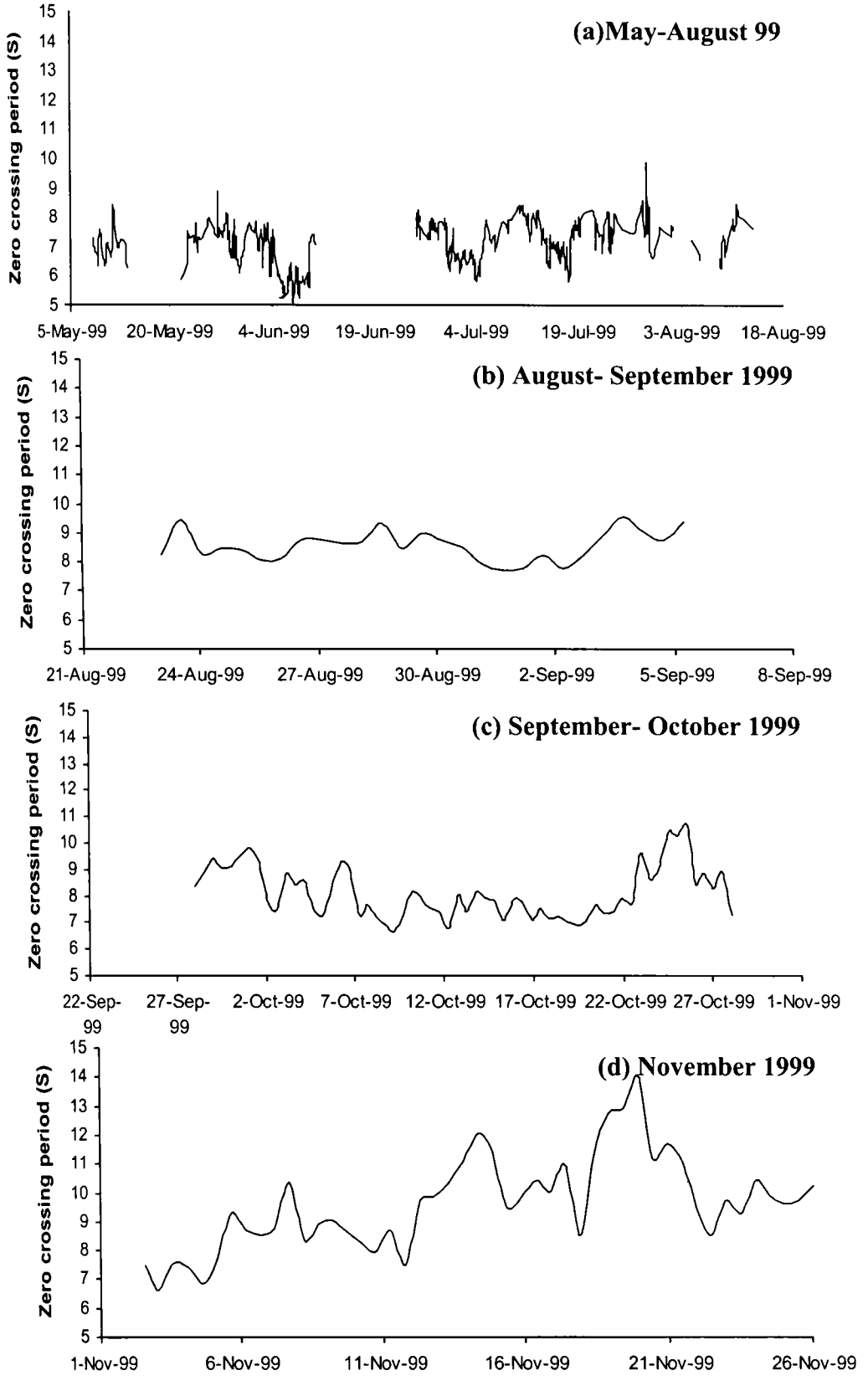

Fig. 3.4 Time series plot of zero crossing period observed during different measurement periods

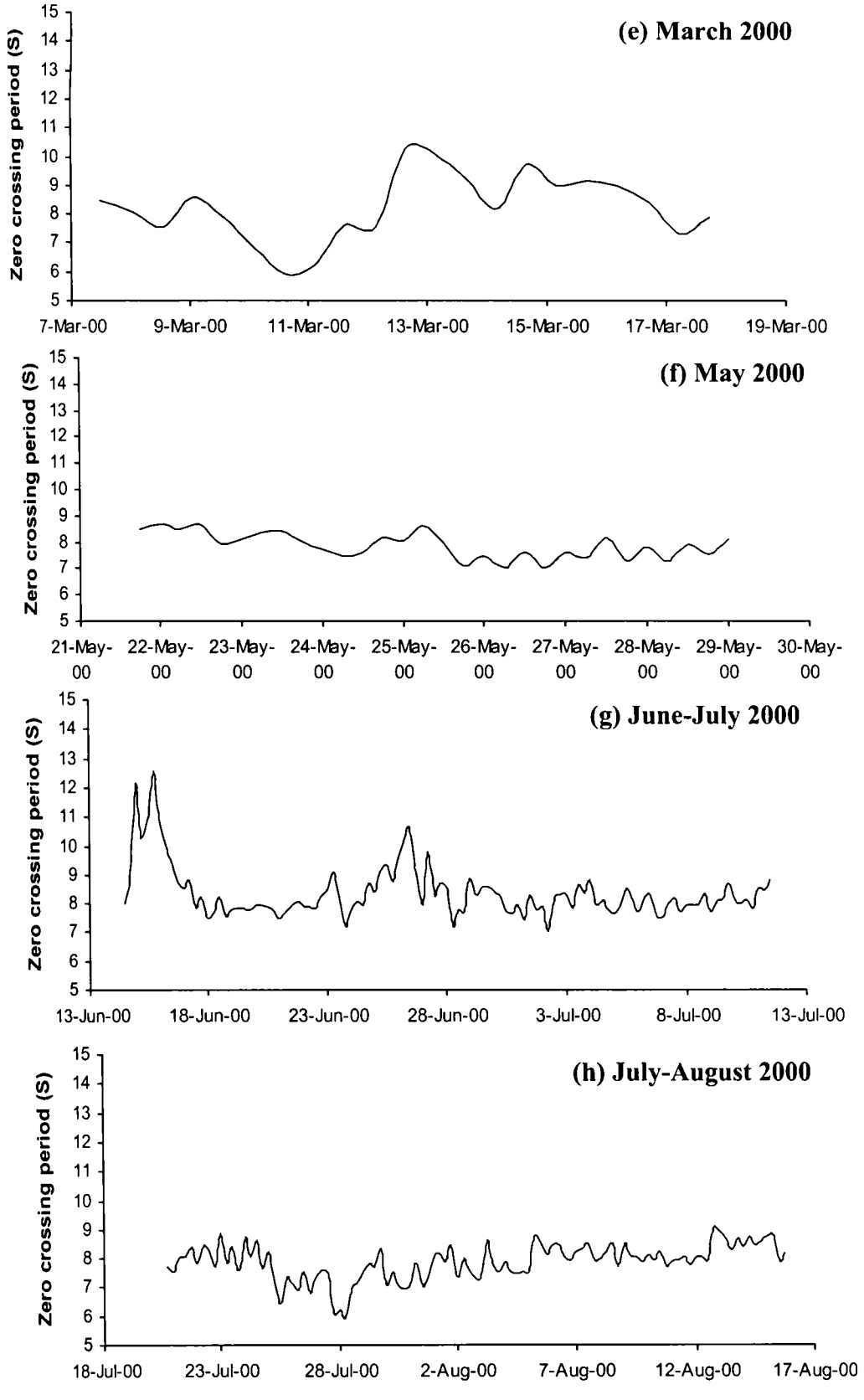

Fig. 3.4 Time series plot of zero crossing period observed during different measurement periods (contd...)

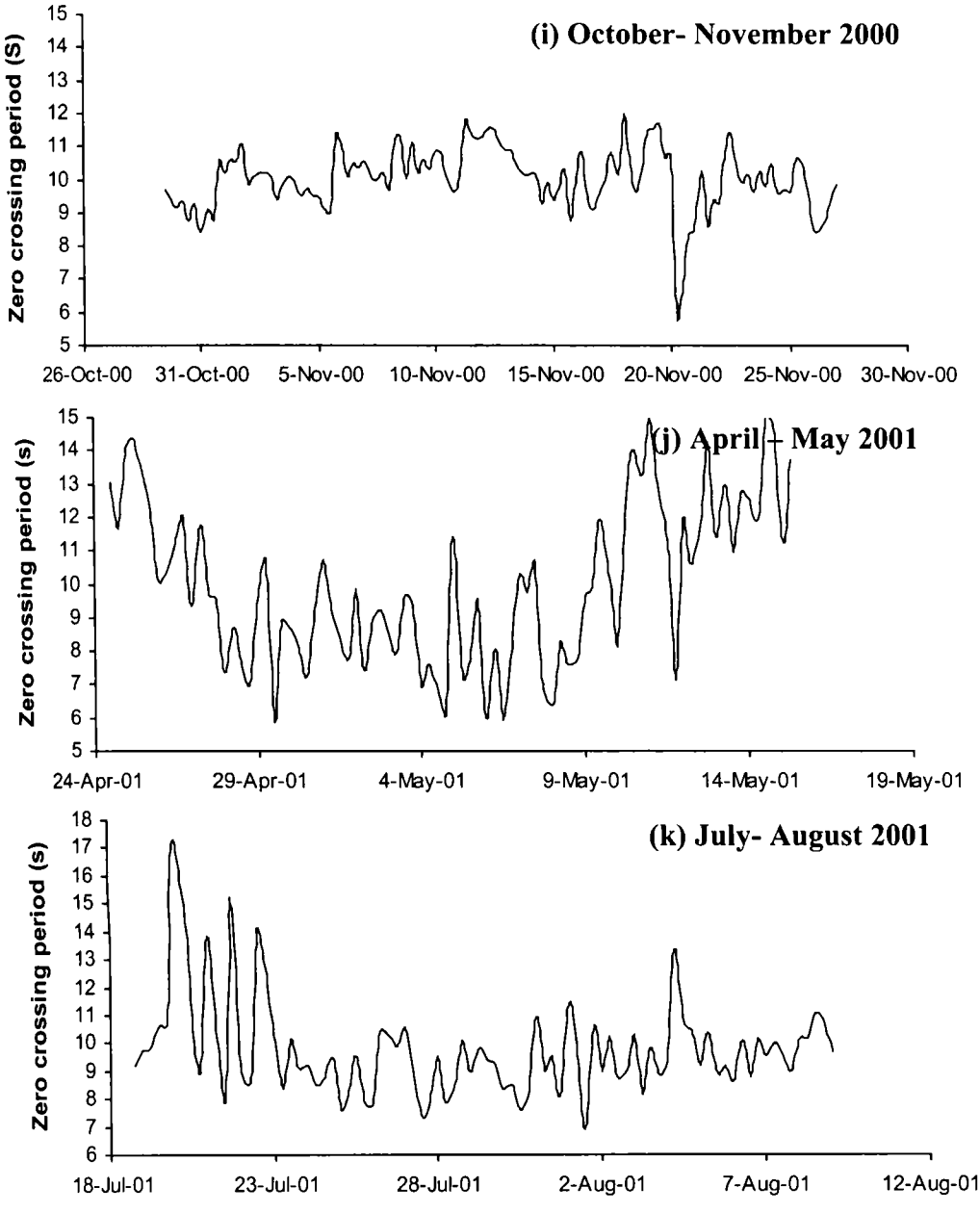

Fig. 3.4 Time series plot of zero crossing period observed during different measurement periods (contd...)

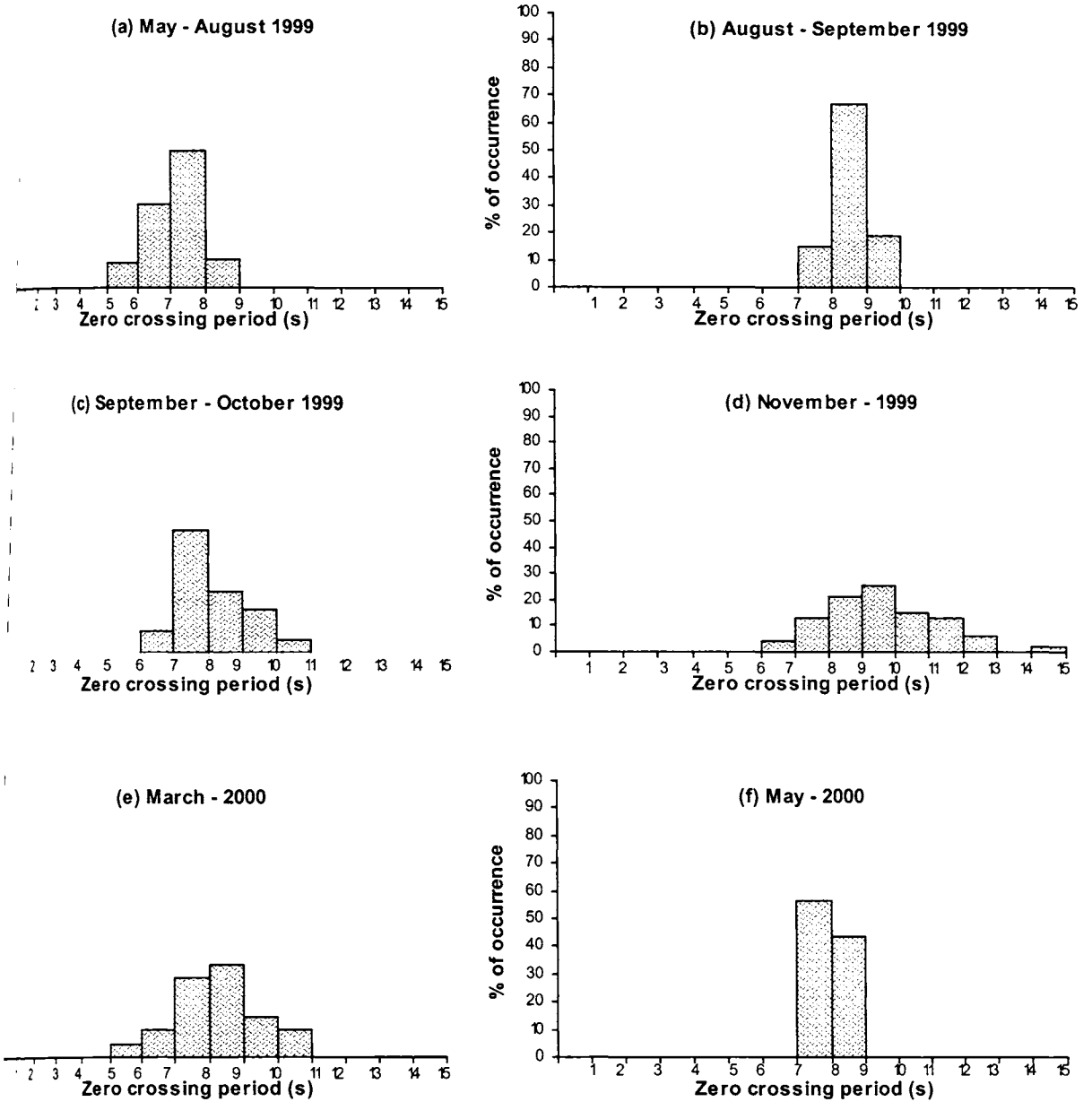

Fig. 3.5 Frequency of occurrence of T_z during different measurement periods

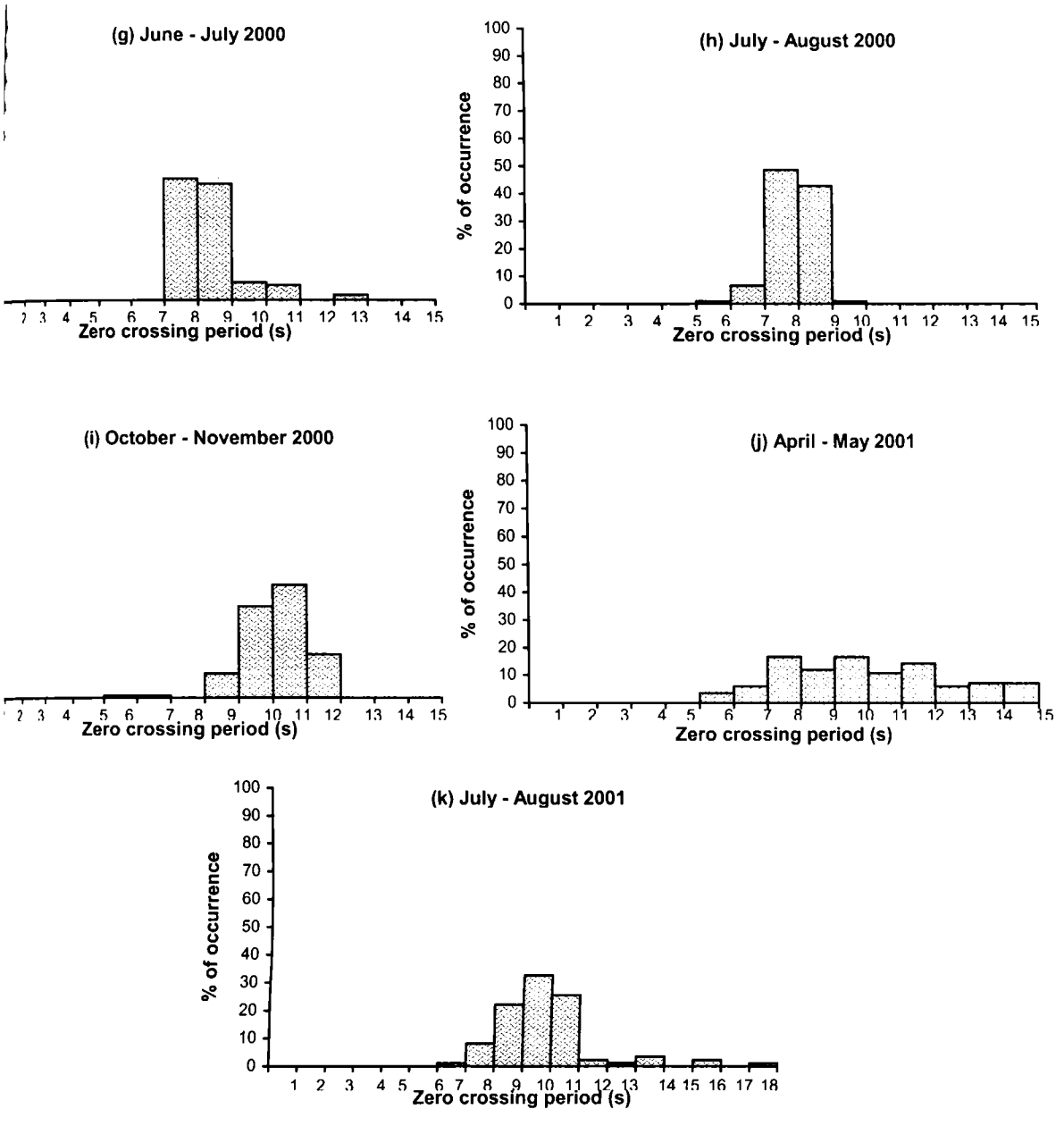

Fig. 3.5 Frequency of occurrence of T_z during different measurement periods (contd...)

3.3 Spectral Width Parameter

The spectral width is an important parameter, which shows the width of the spectrum and it ranges from 0 to 1. It indicates small width for "clean swells" and large width for "messy seas". This parameter helps to deduce whether the waves are purely swells or it is mixture of both swells and locally generated seas. The spectral width is also a good indicator of whether the beach is likely to be eroding or accreting.

The spectral width parameter, denoted by ε, is presented as time series in Fig. 3.6a-k and percentage of occurrence in Fig. 3.7 a-k. The values are in the range 0.53-0.88 with an average of 0.70. The pattern of variation is similar to that exhibited by the wave periods, whereby the variations are minimum during the monsoon months and maximum during the non-monsoon months. The first half of June, the second half of August and the second and third week of October 1999 were the times with low values of spectral width parameter.

During the period May-August 1999 (Fig. 3.6a & 3.7a) the spectral width parameter is in the range 0.6-0.83 with the majority of the values between 0.7 and 0.8. Lower values less than 0.7 occur before the onset of the monsoon and the values pick up with the onset of monsoon towards the end of May. During this period the predominant width is 0.7-0.8 which constitutes 79% of the total occurrence.

During the period August-September (Fig. 3.6b & 3.7b) the spectral width parameters are generally lower with the values crossing 0.7 only for a short period and during this period 74% of ε is in the range 0.6-0.7. In the months of September-October 1999 the range becomes wider (Fig. 3.6c & 3.7c). The predominant ranges are 0.6-0.7 which constitute 50% and 0.7-0.8 which constitute 32% of distribution. In the month of November (Fig. 3.6d & 3.7d) the spectrum becomes further wider, as indicated by the high values of ε and during this period 63% of ε is in the range 0.7-0.8.

During the month of March 2000 the spectral width values are in the range 0.65-0.85 (Fig. 3.6e & 3.7e). The predominant range is 0.7-0.8, which constitutes 81% of all the total cases during the month. In the month of May 2000 (Fig. 3.6f & 3.7f) the predominant width is 0.5-0.60, which is about 16%, and those in the range 0.6-0.7 constitute about 80% of the cases during the period. During the month of June-July (Fig. 3.6g & 3.7h) the range is 0.55-0.8; the values of spectral width are mainly in the range 0.6-0.7 which contributes more than 70% of the occurrences. July-August (Fig. 3.6h & 3.7h) also exhibits a similar pattern of the distribution of spectral width that is characteristic of monsoon. The range is mainly 0.6-0.8 with the predominant values falling in the range 0.6 - 0.7, which constitute 55% of the total cases. The occurrence of spectral width parameter in October-November 2000 (Fig. 3.6i & 3.7i) is characterised by a shift towards higher values with the predominant values occurring in the range 0.7-0.8 (63%).

During the period April-May 2001, the range of spectral width is wide, falling in the range 0.35 to 0.82 (Fig. 3.6j & 3.7j). There are two peaks in the frequency distribution, which are 0.7-0.8 and 0.6-0.7, contributing 29% and 27% respectively to the distribution. The range 0.55-0.75 contributes about two third of the distribution. The time series of the spectral width parameter observed during July-August 2001 is depicted in Fig. 3.6k and the percentage of occurrence in Fig. 3.7k. As expected, the range of spectral width has reduced with majority (about 80%) of the values confined to the range 0.4 to 0.6.

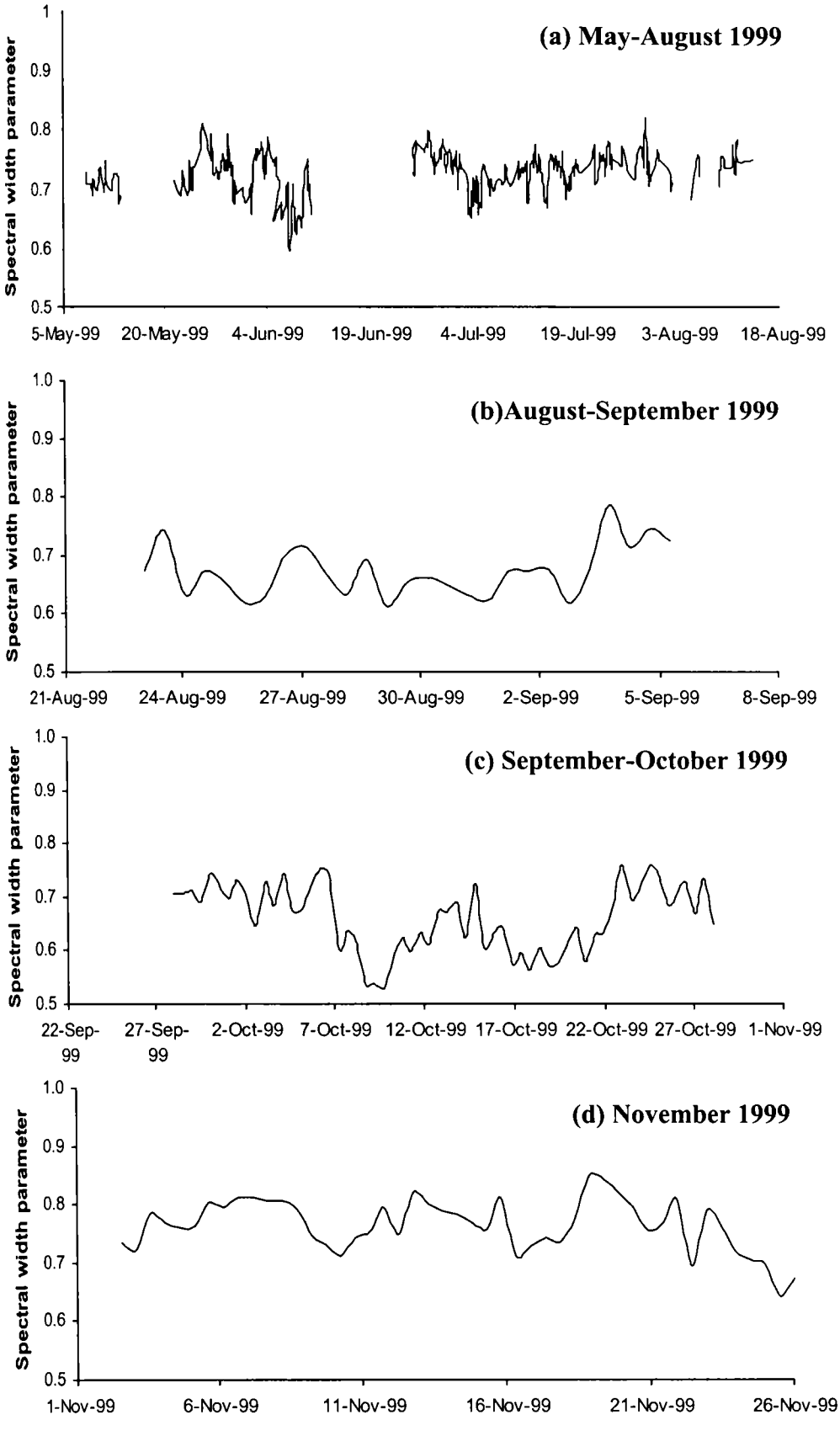

Fig. 3.6 Time series distribution of spectral width parameter during different measurement periods

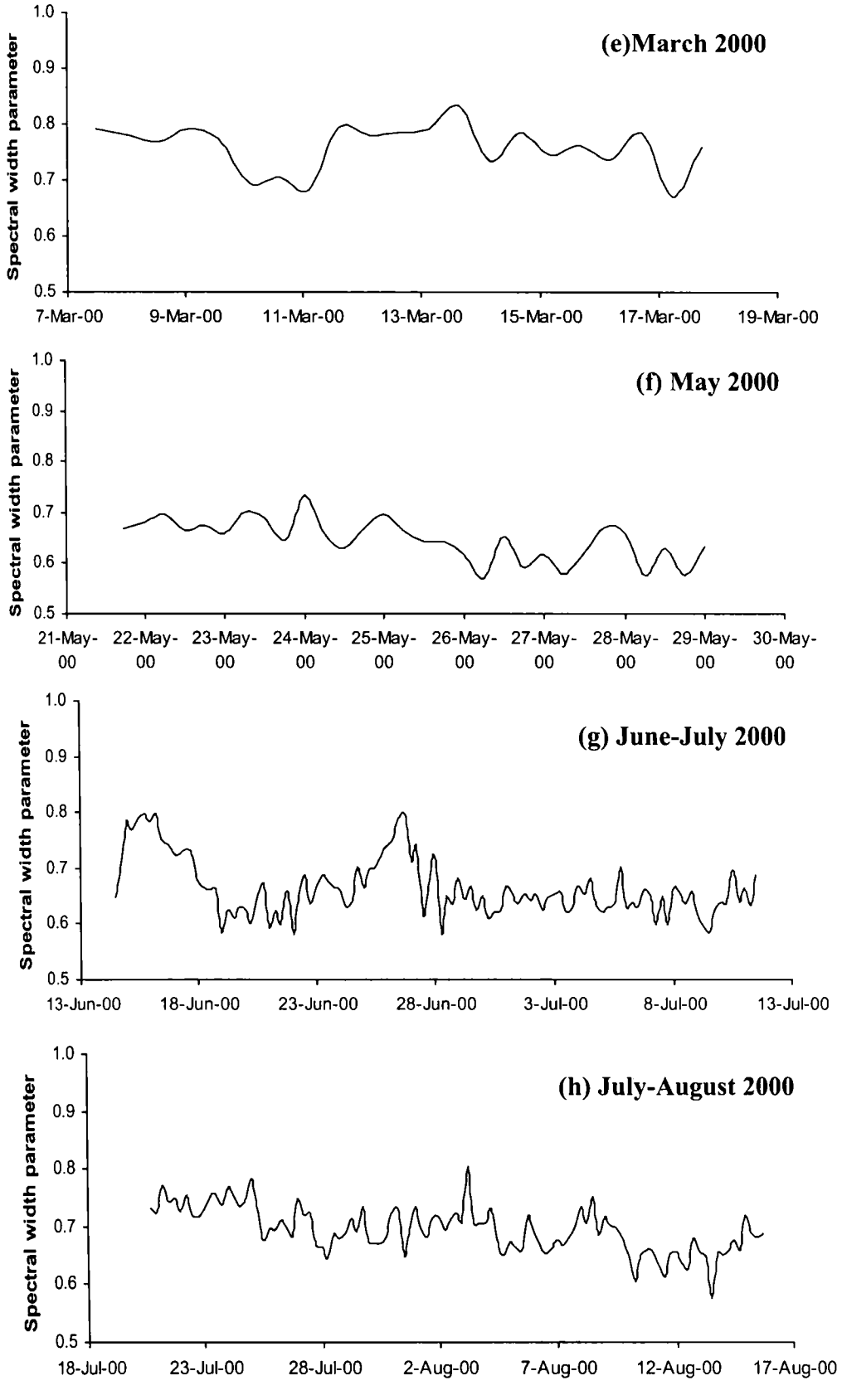

Fig. 3.6 Time series distribution of spectral width parameter during different measurement periods (contd...)

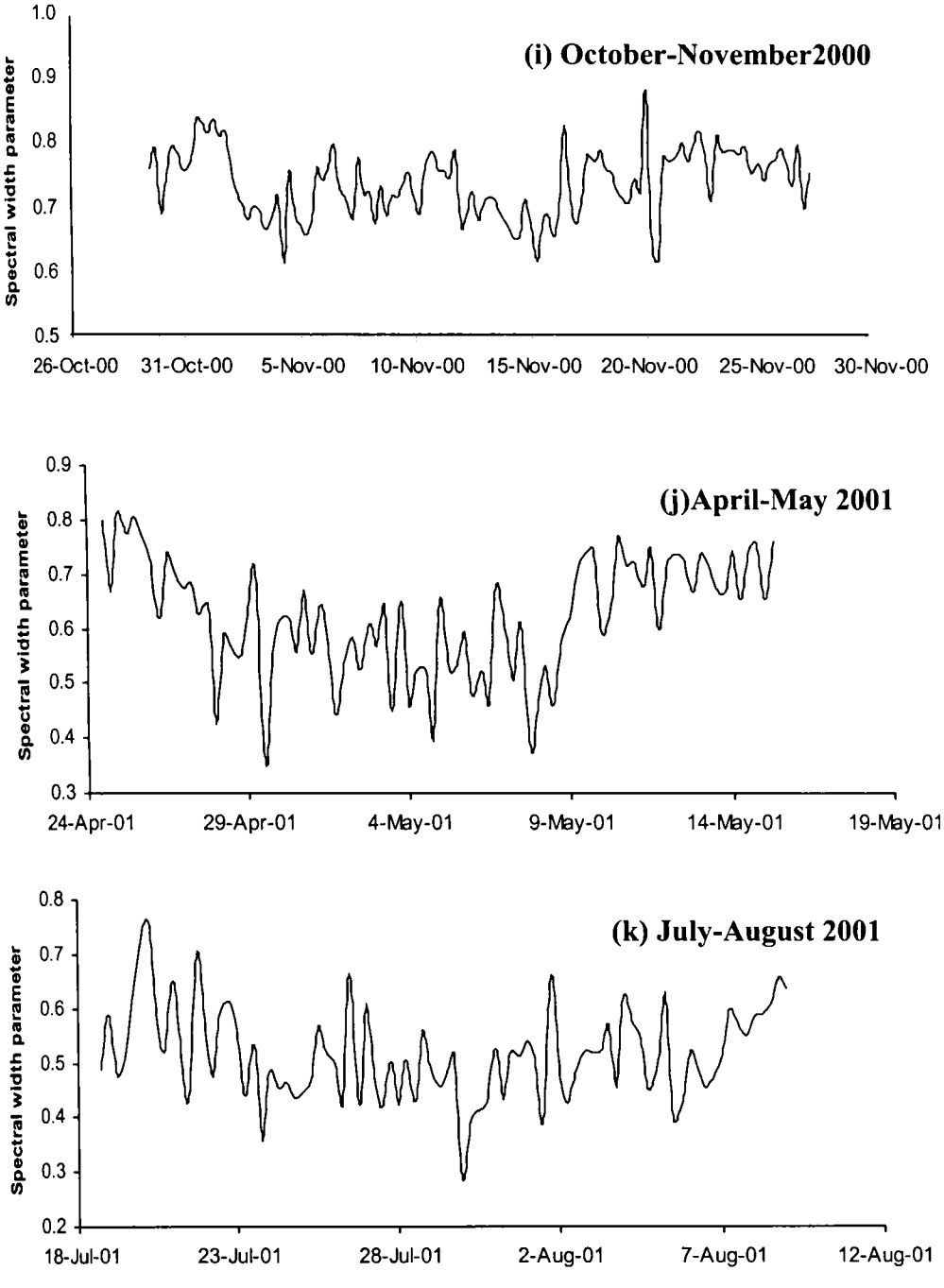

Fig. 3.6 Time series distribution of spectral width parameter during different measurement periods (contd...)

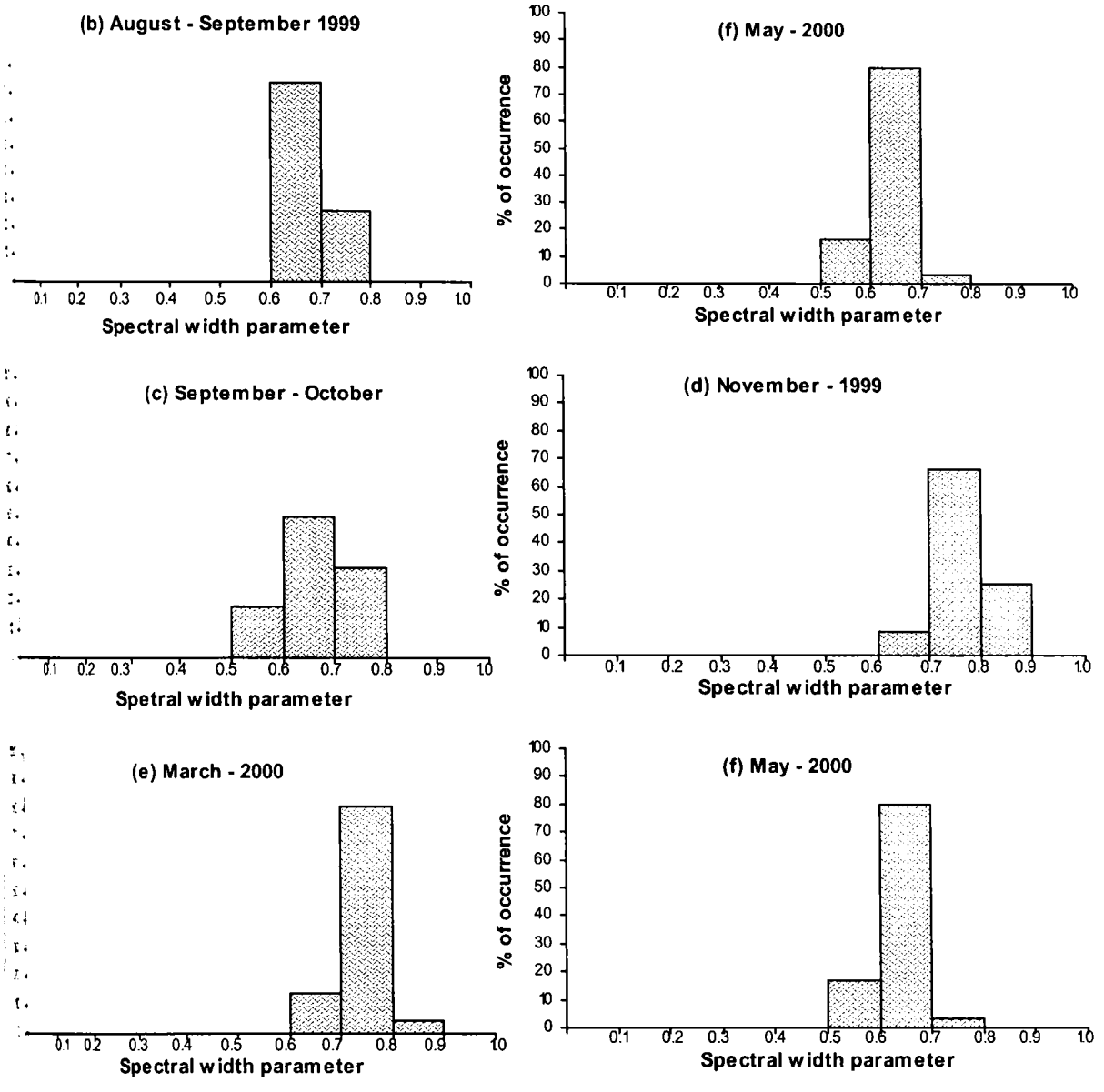

Fig. 3.7 Frequency of occurrence of spectral width parameter during different deployment perioc

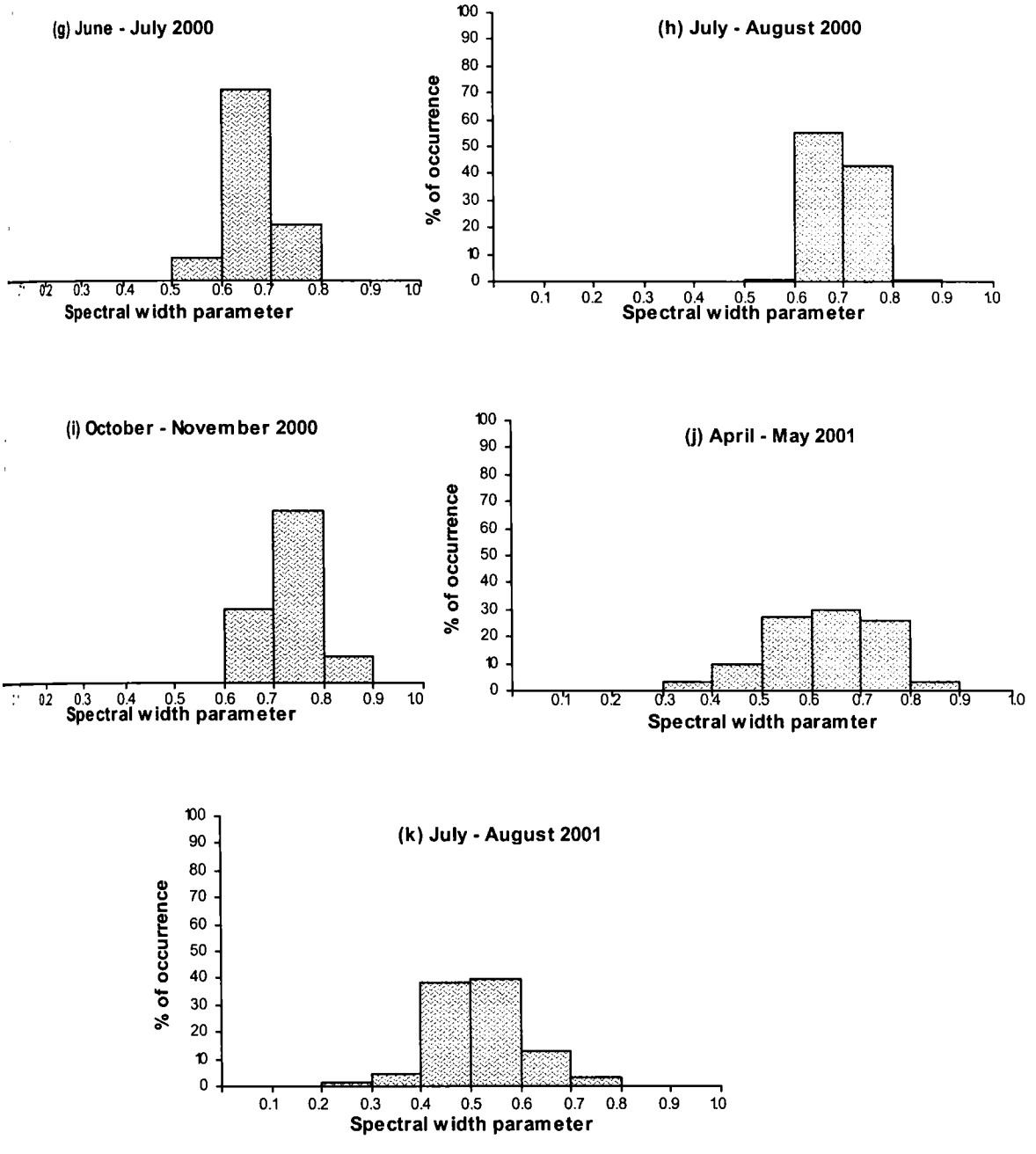

Fig. 3.7 Frequency of occurrence of spectral width parameter during different deployment periods (contd...)

3.5 JOINT DISTRIBUTION

The joint distribution of wave height (H_s) and period (T_z) for different seasons are depicted in Fig. 3.8 a-g. For the grouping of the data into seasons, the months March-April are taken as pre-monsoon, May- September as monsoon and October-November as post-monsoon. The numbers in the diagram represent occurrences per thousand. During monsoon '99 the predominant group has height 1.0-1.2m with period 8s. The post monsoon '99 data indicated three grouping for wave period, the predominant one with height 0.4-0.6m and period 9s followed by the group with height 0.5-0.7m and period 8s and height 1.2-1.4m and period 7s. During the pre-monsoon period of 2000, the predominant group is having period 7-8s and height 1.0-1.2m. The joint distribution of monsoon 2000 is indicative of the lower intensity when compared to 1999. During monsoon 2000, the dominant group is having height 0.4-0.6m with period 7s followed by the group with height 1.0-1.4m and period 7-8s . During post monsoon of 2000 period height 0.6-0.8m with period 10s dominates the distribution. In the pre-monsoon season of 2001, major groups are absent, partly arising out of scarse data. During monsoon period of 2001, height in the range 1.4-1.6m with period 9s is predominant, indicating the rough wave condition typical of monsoon period.

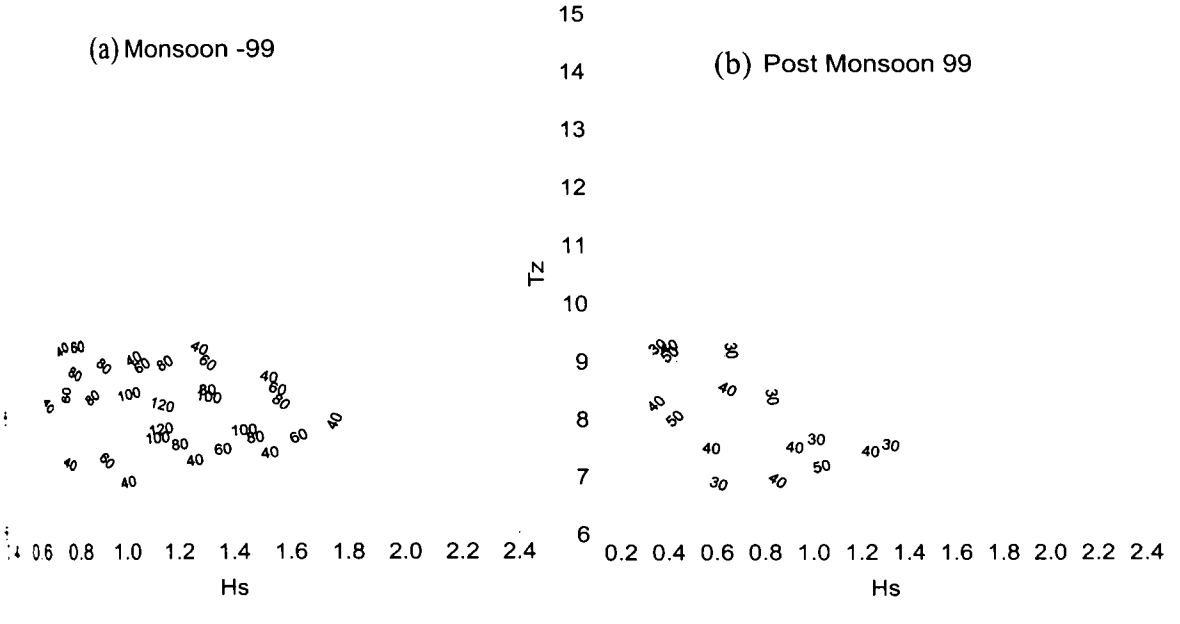

Fig. 3.8 Joint distribution of wave height and period for different seasons

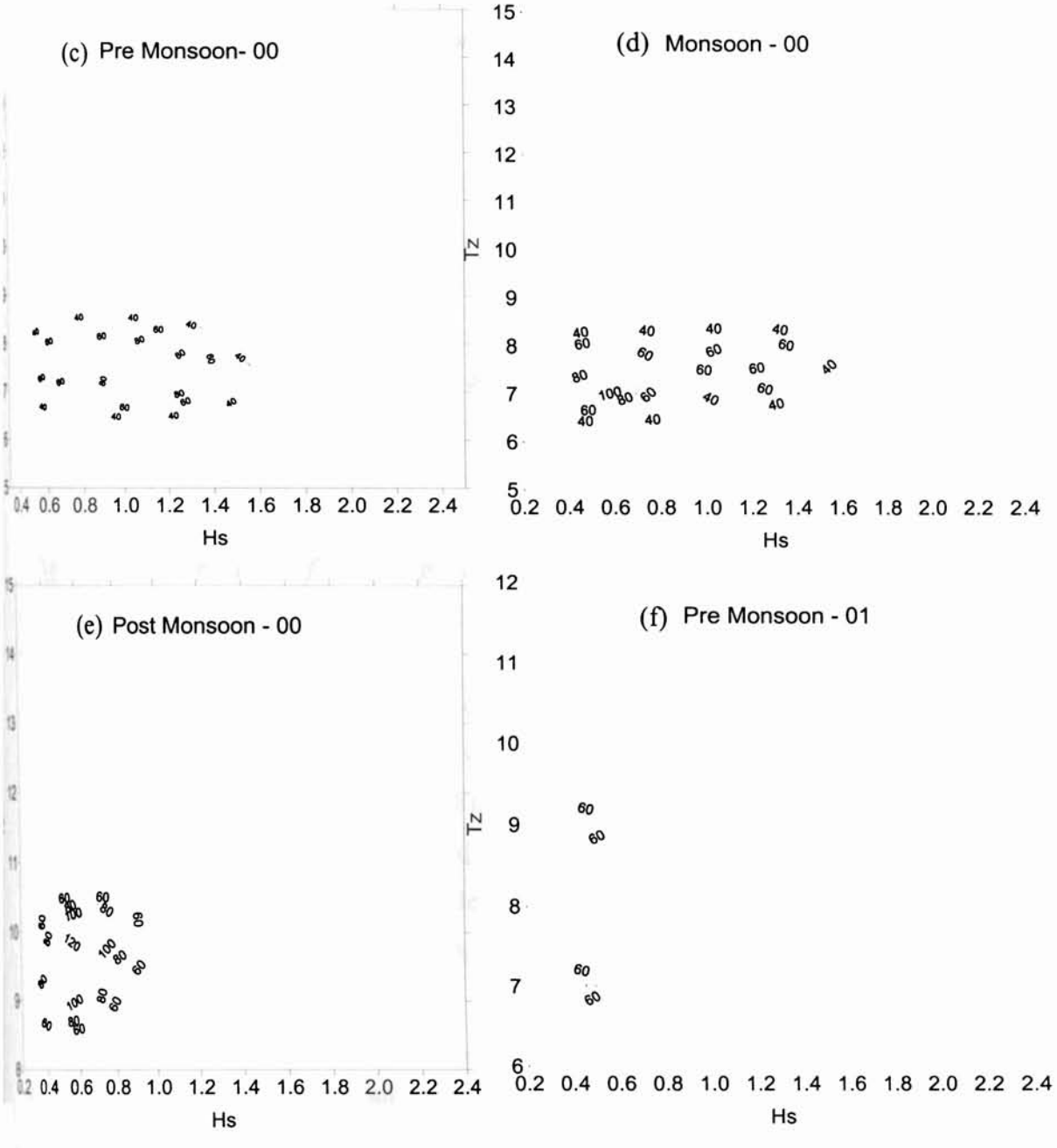

Fig. 3.8 Joint distribution of wave height and period for different seasons (contd...)

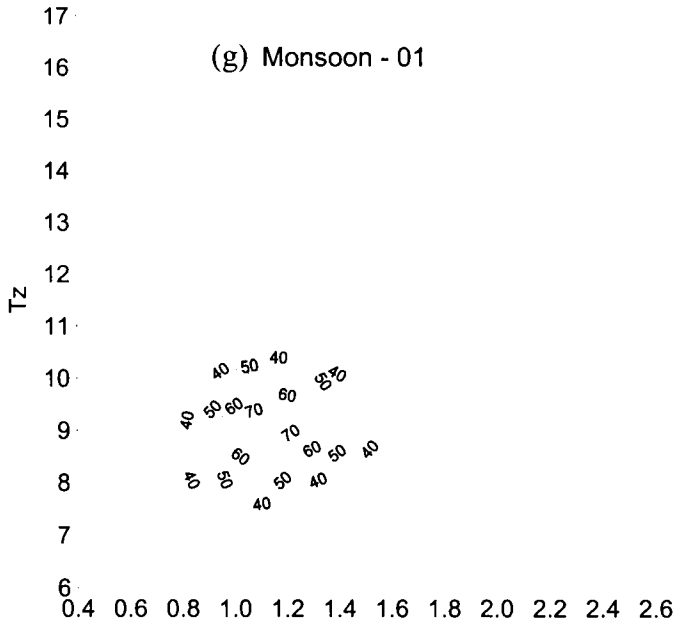

Fig 3.8 Joint distribution of wave height and period for different seasons (contd...)

3.6 DISCUSSION AND SUMMARY

The southwest coast is characterised by differing wave energy levels. The highest wave intensity is reported along the Trivandrum coast which decreases gradually towards north till Tellicherry (Baba, 1988). Kurian (1987) has categorized the coast into different wave energy zones. According to that categorization, the area of the present study belongs to medium energy level. The wave characteristics off Chavara as seen from the present study seem to support that classification.

Like other locations of the west coast, the wave climate of Chavara coast is characterized by monsoonal high and non-monsoonal low wave activity. The seasonal variations are typical of the pattern observed for other locations of the southwest coast of India (Thomas, 1988; Hameed, 1988; Kurian, 1988). The wave characteristics during the peak monsoon period (June, July and August) are characterised by relatively higher wave heights and shorter wave periods, exhibiting minimum variation in these parameters. Intermittent breaks in intensity of waves during monsoon for periods extending for 10 to 15 days are observed in all the three years, which is in tune with the normal characteristic of the monsoonal climate. Wave

characteristics during the pre-monsoon and post-monsoon seasons are characterized by low wave height (<1m) and a wide range in periods (7-15s).

Wind is the driving force for the generation of waves. The wave condition during the peak monsoon period is dominated by the 'sea' waves generated in the Arabian Sea. However, a comparison of the wind and wave data doesn't indicate an increase in the wind speed commensurate with the wave intensity. Even during the peak monsoonal wave activity coupled with the onset of monsoon in May 1999, the wind speed was a maximum of 8m/s only, while the wave height recorded the all time highest value of 3.8m. It is possible that the wind data used being a shorebased measurement may not represent the generating conditions in the offshore, the intensity of which could be much higher. During the non-monsoon months (November '99, May'00, November '01 and April'01) the wind speed remained low (<4m/s), and the wave heights also exhibited lower values, except in the month of November'00, when wind speed as high as 9m/s was recorded with corresponding increase in the wave heights. In November'00, a H_s up to 1.2m was recorded in the middle of November against the normal value of around 0.5m, with a drop in wave period.

The wave periods in general, and particularly during the peak monsoon months, are smaller and the range is less. This could be attributed to the proximity of the coast to the wave generating zones in the Arabian Sea. The wide scatter observed in wave periods during the pre- and post-monsoon seasons is indicative of the presence of sea and swells during that period. The swells as seen from their directions (Thomas, 1988; Hameed, 1988; Kurian, 1988) appear to have its origin in the southern Indian Ocean. Short period waves could be due to the sea waves generated locally by persisting northwest winds.

During more than two years with three monsoon periods covered under the study, though the annual cyclic pattern of changes were same, inter-annual changes were significant. Thus, in 1999, the peak monsoonal characteristics were evident from middle of May, and persisted through the months of June, July and August. Monsoonal breaks as indicated by the wave activity were recorded during the last

week of June, first week of July and the second half of September. During 2000, as indicated by wave height data, the monsoonal effect on wave climate was less pronounced. Very seldom, the significant wave height exceeded the height of 1.5m, the average height for the 1999 peak monsoon period. The wave intensity in the monsoon of 2001 was higher than 2000 but lesser than 1999.

CHAPTER 4

CURRENTS

4. CURRENTS

4.1 INTRODUCTION

Though waves are the most important hydrodynamic force in the coastal zone, currents also are also equally important. While wave orbital motions are strong enough to cause resuspension of sediments in shallow waters the movements are oscillatory in nature. Currents, though relatively weak, are translatory in nature and hence cause transport of resuspended sediments, in addition to other forms of transport. Considering its importance in sediment transport and hence sediment budgeting, an exhaustive set of current data covering different months and periods were collected and the characteristics of currents studied in this chapter. As detailed in Chapter 2, currents were measured both at nearshore and offshore sites. While an S4 current meter was used for measurement at the nearshore site, two FSI current meters were used at the offshore site for measurement at two levels. In addition to these one ADP was installed for one day each in two seasons and the data used for calibration of models.

4.2 LITERATURE REVIEW

Very few direct measurements of currents have been reported in the literature for the Indian coast, particularly for the southwest coast of India. Thus the currents have been mainly inferred from computations using observed data on physical and chemical properties of seawater (eg. Shetye et al., 1990 and 1991; Antony, 1990; Suryanarayana and Rao, 1992; Rao and Murthy, 1992). The available measured data were either very short term spanning for a few days (Sanil Kumar et al., 1989; Sarma and Gangadhara Rao, 1986; Rama Raju et al., 1986; Swamy and Suryanarayana, 1992; Fernandez et al., 1993) or seasonal, occasionally ranging up to a few months (John et al., 1979; Narasimha Rao et al., 1989; Narasimha Rao and Prabhakara Rao, 1989). No work utilising recorded data is seen in the literature for the SW coast of India.

The available literature shows that the Indian Ocean is characterised by seasonal changes of its surface circulation due to two opposite atmospheric regimes, namely

southwest and northeast monsoons. According to Basu et al. (2000) the seasonal variation in the Indian Ocean is greater than that in any other ocean.

A schematic diagram of the north Indian Ocean circulation pattern during northeast (November–March) and southwest (June–September) monsoon is given by Shankar and Shetye (1997) and it is reproduced here as Fig. 4.1. A remarkable feature of the coastal circulation pattern is the formation of an anticyclonic eddy east of Lakshadweep Islands during the northeast monsoon and a cyclonic eddy during the southwest monsoon. The mechanism for the eddy formation is given by Shankar and Shetye (1997) based on their interpretation of previous studies of Nerem et al. (1994) that the sea level starts rising at the southwest coast of India during December, when East India Coastal Current (EICC) is equatorward. The EICC turns around the southern tip of Sri Lanka (Cutler and Swallow, 1984) and joins the poleward current along the west- coast of India (Shetye et al., 1991). During June, the sea level drops at the southwest coast of India, when the current at the western Indian coast, the West India Coastal Current (WICC) is equatorward. Shankar and Shetye (1997) conclude that the formation of the eddy off southwest India during the northeast is one manifestation of an annual cycle of events that are linked not only to the coastal currents around India, but also to the circulation in the southern Arabian Sea as a whole.

Shetye (1998) observed that the West India Coastal Current (WICC) flows northward during November- February and southward during April- September. He attributed the annual cycle of WICC and that of the Lakshadweep high/low to a set of circumstances that are special to North Indian Ocean. Shetye et al. (1998) found that the currents in the North Indian Ocean basin are primarily due to free and forced long waves of three kinds: (1) Equatorial Rossby waves, (2) Equatorial Kelvin waves and (3) Coastal Kelvin waves. They concluded that the surface circulation off Arabian sea is typical of a wind driven system with similar patterns of longshore current and wind stress. They also found that the circulation off the west coast of India is consistent with the dynamics of wind-driven eastern boundary currents only during the southwest monsoon.

Other studies (McCreary et al., 1993; Bruce et al., 1994) also have shown the formation of a cyclonic eddy off the southwest coast of India during northeast monsoon. Recent studies of Bruce et al. (1998) suggests that the anticyclonic circulating feature that forms off the SW coast of India during northeast monsoon is comprised of multiple eddies.

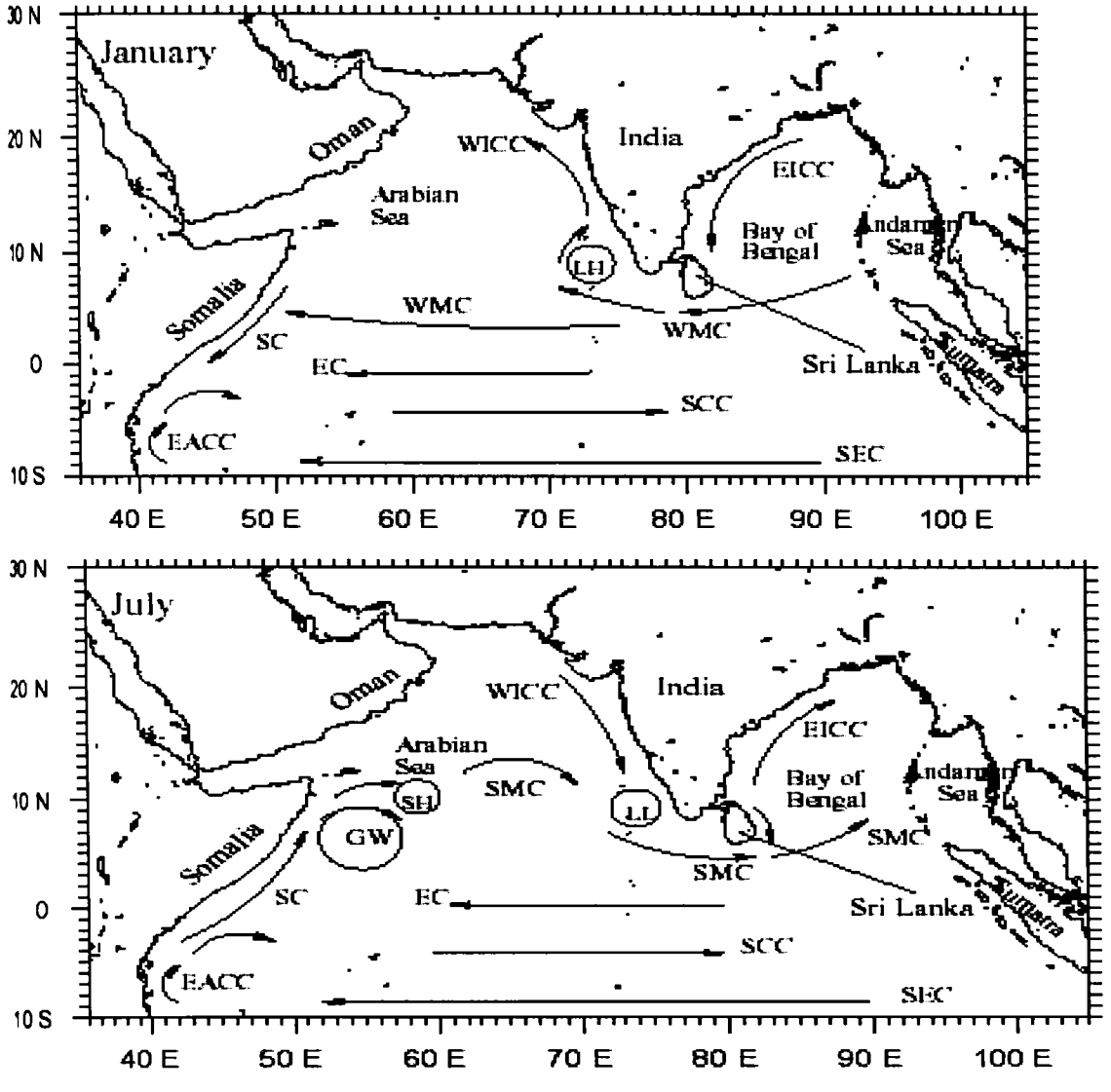

Fig. 4.1 Schematic representation of the circulation in the Indian Ocean during January (winter monsoon) and July (summer monsoon). The abbreviations are as follows. SC, Somali Current; EC, Equatorial Current; SMC, Summer Monsoon Current; WMC, Winter Monsoon Current; EICC, East India Coastal Current; WICC, West India Coastal Current; SCC, South Equatorial Counter Current; EACC, East African Coastal Current; SEC, South Equatorial Current; LH, Lakshadweep high; LL, Lakshadweep low; GW, Great Whirl; and SH, Socotra high (after Shankar and Shetye, 1997)

Shetye et al. (1990) investigated the hydrography and circulation off west coast of India during the southwest monsoon season. They concluded that the circulation off the west coast of India during southwest monsoon season, though weak, is dynamically similar to the wind-driven eastern boundary currents found elsewhere in the ocean.

Shetye et al. (1991) carried out investigation on the coastal current off western India during the northeast monsoon using the hydrographic data obtained from O.R.V. *Sagar Kanya* and described the pole ward coastal current along the west coast of India. They found that longshore pressure gradient overwhelms the winds during the northeast monsoon, whereas during the southwest monsoon the winds dominate.

Shenoi and Antony (1991) collected current data using moored array of current meters from the offshore off Goa. They measured currents for a period of three months and found that the mean flow was towards south during May and March and it was towards north in November. They found that the inertial and semidiurnal frequency motions are the major contributor to the current structure. The inertial currents were concentrated near the surface with a rapid decay towards the bottom. Their analysis indicates that the diurnal and semidiurnal motions are mainly due to baroclinic internal tides rather than due to barotropic surface tides.

Prasada Rao et al. (1996) studied the premonsoon current structure in the shelf water off Cochin using current data collected from the depths of 10,20,40,60 and 80m. They observed a southerly current in near-surface and north-westerly currents in sub-surface. Seasonal fluctuation in the coastal currents off Mangalore was observed by Sahu et al. (1991). They observed a maximum current of 60cm/s during November and a minimum current of 5-9 cm/s during February.

Shankar et al. (2002) described in detail the monsoon currents in the north Indian Ocean using the data from ship drifts, winds and Ekman drifts and geostrophic currents derived from altimetry and hydrography and also by using numerical models. They found that the monsoon currents are seasonally reversing. The Summer

Monsoon Current (SMC) flows eastward during the summer monsoon (May-September) and the Winter Monsoon Current flows westward during the winter monsoon (November-February).

Shetye et al. (1998) observed that it is a consequence of the remote forced Kelvin wave which in turn radiates Rossby waves that cause the formation of a weak, but nonetheless upwelling favourable coastal currents off southwest coast of India, this current being integral to the dynamics of the high.

The flow field off southwest India at 8° N during the southwest monsoon period was measured by Stramma et al. (1996) using ADCP and CTD. They found that the upper ocean between 75°E and 76° 52' E near the south Indian shelf was governed by a northward flow with a subsurface velocity maximum of 25 cm/s at about 100m depth.

Thus the available literature gives a reasonably good picture about the general circulation of the Northern Indian Ocean and the Arabian Sea which is mostly based on the hydrographic data. One notable feature of the currents in the Arabian Sea as understood from the recent studies is the occurrence of an anticyclonic eddy east of Lakshadweep islands during the northeast monsoon and a cyclonic eddy during the southwest monsoon. Lack of literature based on measured current is evident, particularly for the southwest coast of India.

4.3 CURRENTS MEASURED UNDER THE PRESENT INVESTIGATION

4.3.1 Nearshore Site

The time series data for nearshore site are shown in Fig. 4.2 to Fig. 4.8 and the progressive vector plots are shown in Fig. 4.9a-g. An analysis of the velocity into cross-shore (u) and alongshore components (v) of each data is presented along with speed and direction. In October 1999, current speed was generally in the range of 5-10 cm/s, but occasionally high values were observed, and a value as high as 19.30 cm/s was recorded on 19th October (Fig. 4.2). Current speed oscillated between 0

and 360° due to tidal influence. Comparison of alongshore and cross-shore components shows that alongshore components were stronger than cross-shore components. The data indicated a predominant offshore flow in the cross-shore direction. The longshore component changed direction at frequent intervals, with a high frequency of southerly component. The progressive vector plot (Fig. 4.9a) shows a predominant offshore movement with a slight southerly alongshore movement. This is in contrast to the time series where the alongshore component were stronger when compared to the cross-shore. During November 1999 (Fig. 4.3), the currents were weaker except in the first week when speed up to 22 cm/s was recorded. Current direction oscillated from 0 to 360°. During November also the alongshore components were stronger than cross-shore components. The data indicated a strong onshore and southerly current during the first week of the month. Onshore and southerly directions dominated during the rest of the month with reduced speed. The progressive vector plot (Fig. 4.9b) shows more or less same pattern with a net south-easterly movement of water.

In March-April 2000 (Fig. 4.4), current speeds in the range of 5-10 cm/s were common in the beginning with speeds as high as 21 cm/s. After third week of March current speeds were generally less than 5 cm/s but occasionally increased up to 17 cm/s. Cross-shore components were very weak than alongshore components as seen earlier. Alongshore components were predominantly southerly in the first 10 days and thereafter the dominance reduced with occasional northerly currents. The progressive vector plot (Fig. 4.9c) shows intense southerly movement with a weak offshore component.

In May-June 2000 (Fig. 4.5), current speeds were very low and most of the days it was less than 10 cm/s except for a shore period, 7-10th June. During this short period the current speed increased to 58 cm/s and then decreased to values less than 10 cm/s. The direction of current for these 4 days is purely southerly. One notable feature is that the tidal oscillations are masked by this very strong current. As observed during the previous months alongshore components were stronger than cross- shore components. The cross-shore components though weak for major part of the month,

were persistently offshore throughout. The alongshore component was predominantly southerly with very strong speeds during 7-10th June. The progressive vector plot (Fig. 4.9d) for the period confirms the above results. The domination of southerly movement is very much evident.

Current speeds were higher than May-June period during July-August 2000 (Fig. 4.6). The speeds were commonly in the range 5-10 cm/s except for the beginning and end of the recording period. Current speed up to 24 cm/s was recorded during the second week of August. An important feature observed was that, both cross-shore and alongshore components are more or less equal in magnitude during this period. In general offshore flows dominated the observation period. Likewise, southerly currents have dominance over northerly flows, although northerly flows were strong occasionally with speeds exceeding 15 cm/s. The dominance of southerly and offshore flows is reflected in the progressive vector plot (Fig. 4.9e) with net movement of water in the SW direction. During October-November 2000 (Fig. 4.7), the current speeds were less, similar to those recorded in November 1999, with current speeds generally around 5cm/s. Maximum speeds recorded are 19.6 cm/s on 4th November and 19.1 cm/s on 20th November. Comparison of alongshore and cross-shore components shows that, alongshore components are stronger than cross-shore components. The velocity of cross-shore components remains to be less than 5 cm/s throughout the period but persistently onshore. The alongshore components were stronger and predominantly southerly. The flow pattern results in a net transport in the SE direction as seen in the progressive vector plot (Fig. 4.7f).

In April-May 2001, currents were weak, typical of pre-monsoon period, with speeds reaching 10cm/s only a few times (Fig. 4.8). As seen in most of the cases, the alongshore components are stronger than cross-shore. The cross-shore components were predominantly onshore and the alongshore components southerly. The progressive vector plot (Fig. 4.9g) shows a net movement in the SSE direction indicating the dominance of southerly transport over onshore transport.

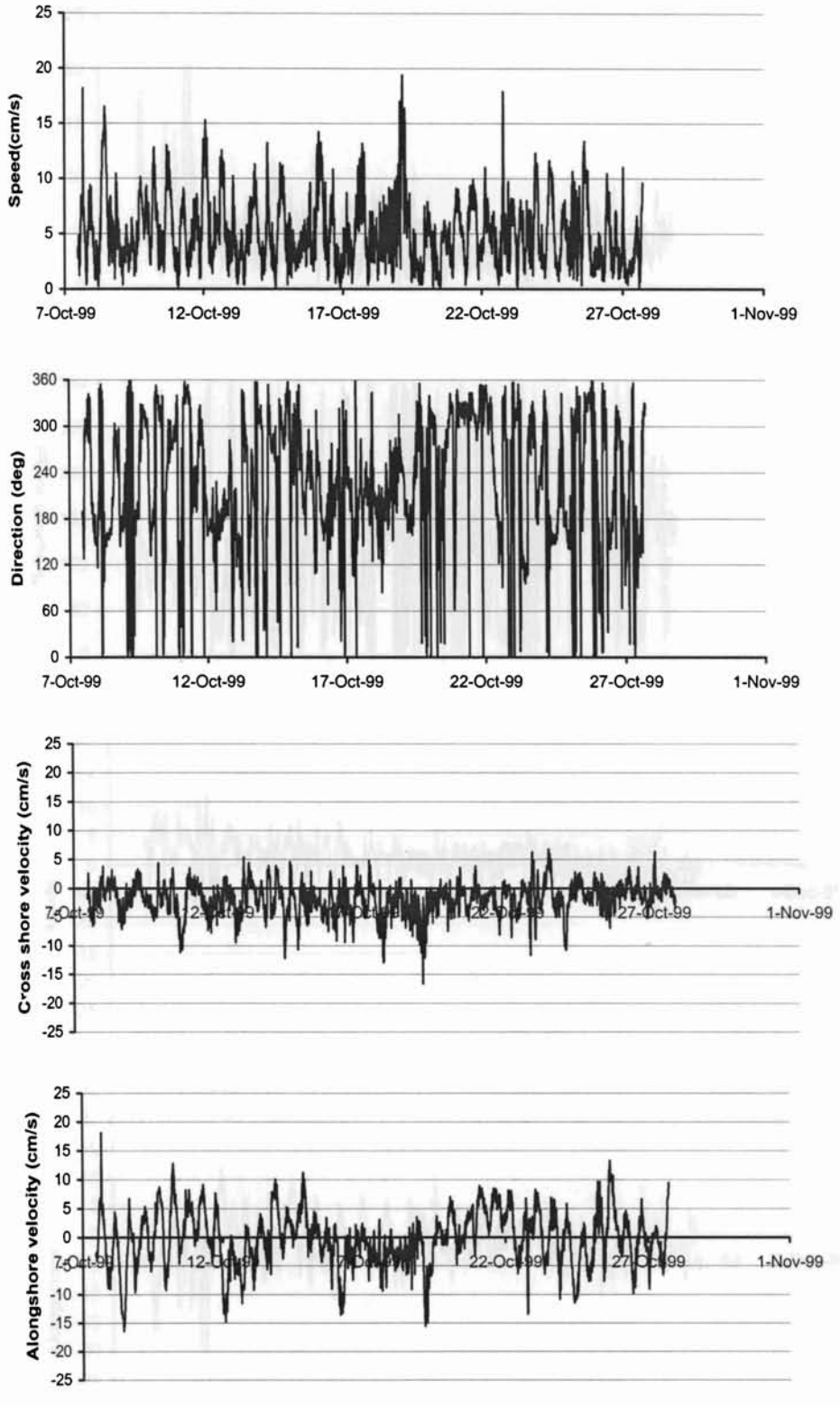

Fig. 4.2 Time series plot of S4 current meter measured mean burst current speed, direction, cross-shore (U cm/s) and alongshore (V cm/s) velocities during the deployment period 07 October – 27 October 1999 at the Nearshore site.

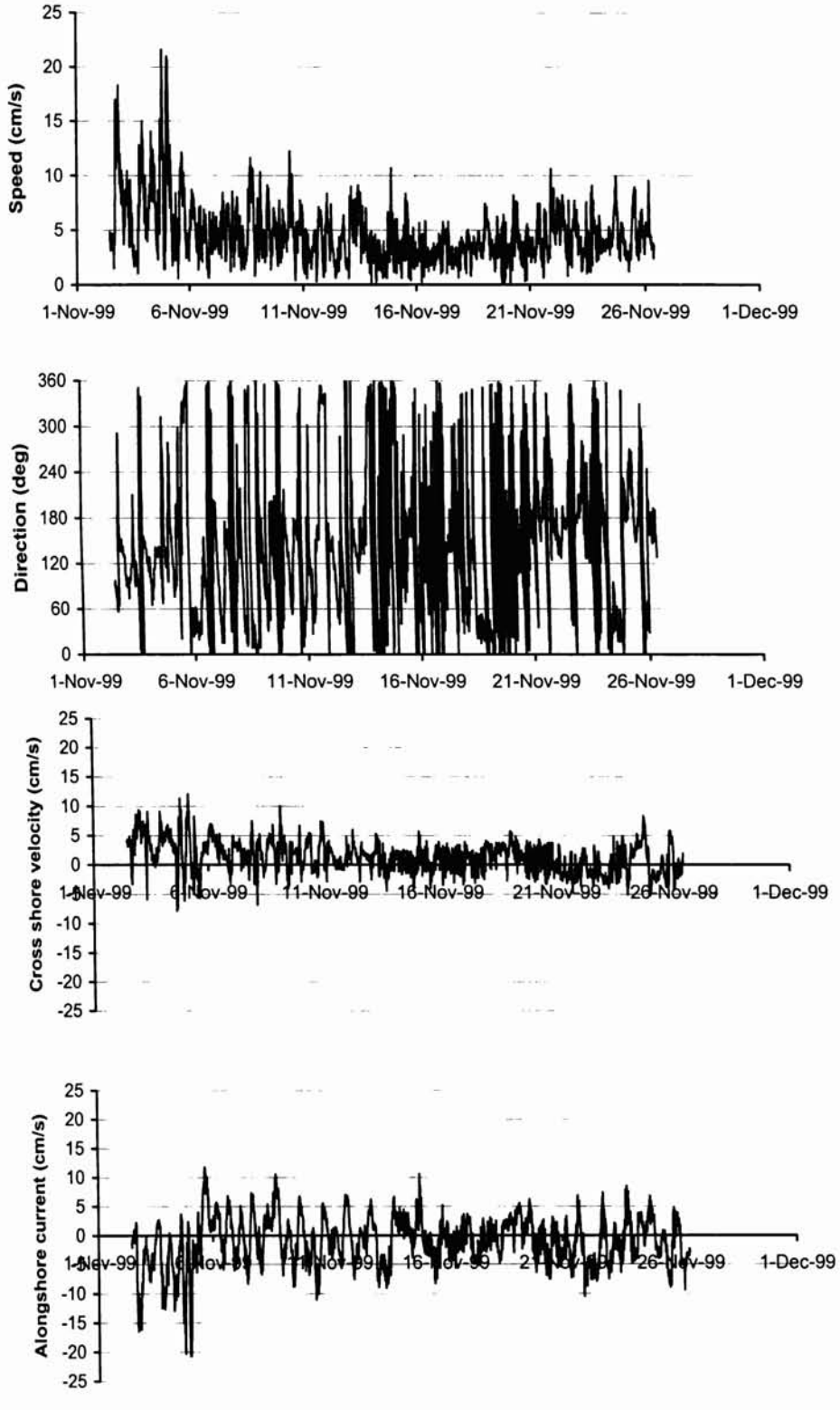

Fig. 4.3 Time series plot of S4 current meter measured mean burst current speed, direction, cross-shore (U cm/s) and alongshore (V cm/s) velocities during the deployment period 02 November – 26 November 1999 at the Nearshore site.

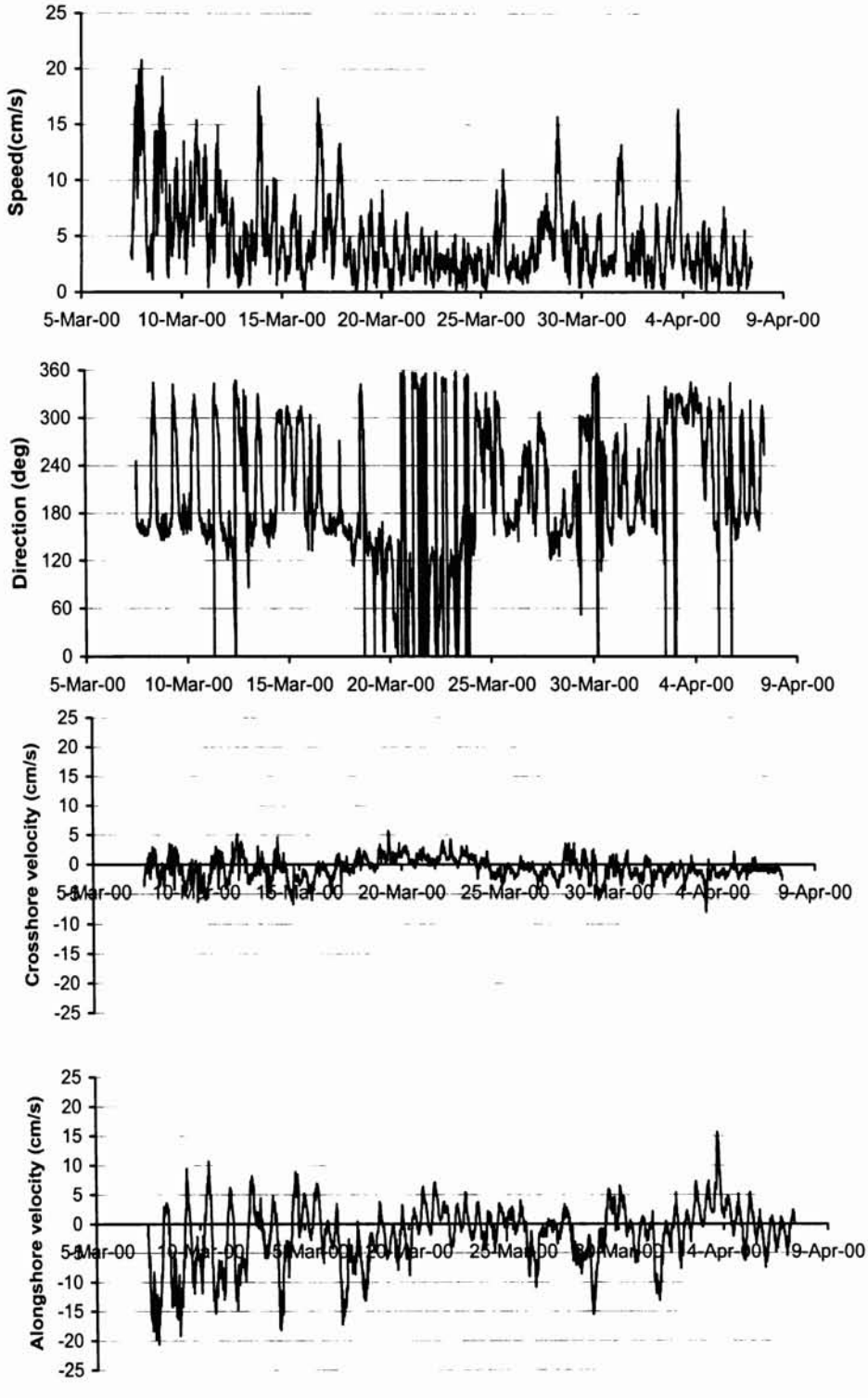

Fig. 4.4 Time series plot of S4 current meter measured mean burst current speed, direction, cross-shore (U cm/s) and alongshore (V cm/s) velocities during the deployment period 07 March– 07 April 2000 at the Nearshore site.

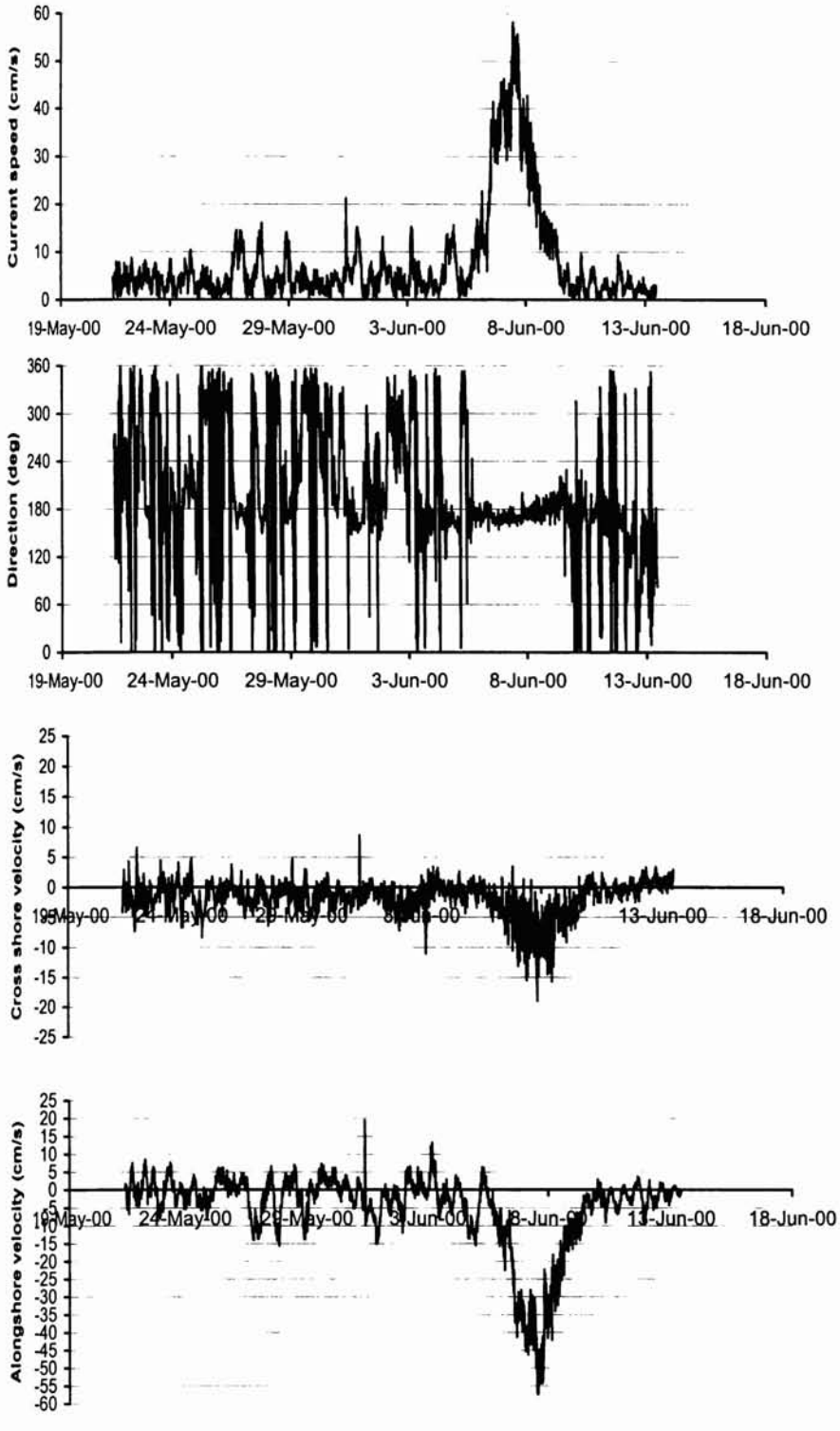

Fig. 4.5 Time series plot of S4 current meter measured mean burst current speed, direction, cross-shore (U cm/s) and alongshore (V cm/s) velocities during the deployment period 21 May – 13 June 2000 at the Nearshore site.

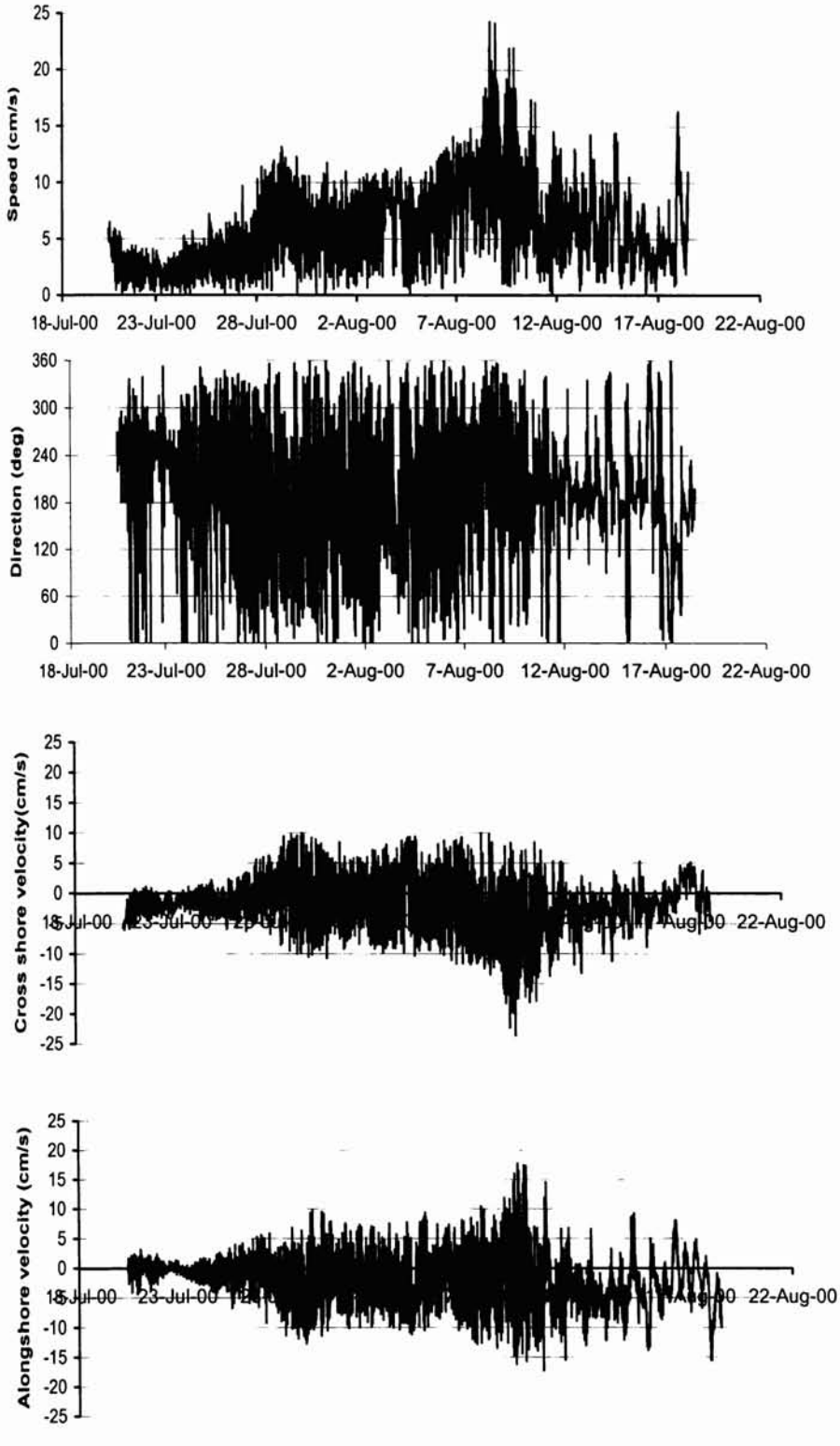

Fig. 4.6 Time series plot of S4 current meter measured mean burst current speed, direction, cross-shore (U cm/s) and alongshore (V cm/s) velocities during the deployment period 20 July– 19 August 2000 at the Nearshore site.

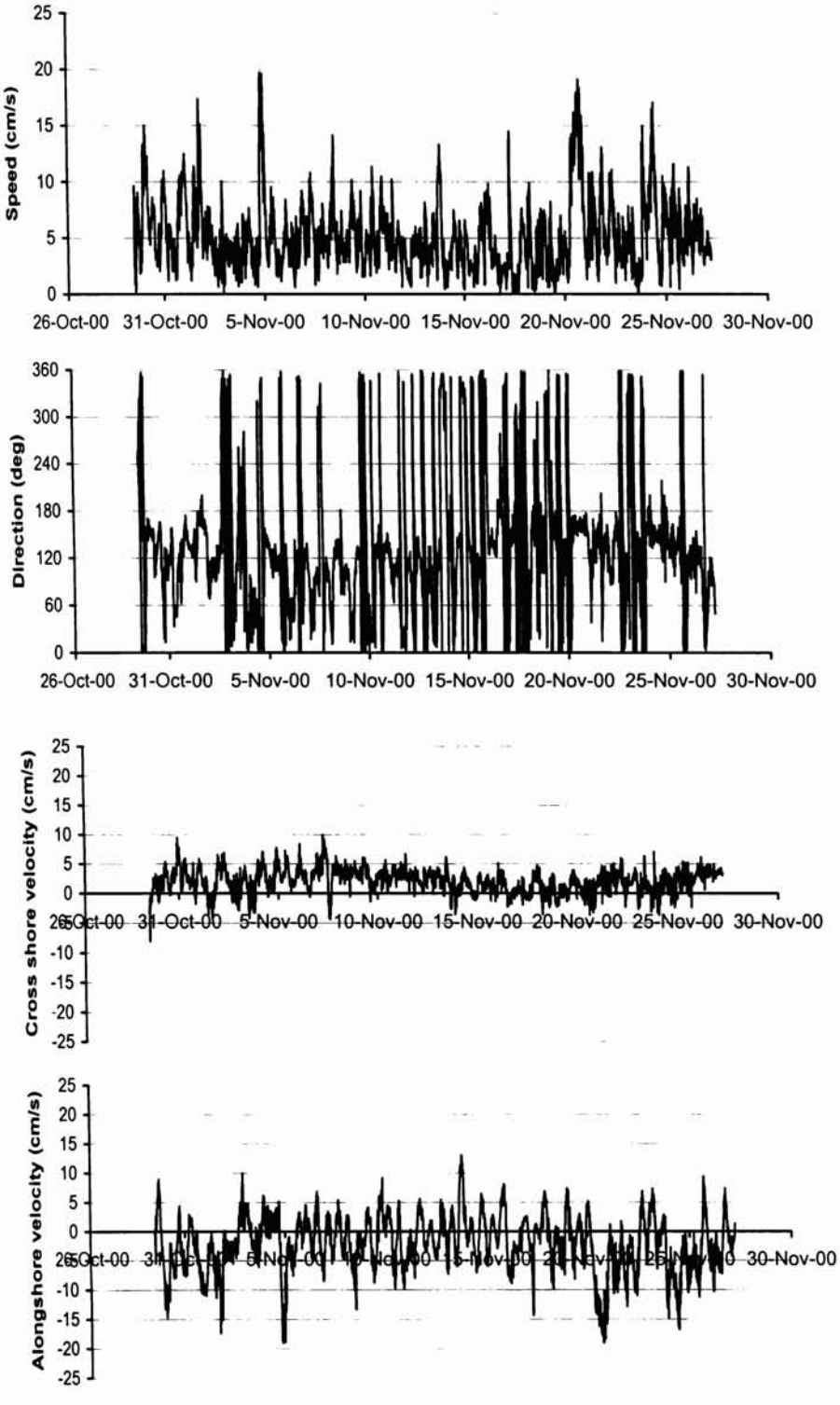

Fig. 4.7 Time series plot of S4 current meter measured mean burst current speed, direction, cross-shore (U cm/s) and alongshore (V cm/s) velocities during the deployment period 29 October – 27 November 2000 at the Nearshore site.

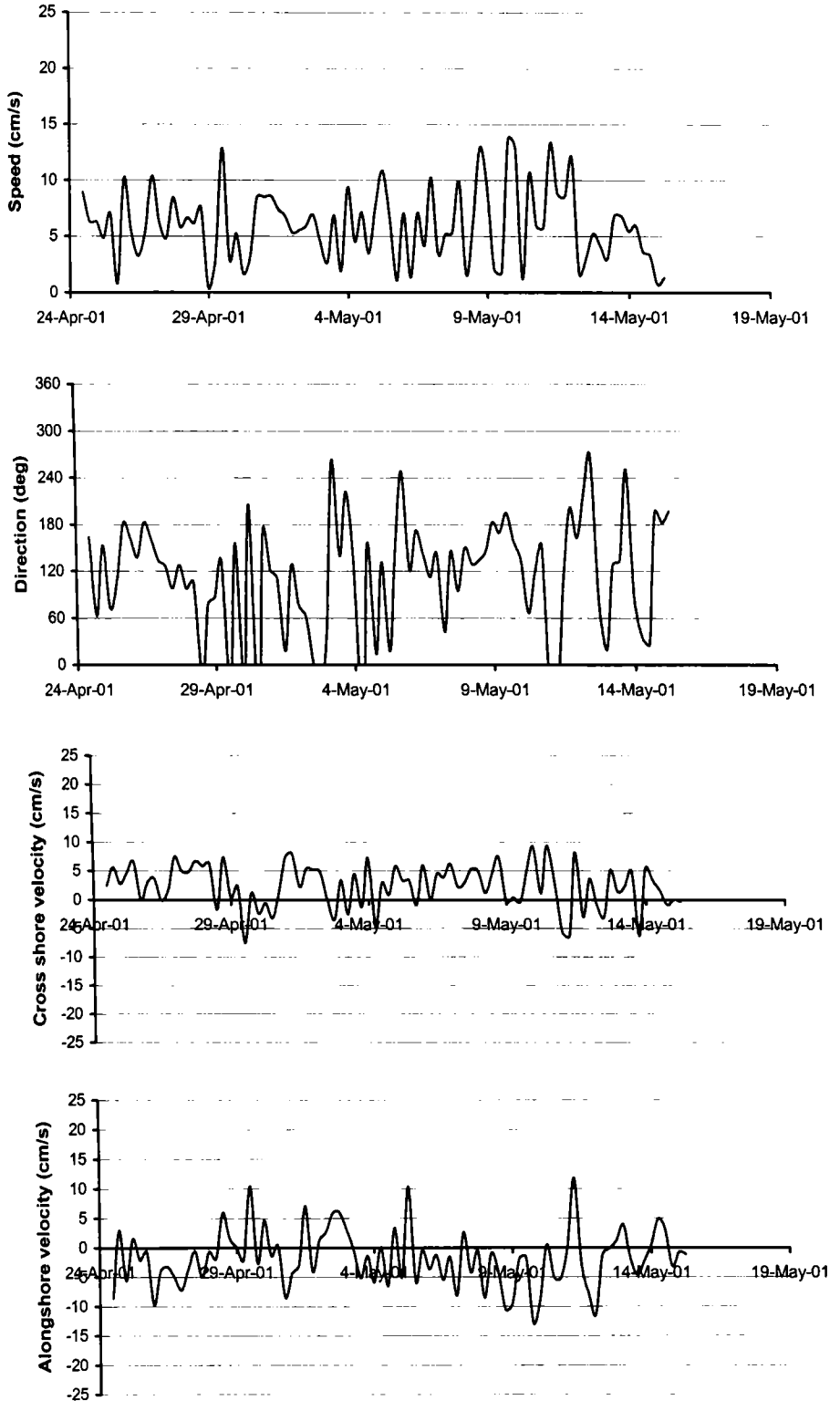

Fig. 4.8 Time series plot of S4 current meter measured mean burst current speed, direction, cross-shore (U cm/s) and alongshore (V cm/s) velocities during the deployment period 25 April – 17 May 2001 at the Nearshore site.

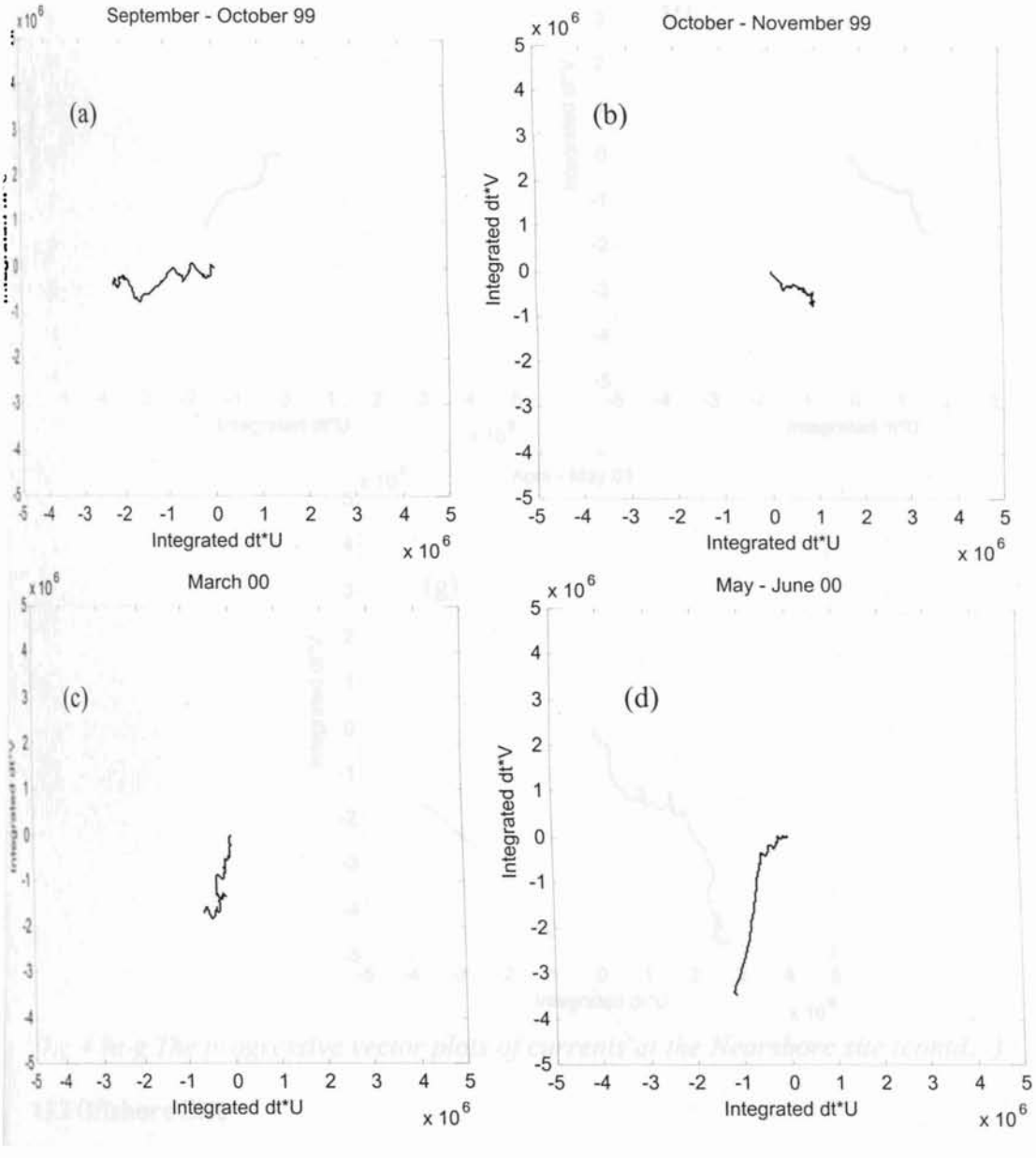

Fig. 4.9a-g The progressive vector plots of currents at the Nearshore site

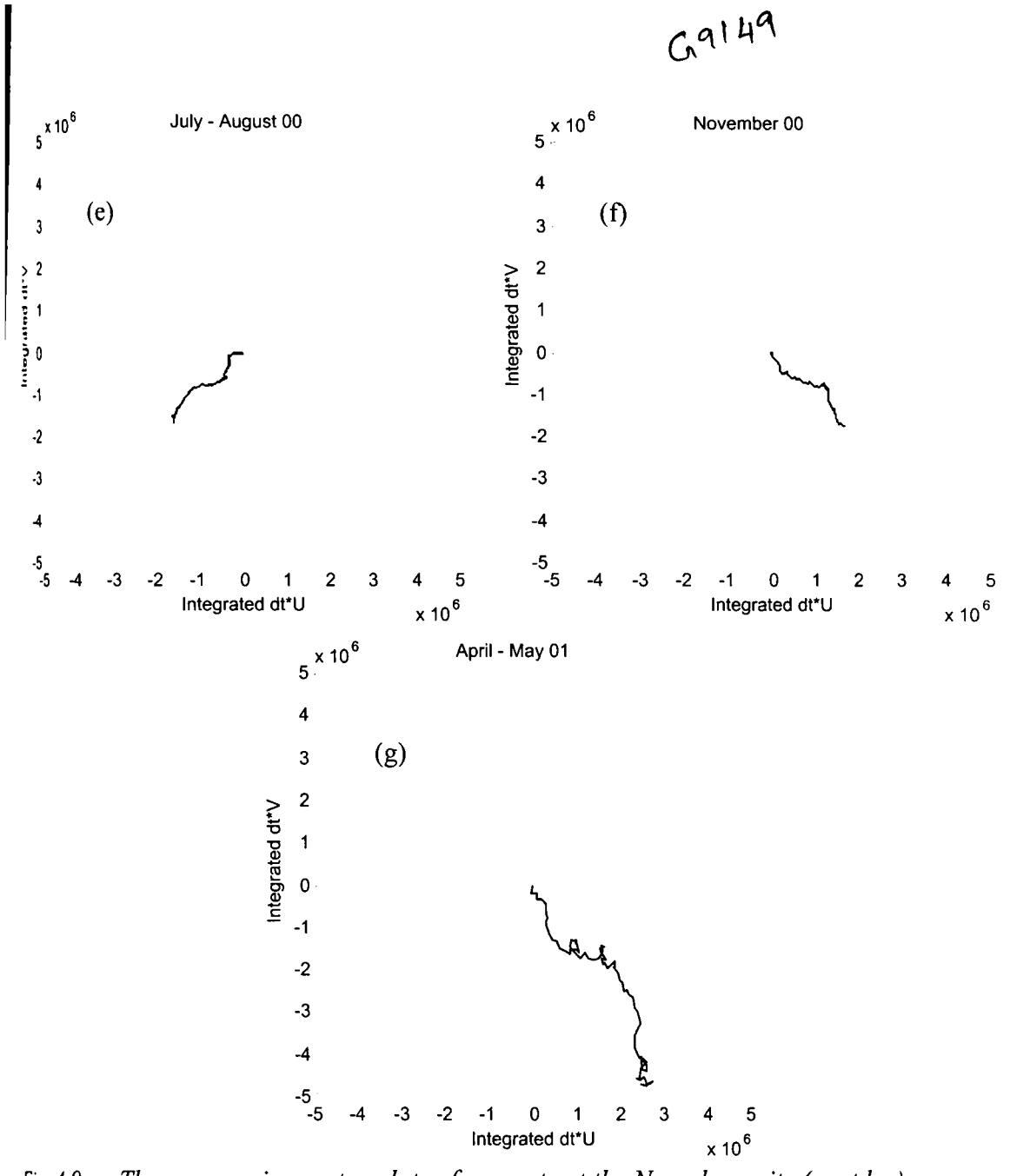

Fig. 4.9a-g The progressive vector plots of currents at the Nearshore site (contd...)

4.3.2 Offshore Site

As mentioned already, the current measurements at the offshore site commenced in May 1999. During May 1999 S4 current meter was deployed in the offshore site. From September 1999 onwards two FSI current meters were used, one at 0.75m and the other at 2.25m above bottom. Due to damage to the equipment on a few occasions, the data for the 2.25m level are not regular.

During the deployment period 7-22 May 1999, the current velocity ranged up to 25 cm/s (Fig. 4.10). The alongshore components were stronger than cross-shore components. Both cross-shore components and alongshore components are

oscillating in directions. However it can be seen that the alongshore component is predominantly in the southerly direction, particularly after the middle of May. This is reflected in the progressive vector plot (Fig. 4.18a), which shows a southerly transport.

During August-September 1999, the bottom current speeds were normally in the range of 5-15 cm/s, and speeds less than 5 cm/s were also recorded frequently (Fig. 4.11). Current direction oscillated between 0 and 360°. In general, the data indicated a predominant onshore flow in the cross-shore direction and northerly flow in the alongshore direction, but during the period when a high current speed of up to 35 cm/s was recorded, the alongshore flow was southerly. Since the recording period was only 2 weeks, the progressive plot doesn't show any significant movement of water (Fig. 4.18b). However, a net southeasterly movement is seen. The current meter deployed at 2.25m above bottom (Fig. 4.12) also recorded similar trends in current speeds, but the current speeds were in general higher, as expected. The cross-shore components were stronger than alongshore components with the domination of onshore flow. Northerly flows were more dominant in alongshore direction, but southerly flows when recorded were stronger than northerly flows. In accordance with the above pattern, the progressive vector plot (Fig. 4.18c) shows significant onshore movement. During the period September-October 1999, current speed was weaker and ranged between 0 and 10 cm/s for most part of the observation period (Fig. 4.13). However, in the last quarter, the current speed increased, and ranged from 5 to 15 cm/s. A maximum speed of 24 cm/s was recorded on 25 October. The cross-shore components were weaker than the alongshore components. Throughout the measurement period, cross-shore flow was offshore. The longshore flow was dominantly northerly in the first three weeks, but when current speeds recorded higher values in the last quarter, the longshore flows were consistently southerly. Progressive vector plot for the period indicates predominantly offshore flow in the first three quarters followed by southerly flow in the last quarter (Fig. 4.18d). Data from the upper current meter was not available during this period.

Due to equipment failures/damages, the next recording available for the offshore station is only in June-July 2000. In June-July 2000, current velocities in the range 0-10 cm/s were recorded on most of the days (Fig. 4.14) though it is considered to be the peak monsoon period. Very rarely current speeds exceeding 15 cm/s were recorded. Current direction oscillates between 0 and 360° due to the tidal influence. During this period, the alongshore components were stronger than cross-shore components. In the cross-shore components of flows, the onshore and offshore flows were equally prevalent and appear to be well balanced. The same is applicable to the alongshore components. The progressive vector plot (Fig. 4.18e) amply demonstrates the above by not showing any net movement. During July-August 2000, the current is stronger than the June-July period. The speeds are commonly in the range 0-10 cm/s (Fig. 4.15). Speeds above 10cm/s too occur several times with a maximum speed of 22.5cm/s. The alongshore components were stronger than cross-shore components. The cross-shore components were distributed more or less equally between onshore and offshore flows. However, among the alongshore components, the northerly flows have a slight edge over southerly flows. Thus the progressive vector plot for this period (Fig. 4.18f) shows a not so significant northerly movement.

During the period October-November 2000 also, the current speed between 0 and10 cm/s is common, but towards the last quarter, there is a significant increase in speed with speed up to 40cm/s (Fig. 4.16). As is the usual case, during periods of strong currents, the direction of current is consistently southerly overcoming the tidal influence. Even during the first three quarters when the currents are weak, the southerly components dominate over the northerlies. Thus the progressive vector plot for this period (Fig. 4.18g) shows a predominant southerly movement.

During July-August 2001, the current speed was generally between 0 and10 cm/s except for a few days (Fig. 4.17). On 1st August the maximum current speed of 29 cm/s was recorded. Both cross-shore and alongshore components have more or less equal magnitude. Among the cross-shore components, there appear to be a slight edge for the onshore flow. The alongshore flow is dominated by southerly components. The progressive vector plots shows a strong southerly movement (Fig. 4.18h)

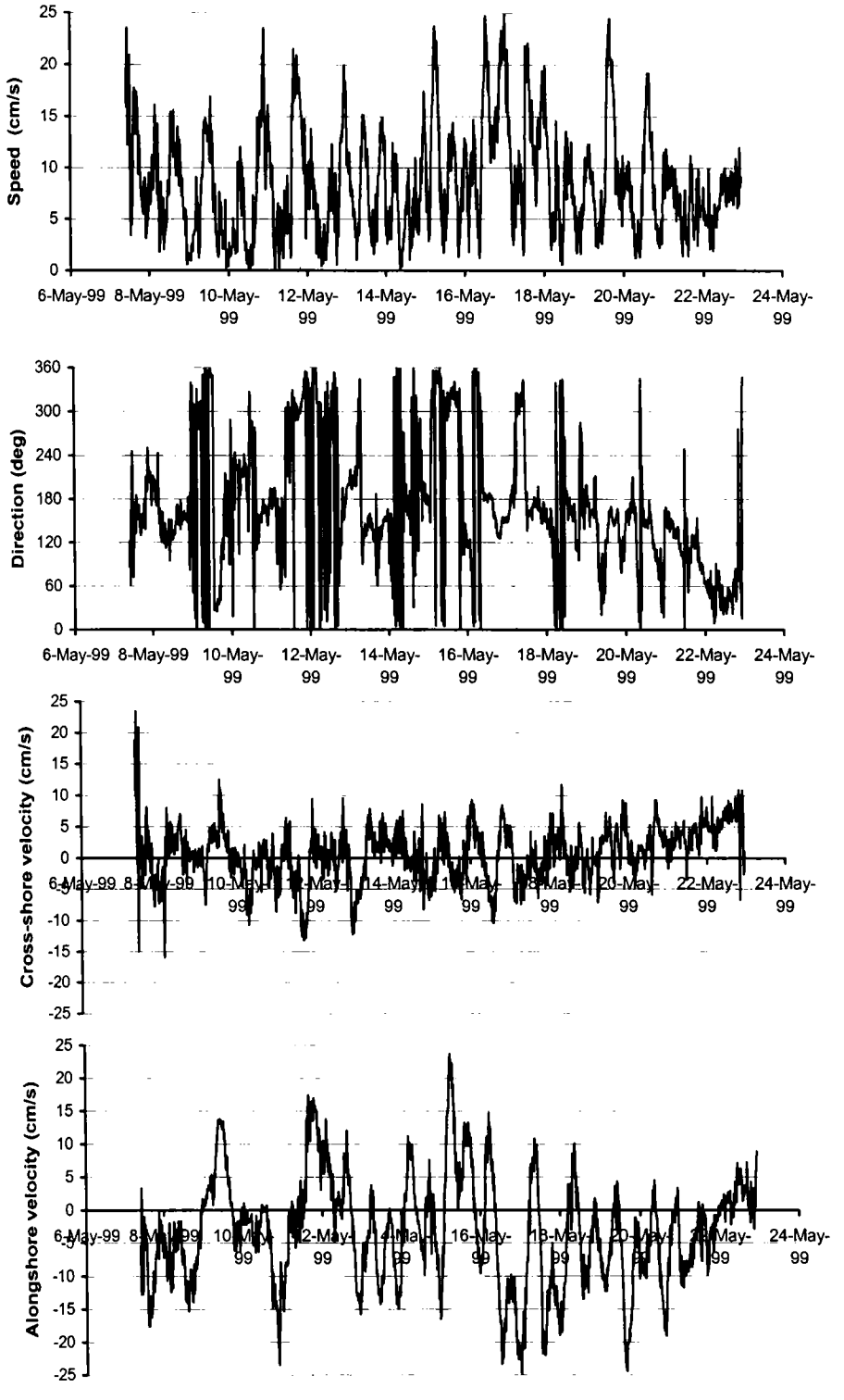

Fig. 4.10 Time series plot of S4 current meter measured mean burst current speed, direction, cross-shore (U cm/s) and alongshore (V cm/s) velocities during the deployment period 7 May – 22 May 99 at the offshore site.

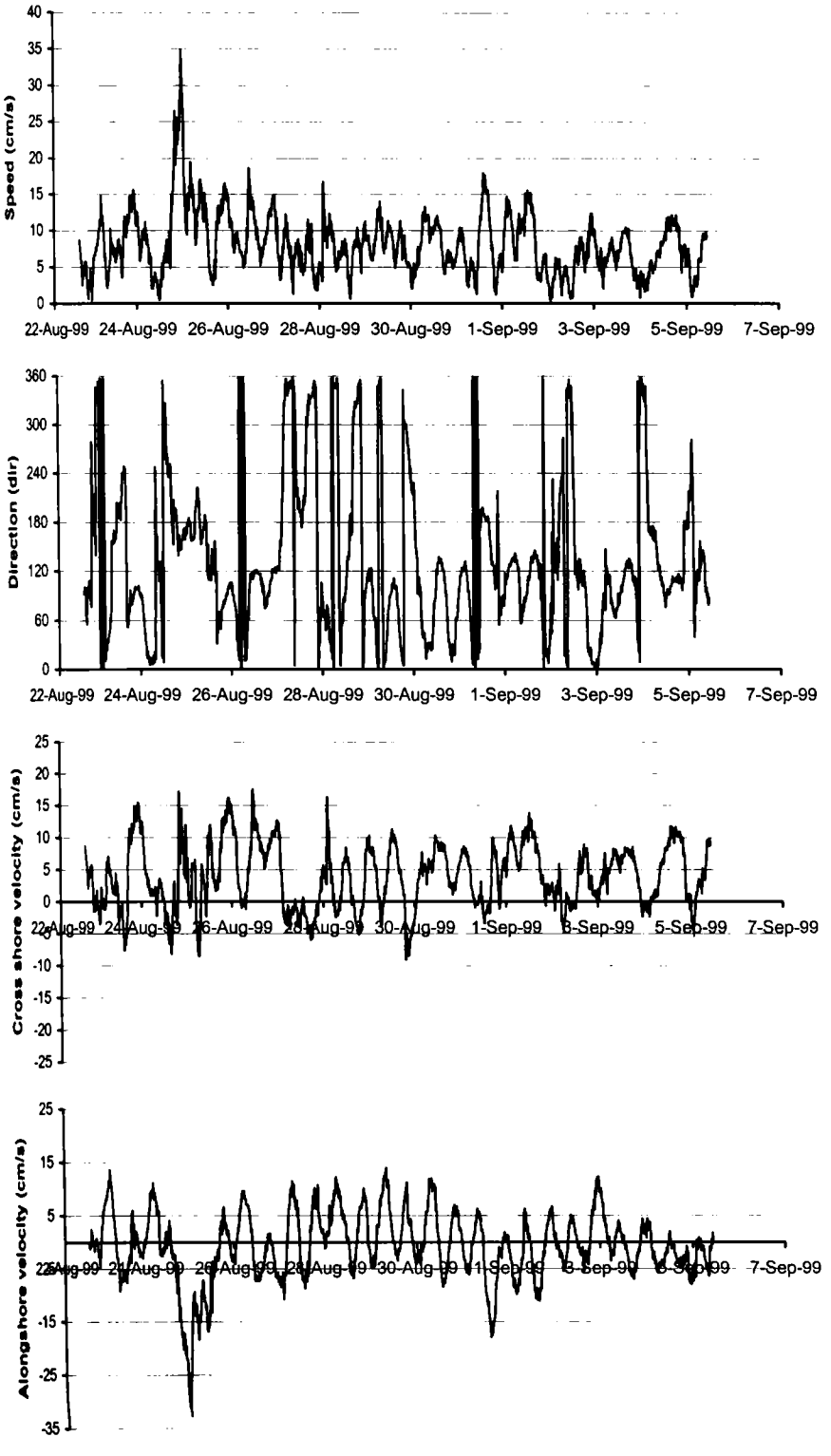

Fig. 4.11 Time series plot of FSI-CTD current meter measured mean burst current speed, direction, cross-shore (U cm/s) and alongshore (V cm/s) velocities during the deployment period 22 August – 05 September 1999 at the offshore site.

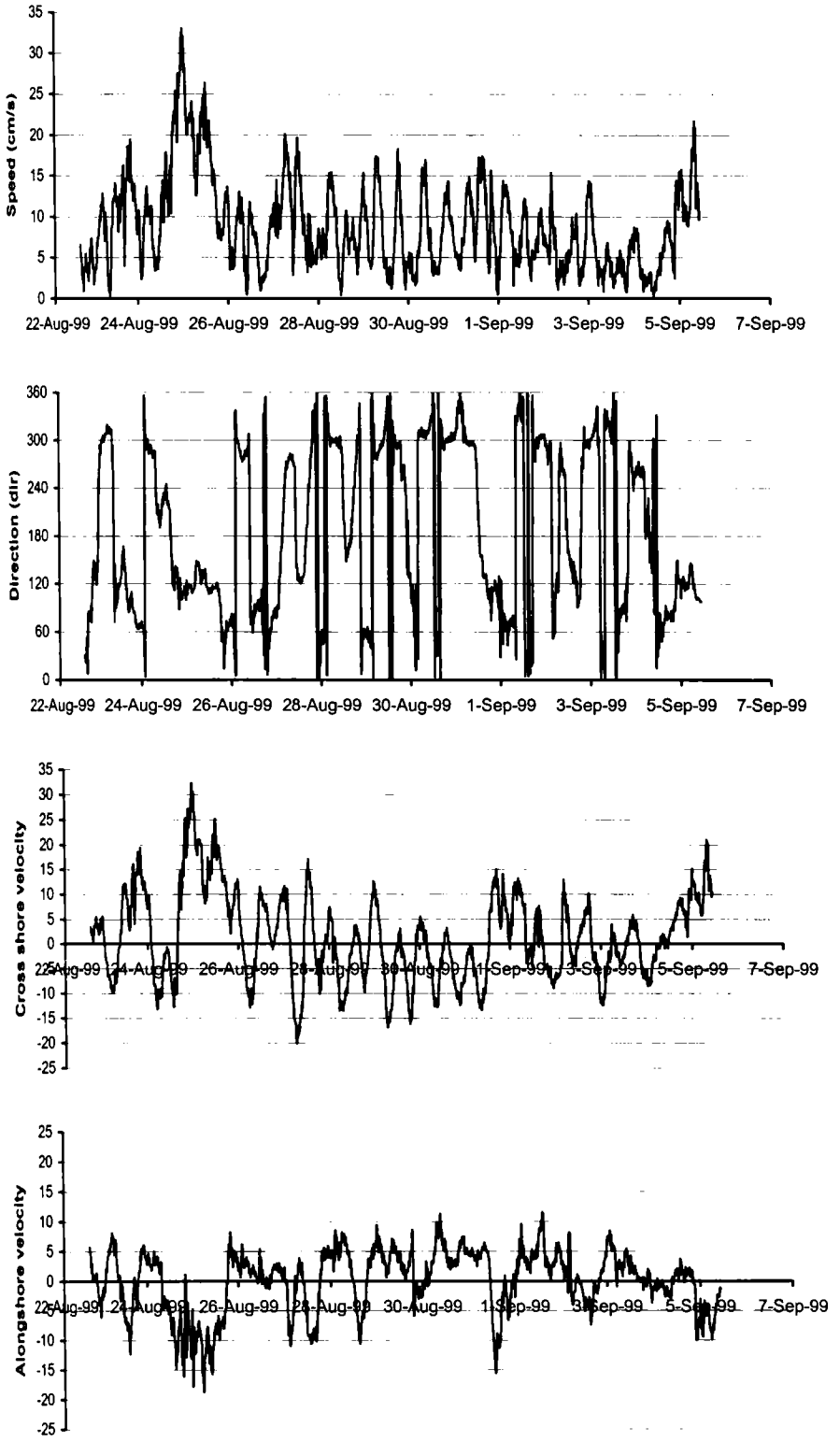

Fig. 4.12 Time series plot of FSI current meter measured mean burst current speed, direction, cross-shore (U cm/s) and alongshore (V cm/s) velocities during the deployment period 22 August – 05 September 1999 at the offshore site.

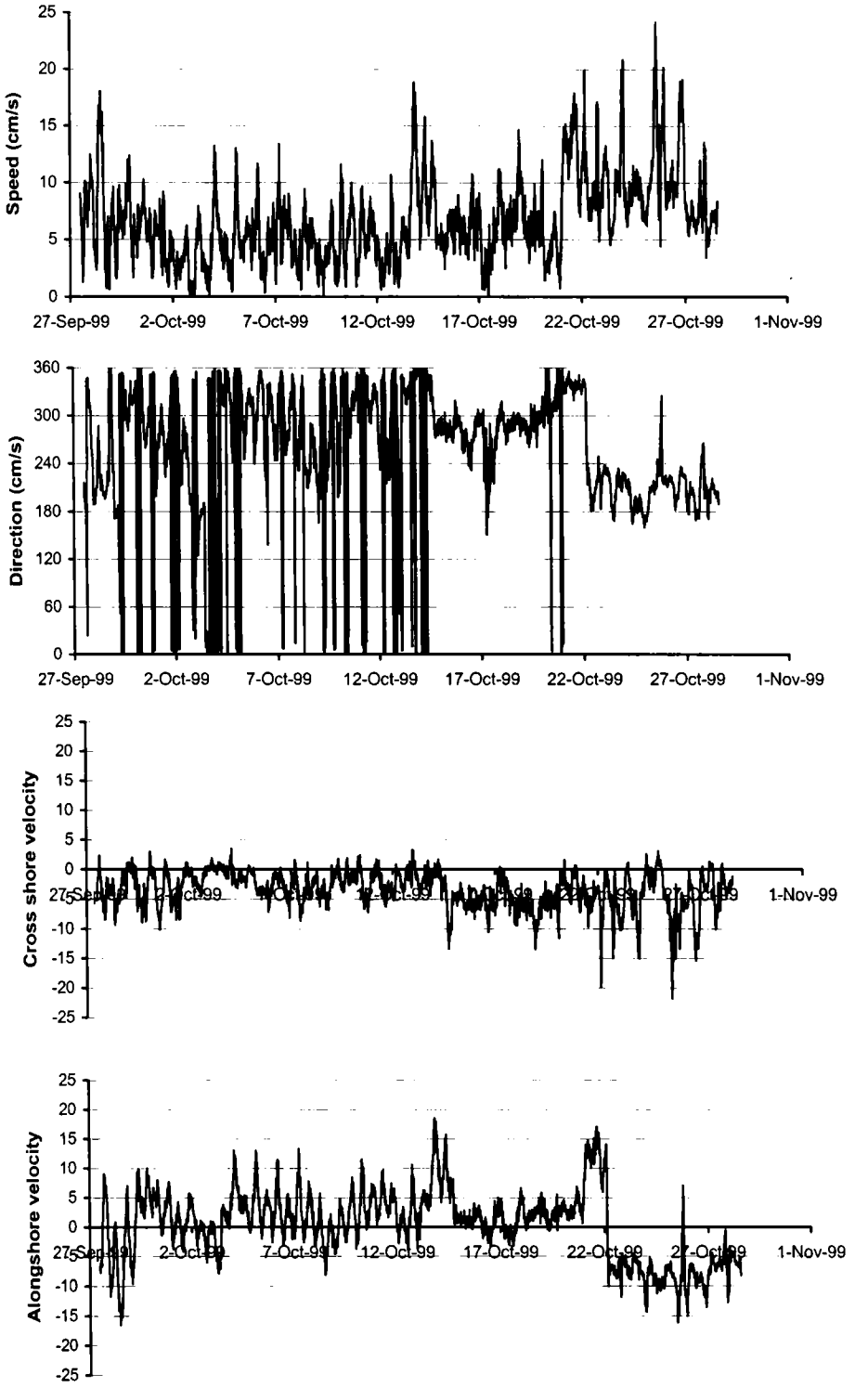

Fig. 4.13 Time series plot of FSI-CTD current meter measured mean burst mean current cross-shore (U cm/s) and alongshore (V cm/s) velocities during the deployment period 27 September – 28 October 1999 at the offshore site.

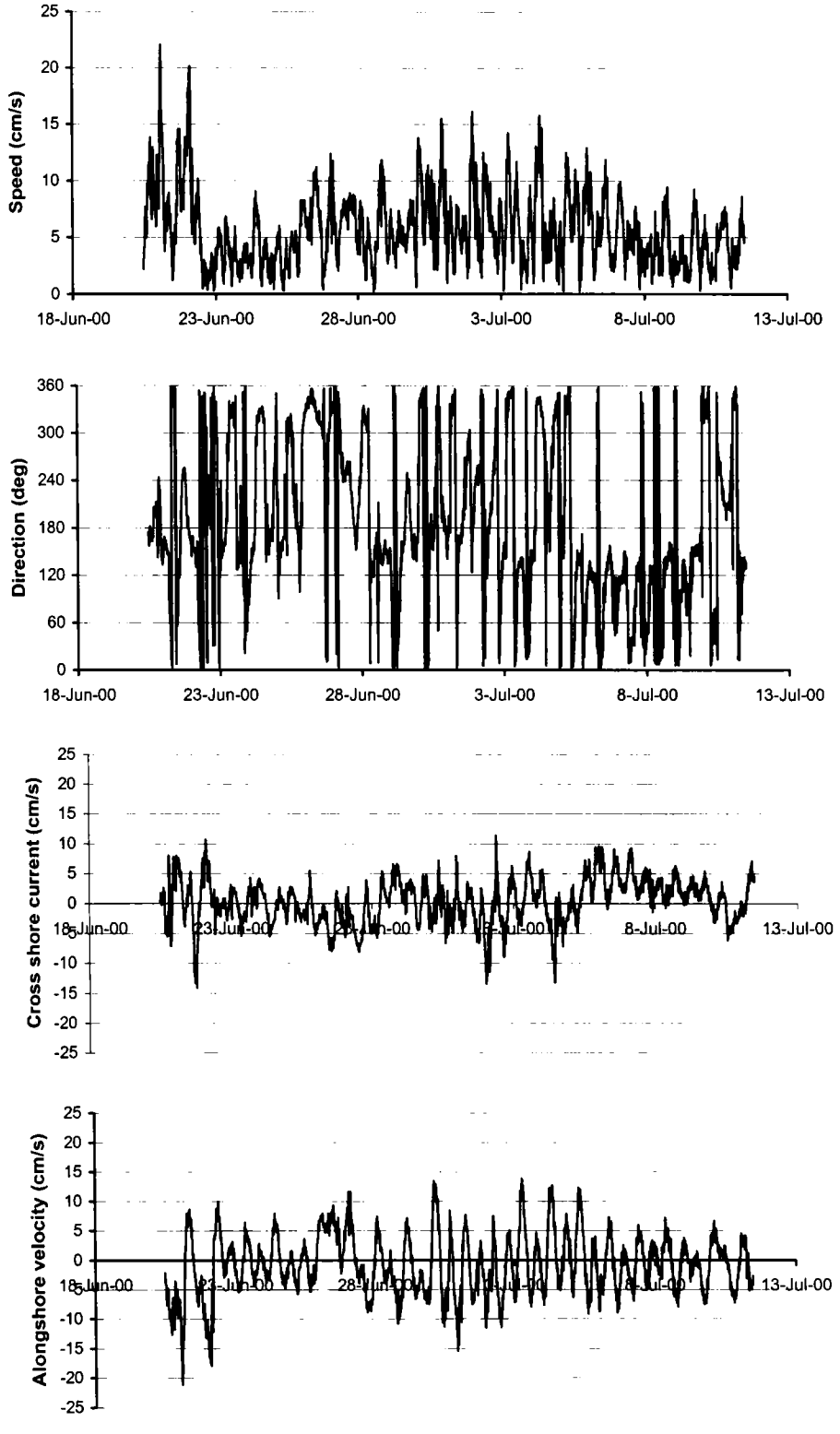

Fig. 4.14 Time series plot of FSI current meter measured mean burst current speed, direction, cross-shore (U cm/s) and alongshore (V cm/s) velocities during the deployment period 20 June – 11 July 2000 at the offshore site.

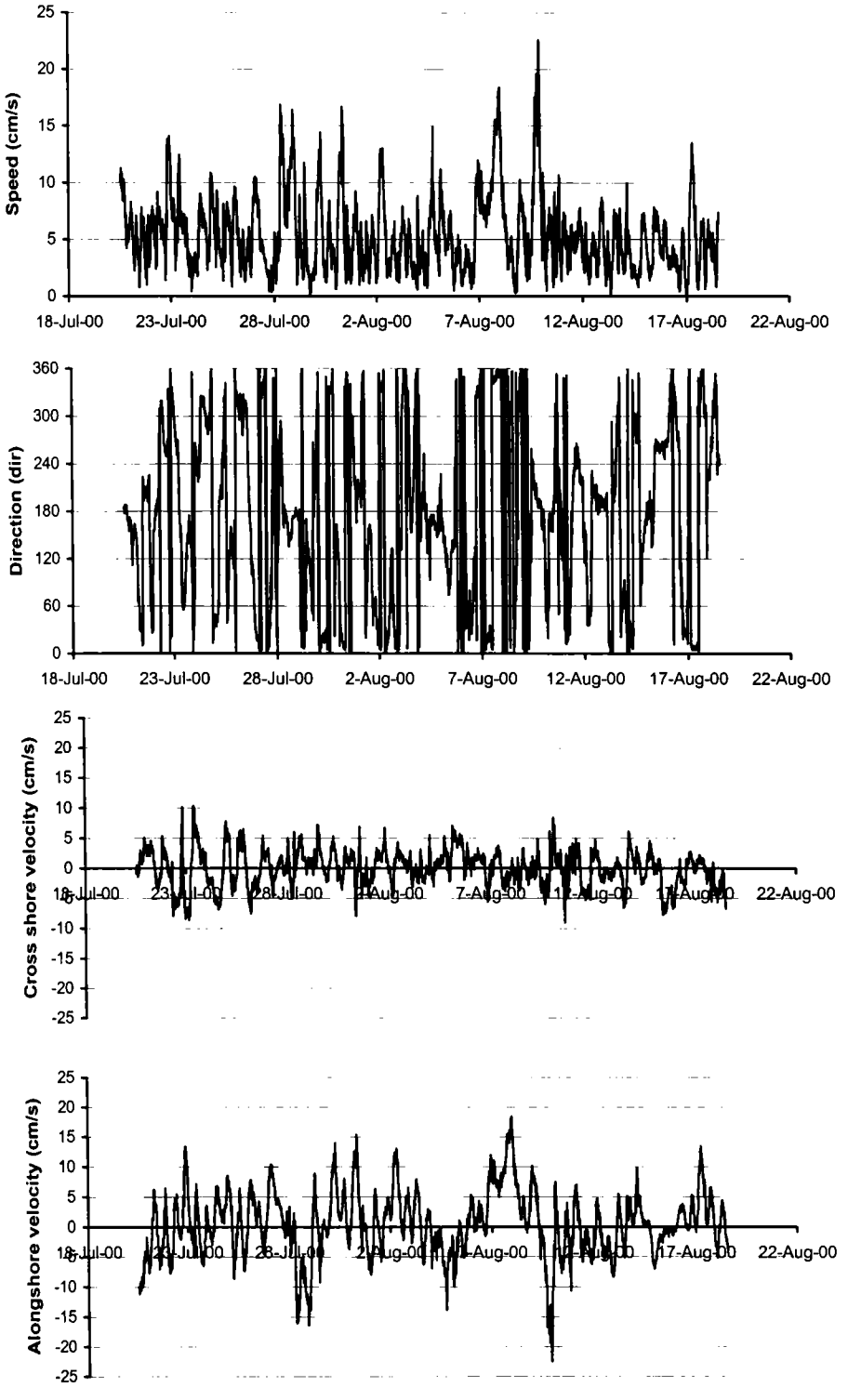

Fig. 4.15 Time series plot of FSI current meter measured mean burst current speed, direction, cross-shore (U cm/s) and alongshore (V cm/s) velocities during the deployment period 20 July – 18 August 2000 at the offshore site.

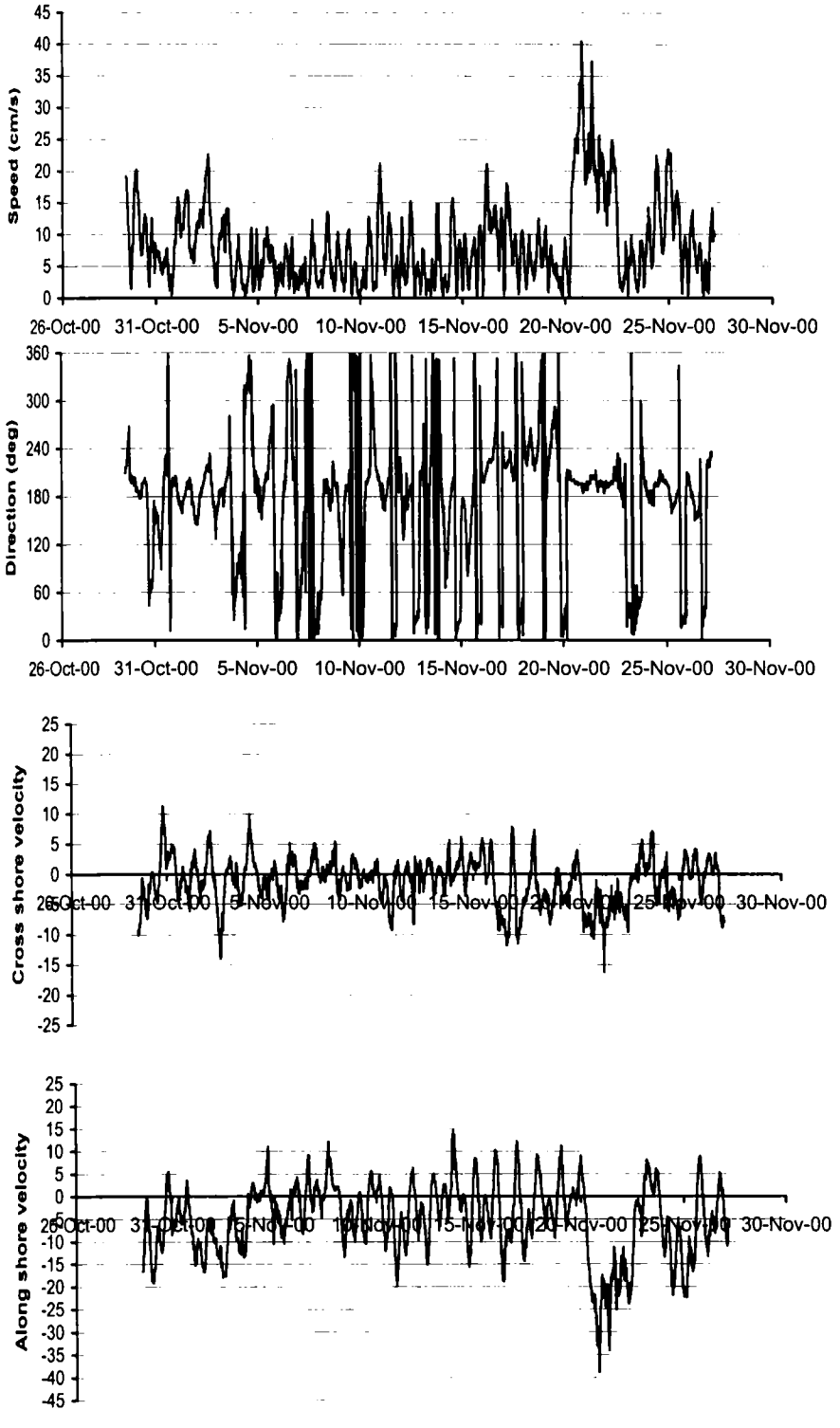

Fig. 4.16 Time series plot of FSI current meter measured mean burst current speed, direction, cross-shore (U cm/s) and alongshore (V cm/s) velocities during the deployment period 29 October – 27 November 2000 at the offshore site.

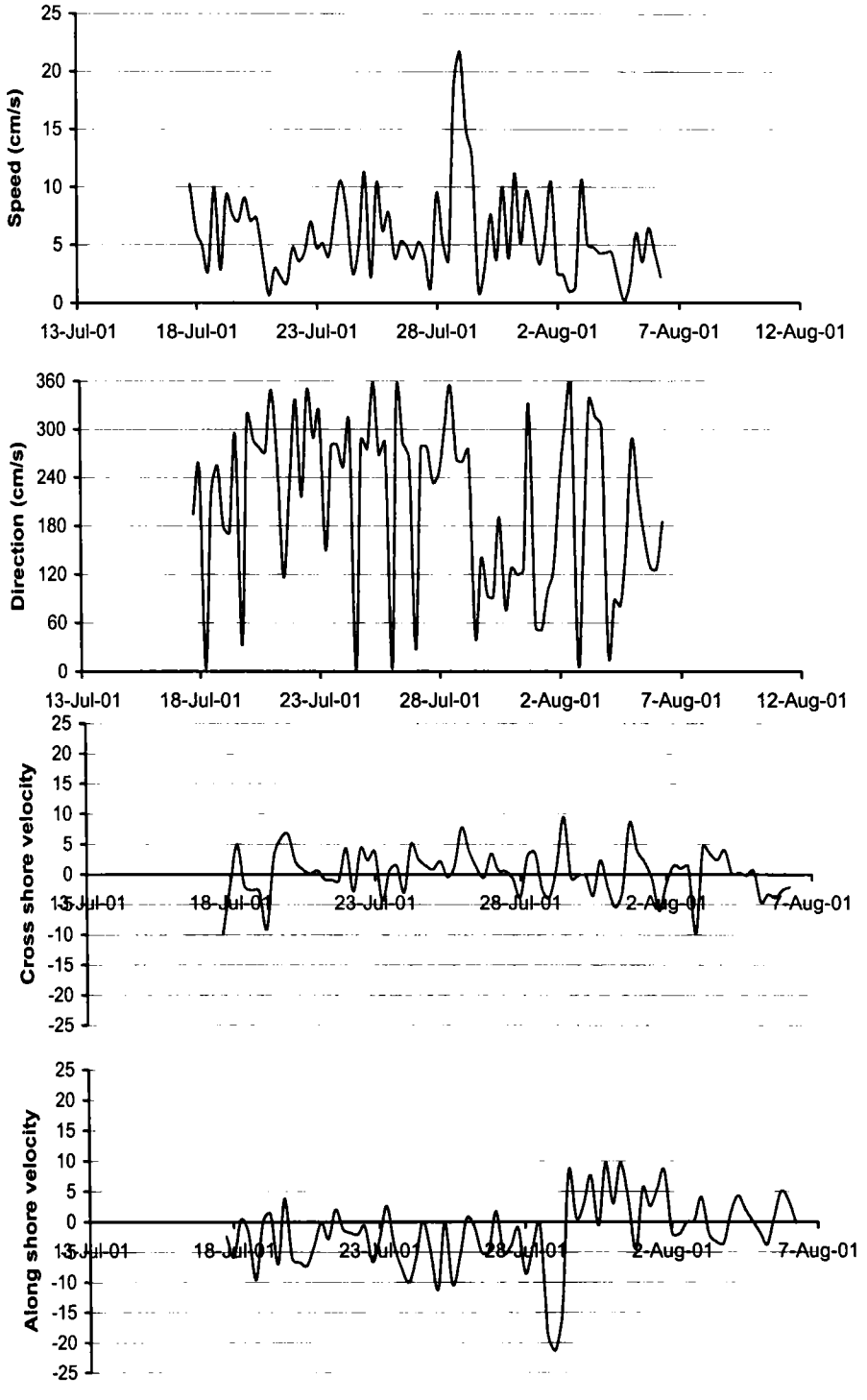

Fig. 4.17 *Time series plot of FSI current meter measured mean burst current speed, direction, cross-shore (U cm/s) and alongshore (V cm/s) velocities and stick plot of current velocity during the deployment period 18July–7August 2001 at the offshore site.*

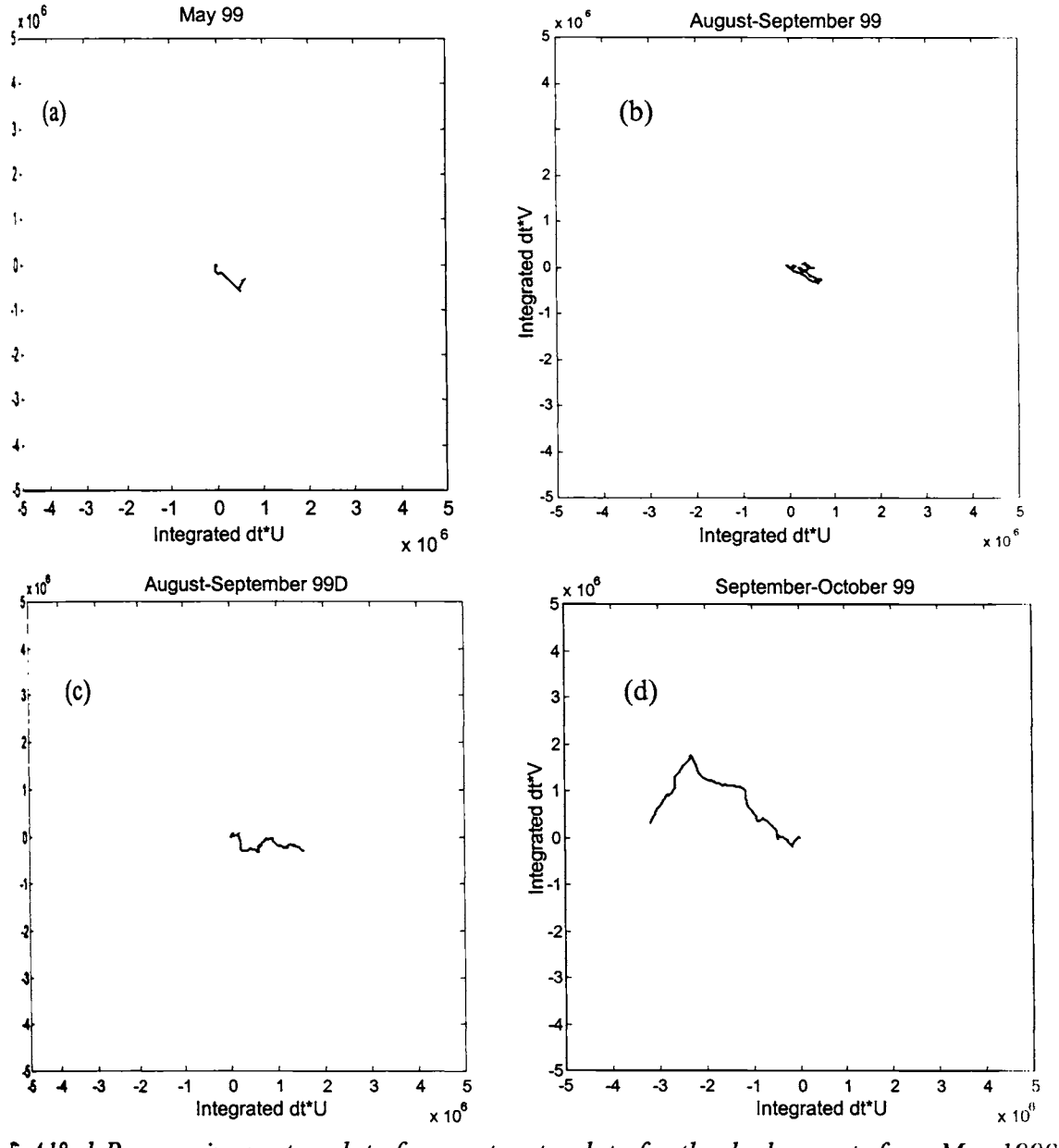

Fig. 4.18a-h Progressive vector plot of current meter data for the deployments from May 1999 to August 2001 at the offshore site.

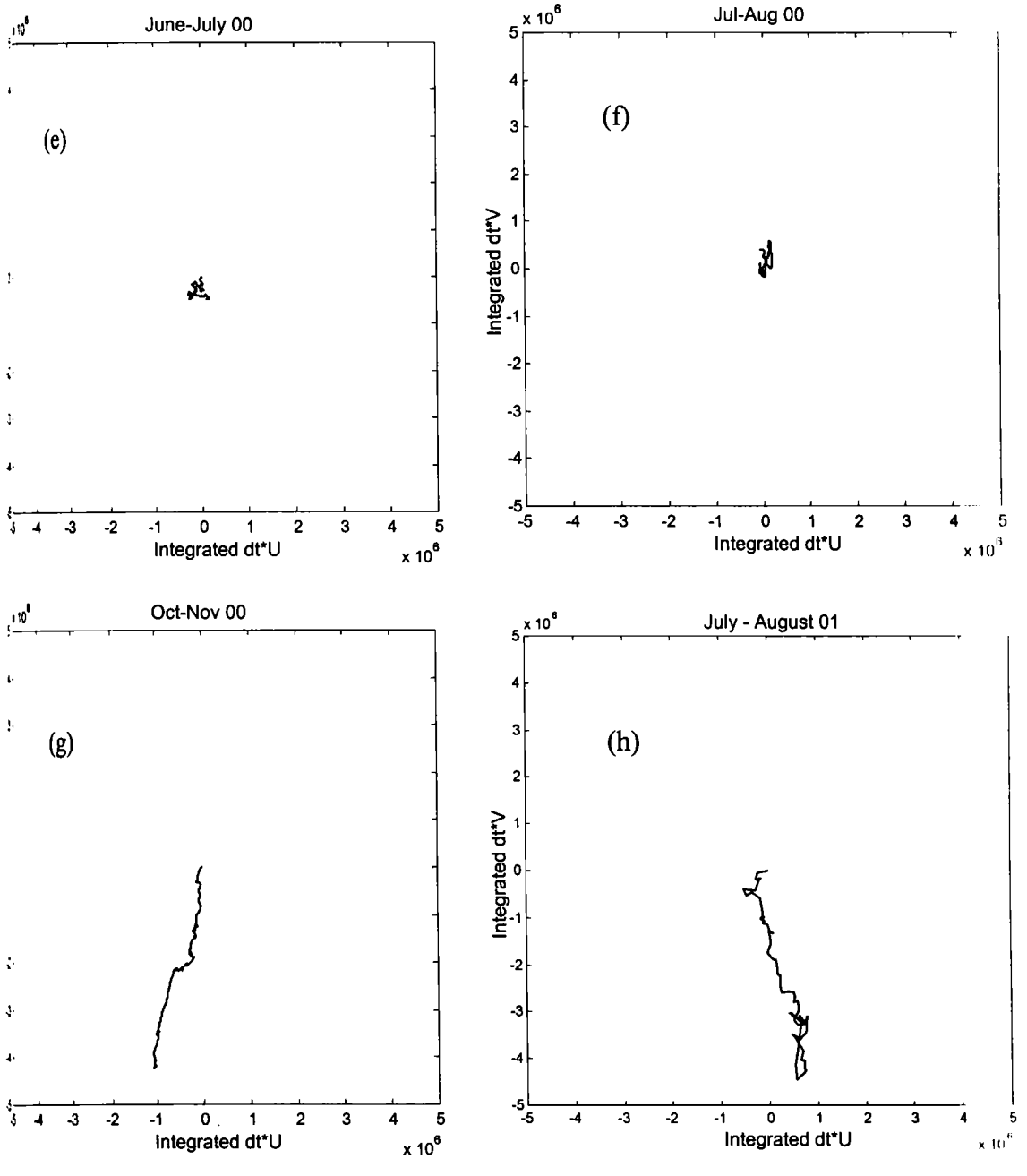

Fig. 4.18 Progressive vector plot of current meter data for the deployments from May 1999 to August 2001 at the offshore site (contd...)

4.3.3 Vertical Profile of Currents

The data used in the earlier sections are mostly bottom currents (1m above sea bed) which are important from the point of view of sediment budgeting. Vertical profile of currents is useful in understanding the relation between wind and currents and calibration of circulation models. Since the instrument required for the same was not available in CESS and was to be hired, only limited data were collected.

An upward-looking Acoustic Doppler Profiler was deployed on a bottom-mounted frame at the offshore and nearshore sites for about 24 hours each on 22 and 23 March 2000 during the non-monsoon and at the offshore site only on July 10, 2000 in the monsoon. The instrument simultaneously measures current speed and direction throughout the water column in a succession of vertical layers of 0.5 m thick. The results are shown as pseudo-colour plots where the horizontal axis shows time, the vertical axis shows elevation above the instrument sensor in the water column and the colours represent scaled velocity and direction in two separate plots (Fig. 4.19-4.21).

During the non-monsoon in March, the maximum currents at the offshore site are of the order of around 25 cm/s (Fig. 4.19). The strongest flows occur at the surface and during the late afternoon when the wind is strongest. The velocity gradient through the water column is largest at this time and is indicative of a surface wind stress forcing which only penetrates to about mid-depth. Currents are onshore to southerly at the surface and offshore at the bed, which also indicates wind-induced downwelling circulation. In the very early morning just after midnight, the flows are mostly longshore to the south and currents are of similar magnitude through the water column, suggesting a response to a large-scale (longshore) pressure gradient, rather than a cross-shore set-up induced by wind. The current speeds show the semi diurnal pattern in the variation with low speed around noon on 22nd. In the afternoon the speed picks up, as already discussed due to the sea breeze. The semidiurnal influence is manifested by low speeds in the evening. In the early morning the speed picks up, but again reduced in the late morning. This semidiurnal pattern is indicative of the domination of tidal current.

At the nearshore site in March, the vertical partitioning is less pronounced (Fig. 4.20). However, similar tendencies occur with the flows onshore at the surface and rotated partially offshore at the bed during the afternoon. The velocity pattern indicates a semi-diurnal response, which is possibly a tidal modulation of the dominantly southerly currents. A northerly reversal when currents are very slow occurs in the late morning in synchrony with the patterns offshore at this time on the previous day. Significant semidiurnal variability in current velocity is indicated. Thus in the late afternoon, surface current velocities achieve the maximum values, most probably under the influence of winds. Then the surface current velocities get decreased, but within six hours of the afternoon maximum values a minimum values is recorded. After that the value gets increased and another maximum is observed though the magnitude of the second peak is slightly reduced. Thus, maximum and minimum values observed in surface current velocity get repeated every six hours, alternatively. This can be the effect of oscillatory tidal currents.

The most striking feature of the profile for monsoon (Fig. 4.21) is a stronger tendency for currents near the surface to be opposite to those near the bed for much of the time. In accordance with the earlier measurements, the current at the seabed during the monsoon is mostly southerly and offshore, although there are periods of slow flow to the north at the bed. The strongest currents occur near the surface, presumably due to the direct action of wind stress and the frictional seabed boundary layer, which reduces near-bed currents. This effect is very strong with periods when currents are around 30 cm/s at the surface and as low as 8 cm/s near the bed. The fastest surface flows occur in the late afternoon when the winds are strongest. The semi-diurnal pattern of variation in the current speed is evident here also, though not to the extend seen in March.

Though the variability of current velocity with depth is not very conspicuous at the nearshore site, significant variation is observed at offshore site. The variability in current speed is mainly caused by the semi-diurnal tidal flows, and the influence of wind on current velocity become evident when the wind activity is strong in the afternoon hours.

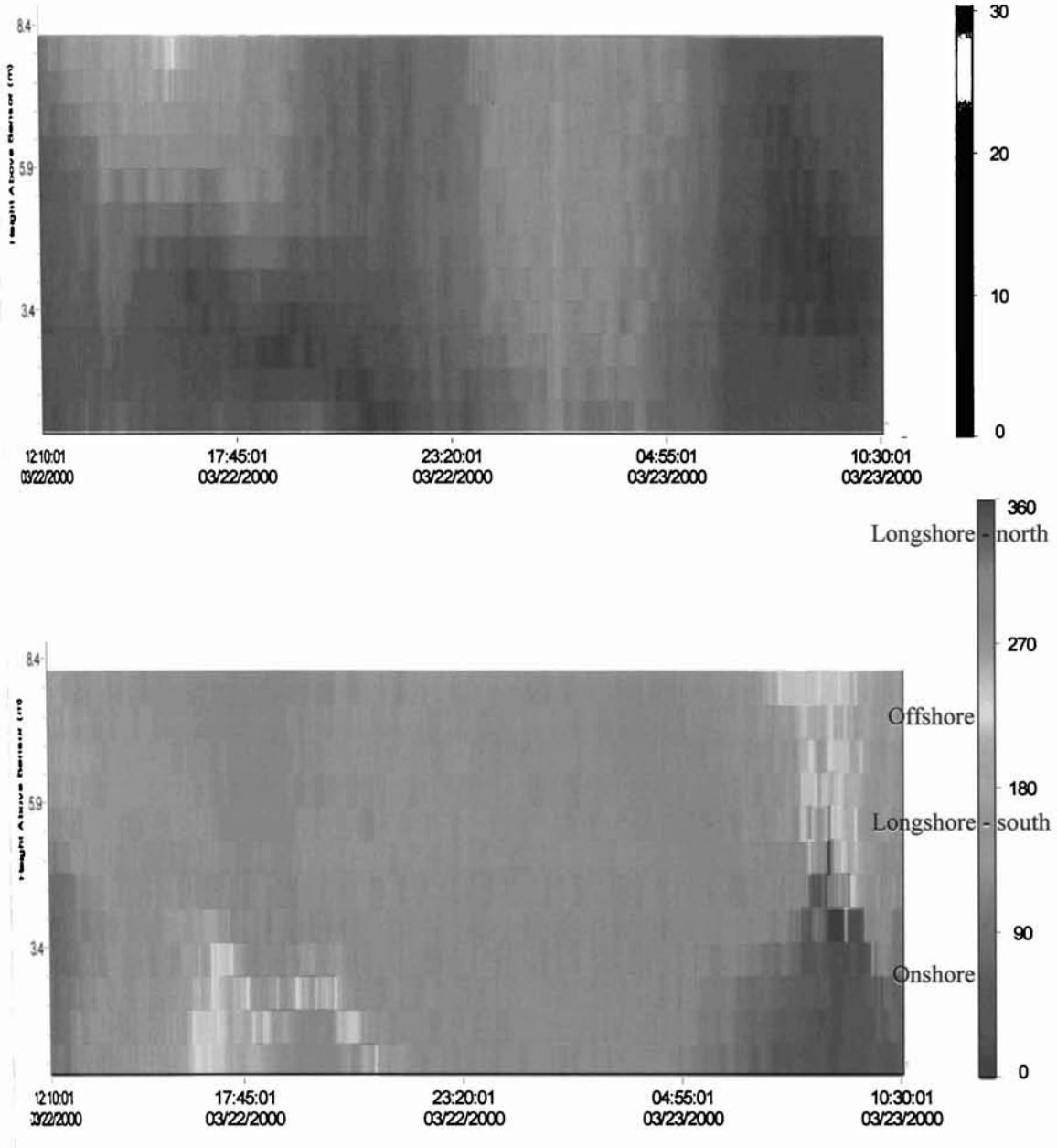

Fig. 4.19 Mean current speed and direction measured by the upward looking Acoustic Doppler Profiler (ADP) at the offshore site on 22-23 March 2000

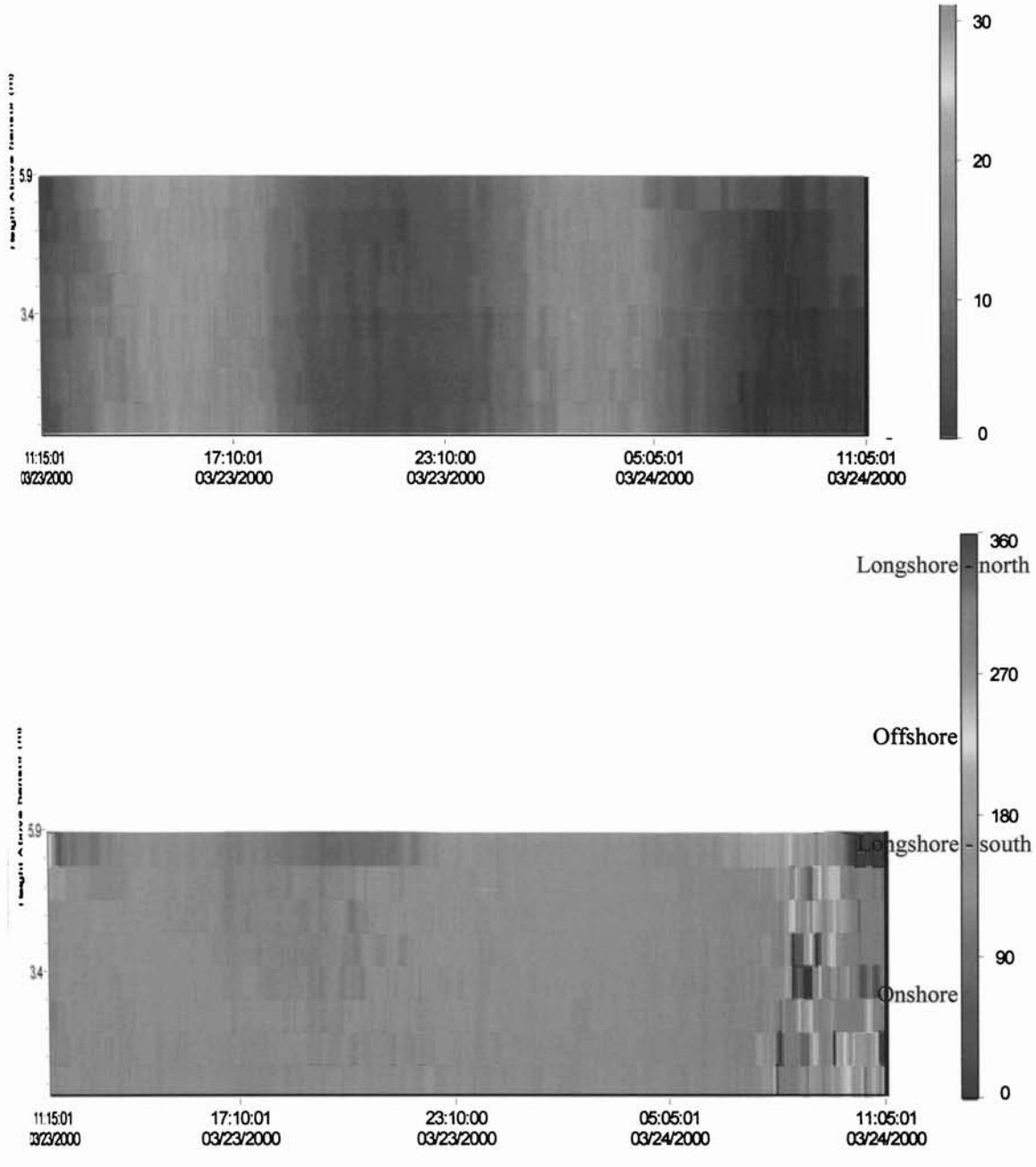

Fig. 4.20 Mean current speed and direction measured by the upward looking Acoustic Doppler Profiler (ADP) at the Nearshore site on 23-24 March 2000

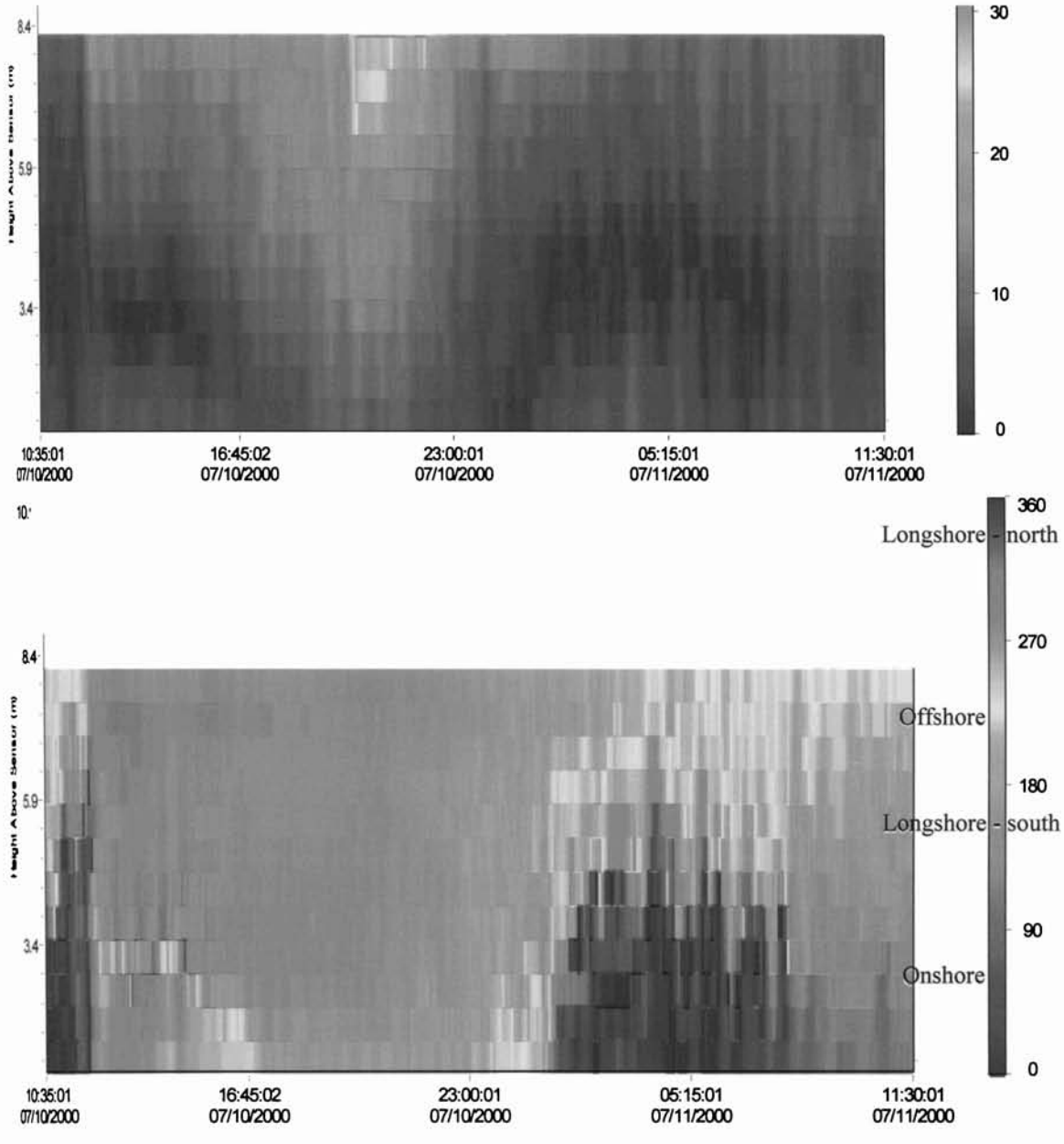

Fig. 4.21 Mean current speed and direction measured by the upward looking Acoustic Doppler Profiler (ADP) at the offshore site on 10-11 July 2000

4.4 DISCUSSION AND SUMMARY

The observed current appears to be a resultant of tidal currents, wind-driven currents and continental shelf currents. The influence of tides on the current is quite evident from the semidiurnal oscillations seen in the time series distributions presented for different measurement periods. However one notable feature is the absence of this tidal influence in occasions when strong currents are present. It is observed that a good relationship exists between wind and currents on many occasions in the study area (Fig. 4.22a-n). Applying the Ekman's theory of wind driven currents, when the wind is onshore, the surface currents will move shorewards on average. This sets up the water level at the coast and creates a cross-shore pressure gradient that drives a return offshore flow at the bed. The reverse occurs in the case of offshore wind when the seabed currents head onshore. The progressive vector plot of current of May 1999 shows a southerly flow while wind vector during this period is northwesterly. In October 1999, westerly to southwesterly flow is observed while the wind is northwesterly. May-June 2000 and July-August 2000 currents show southwesterly flow while the wind vector during this period is predominantly northwesterly. Thus a clear correspondence between the winds and currents is evident in these cases. Exceptions to this correlation are also observed. For example in November 1999, a southeasterly flow was observed while the wind vector is northwesterly for few days and southwesterly after that.

The predominant winds in this region are from the northwest quadrant and so the wind-driven currents are mostly longshore to the south on the inner shelf. The dominance of southerly flow is quite evident from the progressive vector plots for different periods. On this wind-driven pattern is superimposed a shelf current associated with larger-scale circulation in the Indian Ocean. As already seen, this appears to take the form of an eddy, which stretches from Lakshadweep Island to the south-west coast and is opposed to the prevailing flows that pass around Sri Lanka and through the Arabian Sea (see Fig. 4.1). Consequently, the general current is directed north in the monsoon period around July. Thus when the northwest wind abates the shelf currents flows in response to the general circulation, although the net movement is southward. In addition to the three components viz. tidal, wind driven

and continental shelf currents listed above, there could also be the contribution of coastal trapped waves and baroclinic flow associated with the plumes of fresh water coming from the estuaries. The observed currents have lot of implication on the sediment transport in the innershelf and littoral zone. The predominance of southerly flows suggests that sediment in the innershelf is moving to the south. Onshore currents lead to accretion and offshore currents to erosion. The predominant winds are from the NW quadrant. These winds depending on the actual directions induce onshore and offshore currents deciding the net erosion-accretion scenario. This aspect is to be studied in the next chapter on beach process.

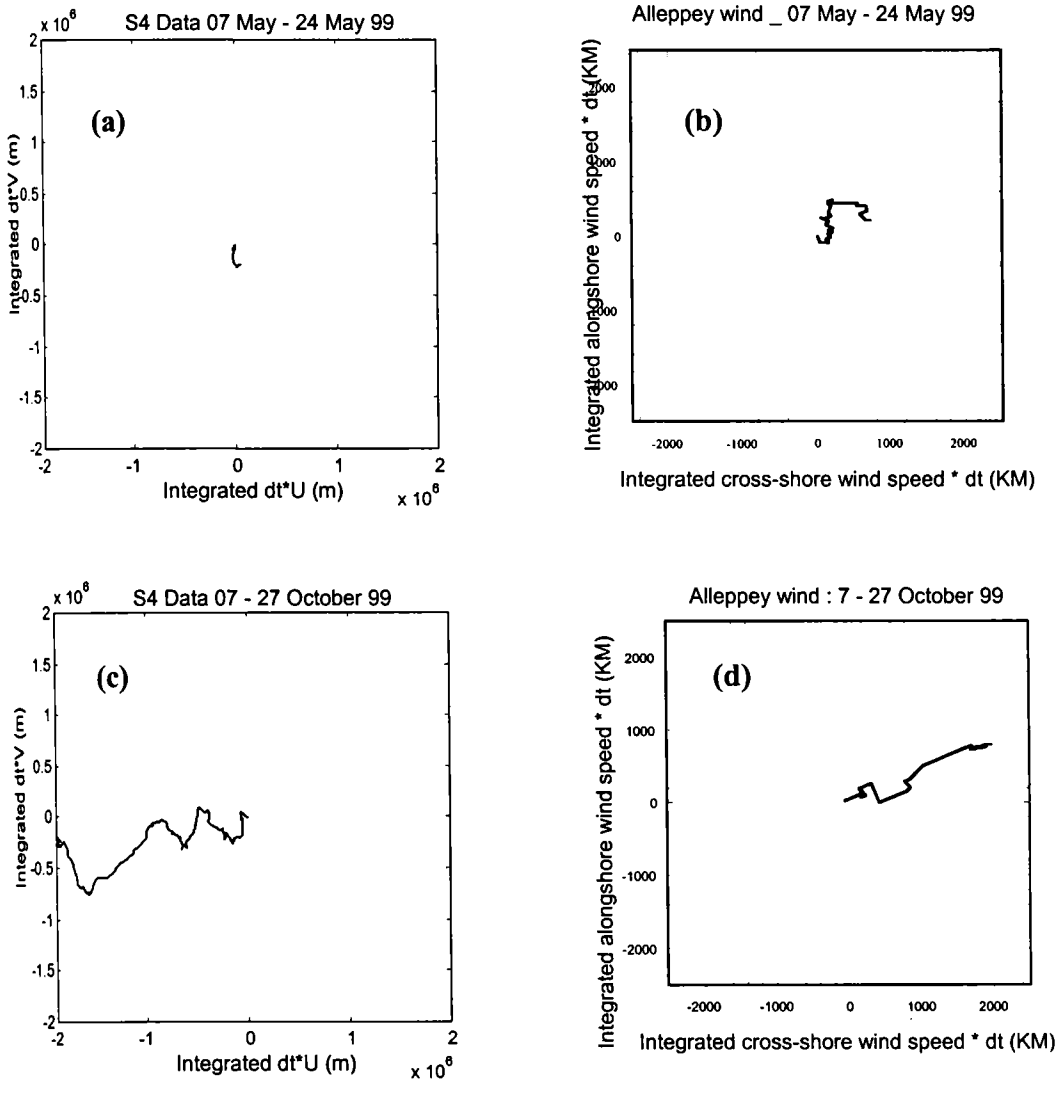

Fig. 4.22a-n Progressive vector plot of burst mean S4 current meter data, for the deployments from May 1999 to November 2000 and Alleppey wind records. The cross-shore and alongshore current velocities are rotated onto a shore-parallel direction (23° relative to True North) to get shore-normal and shore parallel components. North-south is alongshore and positive east is onshore.

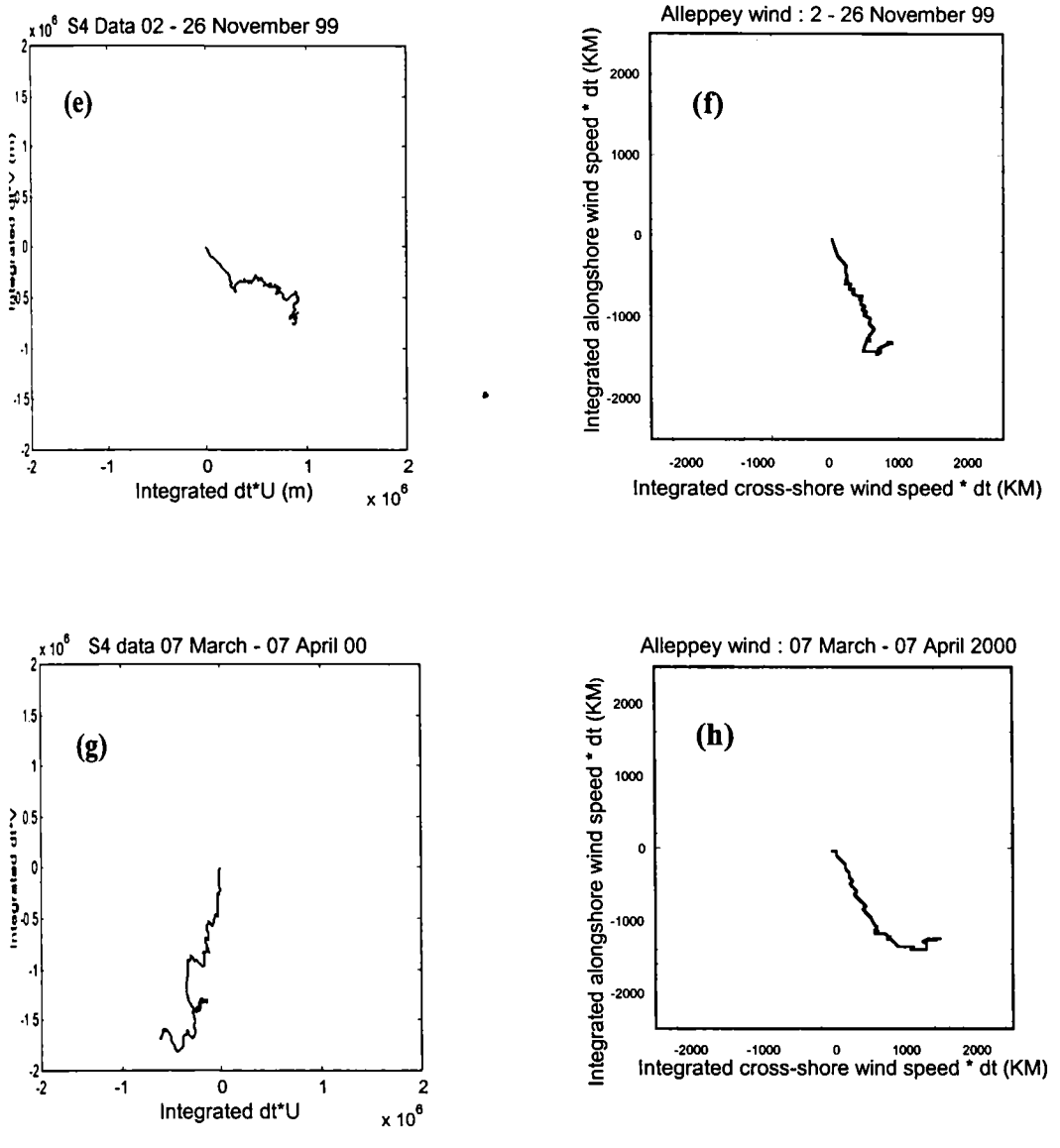

Fig.4.22a-n Progressive vector plot of burst mean S4 current meter data, for the deployments from May 1999 to November 2000 and Alleppey wind records. The cross-shore and alongshore current velocities are rotated onto a shore-parallel direction (23° relative to True North) to get shore-normal and shore parallel components. North-south is alongshore and positive east is onshore.
(contd...)

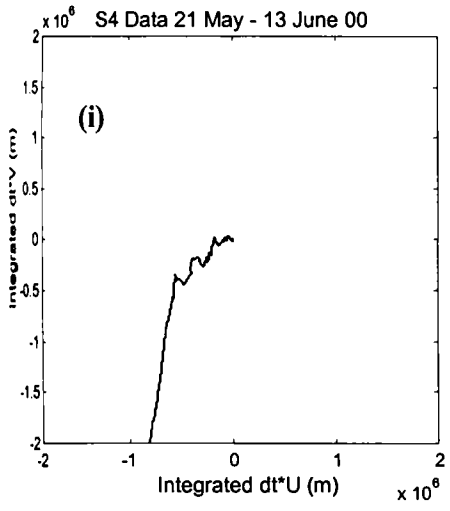

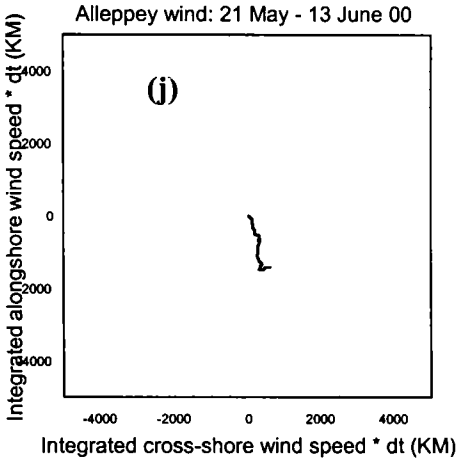

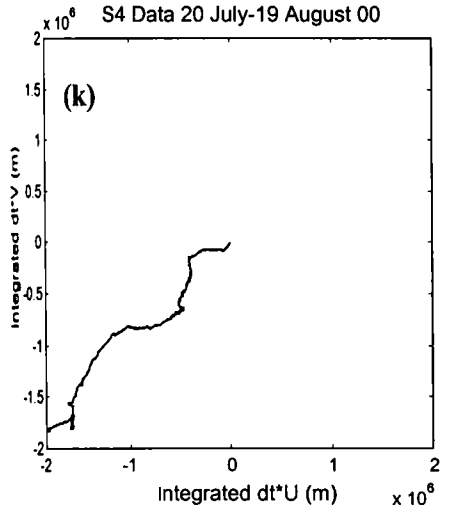

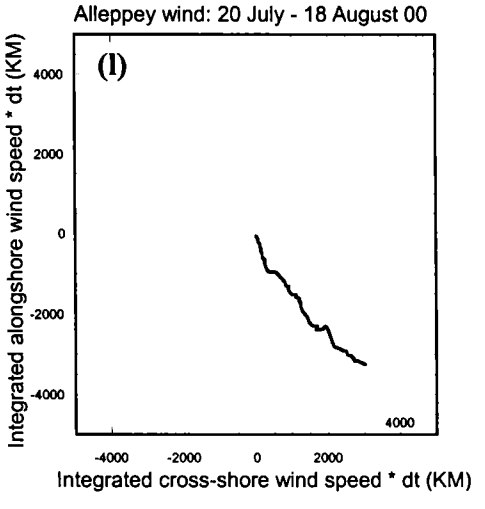

Fig. 4.22a-n Progressive vector plot of burst mean S4 current meter data, for the deployments from May 1999 to November 2000 and Alleppey wind records. The cross-shore and alongshore current velocities are rotated onto a shore-parallel direction (23° relative to True North) to get shore-normal and shore parallel components. North-south is alongshore and positive east is onshore.(Contd..)

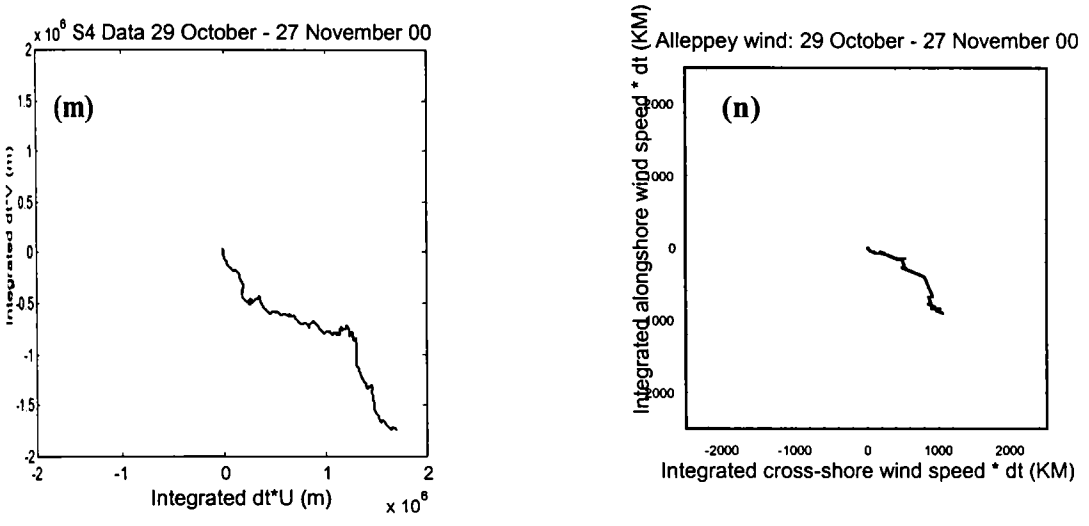

Fig. 4.22a-n Progressive vector plot of burst mean S4 current meter data, for the deployments from May 1999 to November 2000 and Alleppey wind records. The cross-shore and alongshore current velocities are rotated onto a shore-parallel direction (23° relative to True North) to get shore-normal and shore parallel components. North-south is alongshore and positive east is onshore (contd.....)

CHAPTER 5

BEACH PROCESSES

5. BEACH PROCESSES

5.1 INTRODUCTION

The interaction of the hydrodynamic processes with sediment in the beach and nearshelf results in sediment movement, which in turn decides the stability of the beach. Beaches erode, accrete or remain stable depending on the rates at which sediment is supplied to and/or removed from the beach. Profiles across a beach adapt to imposed wave conditions. Important wave characteristics affecting sediment transport near the beach are height, period and direction of breaking waves. Breaker height is significant in determining the quantity of sediments in motion, changes in wave periods affect cross-shore direction of transport and breaker direction is a major factor in determining longshore transport direction and rate. Understanding the evolution of the beach and its erosion/deposition cycles in relation to the forcing factors is of vital importance to sediment budgeting. As stated in Chapter 2, a comprehensive programme of beach measurements and littoral environmental observations were made during the present study period. This chapter presents a study of the beach processes of the area of study.

5.2 LITERATURE REVIEW

Beach processes have attracted attention of scientists and engineers since early sixties. These studies covered different aspects such as breaker wave characteristics, longshore currents, sediment transport, erosion/accretion processes, etc.

Studies on breaker wave characteristics and longshore currents/transport are relatively less when compared to erosion/accretion processes. Thomas (1988), Shahul Hameed (1988), Kurian (1988) and Harish (1988) have discussed the nearshore wave characteristics in relation to beach morphological variations at Valiathura, Alleppey, Calicut and Tellicherry respectively. Thomas (1988) observed that the breaker period was 11 to 12s during March and April and the breaker direction was 210° and 225° except during June-August, when the direction was 230 and 240° at Valiathura. Surf zone widen to around 150m during June-July and the width was practically zero during November- March. He measured longshore currents at six locations and found

that except for three months (June-August) the direction was northerly. During June-August, the direction was southerly.

Shahul Hameed (1988) analysed breaker wave data during 1981-84 and deduced the monthly averages of significant and maximum breaker wave heights, period, direction and type along Alleppey coast. He observed that the heights of breaking waves increase from April and reach a maximum in June. The breaker period ranged from 8 to 15s but most of the time it was between 9 and 11s. The breaker direction generally ranged from 245 to 265°. The longshore currents were generally weak and northerly in direction except during the peak of monsoon. Kurian (1988) observed a maximum breaker height of 2.25m at Calicut. He found that the breaker periods range between 5 and 12s and the direction ranged from 235 to 300°N. He found that the average value of the longshore current reaches as much as 70cm/s. In general, strong longshore currents are observed during the months April-August and low speeds are observed during the postmonsoon months of September-December. Harish (1988) observed that the maximum breaker height generally show a peak during June-July as observed at Valiathura, Alleppey and Calicut. He found that the breaker period varied from 10s during active monsoon to 15s during the calm season. He also observed that the longshore current direction was predominantly southerly during the active monsoon season and the pattern of longshore current during fair season was different on both sides of the pier at Tellicherry.

Jena and Chandramohan (1997) studied the littoral characteristics off Kolachal. They found that breaking wave heights exceeded 1.5m during May to August. Width of the surf zone was wider at about 35m in June to September and November and it was less during the rest of the year. The longshore current direction was towards east (down coast) in September and November to February, and towards west (up coast) during the rest of the year. The longshore current speed was higher exceeding 30cm/s in June to September, November and February and less with values less than 16cm/s in January, March and December. Variation of longshore current and sediment transport along the South Maharashtra coast was studied by Chandramohan et al. (1993). They observed that the longshore current velocity varied between 10 and 33cm/s. The

ngshore current direction was predominantly southward at Ratnagiri, Ambolgarh hile it was variable at Vengurala. Chandramohan et al. (1994a) studied the ngshore current along the Mulgund-Shiroda coast. They found that the longshore irection is not uniform along the coast indicating the presence of variable littoral ansport environment. Longshore current velocity varied predominantly between 8 nd 25cm/s. Chandramohan et al. (1994b) studied the longshore current along the outh Karnataka coast and found that it was stronger in June and relatively low and teady during rest of the year. The current velocity varied from 10 to 50 cm/s.

Some authors have tried computational methods/satellite data for study of longshore urrents and sediment transport. Reddy (1970) used wave refraction diagrams to etermine longshore current pattern and sediment transport along some locations of he west coast. Chandramohan and Rao (1984) used computational methods for the etermination of longshore currents off Visakhapatnam beach. Using modified onguet-Higginson equation and Galvin equation, they computed longhshore currents nd compared it with measured longshore currents. They found that the deviation etween measured and computed was comparatively less in March to July and November to January. During other months, the variation was more and inconsistent. Hameed et al. (1986) computed the longshore current velocities along Alleppey and Valiathura beaches using four widely used models and compared them with measured alues. Longshore currents along the beaches of Mangalore have been studied over a eriod of one year by Jayappa (1996). He found that the sector-wise average ongshore current velocity was high (18, 16 and 17cm/s in the northern, middle and outhern sectors respectively) from March to November at Mangalore. Sajiv et al. 1997) studied the littoral processes at 8 stations spread over the Kerala coast. They btained longshore current values in the range 20-60 cm/s. Santhosh and Reddy 2002) studied the sediment movement and coastal processes along the Mangalore oast using satellite imageries and field measurements. They observed that the ongshore current velocity varied from 10 to 42cm along Mangalore coast.

A number of studies are available on the erosion/accretion regime of the west coast. The earlier investigations on erosion/accretion include a study on the erosion and

protection of Kerala coast by Joseph (1962), an analysis of the problem of beach erosion and its prevention by Menon (1964) and a study on beach nourishment of Purakad beach by Mony and Nambiar (1965). The seasonal variations of some of the beaches of Kerala were discussed by Mony and Nambiar (1966)

Ravindran et al. (1971) studied the shoreline changes along the entire coast of Kerala utilising available historic maps. They reported severe erosion along most of the Kerala beaches excepting West Hill, Vypeen, Ambalapuzha, Neendakara, and Sakthikulangara where accretion was indicated. Thirupad (1971) carried out a detailed investigation on the coastal erosion along Manakodam-Thottapally region using wave refraction analysis and identified areas vulnerable to erosion and accretion. Stability of the coastline from Manakodam to Thottapally was investigated graphically by Varma and Varadachary (1977). Murty (1977) carried out an investigation on the shoreline dynamics at certain places along the West Coast of India including the Kerala coast. John and George (1980), by comparing maps of 1850 and 1966 concluded that the Kerala coast underwent erosion during that time. The interaction between beach topography and wave forces in the presence of seawalls was investigated by Murty et al. (1980). Murty and Varadachary (1980) discussed the profile variations of the Valiathura beach using measured data. Varma et al. (1981) estimated the quantum of sediment involving beach topographic variations utilising field observations on profiles. Shenoi and Prasannakumar (1982) identified areas of possible erosion and accretion along the shoreline from Andhakaranazhi to Azhikode on the Kerala cost. Their study indicated that the coastline showed an erosional tendency under the influence of waves approaching from 220° and 240° and an accretional tendency under the influence of waves from 280° and 300°.

Thrivikramji et al. (1983) studied the shoreline fluctuation over a gap of 55 years (1910-1965) and showed that Kerala coast had gained 41 km^2 by accretion and lost 22 km^2 by erosion during this period. Machado and Baba (1984) investigated the movement of beach sand in Vizhimjam while Machado and Vasudevan (1984) discussed the bathymetric variations over the innershelf off this coast. Sreekala et al. (1998) studied the shoreline changes of Kerala coast using IRS data and aerial

photograph. They compared the recent data with Survey of India Topographic maps of 1967 and found that 148-km of the Kerala coast is eroding and 304 km of the coast is accreting.

At Valiathura, Thomas (1988) found that the volume changes on the sub-aerial beach are systematic with slow erosion over the period from January to June, rapid erosion in June and July and recovery from August to December. The erosion coincides with the onset of the stormy, south-west monsoon. In synchrony with the erosion cycles, the beach slope is maximum during the periods of scour and then reduces as the profile recovers.

Shahul Hameed (1988) and Kurian et al. (1985) studied beach-nearshore morphological changes at Alleppey using profiles that extend more than 300m offshore. They observed a characteristic steep beach above 3 m depth and then a long, near-horizontal platform offshore. By studying the changes in the profile of the beach and nearshore they found that the erosion of the beach is followed by accretion in the nearshore zone and vice versa. Most of the vertical adjustment is restricted to the upper beach around mean water level, but the level of the platform moves considerably in most years. Once again, the maximum beach erosion occurs around June/July and recovery is strongest in November/December. Shahul Hameed (1988) obtained cumulative volume changes of about 60 m^3/m over the accreting phase of the annual cycle which convert to about 0.5 $m^3/m/day$. Notably, the shoreline accreted overall during the 4-year measurement period from 1981-84 inclusive. Further up the coast at Calicut, Kurian (1988) observed similar pattern of changes in the beach profile and volume at sites that he studied.

Chavadi and Bannur (1992) carried out detailed study on beach profiles along Ramangundi beach of North Karnataka Coast (west coast of India). Within the 800 m long pocket type of beach he observed considerable alongshore variability in volume changes and foreshore slopes. Chandramohan et al. (1994a) studied the beach processes between Mulgund and Shiroda and found that the beaches are stable and gain maximum profiles during February to April. The surfzone dynamics along the

south Karnataka coast between Bhatkal and Ullal was studied by Chandramohan et al. (1994b). They found that the beaches are stable. Beaches after being subject to erosional phase during SW monsoon were found to be regain their profile by January or February. The relationship between the surf zone processes and the morphodynamic state of beaches between Vaipar and Tiruchendur along the southeastern coast of Tamil Nadu (India) was studied through 46 beach profile measurements and other morphological features across and along the shoreline by Ramanujam et al. (1996). They found that the dissipative beaches with higher wave heights and low beach gradients yield the higher amount of surf-scale parameter (22.0 to 154.3) whereas at the other extreme, the reflective beaches with steep beach gradients and lower wave height conditions resulted with low surf-scale value (0.5711 to 2.500). Dattatri et al. (1997) also reported that the changes in the south Karnataka coast are cyclic in nature maintaining long term equilibrium. Major changes are observed only at the river mouths and beaches adjacent to river mouths. Nearshore processes along north Karnataka coast were studied by Sanil Kumar et al. (2001a). They selected ten stations for the study and observed the lowest beach levels during the southwest monsoon period except at two stations, where it was observed during northeast monsoon period. The beaches had undergone the seasonal erosion and were stable during the annual processes along the stretch of the coastline between Karwar and Bhatkal.

Some of the salient features that could be summarised out of the available literature with regard to the beach processes of the southwest coast are as follows. The littoral environmental parameters show both spatial and temporal variations. The temporal variations are dictated by the monsoon regime. The spatial variations are determined by the response of the hydrodynamic forces to the geomorphic setup of the beach and innershelf. In general it can be said that southerly longshore currents prevail during the southwest monsoon and northerly currents during the rest of the year. In general three types of beach profiles are observed along the southwest coast: (i) a narrow beach, steep foreshore and longshore bars during the monsoon; (ii) a gently sloping beach face indicative of developing beach during the post-monsoon and (iii) a wide beach, steep foreshore and a well developed berm during pre-monsoon. With inter-

annual variations in the weather and differences in the strength of the monsoon, the magnitudes of seasonal changes vary from year to year.

5.3 BEACH PROCESSES OF THE AREA OF STUDY

5.3.1 Littoral Environmental Processes

5.3.1.1 Breaker wave height

The significant breaker wave heights (H_b) (Fig. 5.1) show seasonal variations as seen in the case of offshore waves (Chapter 3). During the monsoon period H_b was above 1m for most of the time, and sometimes exceeds 2m. During postmonsoon season H_b reduced considerably and was less than 1m in almost all days except for a few cases during the October. During 1999 (with observation starting from May) the values varied from 0.3 to 2.78m with the average value of 1.27m.The most frequently occurring breakers as seen from the frequency distribution are those in the height range of 0.75-1.0 m constituting 55% of the occurrences. More than 70% of the cases fall within the range 0.75-1.5 m. During 2000 also seasonal variations are observed but breaker height is less in comparison with 1999. During 2000, the values of H_b range from 0.29 to 2.22m with average value 0.88m. 68% of the observations are in the range 0.75-1.5m.

During 2001, H_b values recorded the highest value of 4.0m in the 3-year study period. In the month of June 2001, the highest recorded value is only around 2.0 m. However, in the first two weeks of July breaker height was more than 2m in all days and recorded a value as high as 3.5m during that time. After a short calm spell, breaker height further increased in the third week of July and recorded the highest value of 4m. During 2001, H_b values in the range 1-2m constitute 66% of the distribution.

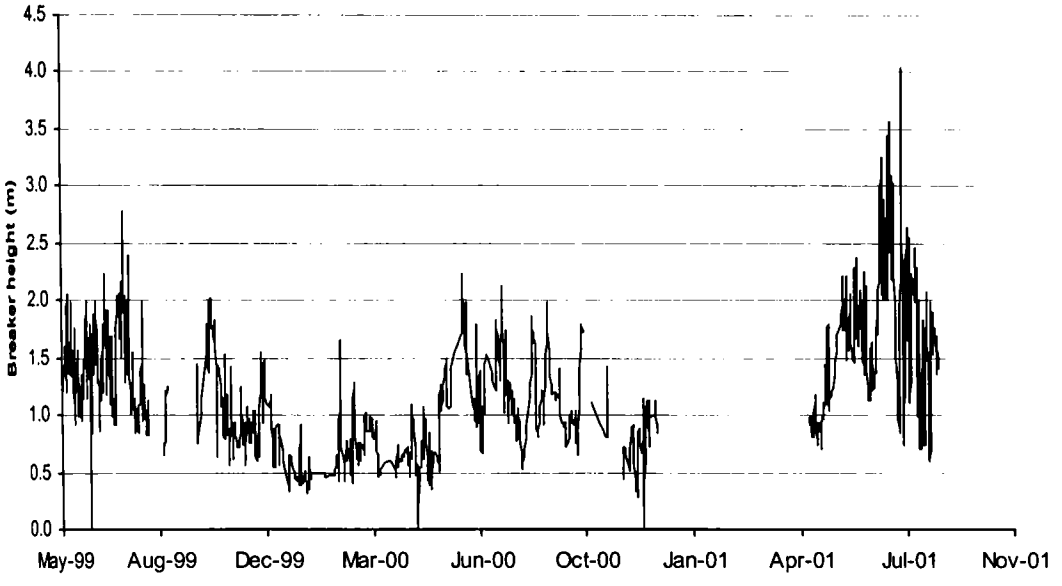

Fig. 5.1 Time series plot of breaker wave height

5.3.1.2 Breaker period

Breaker periods also show seasonal variations (Fig. 5.2). During 1999, breaker period ranges from 7 to 16s. During monsoon months breaker period is around 10s. Breaker periods in the range 9-11s constitute 65% of the distribution in 1999. Though the extent of variations is less, the same patterns of seasonal variations are seen in 2000 too. Breaker periods lower than 10s are seen for a limited period in monsoon. As observed in November 1999, breaker period was high in November 2000 and recorded the highest value of 16s. In 2000, the range 11-13s constitutes 79% of the distribution. During 2001, breaker period ranges from 6 to 16s with a mean of 10.6s. Higher periods were observed in the middle of May. Breaker periods in the range 10-12s constitute 65% of the distribution in 2001 (Observations limited up to August). It is observed, the breaker period values are in general lower during the monsoon and higher during the other periods. Also, the ranges are wider during the post-monsoon period, when long period waves as well as the short period waves due to locally generated wind occur.

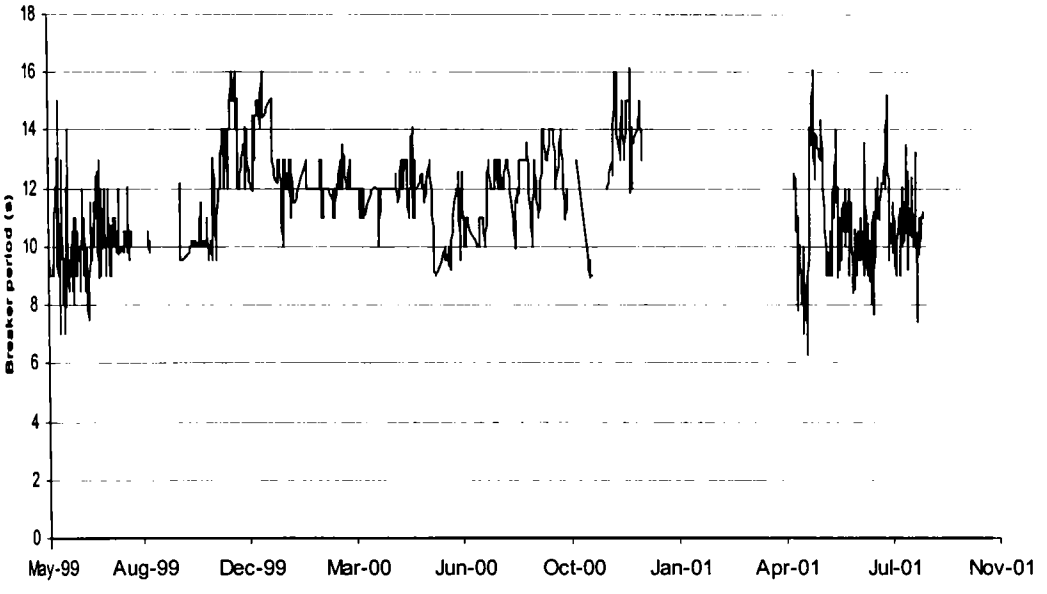

Fig. 5.2 Time series plot of breaker wave period

5.3.1.3 Breaker direction

Breaker direction showed a wide range in this area (Fig. 5.3). During 1999 it ranged from 230 ° N to 280 ° N with an average of 254 ° N. Waves are generally from a direction around 260° N during the monsoon, i.e., they are nearly shore-normal during this season. From the end of July, the direction starts to shift back to the south of the normal with the values between 240 and 250° N till the end of monsoon. During '99 the range 240-260 ° N constitutes 84% of the distribution.

The range of distribution decreased during 2000. During that year, the range 240-260 °N constituted 93% of total distribution. But in 2001, breaker direction distribution showed wider range from 200 ° N to 280 ° N. As observed in 1999 and 2000, the predominant range is 240 ° N to 260 ° N that constitutes 75% of total distribution.

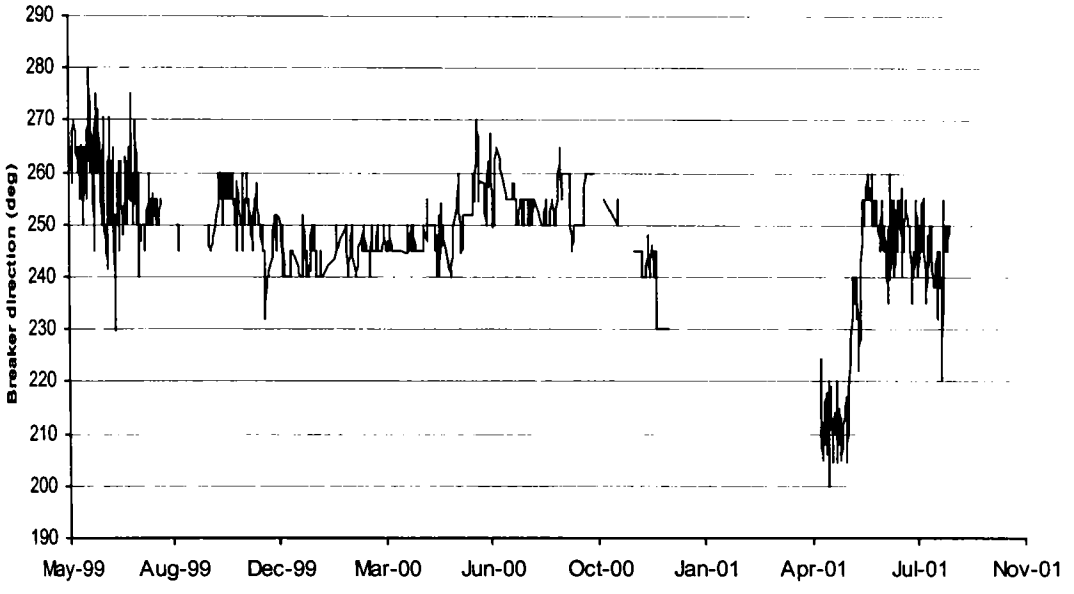

Fig. 5.3 Time series plot of breaker wave direction

5.3.1.4 Surf zone width

The surf zone width is an indication of the wave intensity. It decreases from very low values of the order of 5 m (Fig. 5.4) in the fair weather months of November - April to a maximum of about 750m during the monsoon. Occasionally during the peak monsoon period of June-July, spilling breakers occur quite offshore, and the surf zone width is always high during this period of intense wave activity.

In 1999, surf zone width varied from 3 to 600m. During June 1999, the width was more than 50m in most of the days. Surf zone width decreased considerably during post-monsoon seasons. In 2000 also surf zone width varied seasonally. During monsoon period the width increased up to 720m. During premonsoon and post monsoon months, the width is less than 10m. Surf zone width increased considerably in 2001. Width increased up to 240m in May 2001. In June, surf zone width was comparatively less but in July width increased and recorded a maximum of 750m. In comparison with previous years, surf zone width showed higher values in May-August months of 2001.

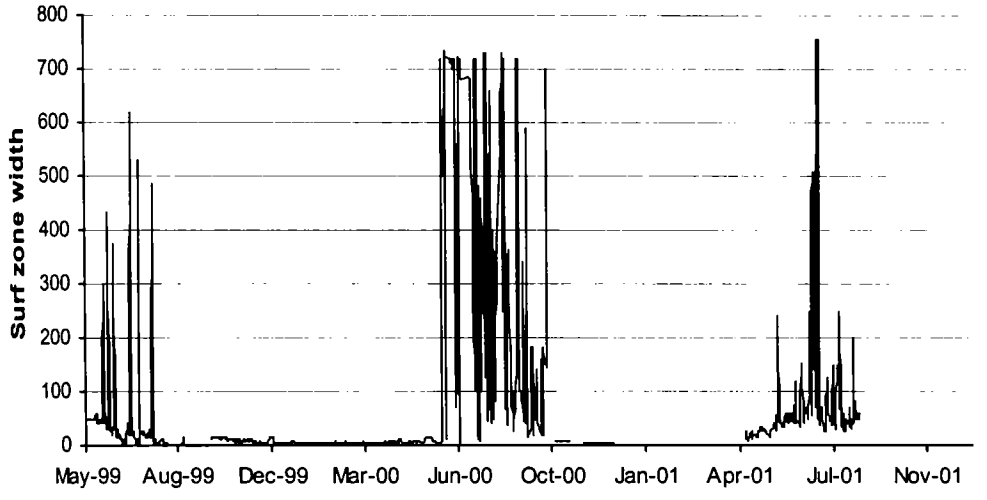

Fig. 5.4 Time series plot of surf zone width

5.3.1.5 Longshore current

Longshore currents also showed strong seasonal variations (Fig. 5.5). In general, longshore current was southerly during monsoon months and northerly during the rest of the year. In 1999, longshore currents were strong in May. The velocity reached up to 80 cm/s during the last week of May and the direction was southerly. Northerly currents up to 30 cm/s were observed during October. In 2000, like other littoral parameters, longshore current values were less except in the first week of June. In the first week of June, strong southerly currents up to 83 cm/s were observed. Strong northerly currents observed in May 1999 were absent in May 2000. Unlike October 1999, southerly longshore currents up to 20 cm/s were observed in October 2000. In 2001, during the observation period of January to August, current velocity was less and recorded a maximum of 33 cm/s during the first week of July.

The longshore currents observed are in tune with the breaker parameters. Southerly currents are generated by breakers north of the shore-normal and vice versa. Intense breakers north of the shore-normal are seen during the peak monsoon activity resulting in strong southerly currents during that time.

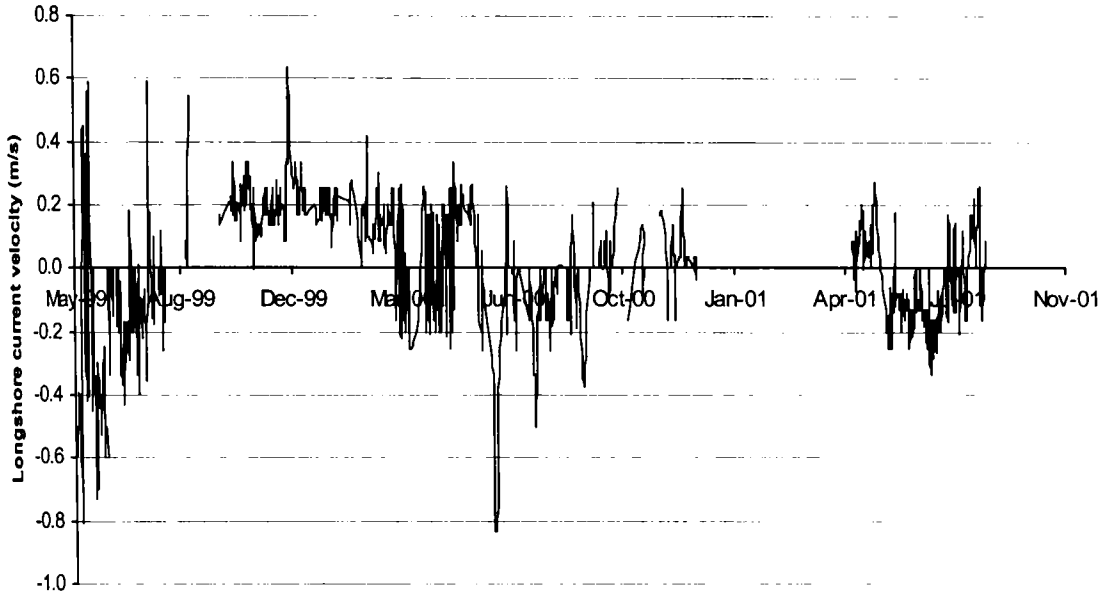

Fig. 5.5 Time series plot of longshore current. Positive values indicate northerly and negative values indicate southerly direction.

5.3.2 Beach/ Nearshore Profiles

5.3.2.1 Beach profiles

As stated in Section 2.7.1, fortnightly beach profile measurements, have been carried out at VMS 1-11 KMS 1-5 which are at close intervals and monthly measurements at stations NK1-19 which are at 1-km interval (Fig. 5.6). Thus beach profiles from a total of 31 stations have been collected regularly during the period May 1999 – August 2001. The beach profiling at 3 stations viz. VMS4, VMS7 and KMS3 was continued till June 2004 (totally 5 years) to understand the long-term trend in the erosion/accretion cycle. Representative beach profiles for the period 1999-2001 are presented in Fig. 5.7, 5.8 & 5.9. As expected, the beach has maximum width during the fair weather months. The profiles reach the nadir during the monsoon and the lowest width of the beach is observed in the months of May-June-July, when the wave intensity is at its maximum. The changes in the beach width are least at stations fronted by sea walls and maximum at stations not fronted by seawalls. The backshore of profiles at mining sites occasionally show bumps indicative of sediments dumped by IREL by scraping from the foreshore (eg. KMS 2, KMS 3, VMS 4, VMS 5 etc.). The vertical and horizontal movements were 4 m and 60 m respectively, at VMS 5.

VMS 7, over 5 m of vertical movement and 60 m of horizontal movement of the each face occurred. At KMS 3, the vertical and horizontal movements were about 3 and 25 m respectively. At NK 4 (about 10 km north of Vellenathuruthu mining site), which is a fishing gap with no sea wall, the vertical and horizontal movements were about 2 m and 30 m respectively.

5.3.2.2 Beach volume changes

The beach volume changes between successive measurement dates were calculated from the beach profile data using a computer program developed by Hameed (unpublished). From this, beach volume changes per day were worked out. The results are presented in Fig. 5.10 and 5.11 for the mining sites of Vellenathurathu and Kovilthottam respectively. Unlike other natural situations the beach profiles and volume changes at the mining sites are influenced by the mining operations too in addition the natural processes. Also, the mining activities bring in anomalies in the beach profiles and volume changes on a temporal and spatial frame due to the dumping of scrapped material in the backshore, which often is collected at a later date. On a temporal scale the volume changes show typical seasonal erosion/accretion pattern. Fig. 5.12 presents the average monthly volume change for the mining sites. In general, significant erosional tendency is observed during the pre-monsoon months of April and May and the monsoon onset month of June. Beach build up tendency starts in the month of July, but is often interrupted during monsoon and continues till March.

As expected, there is noteworthy fluctuation between the stations and not all stations behave identically, which can be explained by the effects of nearshore circulation, presence of sea walls and the influence of the mining operation. At stations fronted by sea walls (eg. VMS 1-3, 10-11, KMS 1&5) the magnitude of the volume change is very nominal except on few occasions when the values reach up to 1.5m^3/m/day. At the mining sites (VMS 4-9; KMS 2-4), which are not fronted by sea walls, the volume changes are significant, and in few cases reach values as high as 9m^3/m/day. At the Vellanathuruthu mining site, maximum changes are noticed at station VMS 5, while at Kovilthottam, the maximum changes are noticed at KMS 3. It may be noted that

these stations of maximum volume changes lie on the northern part of the mining sites. It can be attributed to the intensive beach building process that takes place in these stretches during fair weather periods under the influence of northerly longshore transport.

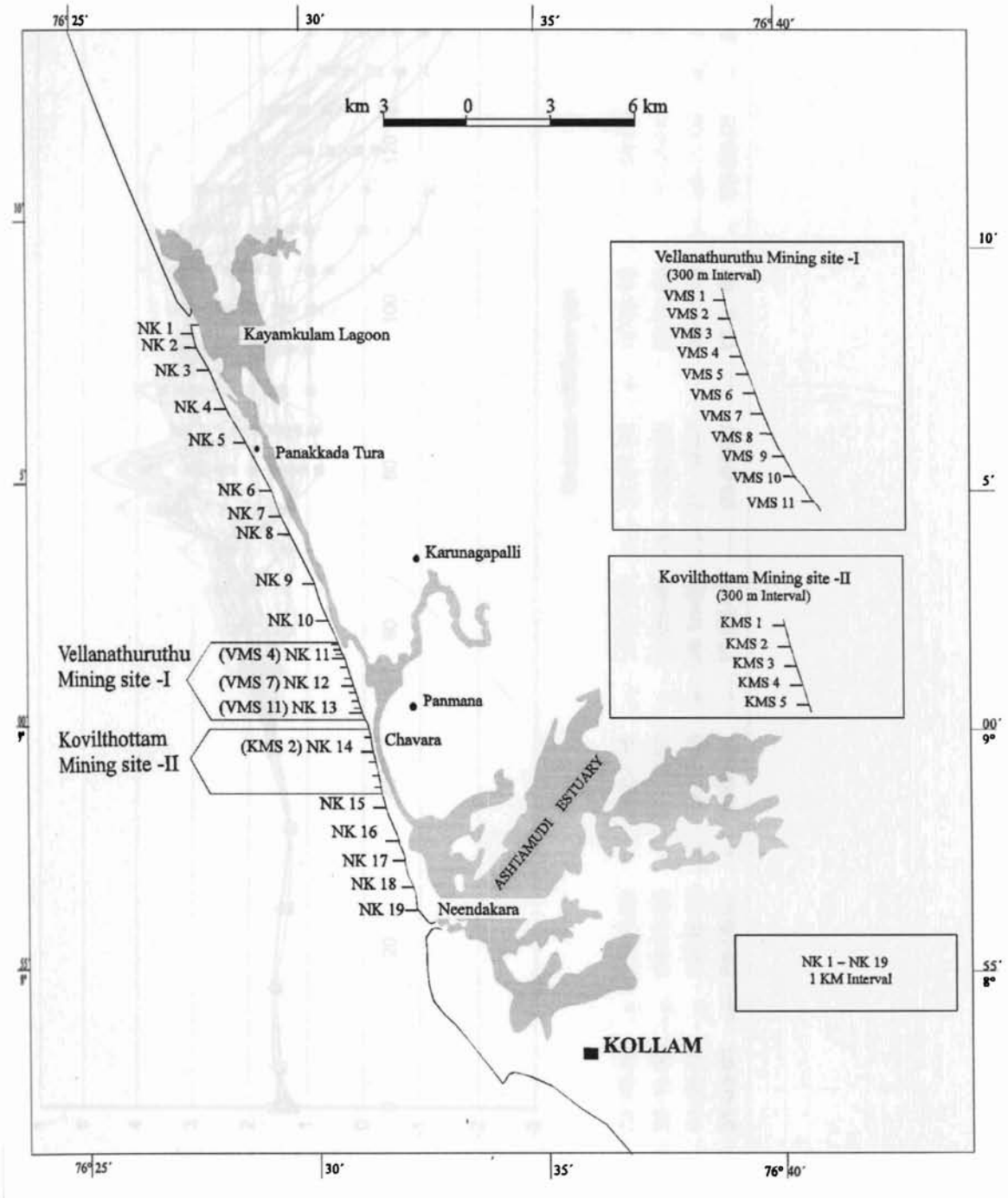

Fig.5.6 (Fig. 2.14 reproduced) Beach monitoring stations along the Neendakara-Kayamkulam coast

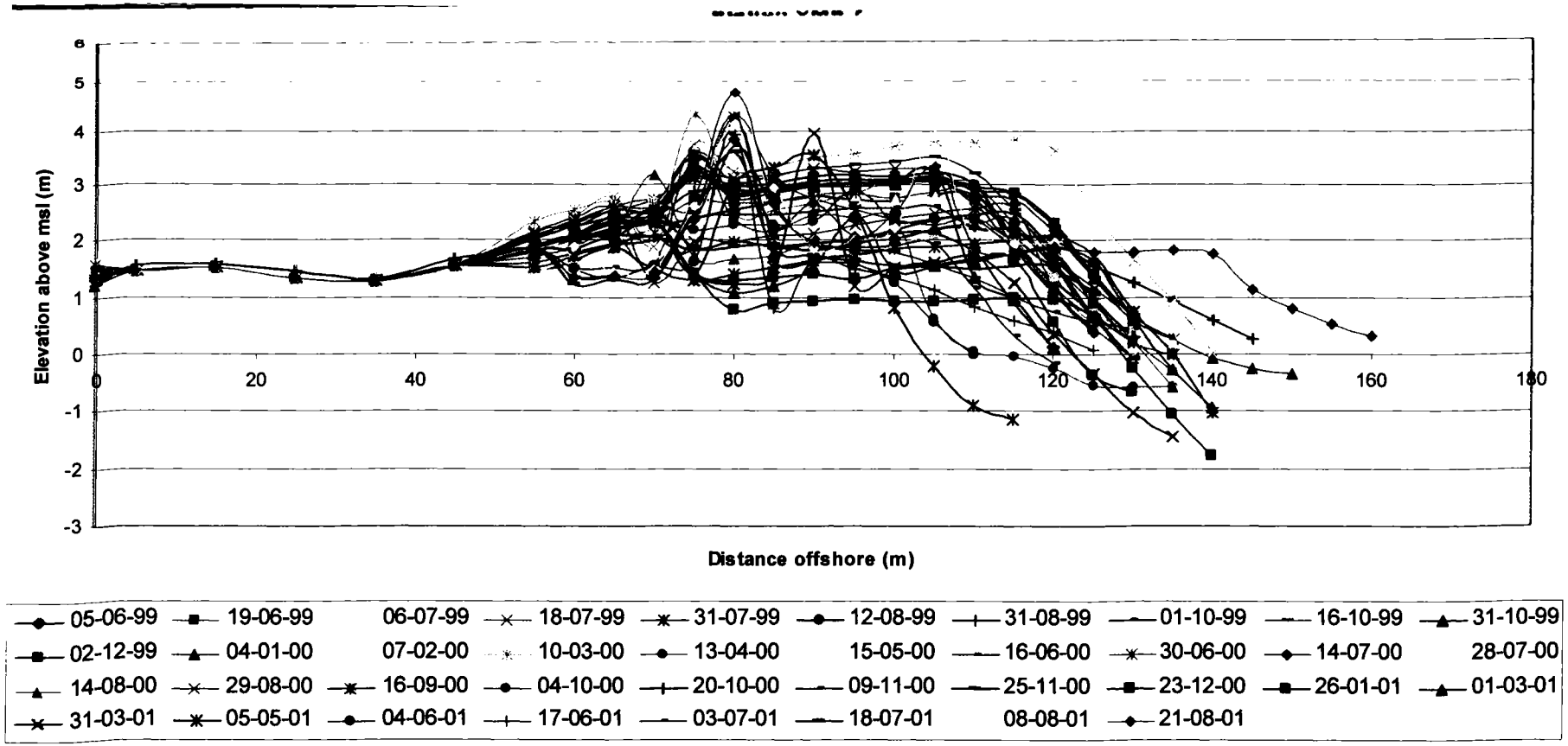
Elevation above msl (m)
6
5
4
3
2
1
0
-1
-2
-3
0
20
40
60
80
100
120
140
160
180
Distance offshore (m)
05-06-99
19-06-99
06-07-99
18-07-99
31-07-99
12-08-99
31-08-99
01-10-99
16-10-99
31-10-99
02-12-99
04-01-00
07-02-00
10-03-00
13-04-00
15-05-00
16-06-00
30-06-00
14-07-00
28-07-00
14-08-00
29-08-00
16-09-00
04-10-00
20-10-00
09-11-00
25-11-00
23-12-00
26-01-01
01-03-01
31-03-01
05-05-01
04-06-01
17-06-01
03-07-01
18-07-01
08-08-01
21-08-01

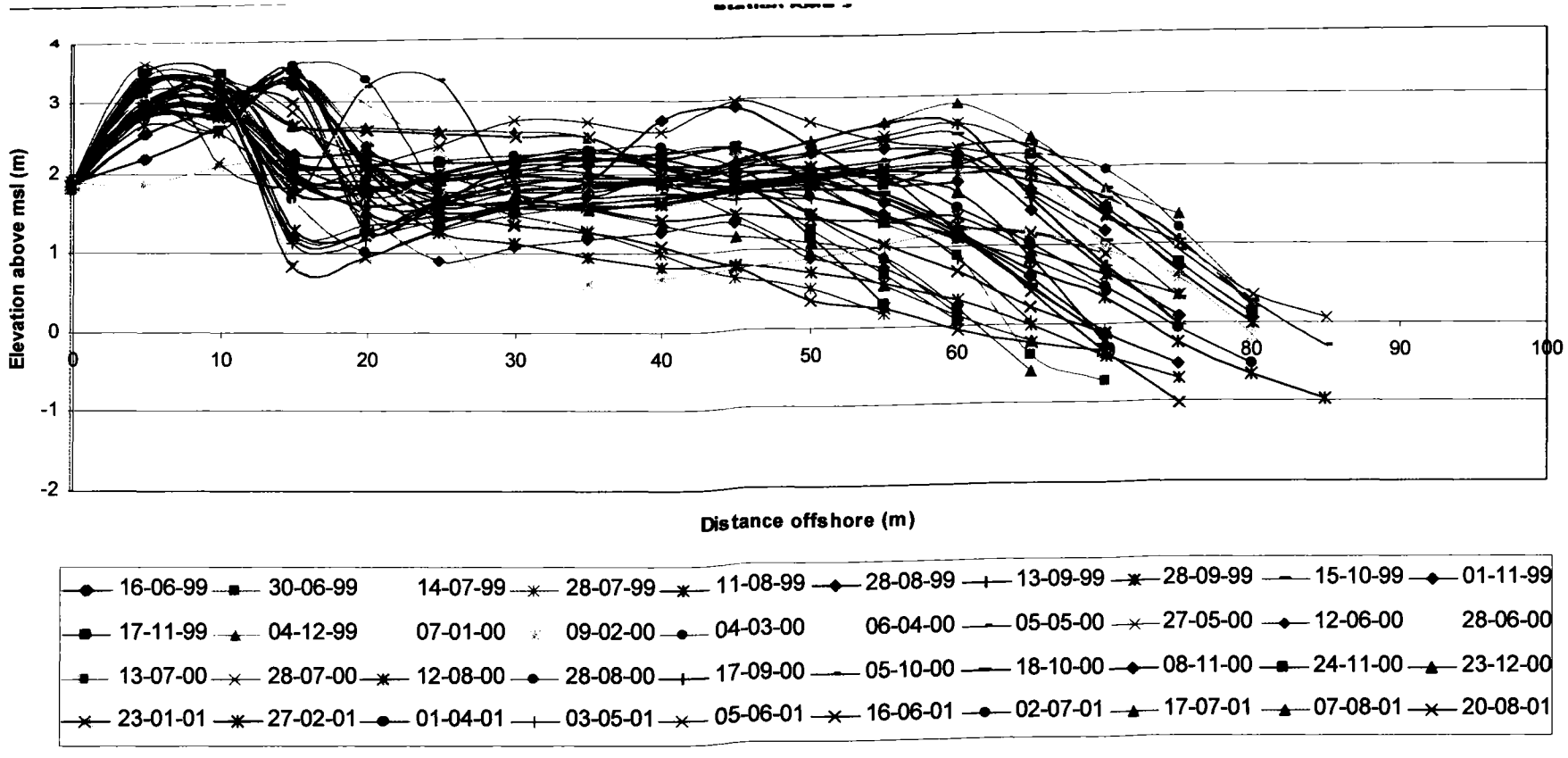
Elevation above msl (m)
4
3
2
1
0
-1
-2
0
10
20
30
40
50
60
80
90
100
Distance offshore (m)
16-06-99
30-06-99
14-07-99
28-07-99
11-08-99
28-08-99
13-09-99
28-09-99
15-10-99
01-11-99
17-11-99
04-12-99
07-01-00
09-02-00
04-03-00
06-04-00
05-05-00
27-05-00
12-06-00
28-06-00
13-07-00
28-07-00
12-08-00
28-08-00
17-09-00
05-10-00
18-10-00
08-11-00
24-11-00
23-12-00
23-01-01
27-02-01
01-04-01
03-05-01
05-06-01
16-06-01
02-07-01
17-07-01
07-08-01
20-08-01

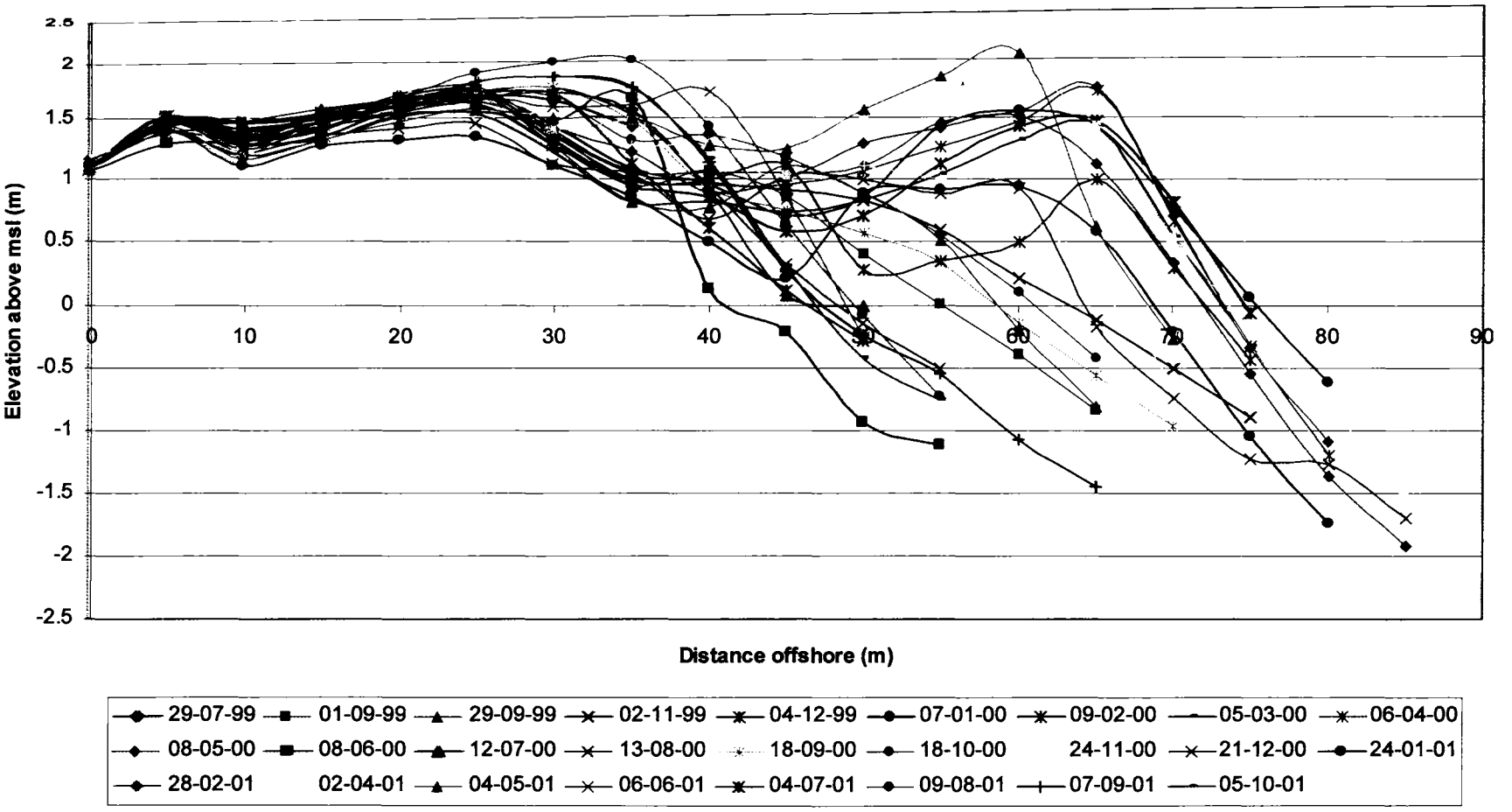
Elevation above msl (m)
2.5
2
1.5
1
0.5
0
-0.5
-1
-1.5
-2
-2.5
0
10
20
30
40
60
70
80
90
Distance offshore (m)
29-07-99
01-09-99
29-09-99
02-11-99
04-12-99
07-01-00
09-02-00
05-03-00
06-04-00
08-05-00
08-06-00
12-07-00
13-08-00
18-09-00
18-10-00
24-11-00
21-12-00
24-01-01
28-02-01
02-04-01
04-05-01
06-06-01
04-07-01
09-08-01
07-09-01
05-10-01

Anomalies in the volume changes are prominently seen in some cases. For example, while significant accretion is found at VMS 5 in the first fortnight of August 99, no volume change is noticed at the adjoining VMS 6. In a similar way, while a huge quantum of accretion is found at VMS 5 in the second fortnight of July 2000, only very marginal accretion is found during this period at VMS 6. These anomalies could be the direct result of the mining activities concentrating on specific sites.

5.3.2.3 Cumulative volume changes along the coast

The cumulative volume change (Fig. 5.13) obtained by successive addition of volume changes for each period gives an indication of the state of erosion or accretion of a beach at any point of time with reference to an initial reference date. It may be noted that the first survey in this study was done in the period of May – June 99 when the beach was partially eroded due to the first monsoonal onslaught by waves. This has to be kept in mind while interpreting the results of cumulative volume change.

Fig. 5.13a shows the cumulative volume change for the sector adjoining the mining sites, protected by sea walls. As seen earlier, the volume change here is the least and thus the cumulative volume change is practically nil. This situation appears to have undergone some change in the pre-monsoon of 2001 when an accretion upto 4 m^3 /m is noticed. This material is however lost with the onset of monsoon and a cumulative erosion of upto about 12m^3/m is observed by the middle of August 2001. This unusual pattern appears to be due to some significant erosion observed at the VMS 3 and VMS 10 stations. Fig. 5.13b gives the cumulative volume changes for the mining sites (VMS 4-9 and KMS 2-4) which are not protected by sea walls. As already mentioned, the reference time is the month of May when the beach monitoring started. With the commencement of accretory processes in July, the cumulative volume shows an increase. However, this upward trend in cumulative volume is interrupted by the erosion that occured in September – October. With the accretory processes setting in again from October, the cumulative volume continues its upward march and reaches its peak value of 60 m^3/m in February when the beach is more or less in an equilibrium condition with maximum width. From February onwards the

volume starts its downward trend with no further accretion, but loss of material takes place on account of the mining by IREL.

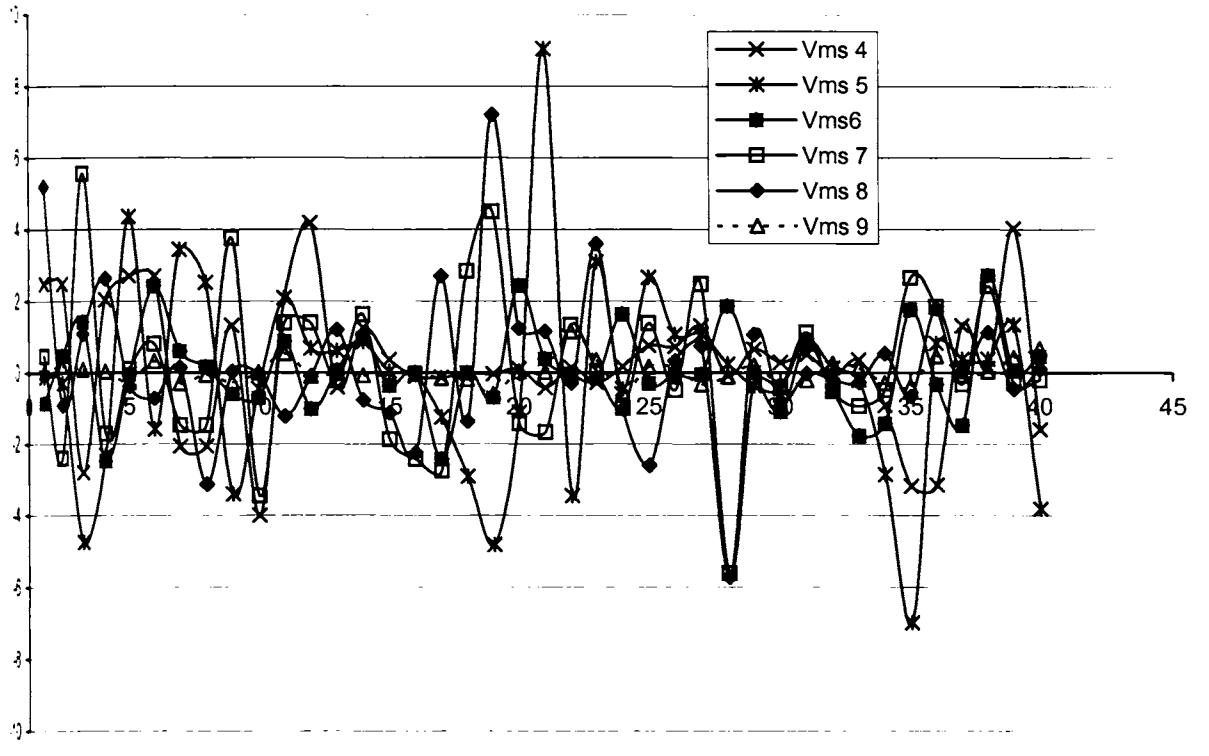

1	05/06/99-19/06/99	11	31/10/99-18/11/99	21	14/07/00-28/07/00	31	26/01/01-01/03/01
2	19/06/99-06/07/99	12	18/11/99-02/12/99	22	28/07/00-14/08/00	32	01/03/01-31/03/01
3	06/07/99-18/07/99	13	02/12/99-04/01/00	23	14/08/00-28/08/00	33	31/03/01-05/05/01
4	18/07/99-31/07/99	14	04/01/00-07/02/00	24	28/08/00-16/09/00	34	05/05/01-04/06/01
5	31/07/99-12/08/99	15	07/02/00-10/03/00	25	16/09/00 -04/10/00	35	04/06/01-17/06/01
6	12/08/99-31/08/99	16	10/03/00-13/04/00	26	04/10/00-20/10/00	36	17/06/01-03/07/01
7	31/08/99-16/09/99	17	13/04/00-15/05/00	27	20/10/00-08/11/00	37	03/07/01-18/07/01
8	16/09/99-01/10/99	18	15/05/00 -16/06/00	28	08/11/00-25/11/00	38	18/07/01-08/08/01
9	01/10/99-16/10/99	19	16/06/00-30/06/00	29	25/11/00-23/12/00	39	08/08/01-21/08/01
10	16/10/99-31/10/99	20	30/06/00-14/07/00	30	23/12/00-26/01/01	40	21/08/01-05/09/01

Fig. 5.10 Beach volume changes (m^3/m/day) between June 1999 and September 2001 at Vellenathuruthu mining site (VMS). The table shows the beach profiling dates and volume computation periods.

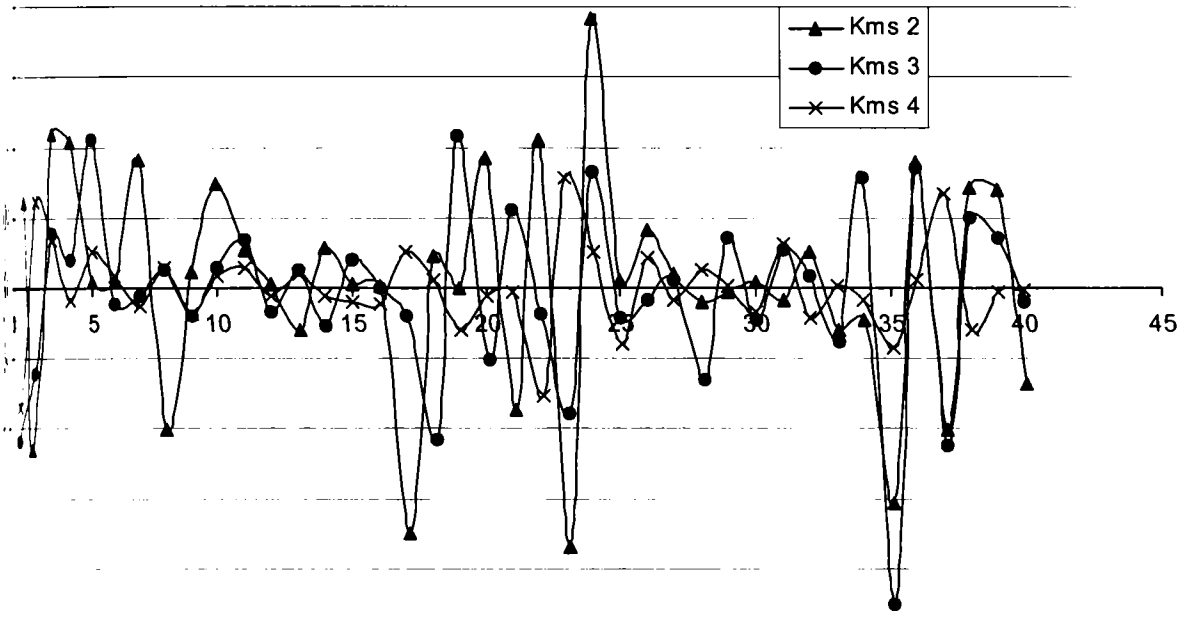

1	16/06/99-30/06/99	11	17/11/99-04/12/99	21	13/07/00-28/07/00	31	23/01/01-27/02/01
2	30/06/99-14/07/99	12	04/12/99-07/01/00	22	28/07/00-12/08/00	32	27/02/01-01/04/01
3	14/07/99-28/07/99	13	07/01/00-09/02/00	23	12/08/00-28/08/00	33	01/04/01-03/05/01
4	28/07/99-11/08/99	14	09/02/00-04/03/00	24	28/08/00-17/09/00	34	03/05/01-05/06/01
5	11/08/99-28/08/99	15	04/03/00-06/04/00	25	17/09/00-05/10/00	35	05/06/01-16/06/01
6	28/08/99-13/09/99	16	06/04/00-05/05/00	26	05/10/00-18/10/00	36	16/06/01-02/07/01
7	13/09/99-29/09/99	17	05/05/00-27/05/00	27	18/10/00-08/11/00	37	02/07/01-17/07/01
8	29/09/99-15/10/99	18	27/05/00-12/06/00	28	08/11/00-24/11/00	38	17/07/01-07/08/01
9	15/10/99-01/11/99	19	12/06/00-28/06/00	29	24/11/00-23/12/00	39	07/08/01-20/08/01
10	01/11/99-17/11/99	20	28/06/00-13/07/00	30	24/12/00-23/01/01	40	20/08/01-06/09/01

Fig. 5.11 Beach volume changes (m^3/m/day) between June 1999 and September 2001 at Kovilthottam mining site (KMS). The table shows the beach profiling dates and volume computation periods.

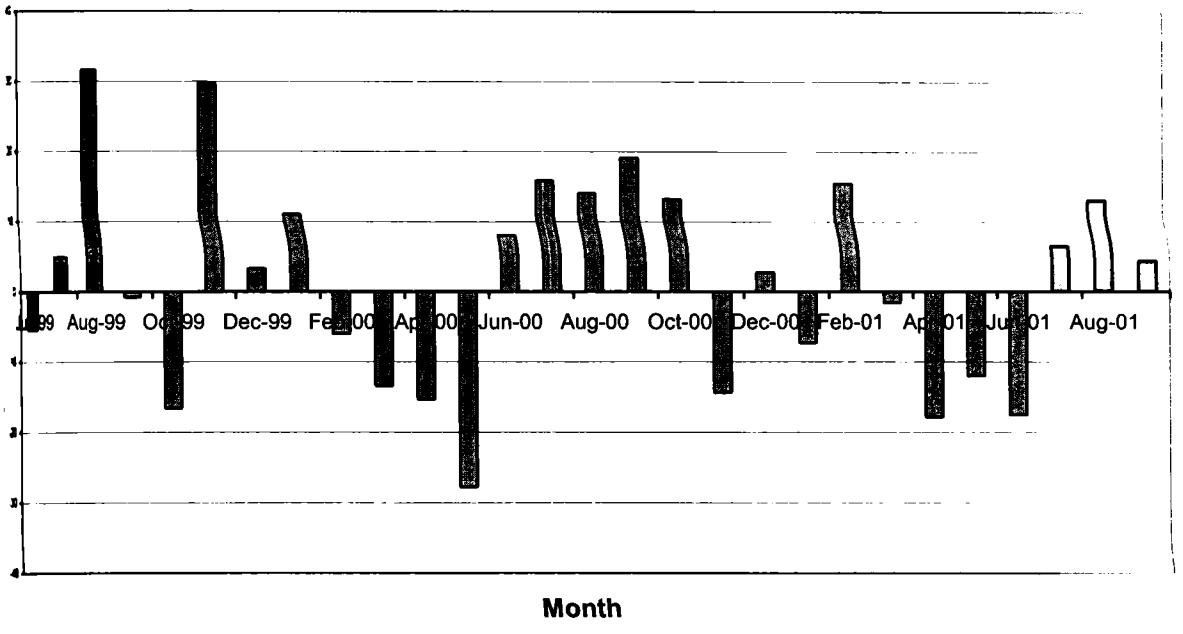

Fig. 5.12 Monthly mean beach volume changes (m^3/m) between June 1999 and September 2001 at the mining sites. [VMS (4-9) and KMS (2-4)]

From April onwards the downward trend is very pronounced due to the erosionary processes set in motion due to pre-monsoonal waves. This is further accelerated with the onset of monsoon and the lowest point is reached again in July. It is interesting to note that over a full year, say May 1999 to May 2000, the cumulative volume is at the same level and there is no net erosion or accretion over this period.

From July 2000, again the cycle is repeated with some minor deviations. In the year 2000, the interruption to the upward trend of the volume is very minimal. Thus, the peak level is reached quite early in this year and the level reaches up to 70 m^3/m, though only for a short period. Surprisingly, the volume level goes down towards the end of the year probably due to the IREL mining and the peak level typical of fair weather period is not maintained. However, the level picks up once again by March from where the dip towards the monsoon low starts. Unlike the previous two years, the dip in the volume doesn't go to the lowest level in 2001. In the post monsoon season of 2001, the trend is once again repeated. By the end of the study period (September 2001), the volume level has reached nearly $40m^3/m$, which is more or less the same level as in previous years.

The maximum observed volume change of 70-80 m^3/m lies between the measurements of Hameed (1988) of 40-80 m^3/m at Alleppey and Thomas (1988) of 100-150 m^3/m at Valiathura.

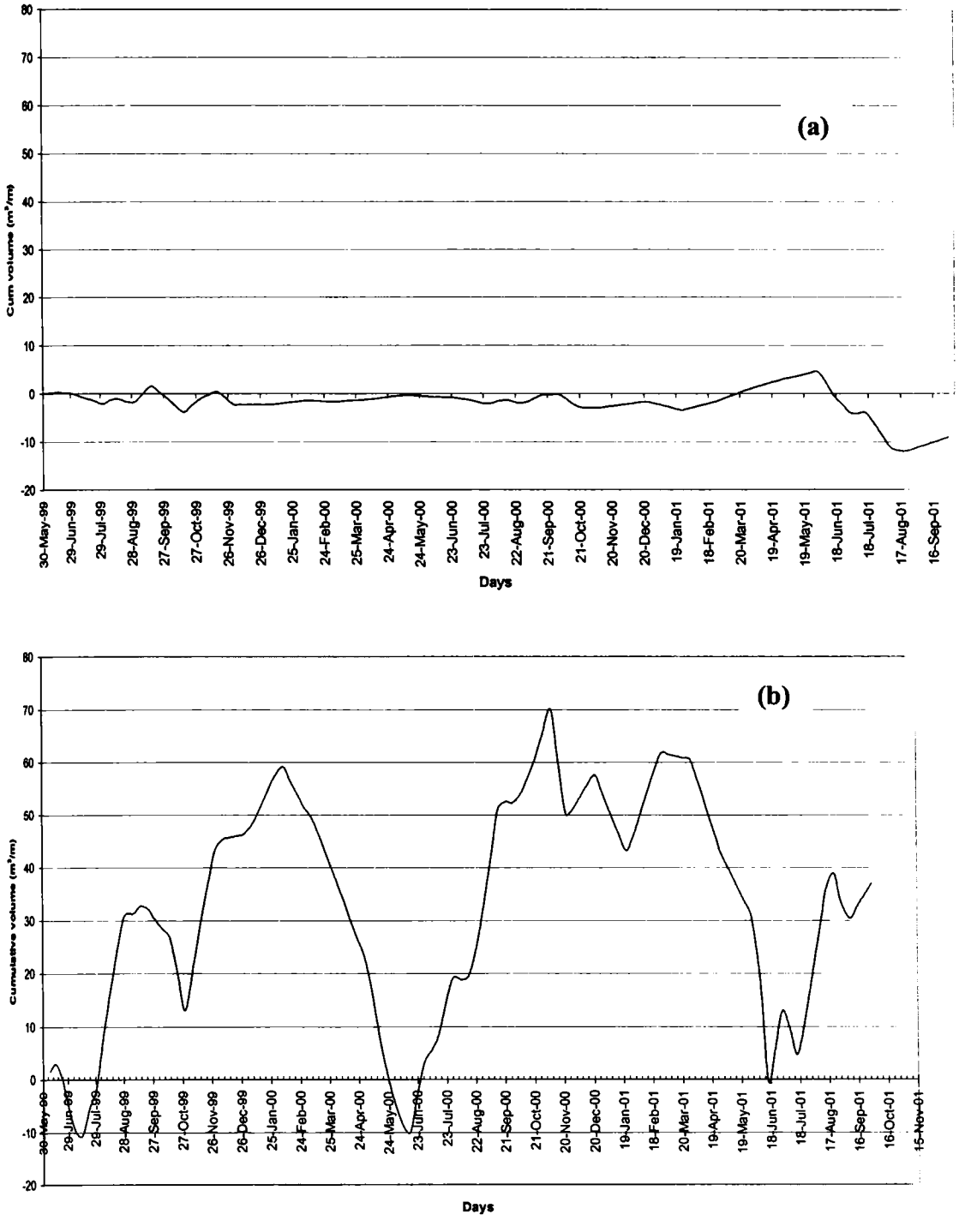

Fig. 5.13 Cumulative volume changes at: (a) sites in front of the sea walls; (b) sites in the mining areas

5.3.2.4 SLED Profiles

As already mentioned in Chapter 2, a SLED was used for measuring nearshore profiles in a few stations in the study area. Unlike the beach profiles, these profiles were taken seasonally since the operation of SLED in the nearshore zone, particularly in the wave breaking zone is a labour-intensive and thus expensive work. Simultaneous to the SLED profiling of nearshore (shoreline to 5m depth), beach profiling (from backshore to shoreline) and echosounding of the offshore (5m to 10m depth) were carried out. The three sets of measurements were reduced to a common datum (MSL) and nearshore profiles drawn. The profiles so obtained at VMS-4, VMS-7 and KMS-2 are presented in Fig. 5.14 a to 5.14c.

VMS 4

At this station the beach face is very steep upto 6m. This doesn't change significantly with season. Comparison between the profiles collected during April 2000 and October 2000 shows erosion all along the transect except for a small zone of 200-400m from the reference point. During the period October 2000 to April 2001, no significant change in the profile is observed. This shows that the effect of monsoon erosion is yet to be replenished even by April 2001. During the period April - November 2001 small erosion is seen in the nearshore zone. Thus, overall, erosion is seen in the innershelf during April 2000 to November 2001.

VMS7

This station has a very steep beach face upto 7m depth followed by a very gently slopping platform out to 10m depth. Unlike VMS4, during April 2000 to October 2000, no significant change in the profile is observed. Erosion and accretion are observed cyclically from the beach towards the offshore along the transect. During the period October 2000 to April 2001, erosion, though not significant, is seen in a major part of the profile. During the period April 01 and November '01, accretion dominates in the beach face while erosion is seen in the offshore portion. Thus during the period April 2000 to November 2001 accretion is seen in the beach face while erosion is seen in the offshore.

KMS 3

The profiles observed at this station which is in the Kovilthottam mining site is different from those observed in Vellenathuruthu. Here the beach face is steep only upto 4m depth. From 4m depth towards offshore the bottom slope is moderate. During the period October 2000 to April 2001, slight accretion is observed in the beach face while significant erosion is observed in the offshore platform. During the period April 2001 and November 2001, accretion is observed in the beach face while significant erosion is observed in a portion of the offshore platform. Thus, during the period October 2000 to November 2001 accretion has taken place in the beach face with erosion in the offshore platform.

Since the profiles during monsoon could not be taken due to operational problems during the rough seas, the offshore bar formation and migration could not be studied.

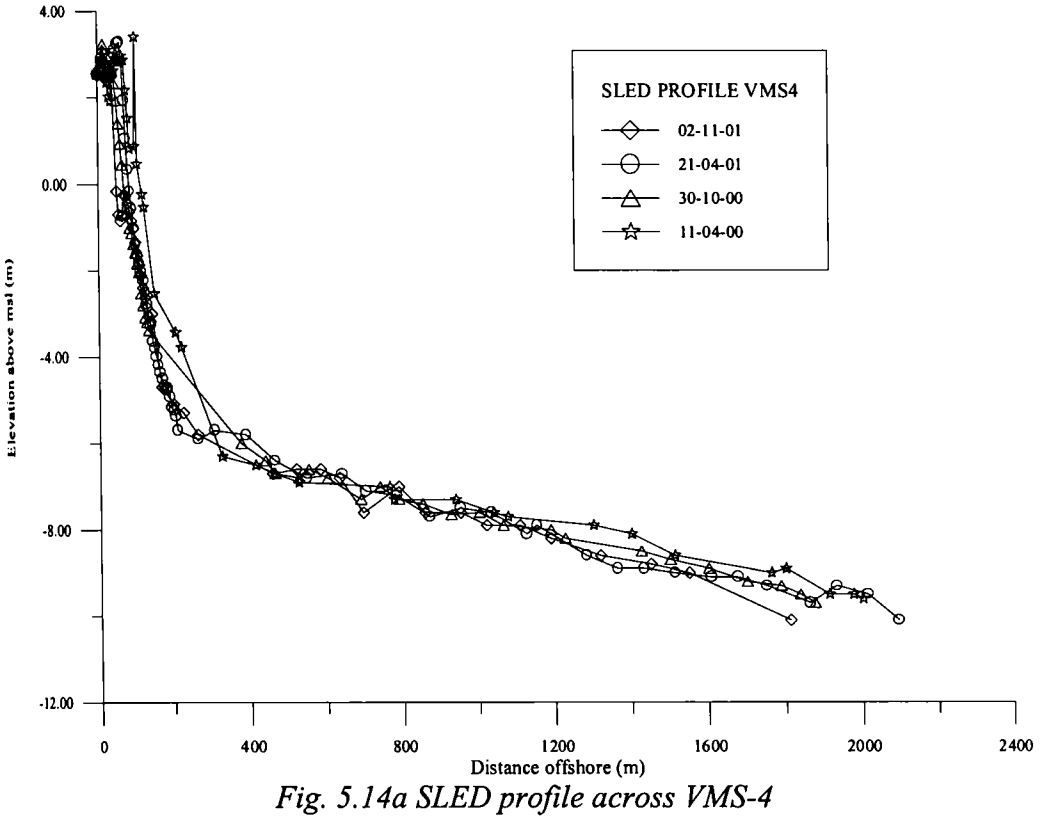

Fig. 5.14a SLED profile across VMS-4

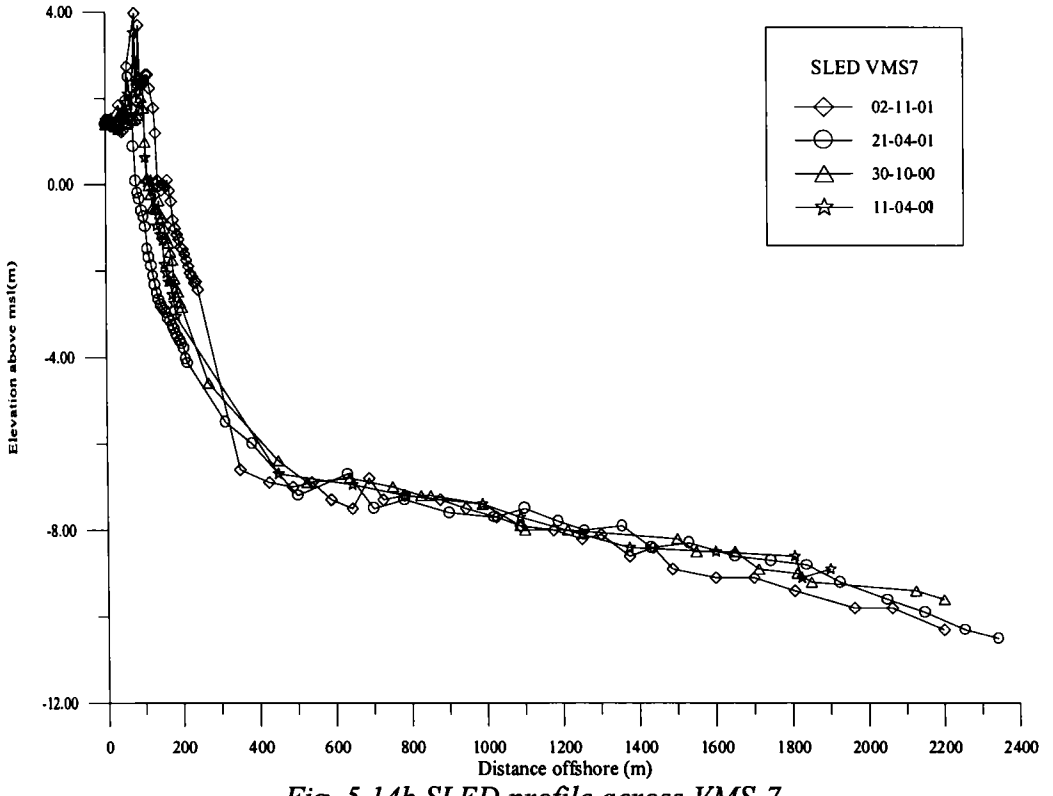

Fig. 5.14b SLED profile across VMS-7

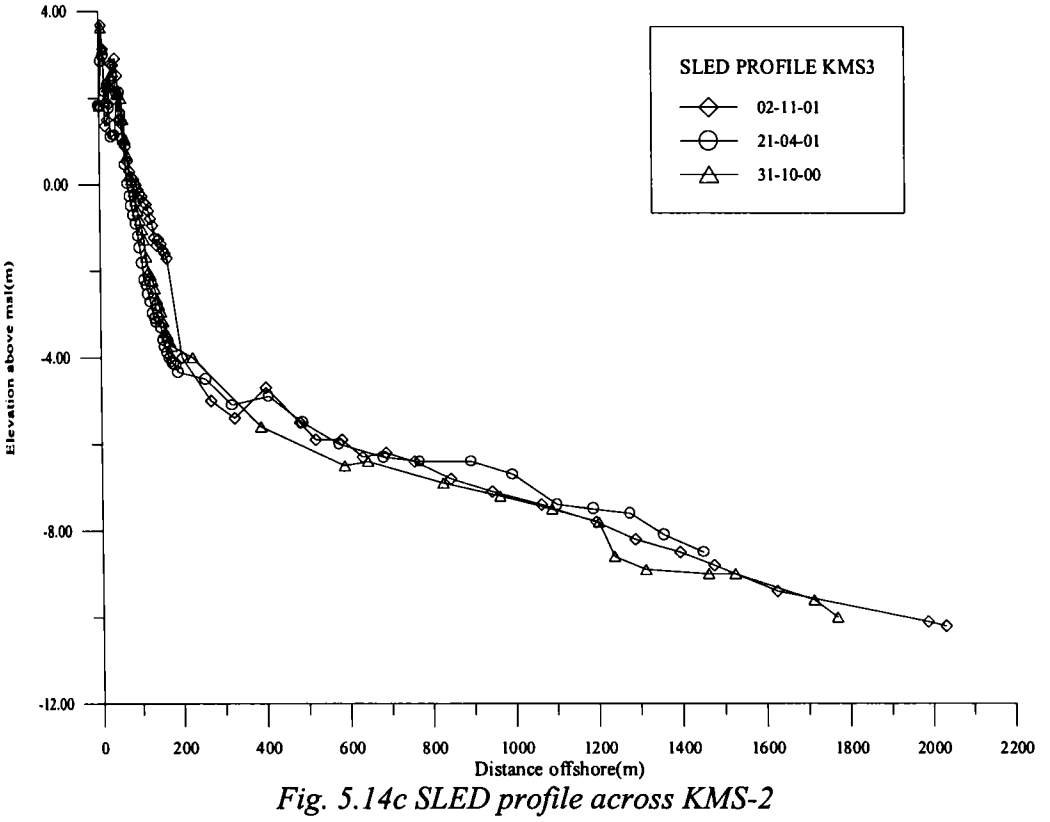

Fig. 5.14c SLED profile across KMS-2

5.4 DISCUSSION AND SUMMARY

The beach processes of the Chavara coast are controlled by the natural processes together with anthropogenic factors. The important natural processes are the wind, waves and currents. The anthropogenic factors of relevance to the area of study are the presence of seawalls and mining of sand.

The seasonal changes exhibited by beaches along the Chavara coast are quite similar with those reported by earlier researchers for different locations of west coast of India (eg. Hameed, 1988; Thomas, 1988; Kurian, 1988). All these studies report maximum width during fair weather months of February, March and April and minimum width during the peak monsoon. Waves are found to be the predominant force bringing about this change. It can be seen that there is very good correlation between wave intensity and beach width. During the peak monsoon when the waves are steep due to high waves of short period, offshore transport of sediments takes place resulting in erosion and beach width reaching its nadir during this period. During the fair weather months, characterized by moderate waves with long period waves, onshore transport of sediments takes places resulting in beach re-building after the erosionary phase. Interruptions in this beach rebuilding process can take place during fair weather months too. E.g., intense erosion was observed in the first two weeks of October 1999 whereas October is normally considered as a period for accretion. It could be correlated to the unusually intense wave action with height up to 1.7m recorded in October 1999 due to winds from SW quadrant.

Longshore currents which are wave induced also contribute to the erosion/accretion processes, particularly during the fair weather. During the rough monsoon period, the longshore currents are generally southerly. This period is dominated by the strong offshore transport which causes erosion all along the coast. However, the excessive erosion observed at VMS5, KMS2 and NK4 could be attributed to this southerly transport which deprives these stations of sediment supply from the north due to sea wall. During the fair weather period, the longshore currents are northerly. This period being an accretionary phase, the imprint of the northerly current is seen clearly

with higher quantum of deposition in the stations towards the north of the mining sites eg. VMS4, KMS2.

While wave is the single predominant force dominating the beach processes, the other hydrodynamic parameters too have a significant role to play. It is interesting to examine the correlation between wind and erosion/accretion pattern of the coast. Fig. 5.15 presents a comparison between progressive plot of cross-shore wind and cumulative beach volume changes. It can be seen that the correspondence between the two is quite high indicating the important role played by wind in the beach processes in the area of study. Wind as a means of transport of sand (deflation) in the beach is ruled out because of the narrow width. It could be summed up that the correspondence between the cross-shore wind and the beach volume change comes out of its role as a driving force of the coastal circulation. Kurian et al (2002) deals in detail with the circulation pattern in the areas of study based on hydrodynamic modeling. According to the simulations, westerly wind generates offshore bottom current while northerly wind generates onshore current. NW wind induces a shore parallel flow. An offshore bottom current induces erosion while onshore current induces accretion. Because the NW wind is dominant in this region, a slight rotation of the wind would lead to changes from net erosion to net accretion along the coast. Thus the observed correspondence between wind and erosion/accretion pattern appearing to be well explained theoretically too.

Sand mining is one of the major anthropogenic factors influencing the beach-innershelf sedimentary system in this area. Two firms, viz. IREL and KMML are mining beach sands from the Chavara coast. Unlike other natural situations the beach profiles and volume changes at the mining sites are influenced by the mining operations too in addition to the natural processes. Major part of the area under present investigation is covered by seawalls except the mining site and few fishing gaps. No frontal beach is observed in the areas fronted by seawalls even during the fair weather season and thus the cumulative volume change is practically nil as seen in Fig. 5.13a. This indicates that the seawall is a hindrance to the normal beach-innershelf sedimentary processes.

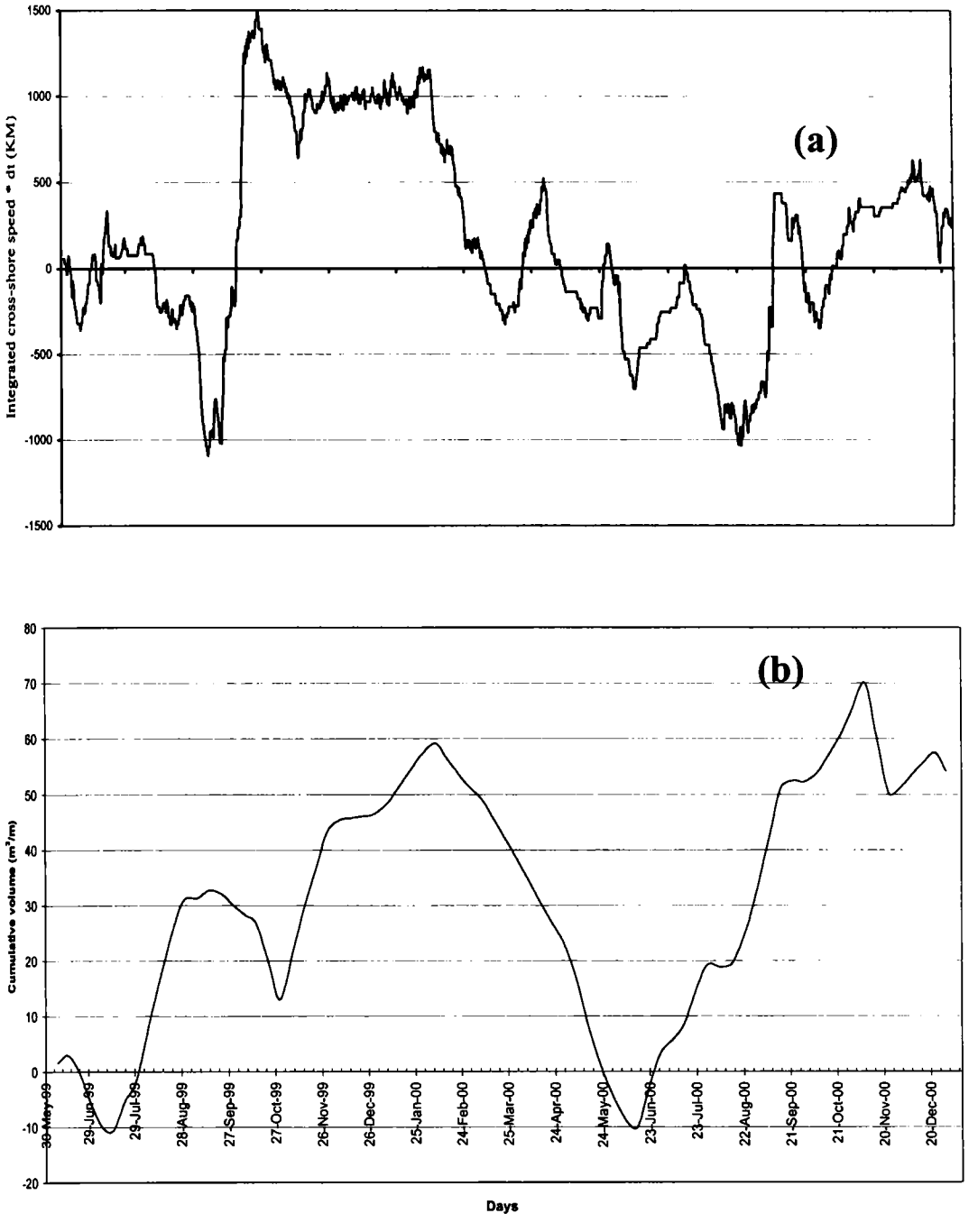

Fig. 5.15 (a) Progressive vector plot of cross-shore wind (km) and (b) cumulative beach volume change (m^3/m)

To conclude, strong monsoonal influence is seen in the beach processes of this coast. Waves are found to be the predominant force bringing about the changes. Offshore transport of sediments induced by steep waves takes place during the peak monsoon leading to intense erosion. Re-building of beach takes place during the fair weather months when onshore transport of sediments takes place. The wave induced longshore currents bring about spatial variations in the erosion/accretion pattern. It is observed that there is a good correlation between the wind and erosion/accretion pattern of beach. This is attributed to the wind induced circulation in the innershelf. Westerly wind generates offshore bottom current leading to erosion while northerly wind generates onshore current resulting in accretion. Winds along this coast being predominantly NW, a slight rotation of wind would lead to changes from net erosion to accretion.

CHAPTER 6

SEDIMENT BUDGET

6. SEDIMENT BUDGET

6.1 INTRODUCTION

The studies detailed in the previous chapters have clearly brought out the hydrodynamic characteristics of the coastal environment under study. It also brought out the beach processes in the area of study, highlighting the role of each driving force in the observed erosion/accretion pattern. With this clear cut understanding of the physical processes in operation in the area, it is intended to go ahead with the final task of computation of sediment budget. It is not an easy task considering the complexity of the processes in operation in the beach-innershelf system. Sediment budget studies are lacking for the Indian coast, as can be seen in the section 6.2 below. Computation of sediment budget has been carried out for the Chavara coast incorporating the components that are relevant for the coast and the results are presented in this chapter.

6.2 LITERATURE REVIEW

As already mentioned sediment budgeting studies are lacking in the Indian scenario. But such studies are available for some coastal locations of the world. Depending on the objective of the study, sediment budgets are constructed with different time frames. Sediment budget on geological time scales has been attempted (Belknap and Kraff, 1985; Oxford et al., 1996; Riggs et al., 1998; Schwab et al., 2000) to bring out the influence of natural forces on the geomorphology of the beach systems. Studies on a historical time frame (several hundred years) are undertaken to unravel the influence of large-scale human activities like dam, jetty and seawall construction on changes in beach systems (Hess and Harris, 1987; Fitz Gerald et al., 1989; List et al., 1991; Pilkey and Dixen, 1996; Cooper and Nevas, 2004). Contemporary (annual-decadal) time scale studies based on sediment budget are planned to bring out the influence of human activities such as dredging, dredge spoil disposal, beach replenishment, sand mining etc. (Pilky et al., 1989; Fenster and Dolan, 1994; Hill et al., 2004).

Bowen and Inman (1966) introduced the general sediment budget concept, based upon coastal geology and longshore sediment transport. The authors estimated longshore sediment transport rates from calculation of the longshore components of wave power and for specified sources (river influx, sea cliff erosion) and sinks (submarine canyons, dune building processes) for the sediment calculation cells (littoral cells).

Carter (1986) constructed a sediment budget for the South Otago continental shelf and coast between Nugget Point and Otago Peninsula. The study revealed that modern (post 6500 y) sediment input was dominated by the Clutha River. Contributions from other sources (Taceri River, adjacent southland shelf and biogenic production of calcareous shell debris) accounted for only 28% of the input. About half of the bed load (sand and gravel) reaching the Otago shelf is stored within a large nearshore sand wedge in the protected waters of Molyneux bay, off the Clutha River. Suspended load (mud) accounts for over half of the sediment input and is nearly all transported from the study area to accumulate in northeasterly shelf and slope. Hess and Harris (1987a&b) compared a series of historical maps and bathymetric charts of coastal areas to evaluate changes in sand volume and to infer directions of sand movement over the past century at Rockaway barrier beach New York. Fitzgerald et al. (1989) also employed similar methodology for evaluating the morphodynamics of the tidal inlet systems in Maine. While evaluating the large-scale coastal evaluation of Louisiana's barrier islands, List et al. (1991) also adopted a similar methodology. Jimenez et al. (1991) constructed the first sediment budget for the Ebro Delta and explained the effects of changing sediment supply on the coastal system and the large scale morphological responses of the coastal system. Sediment budget study conducted by Best and Griggs (1991) for the Santa Cruz littoral cell, California evaluated only the rate of sand movement over limited time periods by directly quantifying sand fluxes in and out of the system.

Gulfenbaum et al. (1999) constructed a regional sediment budget for the Columbia river littoral cell, to gain a better understanding of the Columbia river dispersal system. To help separate natural from human induced changes in the littoral cell,

sediment budgets were constructed separately for prehistoric, historic and contemporary periods. Estimation of the discharge of the Columbia river was a critical component of the sediment budget calculations and it was found that average discharges per annum varied from 20 million m^3 during prehistoric period, through 8.7 million m^3 during early historic periods to 4.3 million m^3 since 1950s. The study also reveals that the early historic shoreline accretion rates are much greater than pre-historic rates, and in general, greater than recent accretion rates. The timing of the rapid accretion in the early part of the century and the longshore variation in the accretion indicated changes in the ebb-tidal deltas after jetty construction as the primary cause.

While constructing a regional sediment budget for the region extending from Fire Island to Montank point, New York, Rosati et al. (1999) demonstrated the essentiality of developing a conceptual sediment budget. A conceptual sediment budget for the 1979-1995 period was formulated based on earlier studies and initial analysis to discern any potential problems with the available data and applied assumptions for each of the littoral cells. The conceptual sediment budget was later modified to account for the imbalances observed. By integrating the data from the inter-connected littoral cells, a regional sediment budget was formulated to represent coastal processes, engineering activities and structure conditions reflected by the 1979-1995 period. Evaluation of the sediment budget in context with sand management during the period highlighted those practices that had been influential in the evolution of the barrier island and inlet systems.

For constructing Holocene geologic framework of the trinity shoal region of the Louisiana continental shelf, Pope et al. (1991) measured the volume of sand in depositional reservoirs of the beach system. Similarly Schwab et al. (2000) studied the influence of inner continental shelf frame work on the evaluation and behaviour of the barrier island inlet and Shinne cock Inlet, Long Island, New York.

Christiansen et al. (2004) constructed a total sediment budget for the Skallingen barrier spit (South Wadden, Denmark) and used the same to establish the relative

importance of sediment transport processes involved in barrier migration. The authors observed strong inter annual variations in the long-term budget, making evaluation of barrier behaviour based on short-term measurements doubtful.

A sediment budget approach was used to study the erosion problems being experienced on the popular tourist beach in St. Queen's Bay, Jercy Channel Islands by Cooper and Pethick (2005). It has been found that the beach lowering and sediment losses being experienced are primarily related to the cessation of sediment input from the finite offshore sources, the construction of a seawall which has exacerbated the erosion and the mining of beach sand. The study provided a fundamental baseline upon which coastal management options could be proposed which offer sustainable solution to the problems being experienced. Park and Wells (2005) studied the littoral processes under a wide range of wave conditions that impact the complicated coastal geometry at the Cape Lookout cuspate forelands, North Carolina, and constructed a regional sediment budget for the region using a numerical wave refraction/diffraction model and through use of aerial photographs and nautical charts.

Kelley et al. (2005) formulated sand budget at geological, historical and contemporary time scales for Saco Bay (Maine, USA) beach system by evaluating the past and present sand-transport pathways, fluxes and reservoir volumes. Black and Healy (1983) discussed several methods to estimate the pathways of sediment transport. The relative magnitude and direction of each pathway can be varied to develop alternative sediment budget solutions. Elliot and Clarke (1982) used statistical analysis based on Fourier transform, least square and empirical orthogonal function to identify characteristic pattern of temporal and spatial variation in sediment volume. Bodge (1997) presented an algebraic method with which a range of sediment budget solution could be developed.

Kraus and Rosati (1999) suggested the inclusion of data on volume change, removal and placement of dredged material or beach fill in the sediment budget studies. Recognising the growing importance of providing quantitative estimates of nearshore

and offshore sand volumes and transport rates, Williams et al. (2003) have compiled an excellent bibliographic source on this topic. Komar (1998) and Kraus and Rosati (1999) discussed the significance of the terms involved in the sediment budget equations and narrated the uncertainties in coastal sediment budgets. According to them significant contributions to true uncertainty enter through natural variability. Such variability includes,

(a) temporal variability (daily, seasonal and annual beach changes)

(b) spatial variability (alongshore and cross shore)

(c) selection of definitions (eg: shoreline orientation, direction of random seas) and

(d) unknowns such as grain size and porosity of the sediment (Rosati, 2005)

As already mentioned sediment budgeting studies in a wholistic sense are lacking in Indian scenario. Most of the studies involved calculation of longshore transport of sediments from littoral environmental observations. Prasannakumar et al. (1983) estimated the probable volume of littoral sediment transport at 2m-depth contour along the shoreline between Munambam and Andhakaranazhi for waves approaching the shore from 200° to 300° with periods varying from 6 to 14 seconds. They estimated that about 9million m^3 of material drifted towards south annualy between Munambam and Vypeen and about 7million m^3 of material drifted towards south between Fort Cochin and Andhakaranazhi. Prasannakumar (1985) observed large variations in the alongshore drift of littoral sediments. In the area between Azhikode and Vypeen, the littoral drift values are higher during rough weather season than the fair weather season. From Munambam to Kuzhipally region the drift decreases in the southerly direction but from Kuzhipally to Narakkal region, the drift value increases. South of Narakal region the drift value is decreasing towards Vypeen region. Chandramohan and Nayak (1991) developed an empirical sediment transport model for the Indian coast on longshore energy flux equation and estimated an annual gross sediment transport of 1.5-2 million m^3 along the south Kerala coast. Chandramohan et. al. (1993) studied the sediment transport along the South Maharashtra coast and estimated that the longshore sediment transport at Ratnagiri, Ambolgarh and Vengurla were 0.12, 0.19 and 0.05 million m^3 respectively towards south.

Jose et al. (1997) studied the longshore transport at three different locations with varying littoral characteristics along the SW coast using the wave energy flux method. They observed a highest transport of 2.9 million m^3 at Vizhimjam and the lowest value of .07 million m^3 at Chavara. Jena and Chandramohan (1997) studied the sediment transport near the Peninsular tip of India based on monthly measurement of littoral environmental data and beach profiles. They estimated that the annual gross longshore sediment transport rate was 0.9 million m^3/year and the annual net transport rate was 0.3 million m^3 towards west (up coast). Sajeev et al. (1997) studied the longshore transport characteristics of the Kerala coast using Waltons equation and found that the net drift was southerly during monsoon periods and northerly during other seasons. The annual net transport was southerly at all the stations except at Trivandrum, Alleppey and Nattika.

The longshore current and sediment transport along Kannirajapuram coast, Tamilnadu were studied by Sanil Kumar et al. (2000). The predominant direction of transport was northerly from March to November and southerly from December to February. They calculated that the annual gross transport was 0.46 million m^3 and annual net was 0.44 million m^3/year towards northeast. Sanil Kumar et al. (2001a) studied the nearshore processes along north Karnataka coast and estimated longshore transport. They estimated that the net transport varied station wise from 0.069 million m^3/year towards north at Arge beach to 0.142 million m^3/year towards south at Gangavalli. Chandramohan et al. (2001) studied the littoral drift sources and sinks along the Indian coast and found that rivers were the major sources for the littoral drift and the annual discharge of sediments to the sea along the Indian coast was about 1.2×10^{12}kg. Jena et al. (2001) computed the longshore transport based on directional waves along North Tamilnadu coast. They found that the transport rate was relatively high (about 0.1 million m^3/month) in November and December and was low showing less than 0.03 million m^3/month in March, April and July. They also found that the annual gross transport was 0.6 million m^3/year, the annual net transport was very low showing less than 0.006 million m^3/year (towards north). Sanil Kumar et al. (2001b) studied the nearshore processes along Tikkavanipalem Beach using waverider buoy. They estimated the longshore currents and longshore sediment transport rate

considering the sea and swell waves separately using the CERC formula. The difference between the gross sediment transport rate estimated based on the Longuet-Higgins and Galvins equation was around 6%. The sediment transport using Walton's equation shows that average annual gross transport was 0.371 million m^3 and the average annual net transport (towards northeast) was 0.173 million m^3.

Sanil Kumar et al. (2002) calculated the longshore sediment transport rate in Nagapattinam coast using CERC formula and found that the average annual gross transport was 0.448 million m^3 and the average net transport (towards south) was 0.098 million m^3. Sanil Kumar et al. (2006) studied the coastal processes along the Indian coastline using measured data on waves and currents. They calculated that the gross sediment transport rate was about 1 million m^3/year along south Kerala and south Orissa coasts.

6.3 SEDIMENT BUDGET COMPONENTS TO BE RECKONED FOR THE COAST

From among the different sediment budget components listed in Table 1.1, the components that are of relevance to the area of study had to be chosen. Considering the geomorphic set up of the area, it could be safely assumed that wind transport, cliff erosion and dune/ridge erosion are practically absent. Thus the components that are relevant for this coast are longshore transport, cross-shore transport, river/estuary input and sand extraction. The study area has two inlets. The one at Kayamkulam is seasonal and while the other at Neendakara is permanent. It has been established by Black and Baba (2001) that the river/estuarine input is practically nil in the area of study. As has already been described in Chapter 1, the area under study is world famous for the rich black sand deposits and the sand was being mined by the Indian Rare Earths Ltd. (IREL). Though the Kerala Minerals and Metals Ltd. (KMML), another public sector company also is engaged in the mining, the intake by them was nominal till 2001 and was increased subsequently. The figures for the intake by the IREL are available. Thus the study ultimately boiled down to the determination of the longshore and cross-shore transports. This was accomplished by using numerical models as described in the ensuing sections.

6.4 NUMERICAL MODELS USED

As already described, the processes in operation in the beach-innershelf systems are very complex and hence sophisticated numerical models that can systematically and simultaneously treat the multiplicity of processes need to be engaged for computation of sediment fluxes. The 3DD suite of numerical process models (© K.P.Black) which is being successfully used for this type of studies (eg. Black, 1996; Black and Vincent, 2001) was chosen for the computation. Three computer models were adopted from the 3DD suite. A brief description of the models is given in the following sections.

6.4.1 WBEND

Model **WBEND** is a 2-dimensional numerical wave refraction model for monochromatic waves or a wave spectrum over variable topography for refraction and shoreline longshore sediment transport studies. The model applies a fast, iterative, finite-difference solution of the wave action equations to solve for wave height, wave period, breakpoint location, longshore sediment transport, bottom orbital currents and near-bed reference concentration of suspended sediments.

WBEND has unique characteristics such as:

- an enhanced shoaling facility to overcome under-prediction of breakpoint wave height which is common to linear wave models
- a pseudo-diffraction algorithm simulating diffusion of height and angle along the wave crests
- multiple bed friction choices
- prediction of bedform geometry in response to prevailing wave conditions, and feed-back into the bed friction term
- coupling to the hydrodynamic model 3DD and sediment model POL3DD for simulation of wave-driven circulation and sediment transport in wave and current environments

6.4.2 GENIUS

Model **GENIUS** is used for the computation of longshore sediment transport. **GENIUS** is similar to its well-known counterpart GENESIS (Hanson and Kraus, 1989) but with some extra features. The model includes frictional attenuation of wave height and a more physically-based treatment of wave transmission factors across submerged reefs.

GENIUS uses a commonly-adopted sediment transport equation which is the CERC formula for longshore sand transport rate given by,

$$Q = (H^2 C_g)_b \left[a_1 \sin(2\theta_{bs})\right]_b \tag{6.1}$$

where

H = wave height

C_g = wave group speed given by linear wave theory

b = subscript denoting wave breaking condition

θ_{bs} = angle of breaking waves to the local shoreline

a_1 is a non-dimensional parameter is given by

$$a_1 = \frac{K_1}{16(\rho_s / \rho - 1)(1 - P)} \tag{6.2}$$

where

K_1 = empirical coefficient, treated as a calibration parameter (typically 0.58)

ρ_s = density of sand (taken as 2650 $kg.m^{-3}$ for quartz sand)

ρ_w = density of water (taken as 1025 $kg.m^{-3}$ for seawater)

P = porosity of sand on the bed (taken to be 0.7)

Knowing the wave height, the equation for depth-limited breaking,

$$H_b = \gamma d_b \tag{6.3}$$

(where γ = breaker index often taken as 0.78) is adopted to obtain the wave group speed. Finding d_b from eqn (6.3), the wave group speed is obtained from the shallow water approximation given by,

$$C_g = (g\, d_b)^{1/2} \tag{6.4}$$

6.4.3 SFLUX_3DD

Model SFLUX_ 3DD is used for the computation of cross-shore sediment transport. This model is capable of computing the cross-shore transport under the combined effect of waves and currents. The following equation is used in SFLUX for the computation of sediment flux:

$$F = \sum_z U(z)C(z)\Delta z \tag{6.5}$$

where *C(z) is* vertical profile of suspended sediment concentration and *U(z) is* the velocity profile.

The detailed computational procedure is given in Section 6.7

6.5 BATHYMETRIC GRIDS USED

Two depth grids of varying sizes and resolutions as described below are prepared for the computations using the models.

6.5.1 Meso Grid

The Meso-scale grid from Paravur to Thottappaly covering a coastline of length 70km was developed from a high quality bathymetric survey undertaken in November - December, 2000. The survey provided high resolution bathymetric data for the innershelf waters of this coast extending out to 60 m depth. The survey lines are shown in Fig. 6.1 and the data intensity is high. Given the large size of the area, the survey involved 14 days at sea. In addition, surveys of the shoreline along the crest of the seawall were undertaken using a GPS to fix the position of the wall for development of the model grid. Data were interpolated and gridded with the software

package Surfer. With these data, a high-resolution grid was developed of 300 m square cells, which led to a grid of 119 cells cross-shore by 249 cells longshore (Fig. 6.2a&b). While considerable effort was required to collect the data, the high quality of the data leads to confidence in the model outputs.

6.5.2 Very Fine Grid

This grid was a very-fine resolution 2 m grid extending out to 10m depth adopted by Model GENIUS for calculation of the longshore surf zone sediment fluxes (Fig. 6.3). Given the strong similarity of the various SLED profiles, the average of all SLED profiles is used for the preparation of this grid.

To eliminate longshore perturbations, longshore depth variability was neglected.

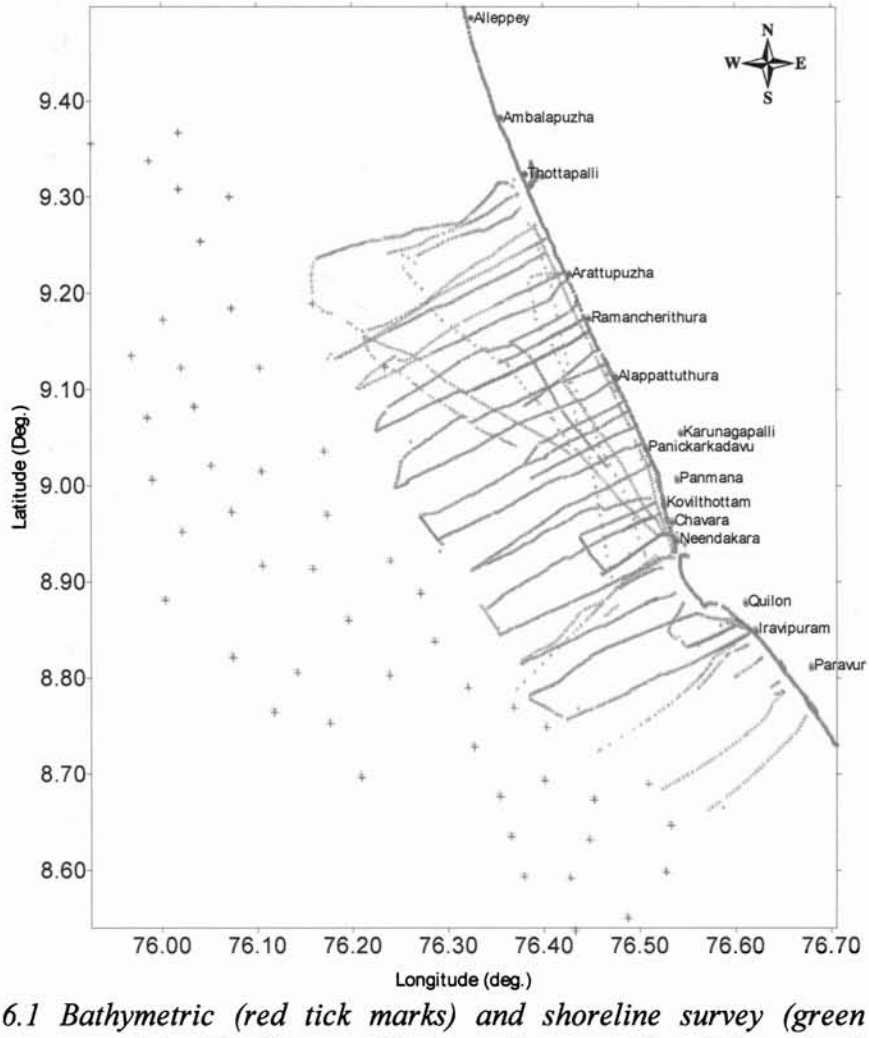

Fig. 6.1 Bathymetric (red tick marks) and shoreline survey (green tick marks) coverage plot of the Paravur-Thottappally coast. Blue tick marks show the points digitized from Naval Hydrographic Chart No.220-222 for depths beyond 55 m.

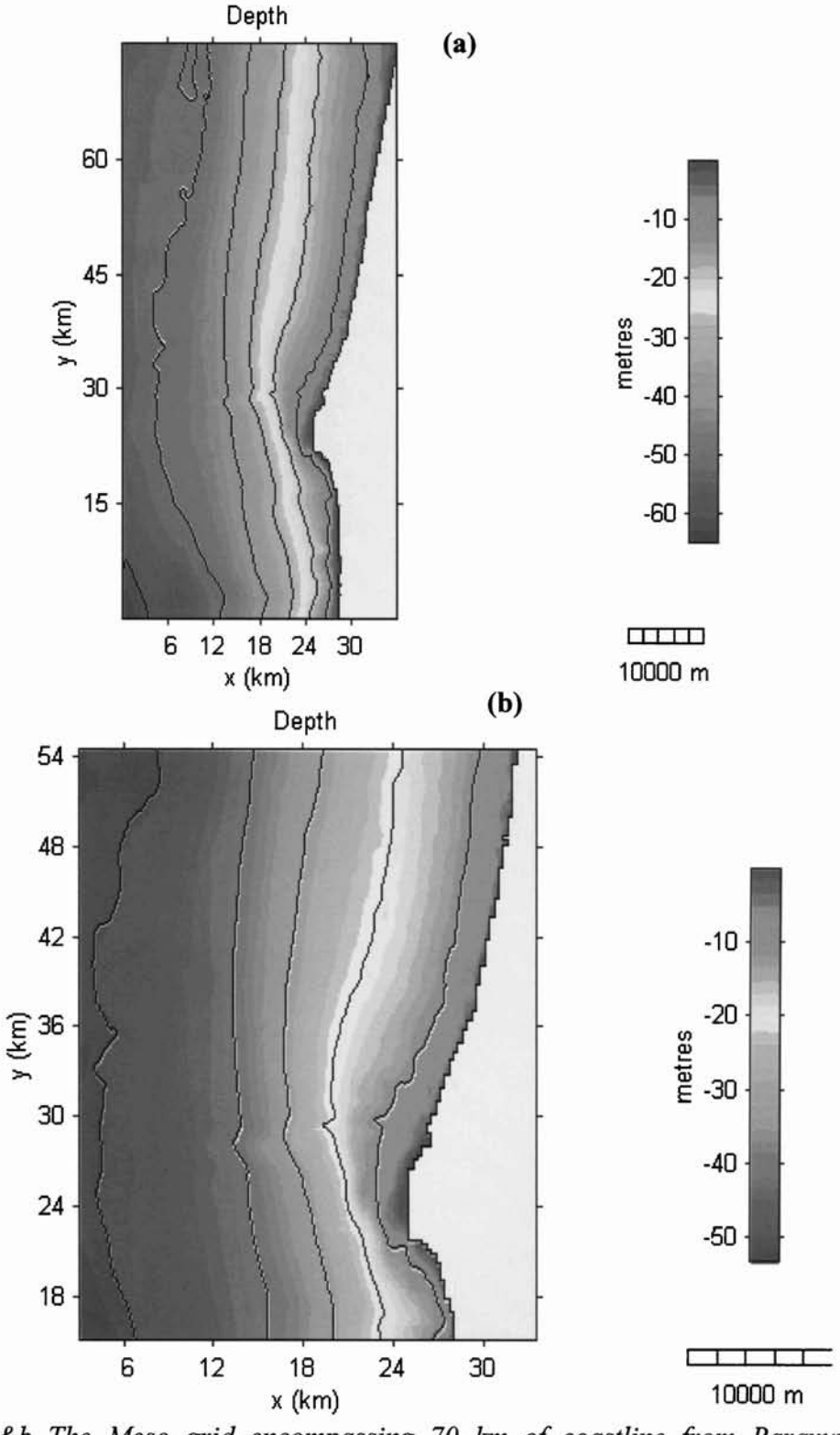

Fig. 6.2a&b The Meso grid encompassing 70 km of coastline from Paravur to Thottappally. The grid was created using a detailed bathymetry survey undertaken in November - December, 2000. The lower panel shows the region around IREL in more detail.

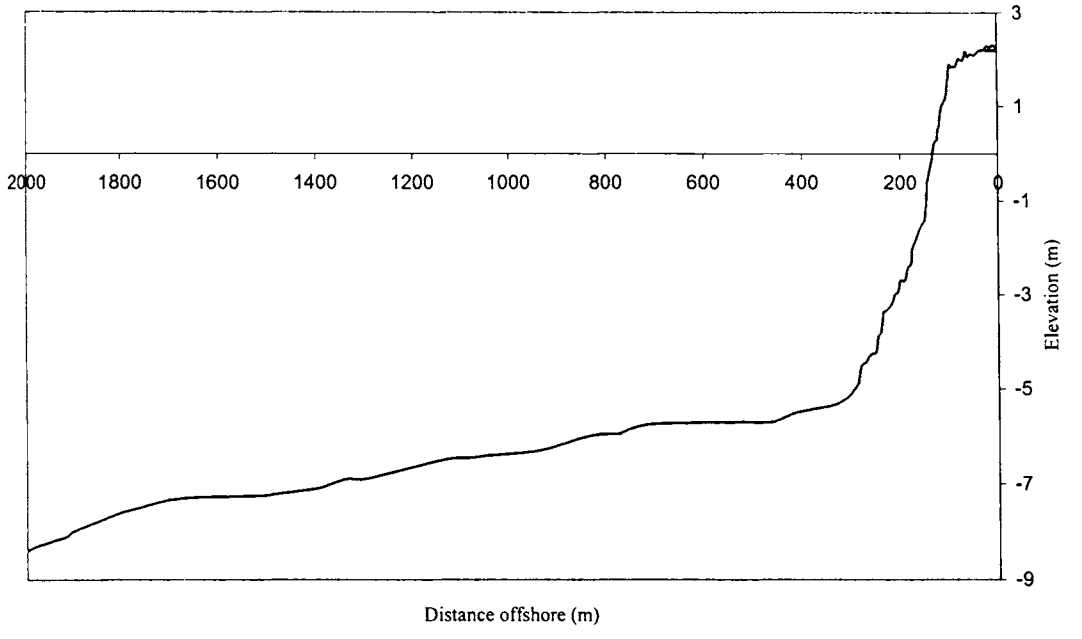

Fig. 6.3 Bathymetry grid produced using the SLED profile measurements

6.6 COMPUTATION OF LONGSHORE SEDIMENT TRANSPORT FLUXES

6.6.1 Computational Procedure

Longshore surf zone transport was calculated by Model GENIUS using wave boundary conditions created with Model WBEND. The methods can be summarized as follows:

1. Development of a boundary file containing probability of occurrence, wave height, period and direction from deep water wave measurements (Baba et al., 1992). Some 356 different cases were involved.
2. Simulation of all of these 356 cases with Model WBEND on the Meso grid
3. Extraction of the wave conditions from the 356 WBEND simulations at the offshore end of the very high-resolution bathymetry grid
4. Remodelling of the waves on the very high-resolution grid as they propagate towards the beach and break, using Model GENIUS.
5. Prediction of the longshore sediment transport for each case
6. Working out the annual longshore transport fluxes including weighting according to the probability of occurrence.

The shoreline has distinctly different orientations to the south and north of the Field station. Thus, the calculations are repeated for these two sections of coast.

The frictional height losses in Model GENIUS are calculated as in Model WBEND. The total sediment flux is obtained by summing the fluxes for each case over the full year. The equations include the sediment density and for this the mean density of the beach samples of 3350 kg/m^3 (Kurian et al., 2002) was used.

The retarding effect of the seawalls is not considered. Instead, the maximum flux that would occur along this coast in the absence of the seawalls was determined. The walls are likely to cause a reduction in longshore transport because the beach widths in front of the walls are narrower or beach itself is missing for some area.

6.6.2 Results

The results of the computations are presented in Table 6.1. The shoreline orientation to the north and south of the mining sites are different and accordingly the breakpoint angles are also different, as can be seen from the Table. Since the breaker angle is the most critical parameter deciding the longshore flux and the shoreline south of the mining site has a higher breaker angle of 8.1°, the flux is also much higher in this sector. The longshore flux northward and southward in the southern sector are 2,91,000 m^3/yr and 82,000 m^3/yr respectively, resulting in a net northerly transport of 2,09,000 m^3/yr. The northward flux in the northern sector is much less, resulting in a net flux of only 1,25,000 m^3/yr. Thus the average net yearly longshore transport for the coast works out to a sizable quantity of 1,67,000 m^3/yr in the northerly direction.

Table 6.1 Longshore sediment transport calculations

Parameter	Shoreline south of mining site	Shoreline north of mining site
Mean height at breakpoint (m)	1.17	1.18
Mean angles at breakpoint (° relative to the beach normal)	8.10	5.49
Net flux (m^3/yr)	209,000	125,000
Northward flux (m^3/yr)	291,000	211,000
Southward flux (m^3/yr)	-82,000	-86,000

6.7 COMPUTATION OF CROSS-SHORE SEDIMENT TRANSPORT FLUXES

The computation of cross-shore sediment transport fluxes involved the calculation of bed reference concentration and vertical mixing length parameter. Towards this detailed data on suspended sediment concentration were collected using sediment traps and automated water sampler as described in Chapter 2. The following sections describe the data collected and the procedures followed for the computations of cross-shore sediment flux.

6.7.1 Sediment Trap Collection

Although eleven deployments of sediment traps at elevations between 0.26 and 3.15 m above sea bottom were made at both the nearshore and offshore stations covering monsoon and non-monsoon seasons a few data sets could not be used as the mooring frame was found in a slanting position at the time of retrieval. After the retrieval of sediment traps from the sea, the samples were brought to the laboratory for analysis. All the samples from the traps were wet sieved using 0.045 mm size mesh, the washings collected, dried and weighed. Further analysis to determine the sand, silt and heavy mineral contents also was carried out. The results are given in Fig. 6.4 and 6.5.

At the nearshore site (Fig. 6.4), the mass of sediment trapped is highest at the bottom traps and decreases gradually upwards. Maximum deposition (3.08 $g/cm^2/day$) was during the pre-monsoon deployment of April -May 2001, followed by (2.68$g/cm^2/day$) during pre-monsoon deployment during March-April 2000, although the monsoon deployments of August-September 1999 (2.53 $g/cm^2/day$) and May-June 2000 (2.16 $g/cm^2/day$) registered high rates (Fig. 6.4). During the monsoon deployments (May-June, June-July and July-August), the sediment deposition rates at the upper levels were also relatively high whereas for the non-monsoon deployments, higher values were limited to the near-bottom traps. The results can be explained by the presence of large swell events in the non-monsoon causing high near-bed suspended load, while the high load in the upper traps during the monsoon is likely to relate to the higher water column turbulence during the rough monsoon season.

At the offshore site (Fig. 6.5), there is a more rapid reduction in sediment trapped above 1 m elevation than nearshore (Fig. 6.4). The maximum sediment deposition at the bottom trap (26 cm above bed) was during the monsoon deployments of August-September 1999 (2.36 g/cm^2/day) and May-June 2000 (2.08 g/cm^2/day) (Fig. 6.5). An increase in the sediment deposition at the elevated traps was evident during the monsoon deployments; otherwise the upper level traps (above 64 cm from the bed) received only negligible quantities of sediment. This confirms that the increased sediment deposition at the upper levels during the monsoon deployments is due to wave breaking and turbulence during the monsoon period in association with the rougher seas.

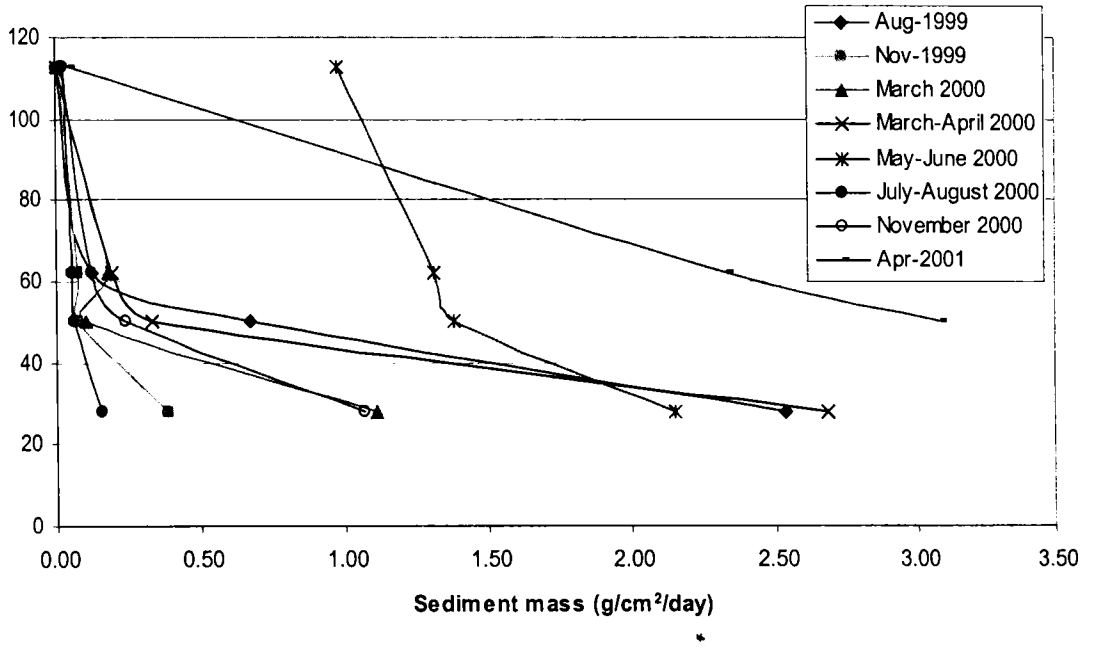

Fig. 6.4 Average sediment mass (g) collected per day at the nearshore station during the deployment period between August 1999 and April 2001. Traps were at 28, 50, 62 and 113 cm above the bed.

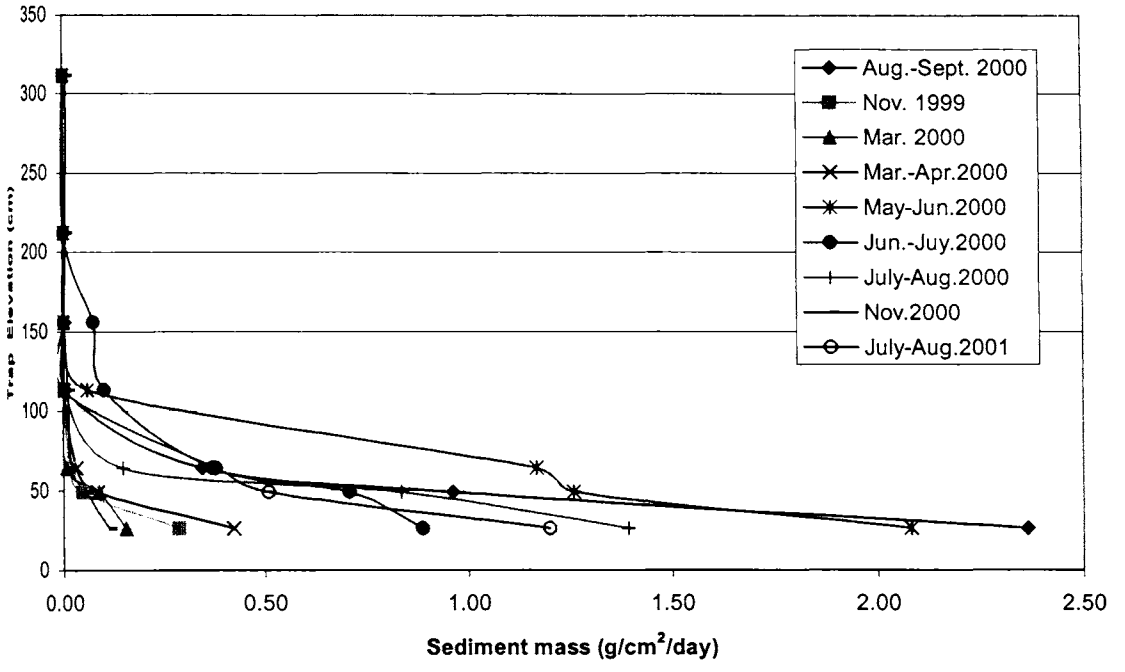

Fig. 6.5 Average sediment mass (g) collected per day at the offshore station during the deployment period between August 1999 and Aug 2001. Traps were at 26, 49, 64, 113, 156, 212 and 312 cm above the bed.

6.7.2 Suspended Sediment Load from Water Samples

Suspended sediment load was estimated from water samples collected from the offshore station using the Automatic Water Sampler and boat-based pumps. The automatic sampler was programmed to collect the water samples at 6/12/24 hourly intervals. On retrieval of the sampler from the sea, all the 20 water bags were taken to the laboratory where the quantity of water was measured, sieved with 0.045 mm size mesh and the sediments collected. The collected sediment was dried and weighed and used for further analysis. The results of the analysis are given in Table 6.3a-d. The sediment load ranges from 0.18 to 2.49 g/l during the monsoon deployment of 22-27 August 1999 (Table 6.3a), and 0.02 to 0.06 g/l during 21 May to 14 June 2000 (Table 6.3b). The concentration of near-bed samples pumped from heights of 27 cm and 67 cm from bottom during November 2000 ranges from 0.03 to 0.07 g/l (Table 6.3c). The sediment load ranges from 0.1 to 3.19 g/l during 20 July to 7 August 2001(Table 6.3d) which is comparable with the monsoon data of 1999.

Table 6.3a Suspended sediment concentration from water sampler during 22.08.99 to 27.08.99

Sl. No.	Date	Time (Hrs)	Volume of Water in (ml)	Suspended sediment load (g.)	Suspended Sediment/litre (g)
1	22.8.99	18.30	2650	0.47	0.18
2	23.8.99	0.30	2600	1.08	0.42
3	"	6.30	2310	3.46	1.50
4	"	12.30	2700	1.02	0.38
5	"	18.30	2650	0.94	0.35
6	24.8.99	0.30	2780	0.86	0.31
7	"	6.30	2760	2.11	0.76
8	"	12.30	2620	1.47	0.56
9	"	18.30	2700	2.52	0.93
10	25.8.99	0.30	2240	0.51	0.23
11	"	6.30	2660	3.41	1.28
12	"	12.30	2680	3.58	1.34
13	"	18.30	2760	2.92	1.06
14	26.8.99	0.30	2670	4.00	1.50
15	"	6.30	2690	6.69	2.49
16	"	12.30	2520	1.77	0.70
17	"	18.30	2770	2.31	0.83
18	27.8.99	0.30	2720	2.30	0.85
19	"	6.30	2680	6.60	2.46
20	"	12.30	2730	2.40	0.88

Table 6.3b Suspended sediment concentration from water sampler during 21.05.2000 to 14.06.2000

Sl.No.	Date	Time (Hrs.)	Volume of water (ml)	Total suspended sediment load in (g)	Suspended Sediment/litre (g)
1	21.05.2000	12.00	4610	0.23	0.050
2	22.05.2000	12.00	3250	0.16	0.049
3	23.05.2000	12.00	2800	0.16	0.057
4	24.05.2000	12.00	3260	0.15	0.046
5	25.05.2000	12.00	3350	0.10	0.030
6	26.05.2000	12.00	3090	0.08	0.026
7	27.05.2000	12.00	3460	0.02	0.006
8	28.05.2000	12.00	3470	0.13	0.037
9	29.05.2000	12.00	Sample cover broken	-	-
10	30.05.2000	12.00	3540	0.10	0.028
11	31.05.2000	12.00	3550	0.12	0.034
12	01.06.2000	12.00	Sample cover broken	-	-
13	02.06.2000	12.00	3680	0.08	0.022

14	03.06.2000	12.00	3570	0.14	0.039
15	04.06.2000	12.00	3280	0.08	0.024
16	05.06.2000	12.00	3470	0.10	0.029
17	06.06.2000	12.00	3370	0.10	0.030
18	07.06.2000	12.00	3400	0.16	0.047
19	08.06.2000	12.00	3370	0.11	0.033
20	09.06.2000	12.00	3100	0.14	0.045

Table-6.3c Suspended sediment concentration from pumped samples.

Sl.No.	Date	Time (Hrs.)	Sample withdrawal	Volume of water (ml)	Total suspended sediment load in (g)	Suspended Sediment/litre (g/l)
1	15.11.2000	12.30	0.27 m from bottom	3200	0.22	0.069
2	15.11.2000	12.45	0.65m from bottom	3230	0.12	0.037
4	24.11.2000	15.45	0.27 from bottom	3650	0.13	0.036
3	24.11.2000	16.00	0.65m from bottom	4100	0.11	0.027
5	27.11.2000	11.00	0.65m from bottom	3600	0.09	0.025

Table 6.3d Suspended sediment concentration from water sampler during 20.07.2001 to 07.08.2001

Sl.No.	Date	Time (Hrs.)	Volume of water (ml)	Total suspended sediment load in (g)	Suspended Sediment/litre (g)
1	20.7.01	12	2000	0.20	0.10
2	21.7.01	12	Sample cover broken	-	-
3	22.7.01	12	1700	0.71	0.42
4	23.7.01	12	1440	3.03	2.10
5	24.7.01	12	Sample cover broken	-	-
6	25.7.01	12	2000	0.06	0.03
7	26.7.01	12	2000	0.14	0.07
8	27.7.01	12	2050	0.16	0.08
9	28.7.01	12	2020	1.63	0.81
10	29.7.01	12	Sample cover broken	-	-
11	30.7.01	12	2040	0.44	0.22
12	31.7.01	12	Sample cover broken	-	-
14	1.8.2001	12	2020	3.16	1.56
15	2.8.2001	12	1850	5.91	3.19
16	3.8.2001	12	2010	3.16	1.57
17	4.8.2001	12	Sample cover broken	-	-
18	5.8.2001	12	1750	3.01	1.72
19	6.8.2001	12	2000	1.90	0.95
20	7.8.2001	12	2100	0.41	0.20

6.7.3 Calculating Concentrations from Trapped Masses

The masses caught in the traps can be converted to record-duration average suspended sediment concentration (SSC, g/l) at the level of the sediment trap entrance as follows:

$$SSC = M/(Awt) \tag{6.7}$$

where M is the mass trapped (g) over the duration of the deployment t (s), A is the area of the trap orifice (m^2) and w is the fall velocity of the sediment in the trap (m/s). The conversion is achieved using the fall velocity distribution which was measured separately and is available in Kurian et al. (2002). The concentration for each size fraction is then calculated individually with eqn (6.10) and the total concentration obtained by summing the individual components. The results of the analysis are presented in Table 6.4a&b.

Table 6.4a Concentrations calculated from the sediment traps measurements.

Trap elevation (m)	**0.28**	**0.5**	**0.62**	**1.13**
Instrument deployment (Inshore site)	**Cz ($kg.m^{-3}$)**	**Cz ($kg.m^{-3}$)**	**Cz ($kg.m^{-3}$)**	**Cz ($kg.m^{-3}$)**
22/8/99	0.02882	0.00674	0.00230	0.00006
28/10/99	0.00464	0.00104	0.00093	0.00023
7/03/00	0.01266	0.00115	0.00201	0.00003
29/03/00	0.01225	0.00154	0.00089	0.00001
21/05/00	0.01554	0.01320	0.01394	0.01142
14/06/00	0.00007	0.00015	0.00208	0.00132
20/07/00	0.00013	0.00011	0.00227	0.00034
27/10/00	0.01496	0.00339	0.00179	0.00032
25/04/01	No data	0.06240	0.04089	0.00255

(Table 6.4 contd...)

Table 6.4b Concentrations calculated from the sediment traps measurements.

Trap elevation (m)	**0.26**	**0.49**	**0.64**	**1.13**	**1.56**	**2.12**	**3.12**
Instrument deployment (Offshore site)	**Cz ($kg.m^{-3}$)**	**Cz ($kg.m^{-3}$)**	**Cz ($kg.m^{-3}$)**	**Cz ($kg.m^{-3}$)**	**Cz ($kg.m^{-3}$)**	**Cz ($kg.m^{-3}$)**	**Cz ($kg.m^{-3}$)**
22/8/99	0.00352	0.01258	0.00540	0.00005	0.00001	0.00001	0.00000
28/10/99	0.00456	0.00206	0.00026	0.00007	0.00004	0.00001	0.00001
7/03/00	0.00172	0.00089	0.00008	0.00013	0.00000	0.00000	0.00000
29/03/00	0.00609	0.00107	0.00051	0.00001	0.00000	0.00000	0.00000
21/05/00	0.01234	0.04411	0.01394	0.00078	0.00001	0.00002	0.00002
14/06/00	0.01799	0.00439	0.01267	0.00223	0.00127	0.00002	0.00001
20/07/00	0.02588	0.00921	0.00204	0.00006	0.00001	0.00002	0.00004
27/10/00	0.00026	0.00435	0.00005	0.00003	0.00001	0.00002	0.00002
18/7/2001	0.01469	0.01218	0.00338	0.00002	0.00001	0.00008	0.00003

6.7.4 Curve fitting to find Reference Concentration and Mixing Length

In order to determine the bed reference concentrations (C_0) and mixing length l_s, the sediment trap concentrations have been plotted in log-linear space on Fig. 6.6-6.22 and the regression procedure used to find intercept and gradient. According to Nielson (1986) the intercept at the bed (z=0) in each case gives C_0 and l_s is given by the equation $l_s = -1/\alpha$ where α is the gradient of the regression line.

As expected in log-linear space, the concentration profile is nearly linear close to the seabed, but several of the profiles exhibit the classic concave-up shape that results from a combination of grain size fining and increasing mixing length with elevation. The calculated value of C_0 are presented in Table 6.5.

Table 6.5 Calculated bed reference concentrations (C_o) for the sediment trap deployments.

Instrument deployment date	Nearshore site C_o (kg/m^3)	Offshore site C_o (kg/m^3)
22/8/99	0.238753	0.060164
28/10/99	0.008019	0.007667
7/03/00	0.07586	0.004329
29/03/00	0.137451	0.023781
21/05/00	0.016607	0.023781
14/06/00	No data	0.023457
20/07/00	No data	0.120739
27/10/00	0.035808	0.001892

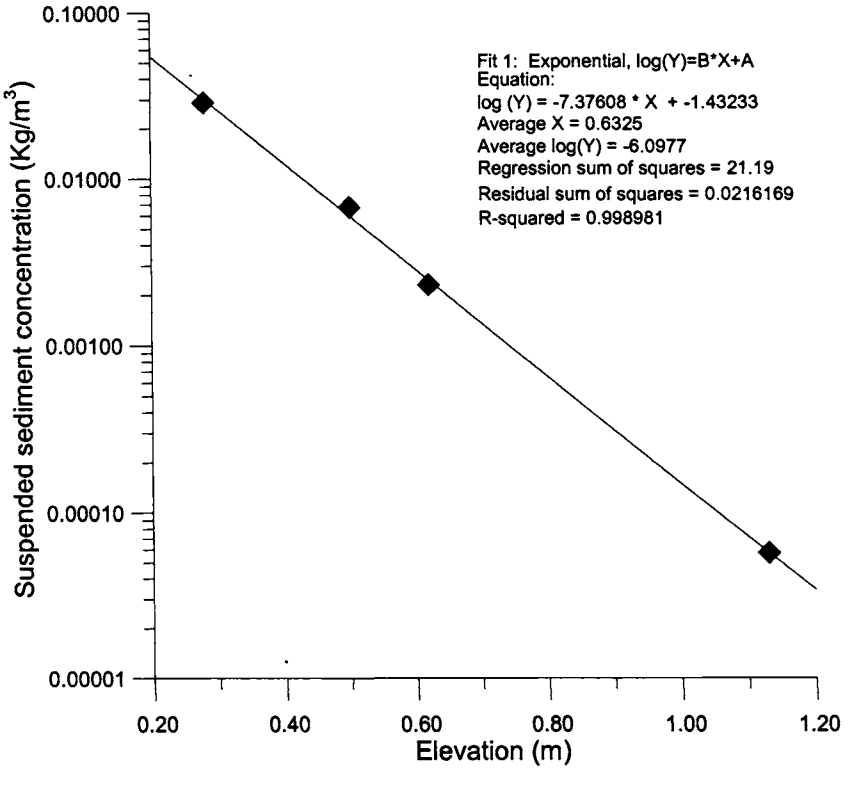

Fig. 6.6 Plot of elevation vs. suspended sediment concentration for the nearshore deployment date of 22 August 1999 – 05 September 1999

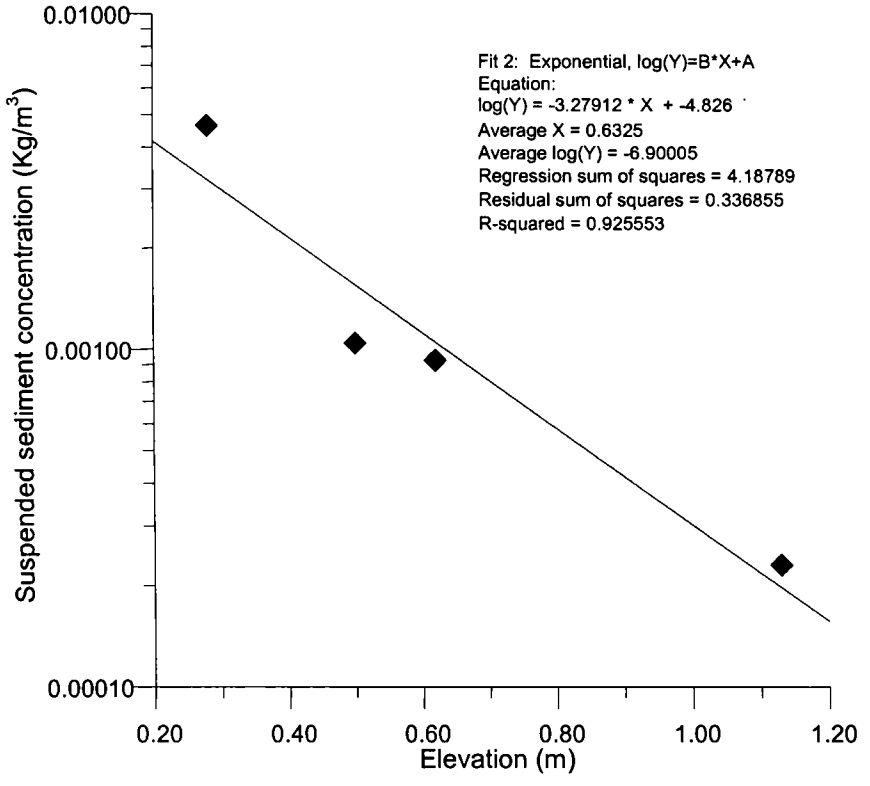

Fig. 6.7 Plot of elevation vs. suspended sediment concentration for the nearshore deployment date of 28 October 1999 – 26 November 1999

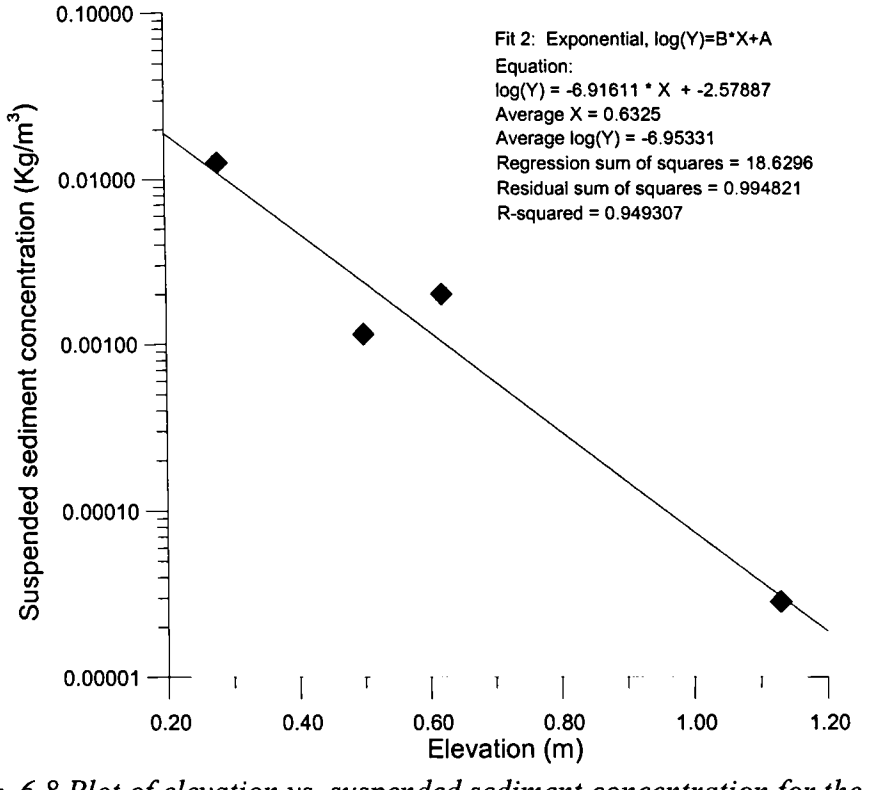

Fig. 6.8 Plot of elevation vs. suspended sediment concentration for the nearshore deployment date of 07 March 2000 – 29 March 2000

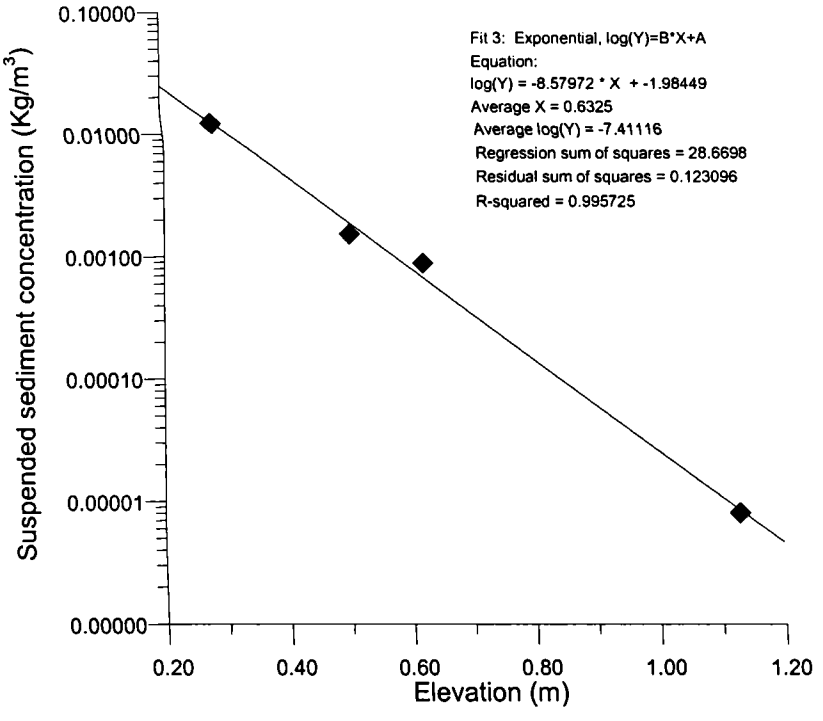

Fig. 6.9 Plot of elevation vs. suspended sediment concentration for the nearshore deployment date of 29 March 2000 – 07 April 2000

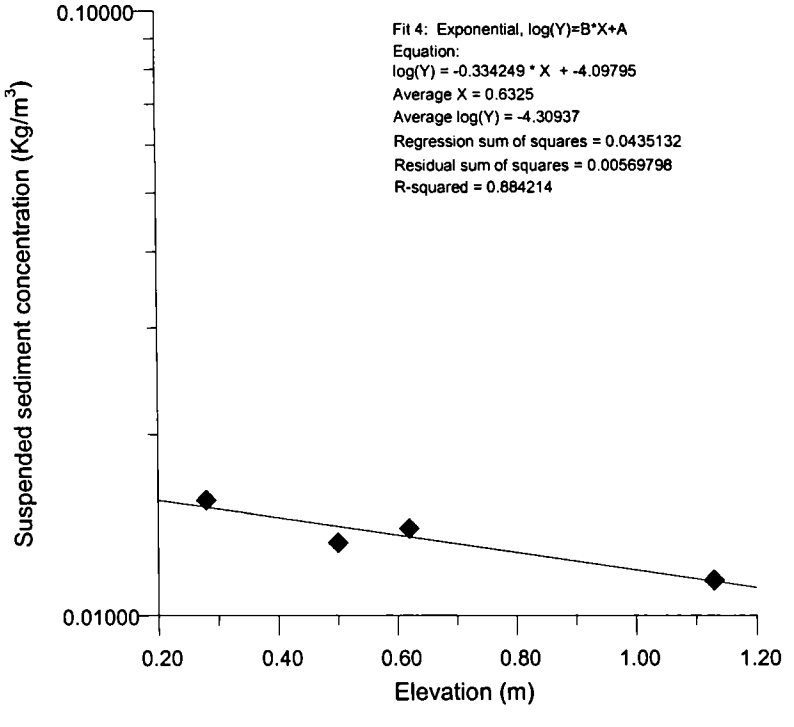

Fig. 6.10 Plot of elevation vs. suspended sediment concentration for the nearshore deployment date of 21 May 2000 – 14 June 2000

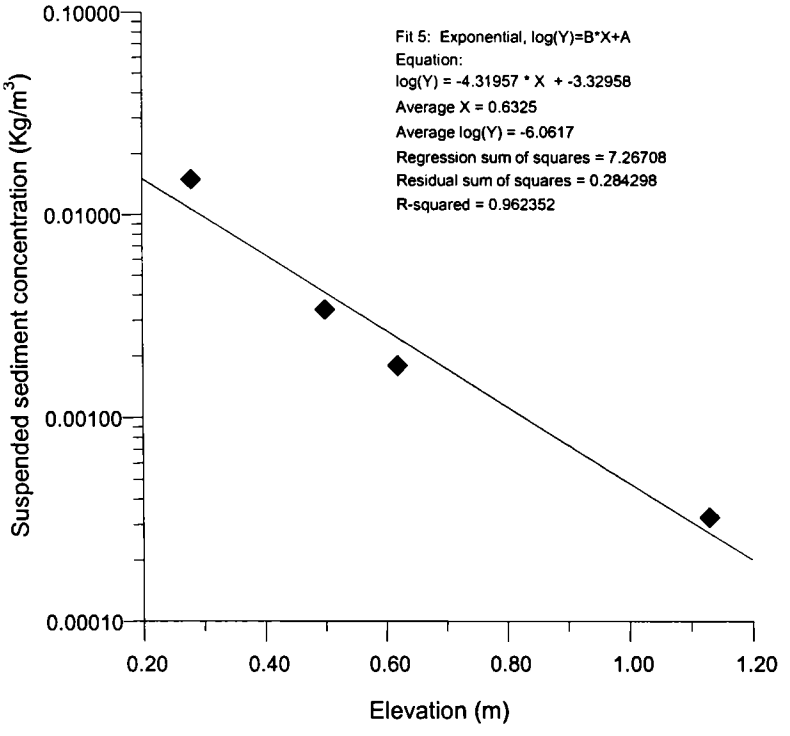

Fig. 6.11 Plot of elevation vs. suspended sediment concentration for the nearshore deployment date of 27 October 2000 – 27 November 2000

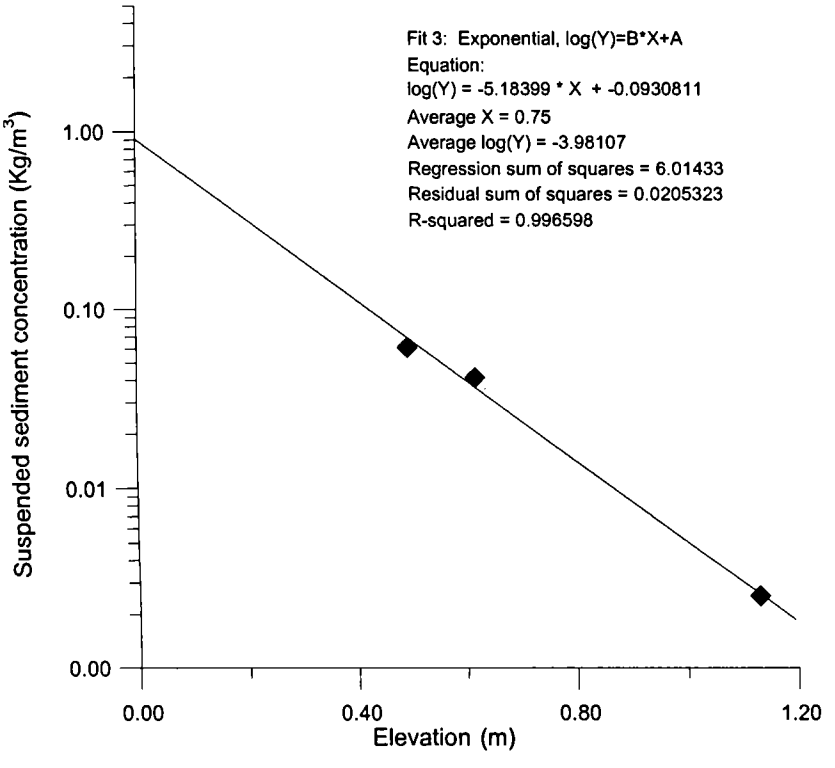

Fig. 6.12 Plot of elevation vs. suspended sediment concentration for the nearshore deployment date of 25 April 2001 – 16 May 2001

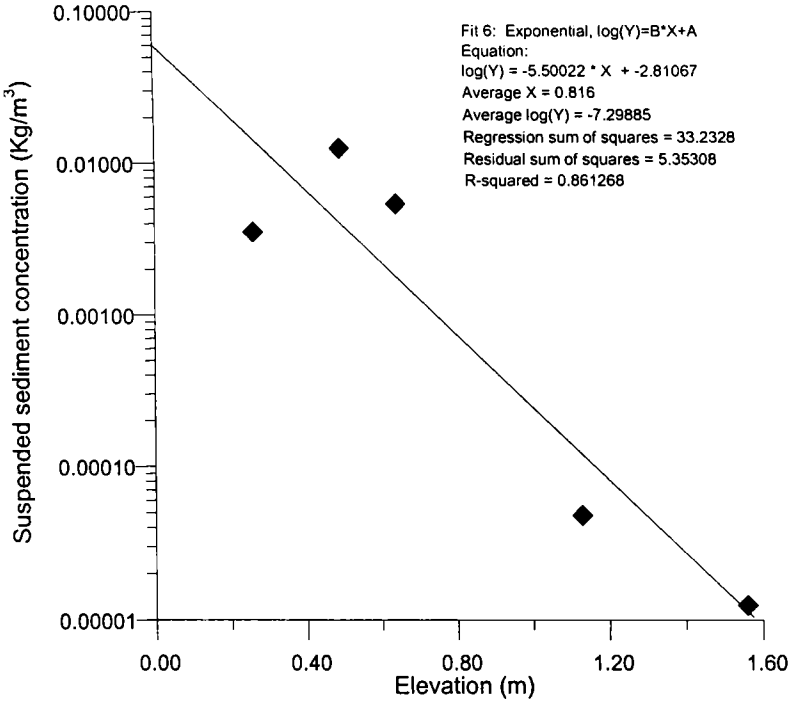

Fig. 6.13 Plot of elevation vs. suspended sediment concentration for the offshore deployment date of 22 August 1999 – 05 September 1999

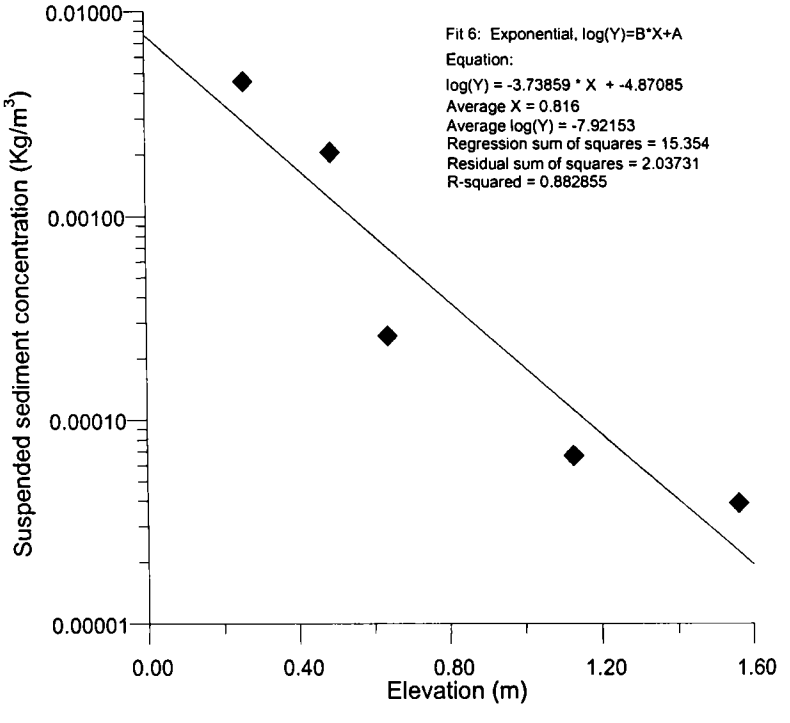

Fig. 6.14 Plot of elevation vs. suspended sediment concentration for the offshore deployment date of 28 October 1999 – 26 November 1999

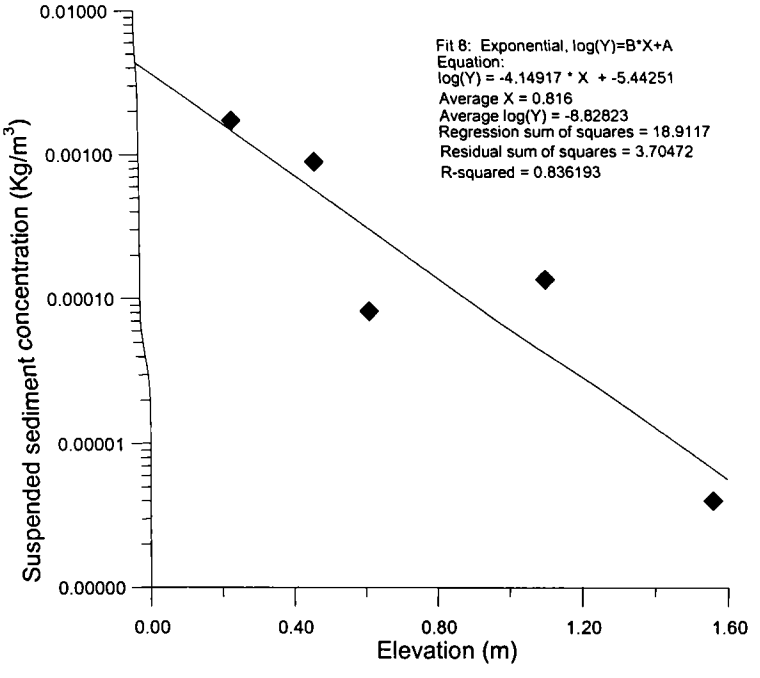

Fig. 6.15 Plot of elevation vs. suspended sediment concentration for the offshore deployment date of 07 March 2000 – 29 March 2000

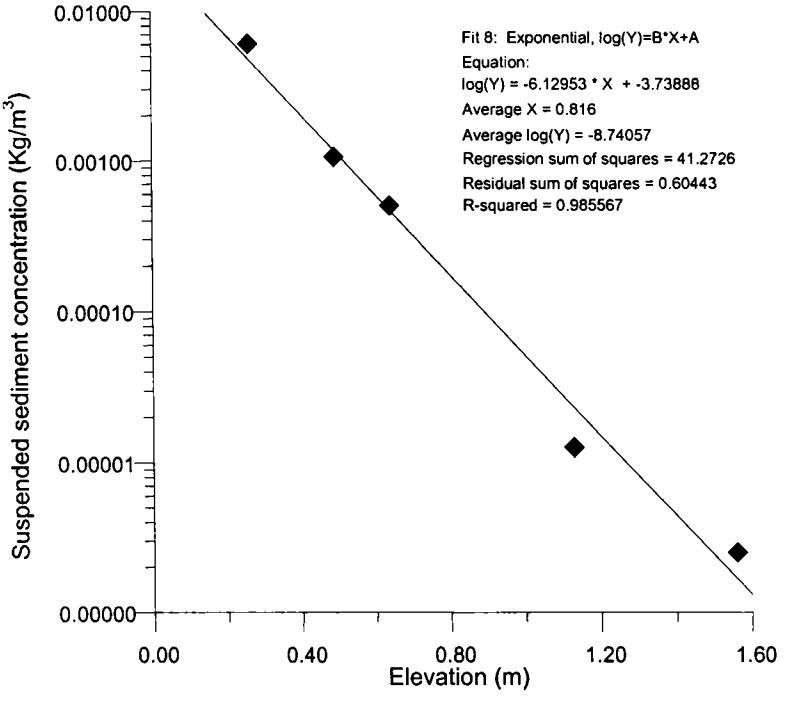

Fig. 6.16 Plot of elevation vs. suspended sediment concentration for the offshore deployment date of 29 March 2000 – 07 April 2000

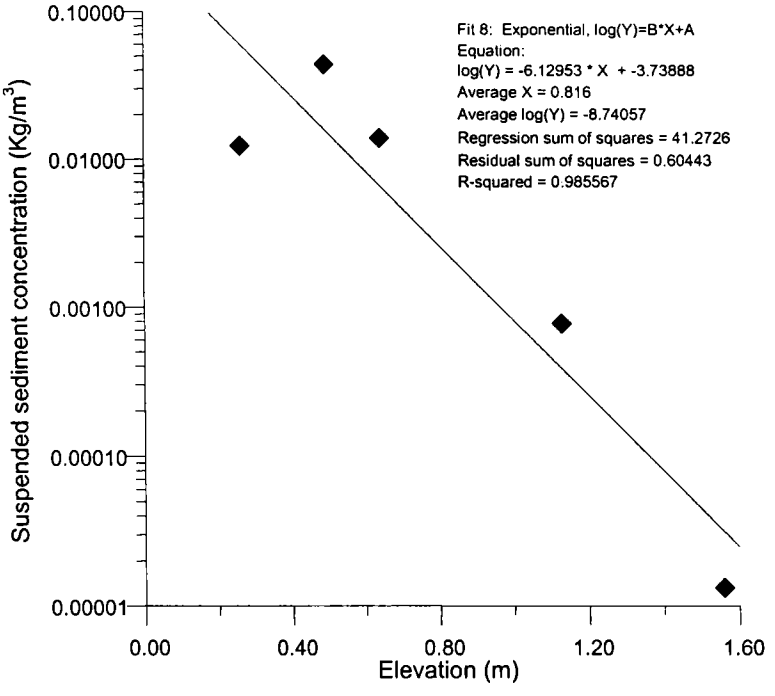

Fig. 6.17 Plot of elevation vs. suspended sediment concentration for the offshore deployment date of 21 May 2000 – 14 June 2000

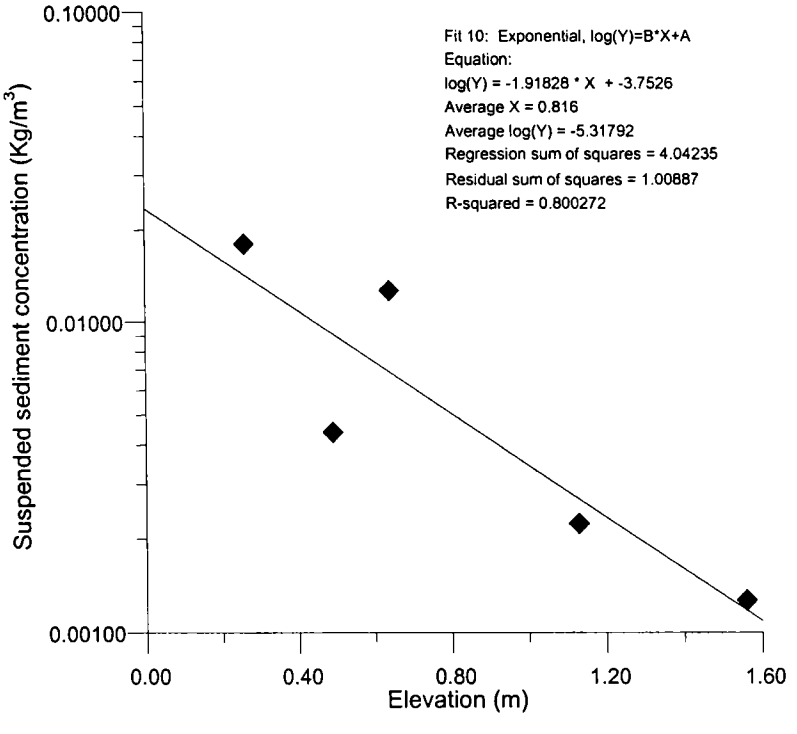

Fig. 6.18 Plot of elevation vs. suspended sediment concentration for the offshore deployment date of 14 June 2000 – 11 July 2000

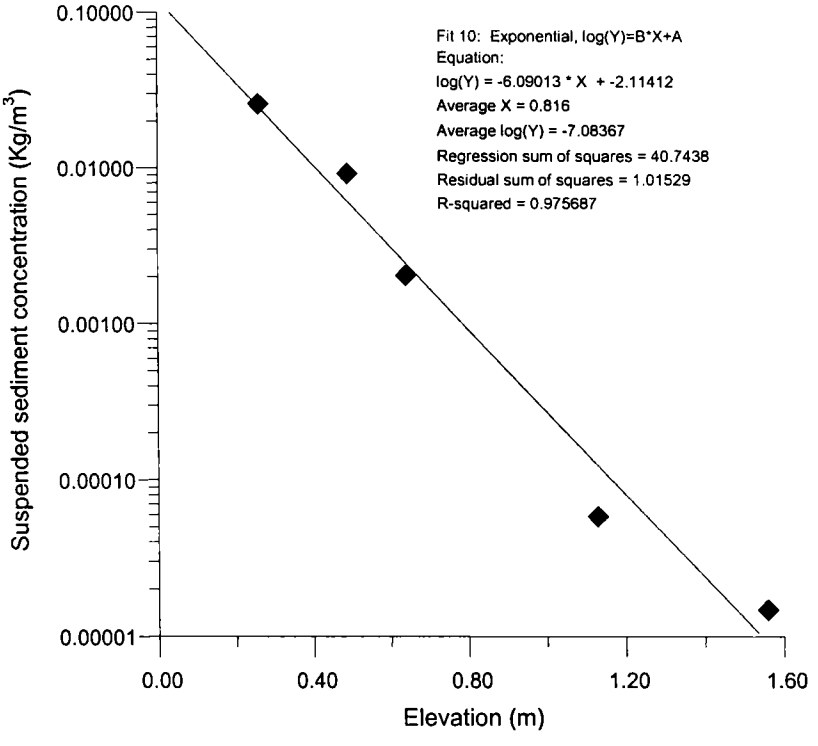

Fig. 6.19 Plot of elevation vs. suspended sediment concentration for the offshore deployment date of 20 July 2000 – 19 August 2000

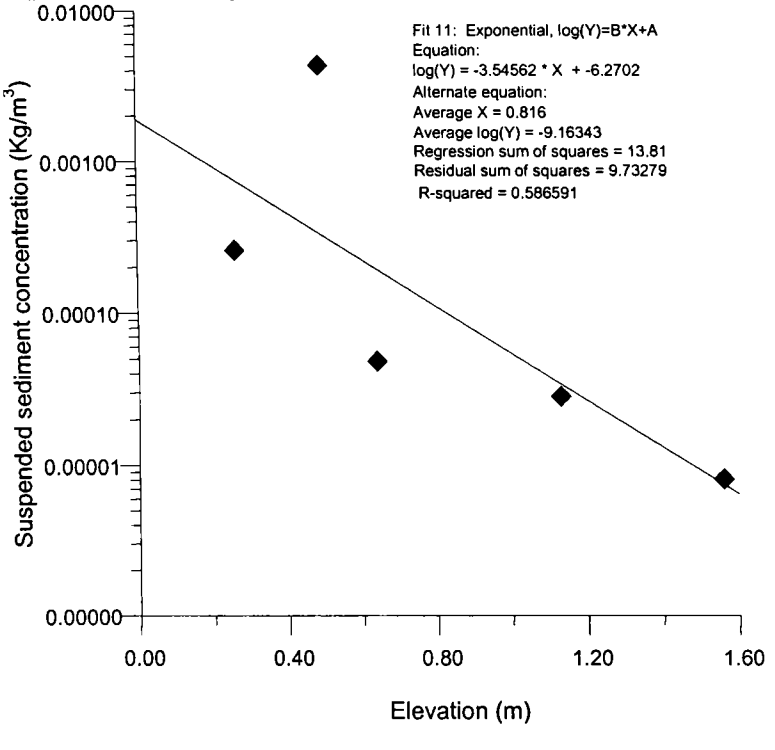

Fig. 6.20 Plot of elevation vs. suspended sediment concentration for the offshore deployment date of 27 October 2000 – 27 November 2000

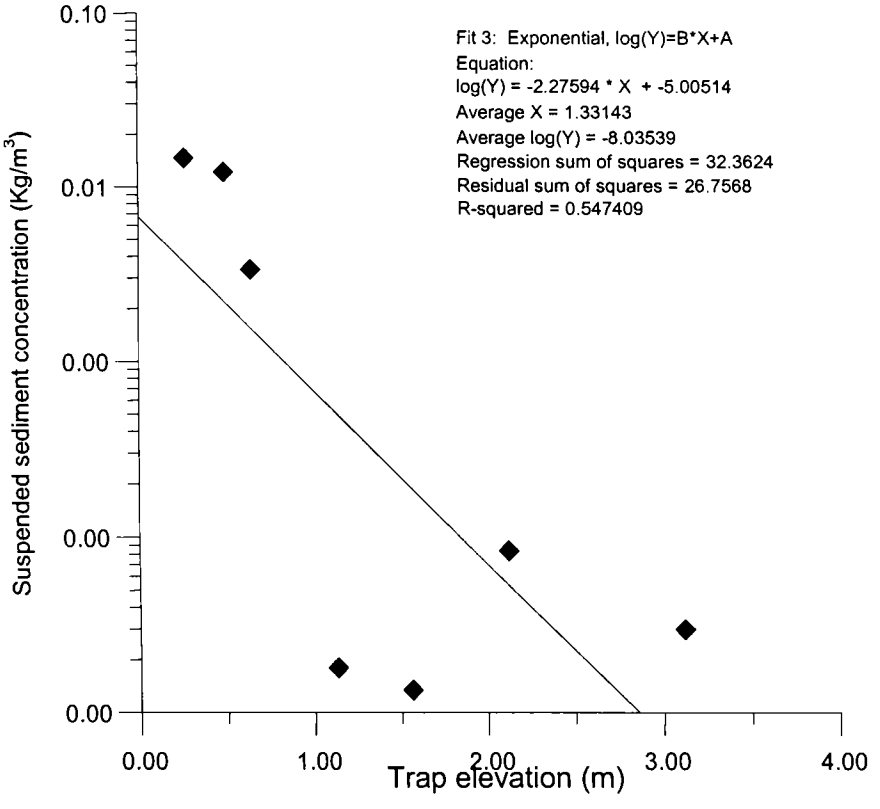

Fig. 6.21 Plot of elevation vs. suspended sediment concentration for the offshore deployment date of 18 July 2001 – 19 August 2001

6.7.5 Computational Procedure

As already stated in Section 6.4.3 the cross-shore flux is computed using equation 6.5. The vertical profile of sediment concentration C(z) and the velocity profile U(z) are the inputs to the above equation. C(z) is calculated using the equation by Nielsen (1992) as

$$C(z) = C_a \exp^{(-z/\ l_s)} \tag{6.6}$$

where C(z) is the SSC at elevation z, and C_a is the near-bed reference concentration and is defined at bed level as C_o and l_s is the mixing length.

The velocity profile U(z) is taken as logarithmic and the velocity at any level is,

$$U(z) = U_m \log_{10}(z_m / z_o) / \log_{10}(0.37d / z_o) \tag{6.7}$$

where U_m is the measured velocity at elevation z_m, while z_o is the roughness length and d is water depth.

In SFLUX, the bed reference concentration is obtained by adopting the formula after Nielsen (1992),

$$C_0 = 0.005(\theta')^3 \tag{6.8}$$

where θ' is called shields parameter and is expressed as

$$\theta' = \frac{0.5\, f_w U^2}{[(s-1)gD]} \tag{6.9}$$

where s is the specific density given by

$$s = \frac{\rho_s - \rho}{\rho} \tag{6.10}$$

where ρ_s and ρ are the sediment and water densities respectively, g is the acceleration of gravity, D is the mean grain size and f_w is the friction factor. The current U is the maximum wave orbital velocity on a wave-by-wave basis (Black, 1994).

6.7.6 Sediment Flux Model Calibration

To calibrate the model the near-bed reference concentrations calculated from the theoretical equations above was compared with the near-bed concentrations measured using the sediment traps. In Table 6.6, comparison of calculated and measured near-bed reference concentrations for a series of deployments is given. Of these, there are 3 when a large number of data points were recorded and good sediment information was also obtained. These are "periods" 3, 8 and 10 in Table 6.6. When these are averaged, it was found that the measured near-bed reference concentration values average 0.030 $kg.m^{-3}$ while the calculated values average 0.037 $kg.m^{-3}$. The ratio of these values is 1.22, which is the calibration factor. This is a very good first agreement as the calculations are sensitive to bedforms, which were not able to be measured. Very steep bedforms will increase the suspended load by upto a factor of about 20 times. The calculation is dominated by the large event #10, and only limited measurements were made at this time. If we consider the lower wave conditions in events #3 and 8 only, then the calibration factor is 3.8. It is appropriate to use the latter factor because more data was recorded during these two periods. Thus, a factor of 3.8 is applied for calculations of the fluxes.

Table 6.6 Comparison of calculated and measured near-bed reference concentrations for a series of deployments

Serial No	Start Day	End day	Calculated	Measured
1	22.08.99	05.09.99	0.2390	0.0000
2	28.10.99	26.11.99	0.0080	0.0000
3	7.03.00	29.03.00	0.0760	0.0167
4	29.03.00	08.04.00	0.1370	0.0000
5	21.05.00	14.06.00	0.0170	0.6415
6	14.06.00	11.07.00	0.0000	0.0000
7	20.07.00	19.08.00	0.0000	0.0193
8	27.10.00	27.11.00	0.0360	0.0121
9	25.04.01	16.05.01	0.0000	0.0624
10	18.07.01	19.08.01	0.9380	0.8930

6.7.7 Results

The results of the computations using the model are as follows:

Average onshore flux:0.201 m^3/m/day

Average offshore flux:0.437 m^3/m/day

Average longshore flux:0.236 m^3/m/day to the south

In order to convert the average daily flux values as above to yearly values we need to know the period for which the onshore and offshore fluxes prevail during a year. It can be roughly taken that offshore flux prevails during the erosive monsoon period and onshore flux prevails during the non-monsoon period. Based on the field data it can be safely assumed that monsoon conditions prevail for about 100 days and non-monsoon conditions for the rest of the period. Based on the above assumption the average daily values can be converted to yearly values by multiplying with the relevant number of days ie, 100 days for offshore flux, 265 days for onshore flux and 365 days for longshore flux. Thus the yearly flux values are:

Onshore flux:53 m^3/m/year

Offshore flux:44 m^3/m/year

Longshore flux:86.14 m^3/m/year to the south

The longshore flux calculated above is for a width of 1m. Assuming that this flux is applicable for the active wave stirring zone of innershelf up to a depth of 10m which is approximately of 2km width, the total longshore flux across this width of the shelf can be calculated by multiplying with 2000. Thus:
Total innershelf longshore flux: 1,72,000 m^3/year to the south

The duration and strength of the onshore/offshore fluxes vary from year to year. In general, it appears to be a situation where the onshore and offshore fluxes are more or less balanced, i.e. nature brings about 50 m^3/m/year onshore during the non-monsoon and then takes it back offshore again in the monsoon. This agrees closely with the estimate of about 60 m^3/m/year from the beach profiles, noting that these vary from year to year and so perfect agreement is not possible.

6.8 SUMMARY OF SEDIMENT BUDGET

Based on the computations using the model and other data available, the annual sediment budget for the Chavara coast can be summarized as below:

Net longshore transport in the surf zone: 1,67,000 m^3 (towards north)
Net longshore transport in the innershelf: 1,72,000 m^3 (towards south)
(computed for 2 km width from the shore)

Cross-shore transport-onshore: 53,000 m^3
(over a 1 km stretch of mining site)
Cross-shore transport-offshore: 44,000 m^3

Thus, there is a sort of balancing between the longshore and cross-shore transport. This is offset by the mining by the IREL which results in a deficit budget for the coast, as is expected in any sand mining scenario. The quantum of mining decides the deficit in the budget, the implication of which is discussed in the following section.

6.9 EROSION OF THE COAST IN RELATION TO SAND MINING

As already seen, the movement of sediment in the alongshore and cross-shore directions are more or less balanced leading to a dynamic equilibrium. The existence of such a dynamic equilibrium also points to a strong connection between the beach and the innershelf. This is in contrast to the situation where either the longshore or cross-shore transport or both are missing resulting in local impact of the mining as shown in Fig. 6.22a-b. The coast under study can be called an "open system" (Fig. 6.22c) where both the longshore and cross-shore transports are active. The impact of mining will not be felt in the beach in such systems as along as the mining is within the replenishable level.

The foreshore of this coast down to 5m depth is very steep (gradient about 1:30), but the innershelf has a low gradient of about 1:500. The data shows clearly that considerable volume of sand is moving about on the innershelf out to 8m depth. As in the case of other coasts worldwide with similar wave climate, a noteworthy sediment mobilisation out to at least 45m depth is expected (Black and Oldman, 1999). The input to the shoreline from offshore during the accretionary phase is large. The measurements indicate an input of no less than $60m^3/m$. Over the shoreline from Neendakara to Thottappally (about 40km), the volumes arriving at the beach from the inner continental shelf each year are therefore about 2.4 million m^3. Mining volumes of the order of 68,000 m^3 (Kurian et al., 2002) which the IREL is mining are about 3% of the total inputs that arrive at the Neendakara-Thottappally stretch each year. When sand is extracted at the beach, then the volumes available to be returned to the innershelf in the erosive periods are reduced and the ultimate impact of mining is to deplete the innershelf source and lower the overall level of the shelf. Spread over a shelf width of 17 km (45m isobath) and along the 40 km of coast, the effect of the extraction is to lower the shelf sediment level by 0.10 mm every year without causing any significant erosion in the beach.

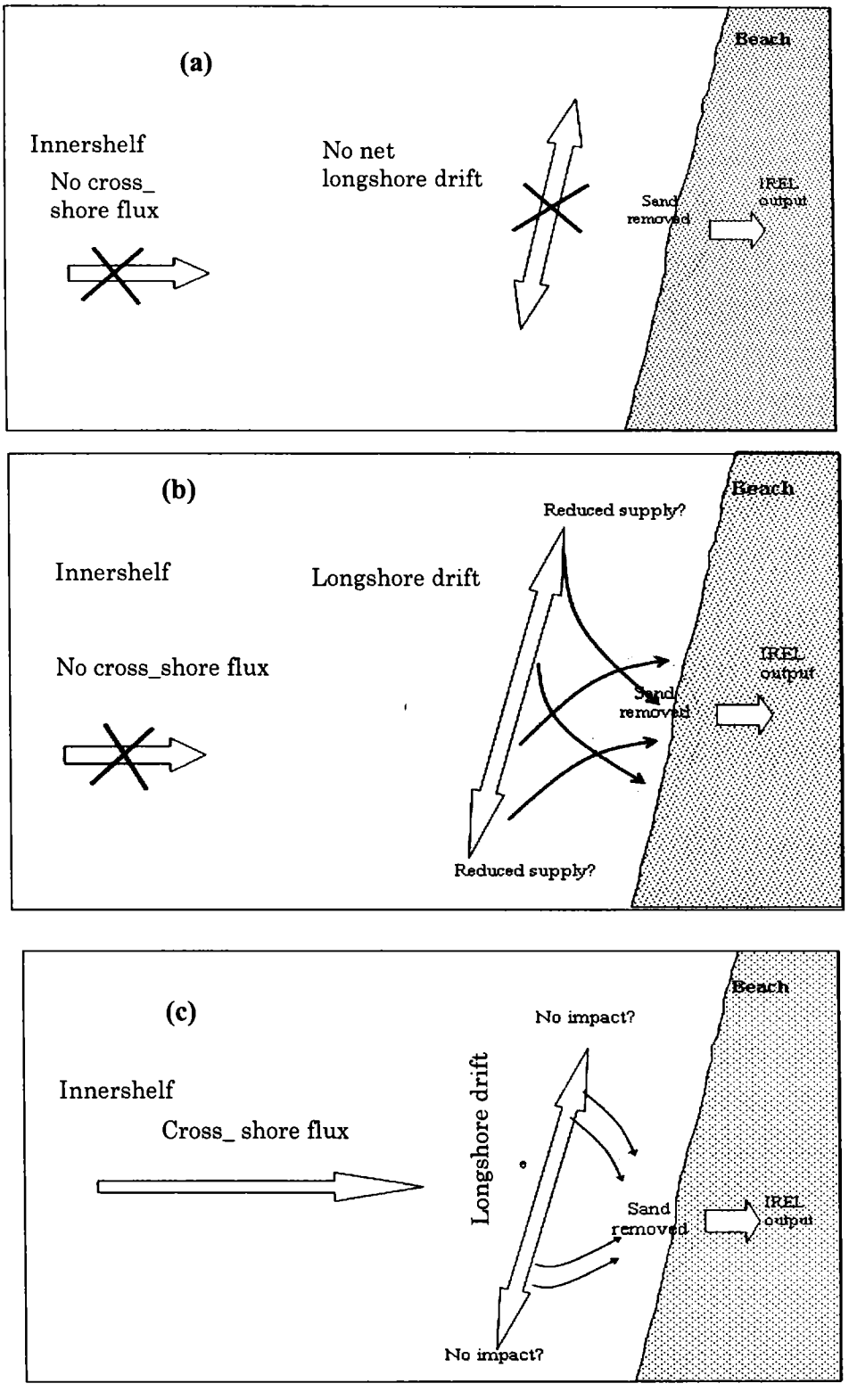

Fig. 6.22 Schematic diagrams showing the impact of beach sand mining when there is (a) no offshore sediment input and no net longshore transport, (b) no offshore sediment input but longshore input occurs and (c) sediment input from offshore and longshore

However, the scenario described above (ie no net erosion in the beach) is applicable only when the quantum of mining is limited to the annual replenishment of sand on the beach by the natural processes (i.e. 60,000-70,000 m^3 along a 1km stretch of beach in the present case). If the quantum of mining exceeds this level, it can cause local impacts on the beach. Indeed the mining scenario changed in the area of study since 2001. While IREL was the major player in the area till 2001, the Kerala Minerals and Metals Ltd. (KMML), another public sector company exploiting the heavy mineral resources, expanded its mining operations in a major way starting from 2001. Though the data for their mining are not made available by KMML, it is estimated that their intake from the area could be a sizable fraction of the intake by IREL. Thus the intake by IREL and KMML together starting from 2001 constitute a quantity much more than the annual replenishment and could upset the dynamic equilibrium seen in beach volume changes till 2001 as in Fig.5.13.

The continuation of beach profile measurements at a few stations (see Section 5.3.2.1) enabled verification of this hypothesis. Figure 6.23 presents the cumulative beach volume changes at stations VMS 4, VMS7 and KMS3 stations for the period 1999-2004. It can be seen that while KMS 3 maintains its dynamic equilibrium and VMS4 even shows an upswing, VMS 7 shows cumulative loss of material showing the imbalance. It is pertinent to note that the beach adjoining the station VMS7 is the intake area of KMML too. Thus it is obvious that the combined mining by KMML and IREL has offset the dynamic equilibrium in beach volume changes seen till 2001 at VMS 7. The field data conclusively support the hypothesis that any intake more than the annual replenishment could have serious consequences on the beach.

6.10 DISCUSSION AND SUMMARY

The investigation shows that the sediment budget of the coast is constituted by the longshore and cross-shore sediment transports together with the quantum of sand mining. The computations show that the coast under study is an open system with considerable inputs by the longshore as well as the cross-shore transports. The longshore transport through the surf zone of the study area is 1,67,000 m^3/year. This value is in close agreement with the results of Jose et al. (1997) for Chavara coast.

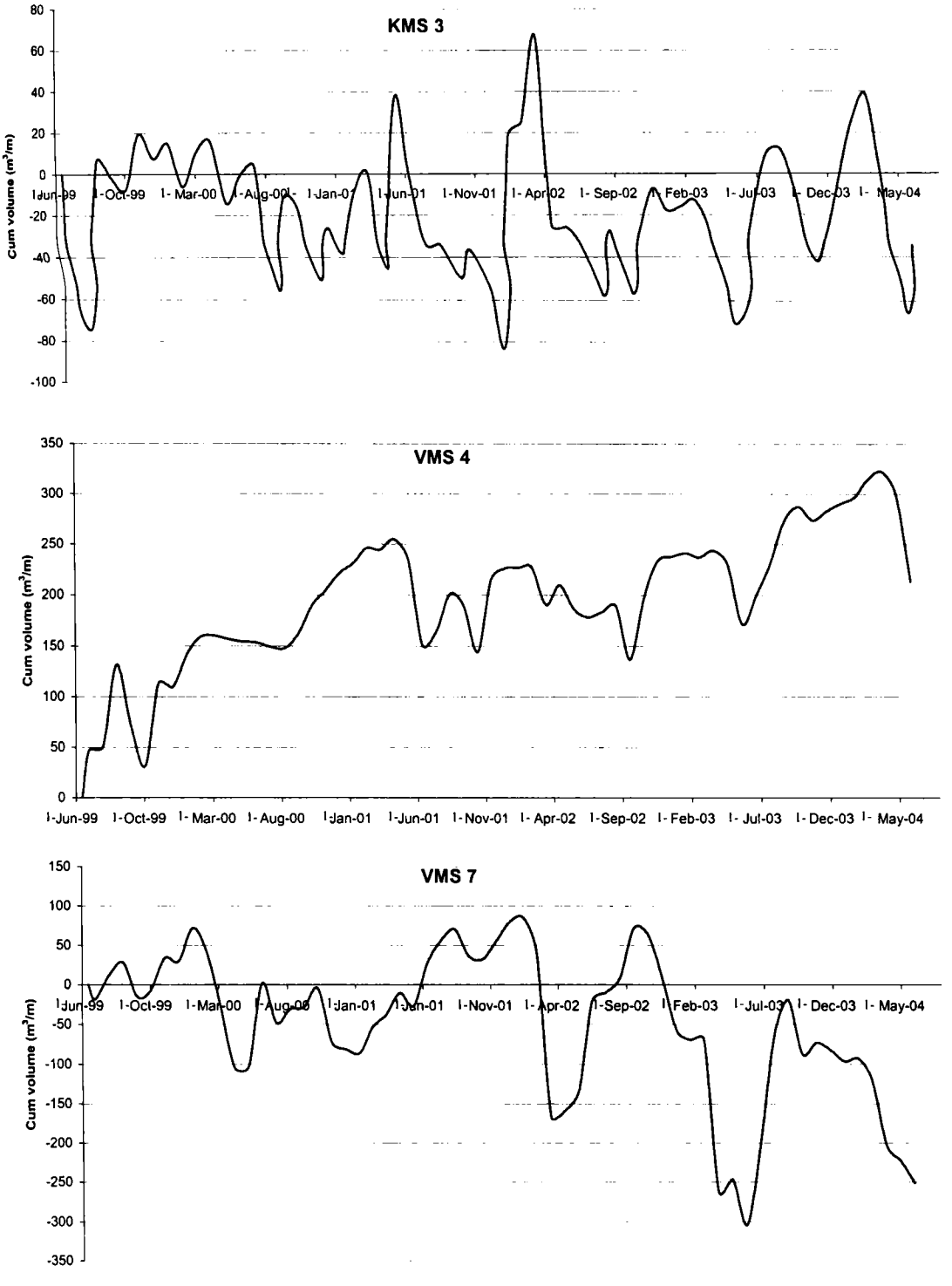

Fig. 6.23 Five year cumulative volume changes (June 1999 to June 2004) at KMS 3, VMS 4 and VMS 7.

Chandramohan and Nayak (1991) estimated an annual net sediment transport of 9,50,000 m^3/year towards south along the Kollam coast. Sanil Kumar et al. (2006) estimated that the net sediment transport rate for Kollam coast was 3,83,784 m^3/year towards south. The longshore transport values observed by these authors which are many times higher than the present results does not appear to be true from field conditions since there are no visible sign of such a huge transport. Also, the net southerly transport obtained by them does not appear to be correct as can be seen by the deposition on the southern side of the Kayamkulam inlet breakwater (Fig. 1.6) which is indicative of northerly transport. Thomas (1988) observed for the Trivandrum coast that the longshore currents are directed north on average for 9 of the 12 months when averaged over 5 years from 1980-84. A similar pattern was measured by Shahul Hameed (1988) at Alleppey. This ratio between the northward and southward fluxes is true in the present case too.

It is calculated that the onshore flux is 53 m^3/m/year and the offshore flux is 44 m^3/m/year. Unfortunately, the studies to estimate the cross-shore sediment transport are lacking in Indian Scenario. However, the cumulative beach volume changes of 60-70 m^3 seem to support these computed results.

Black et al. (2006) describes the beach–innershelf sedimentary system of Chavara as a "step-ladder" coast. The main supports of the ladder, according to them, are the two longshore fluxes of sediment. The first one is the flux to the north along the beach in and adjacent to the surf zone driven by the waves that approach predominantly from the south to south-west quadrants. The second flux is to the south on the inner continental shelf, beyond the surf zone, driven by prevailing wind from the north to north-west quadrant that induces southbound currents for much of the year. The rungs of the ladder are cross-shore exchanges of sediment between the inner shelf and beach. The onshore and offshore fluxes, the rungs of the ladder, are also balanced.

On this balanced beach-innershelf sedimentary system is superimposed the mining which is a sink in the system. The impact of mining is focused on small regions where the mining occurs. While the long-term impact is regional and small, the short-

term impacts are larger around the sink, until the effects diffuse into the broader system. The short-term impacts are primarily scaled by the local longshore and cross-shore transport rates. For this, the quantum of mining has to be less than the volume of arrival of sand. When the quantum of mining exceeds the local supply of sand by longshore and onshore transport, local impacts will be visible as cumulative erosion in the beach as seen in the present investigation.

To conclude, the beach sediment budget of the Chavara coast is constituted by the longshore and cross-shore transport together with the intake due to mining. There is a balancing between the sediment fluxes leading to a dynamic equilibrium. Sand mining from the beach makes this coast one with deficit sand budget. However, due to the strong connection between the beach and innershelf, the impact of sand mining is not felt on the beach as long as the mining is kept at an optimum level. When the quantum of mining exceeds the supply of sand by the natural processes, local impacts by way of beach erosion is seen. Though sand extraction will cause erosion in the innershelf, the level and time taken for a measurable impact can be long if the extraction volumes are much less than the volumes being moved naturally on/offshore and alongshore.

Chapter 7

SUMMARY AND CONCLUSIONS

7. SUMMARY AND CONCLUSIONS

Sediment budgeting studies are done to bring out the coastal processes at work, to understand the beach-innershelf sedimentary dynamics and to assess the stability of any coastal stretch. There is a dearth of such studies as far as the Indian coast is concerned. The Chavara coast of Kollam district, Kerala, is world famous for its rich heavy mineral resources. These mineral resources are being commercially mined by the Indian Rare Earths Ltd. (IREL) and Kerala Minerals and Metals Ltd. (KMML), two Public Sector Undertakings located in the area. The impact of mining on stability of the beach has been a point of debate among the local people as well as researchers. Hence a sediment budgeting study was taken up for this coast as it offered a very interesting and challenging research problem. The study was taken up with the following objectives:

- Study the hydrodynamic processes and mechanisms involved in the sediment movement along the Chavara coast
- Identify the different sources and sinks of beach sand along the coast
- Quantify the sediment input/output into/from the coast
- Assess the erosion/accretion scenario of the coast based on the study

The investigation covered the coastal stretch of 22km length from Neendakara to Kayamkulam which is referred to as the Chavara coast. A comprehensive field measurement programme taking care of the data requirements for the investigation was meticulously planned and implemented. Wave and current data for different periods spanning over a period of 27 months (ie. more than 2 years) were collected and analysed. Beach based field programmes were also implemented successfully. Close grid beach profiling was carried out at two sites while coarse grid profiling was carried out along the rest of the 22km long coastline. Bathymetric survey was carried out over a region extending 70 km along the coast encompassing the study area and extending out to 60m depth. In addition, seasonal bathymetric surveys were carried out in the inshore regions coupled with SLED measurements to study the seasonal changes in the nearshore profile. The field data were processed to understand the

hydrodynamic and beach-innershelf sedimentary processes and to set up numerical models for sediment budget computations.

A study of the wind pattern in the area was taken up using the IMD data for Alleppey, considering the importance of wind as an important forcing factor in the hydrodynamic regime. The distribution of wind is characterized by the seasonal variation. During fair weather period of November-April, the speeds are generally low with a good scattering. In the rough weather months of May-October, the speeds are higher with a focusing of the direction in the SW-NW quadrants. However, during the rough weather also, the easterlies which are generally weak when compared to the strong westerlies are prevalent. The highest wind speed recorded in the study area was 11m/s.

Analysis of the extensive wave data shows that the wave climate of Chavara coast in general is characterized by monsoonal high and non-monsoonal low wave activity. The seasonal variations are typical of the pattern observed for other locations of the southwest coast of India. The wave characteristics during the peak monsoon period (June, July and August) are characterised by relatively higher wave heights and shorter wave periods. This is attributed to the proximity of the coast to the wave generating zones in the Arabian Sea during the peak monsoon. The highest wave recorded during the study period has a height of 3.8m. Intermittent breaks in intensity of waves for periods extending for 10 to 15 days are observed during monsoon in all the three years and this is in tune with the normal characteristic of the monsoonal climate. Low wave heights (<1m) and a wide range in periods (7-15s) characterize the waves during the pre-monsoon and post-monsoon seasons. The long periods are associated with swells that originate far away in the Indian Ocean. The shorter wave periods recorded during these seasons indicate sea waves generated locally by persisting NW wind. During the period of wave recording that covered three monsoon periods, though the annual cyclic pattern of changes were same, inter-annual changes were significant.

The exhaustive set of measured current data at two offshore sites spanning over a period of more than two years, which is unique for the Indian coast, is used to study the currents. Currents show seasonal changes with stronger currents during monsoon and weaker currents during fair weather. The maximum observed current is 70 cm/s and the common maxima are around 15-20 cm/s. It is found that both in nearshore and offshore sites alongshore components of the currents are mostly much stronger than the cross-shore flows. The observed current appears to be a resultant of tidal currents, wind-driven currents and continental shelf currents. The influence of tides on the current is quite evident from the semidiurnal oscillations seen in the time series distributions for different measurement periods. A good correspondence is seen between wind and currents on many occasions in the study area. The predominant NW winds in this region, according to theory, can generate currents mostly longshore to the south on the inner shelf. The dominance of southerly flow is quite evident from the recorded data. On this wind-driven pattern is superimposed a shelf current associated with larger-scale circulation in the Indian Ocean which is characterised by the Lakshadweep High and Low. It is deduced from the data that when the northwest wind abates the shelf currents flows in response to the general circulation, although the net movement is southward. In addition to the tidal, wind driven and continental shelf currents, there could also be the contribution of coastal trapped waves and baroclinic flow associated with the plumes of fresh water coming from the estuaries.

Significant seasonal variability is observed in the case of littoral environmental parameters in line with the variability in wave parameters observed in the offshore zone. The beach generally has maximum width during the fair weather months and the lowest in the months of May-June-July, when the wave intensity is at its maximum. The seasonal cycle is maximum at sites, which are not fronted by sea walls. During the period June '99 to June '00 volume change is 60 m^3/m of beach while in the subsequent year the volume change is 70 m^3/m, indicating a more or less steady condition on an annual basis. Five-year beach profile data at selected stations show conditions different from this starting from 2001 with cumulative erosion at station VMS7.

Wave is found to be the predominant force influencing the beach processes. Offshore transport of sediments induced by steep waves takes place during the peak monsoon leading to intense erosion. Re-building of beach takes place during the fair weather months when onshore transport of sediments takes place. The wave induced longshore currents bring about spatial variations in the erosion/accretion pattern. It is observed that there is a good correlation between the wind and erosion/accretion pattern of beach. This is attributed to the wind induced circulation in the innershelf. Westerly wind generates offshore bottom current leading to erosion while northerly wind generates onshore current resulting in accretion. Winds along this coast being predominantly NW, a slight rotation of wind would lead to changes from net erosion to accretion. Mining of beach sand for heavy mineral extraction is an anthropogenic activity which has an impact on the beach as seen at station VMS7.

Based on the investigation, it is concluded that the beach sediment budget of the Chavara coast is constituted by the longshore and cross-shore transport together with the intake due to mining. There are two longshore fluxes; first, there is a flux to the north of an average yearly value of 1,67,000 m^3 along the beaches in and adjacent to the surf zone which is driven by the waves that approach predominantly from the south to south-west quadrants. The second flux is to the south on the inner continental shelf of value 1,72,000 m^3, beyond the surf zone. This is driven by a prevailing wind from the north to north-west quadrant that induces southbound currents for much of the year. The two longshore transports are linked by the onshore and offshore transport which are also more or less balanced. Thus there is a balancing between the longshore and cross-shore transport leading to a dynamic equilibrium.

Due to the strong connection between the beach and innershelf, the impact of sand mining is not felt on the beach when the mining is within an optimum level equivalent to the quantum of sand replenished by the natural processes. When the quantum of mining exceeded the supply of sand by the natural processes, local impacts by way of beach erosion is seen. The five yearly beach profile data which shows cumulative erosion at station VMS7 starting from 2001 conclusively proves this point. It is concluded that, though sand mining will cause erosion in the innershelf, the level and

time taken for a measurable impact can be long if the extraction volumes are much less than the volumes being moved naturally on/offshore and alongshore.

Recommendations for Future Work

The present work is a pioneering effort in sediment budgeting studies. The study has proved beyond doubt the usefulness of such studies in understanding the beach-innershelf sedimentary system, in apportioning the role of each contributing factor in the erosion/accretion scenario of the coast and for making a final assessment of the stability of the coast under different scenarios. Thus sediment budgeting studies should be made mandatory for all coastal systems that are critically eroding or are under threat due to anthropogenic activities such as mining or coastal engineering projects.

While all efforts have been made to conduct the study within reasonable accuracy level utilizing the then available infrastructure and numerical models, future studies could be directed to take care of some of the limitations of the study with regard to numerical models and instrumentation. Some of the efforts in future that would greatly enhance the reliability of the sediment budgeting studies are given below.

- Longshore transport models are very sensitive to wave breaker angles. Though a directional wave gauge was initially used in the present study, the data collection could not be continued due to malfunctioning of the equipment. A directional wave gauge should be made an essential component of the instrumentation system.
- The vertical profile of currents is another desirable data that could help in the calibration of models and computation of cross-shore sediment flux. An ADCP could ideally replace the current meters.
- An important addition to the offshore instrumentation could be an underwater video camera that could give vital information on bed form, which is required in understanding the physical environment as well as providing some empirical coefficients in numerical modelling.

- Wind data is very essential in sediment budgeting studies. Shore-based records of wind have limitations as seen in the present study. Hence wind data based on offshore data buoys would be the ideal choice.

Further refining of numerical models engaged for the work is essential. Attempts could be focused in the following directions.

- Many of the beaches are fronted by sea walls. In such a condition the longshore transport model in its present form which doesn't take care of this situation should be appropriately modified. The longshore transport rates estimated using the present models in such cases are over estimates.
- Coefficients/constants relevant for the coast should be worked out for input into the models. Under water video images should be used for providing appropriate values for bed characteristics and friction coefficient.

It can be said with confidence that sediment budgeting studies incorporating the above suggestions will be a real boon for investigation of coastal erosion problem including future projections and suggestion of appropriate mitigation measures.

REFERENCES

Aagaard, T. and Greenwood, B., 1994. Suspended sediment transport and the role of infragravity waves in barred surfzone. *Marine Geology*, 118, 23-48.

Antony, M.K., 1990. Northward undercurrent along west coasts of India during upwelling- some inferences. *Indian Journal of Marine Sciences*, 19, 95-101.

Baba, M. and Joseph, P.S., 1988. Deepwater wave climate off Cochin and Trivandrum. In: *Ocean waves and beach processes of south west coast of India and their prediction* (Eds: Baba, M. and Kurian, N.P.), CESS, Trivandrum, 129-139.

Baba, M. and Kurian, N.P., 1988. Ocean waves and beach processes of south west coast of India and their prediction. Centre for Earth Science Studies, Trivandrum, December 1988, 249p.

Baba, M., 1988. Wave characteristics and beach processes of the southwest coast of India-a summary. In: *Ocean waves and beach processes* (Eds: Baba, M. and Kurian, N.P.), CESS, Trivandrum, 225-239.

Baba, M., Hameed, T.S.S., Kurian, N.P. and Subaschandran, K.S., 1992. Wave power of Lakshadweep Islands. *Project Report*, CESS, Trivandrum, 178p.

Basu, S., Meyers, S.D. and O'Brien, J.J., 2000. Annual and inter annual sea level variations in the Indian Ocean from TOPEX/POSEIDON observations and ocean model simulations. *Journal of Geophysical Research*, 105, 975-994.

Belknap, D.F., Kraft, J.C., 1985. Influence of antecedent geology on evolution of barrier systems. In: Special Issue: *Marine Geology* (Eds: Oertel, G. and Leatherman, S.P.), 63, 235–262.

Best, T.C., Griggs, G.B., 1991. A sediment budget for the Santa Cruz littoral cell, California. In: *From Shoreline to Abyss: Contributions in Marine Geology in*

Honor of Francis Parker Shepard, (Ed: Osborne, R.H.), Special Publication, Society Econ. Paleontology Mineralogy, 46, 35–50.

Black, K.P. and Baba, M., 2001. Developing a management plan for Ashtamudi Estuary, Kollam, India. *Project Report*, ASR Ltd., New Zealand and CESS, Thiruvananthapuram. 546p.

Black, K.P. and Healy, T.R., 1983. Side-scan Sonar Survey, Northland Forestry Port Investigation, Northland Harbour Board. *Project Report*, ASR, 88p.

Black, K.P. and Rosenberg, M.A., 1991. Suspended load at three time scales. *Proc.* Coastal Sediments '91, ASCE, 313-327.

Black, K.P. and Vincent, C.E., 2001. High-resolution field measurements and numerical modelling of intra-wave sediment suspension on plane beds under shoaling waves. *Coastal Engineering*, 42, 173–197.

Black, K.P., 1994. Suspended sediment load during an asymmetric wave cycle over plane bed. *Coastal Engineering*, 23, 95-114.

Black, K.P., 1996. Lagrangian Dispersal and Sediment Transport Model POL3DD, 21, University of Waikato.

Black, K.P., Kurian, N.P., Mathew, J. and Baba, M., 2006. Open tropical beach dynamics. *Journal of Coastal Research* (In press).

Bodge, K.R., 1999. Inlet Impacts and Families of Solutions for Inlet Sediment Budgets. *Proc.* Coastal Sediments '99, ASCE, 703–718.

Bowen, A.J. and Inman, D.L., 1966. Budget of Littoral Sands in the Vicinity of Point Arguello, California. CERC Technical Memorandum. No. 19, 41p.

Bruce, J.G., Johnson, D.R., and Kindle, J.C., 1994. Evidence of eddy formation in the eastern Arabian Sea during the northeast monsoon. *Journal of Geophysical Research*, 99, 7651-7664.

Carter, L., 1986. A budget for modern-Holocene sediment on the South Otago continental shelf. *New Zealand Journal of Marine and Freshwater Research*, 20, 665-676.

Chandramohan, P. and Nayak, B.U., 1991. Longshore sediment transport along the Indian coast. *Indian Journal of Marine Sciences*, 20, 110-114.

Chandramohan, P. and Rao, T.V.N., 1984. Study of longshore current equation for currents in Visakhapatnam coast. *Indian Journal of Marine Sciences*, 13, 24-28.

Chandramohan, P., Jena, B.K. and Sanil Kumar, V., 2001. Littoral drift sources and sinks along the Indian coast. *Current Science*, 81, 292-297.

Chandramohan, P., Nayak, B.U., Sanil Kumar, V. and Pathak, K.C., 1994a. Beach process between Mulgund and Shiroda, West coast of India. *Indian Journal of Marine Sciences*, 23, 102-104.

Chandramohan, P., Sanil Kumar, V., Nayak, B.U. and Pathak, K.C., 1993. Variation of longshore current and sediment transport along the south Maharashtra coast, West coast of India. *Indian Journal of Marine Sciences*, 22, 115-118.

Chandramohan, P., Sanil Kumar, V., Nayak, B.U. and Raju, N.S.N., 1994b. Surf zone dynamics along the south Karnataka coast between Bhatkal and Ullal, West coast of India. *Indian Journal of Marine Sciences*, 23, 189-194.

Chavadi, V.C. and Bannur, C.R., 1992. Beach profile study along Ramangundi beach of North Karnataka coast. *Indian Journal of Marine Science*, 21, 107-110.

Christiansen, C., Aagaard, T., Bartholdy, J., Christiansen, M., Nielsen, J., Nielsen, N., Pedersen, J.B.T and Vinther, N., 2004. Total sediment budget of a transgressive barrier-spit, Skallingen, SW Denmark: A review. *Danish Journal of Geography,* 104, 107-126.

Cooper, J.A.G. and Nevas, F., 2004. Natural bathymetric change as a control on century-scale shoreline behavior. *Geology*, 32, 513– 516.

Cooper, N.J. and Pethick, J.S., 2005. Sediment budget approach to addressing coastal erosion problems in St. Queen's Bay, Jersey, Channel Islands. *Journal of Coastal Research,* 21, 112–122.

Corso, W. and Joyce, P.S., 1995. *Oceanography.* Springhouse Corporation, Spring house, 182p.

Cutler, A.N. and Swallow, J.C., 1984. Surface currents of the Indian Ocean (to 25°S, 100°E): Compiled from historical data archived by the Meteorological Office, Bracknell, U.K. Rep. 187, 36 charts, 8 p., Institute of Oceanographic Science., Wormley, England.

Das, V.K., Varkey, M.J. and Raju, D.V.R., 1979. Wave characteristics of the Laccadive Sea. *Indian Journal of Marine Sciences*, 8, 203-210.

Dattari, J., Rao, N.B.S., Rao, S., Dwarakish, G.S. and Kumar, B.N., 1997. Beach profile studies along Dakshina kannada coast of Karnataka state. *Proc.* Indian National Conference on Harbour and Ocean Engineering, 1135-1144.

Deigaard, R., Fredsoe, J. and Hedegaard, I.B., 1986. Suspended sediment in the surf zone. *Journal of Waterway, Port, Coastal and Ocean Engineering*, 112, 115-127.

Diwan, S.G., Suryavaunshi, A.K. and Nayak, B.U., 1985. NIO's experience in Datawell wave rider buoys. *Proc.* 1st National Conference on Dock and Harbour Engineering, Bombay, 2: E, 143-156.

Einstein, H.A., 1950. The bed-load function for sediment transportation in open channel flows. U.S. Dep. Agric. Tech. Bull., 1026, 71p.

Fairbridge, R.W., 1966. The encyclopedia of Oceanography. Dowden, Hutchinson & Ross Inc., USA. 1021p.

Fenster, M. and Dolan, R., 1994. Large-scale reversals in shoreline trends along the U.S. mid-Atlantic coast. *Geology,* 22, 543– 546.

Fernadez, A.A., Chandramohan, P. and Nayak, B.U.T.I. 1993. Observed currents at Bombay High during a winter. *Mahasagar,* 26, 95-104.

FitzGerald, D.M., Lincoln, J.M., Fink, L.K., Caldwell, D.W., 1989. Morphodynamics of tidal inlet systems in Maine. In: *Studies in Marine Geology 5*: (Eds: Tucker, R.D. and Marvinney, R.G.). Quaternary Geology. ME Geological Survey, Augusta, ME, 67-96.

Fredsoe, J. and Deigaard, R., 1992. *Mechanics of Coastal Sediment Transport. World Scientific, Singapore, 369p.*

Fredsoe, J., Anderson, O.H. and Silberg, S., 1986. Distribution of suspended sediment in large waves. *Journal of Waterway, Port, Coastal and Ocean Engineering*, 111, 1041-1059.

Gelfenbaum, G., Sherwood, C.R., Peterson, C.D., Kaminsky, G.M., Buijsman, M., Twichell, D.C., Ruggier, P., Gibbs, A.E. and Reed, C., 1999. The Columbia river littoral cell: a sediment budget overview. *Proc.* 4th International Conference on Coastal Engineering and Coastal Sediment Processes American Society of Civil Engineers.

Glenn, S.M. and Grant, W.D., 1987. A suspended sediment stratification correction for combined wave and current flows. *Journal of Geophysical Research*, 92, 8244-8264.

Graber, H.C., Beardsley, R.C. and Grant, W.D., 1989. Storm-generated surface waves and sediment resuspension in the East China and Yellow Seas. *Journal of Physical Oceanography*, 19, 1039-1059.

Grant, W.D and Madsen, O.S., 1979. Combined wave and current interaction with a rough bottom. *Journal of Geophysical Research*, 84, 1797-1808.

Green, M.O. and Vincent, C.E. 1990. Wave entrainment of sand from a rippled bed. *Proc. International Conference in Coastal Engineering*, ASCE, 1990, 2200-2212.

Greenwood, B., Osborne, P.D., Bowen, A.J., Hazen, D.G. and Hay, A. 1990. Nearshore sediment flux and bottom boundary transport programme (C-COAST). *Proc.* International Conference in Coastal Engineering, ASCE, 2227 - 2240.

H.M.S.O. 1949. Monthly Meteorological Charts of the Indian Ocean. No. 519, H.M. Stationary office, London.

Hameed, T.S.S., 1988. Wave climatology and littoral processes at Alleppey. In: *Ocean waves and beach processes of south west coast of India and their prediction*, (Eds: Baba, M. and Kurian, N.P.), CESS, Trivandrum, December 1988, 67-90.

Hameed, T.S.S., Baba, M. and Thomas, K.V., 1986. Computation of longshore currents. *Indian Journal of Marine Sciences*, 15, 92-95.

Hanson, H., and Kraus, N.C. 1989. "GENESIS: Generalized Model for Simulating Shoreline Change. Technical Report CERC-89-19, U.S. Army Engineer Waterways Experiment Station, Vicksburg, MS.

Hareesh Kumar, P.V. and Sanil Kumar, K.V., 2004. Long period waves in the coastal regions of north Indian Ocean. *Indian Journal of Marine Sciences*, 33, 150-154.

Harish, C.M., 1988. Waves and related nearshore processes in a complex bay beach at Tellicherry. In: *Ocean waves and Beach processes of the South-west coast of India and their prediction*, (Eds: Baba, M. and Kurian, N.P.), CESS, 111-128.

Hess, L. and Harris, W.H., 1987a. Morphology and sediment budget during recent evolution of a barrier beach, Rockaway, New York. *Geology*, 9, 94–109.

Hess, L. and Harris, W.H., 1987b. Effect of storm energy and shoreline engineering on the sediment budget of a barrier beach, Rockaway, New York. *Geology*, 9, 110–115.

Hill, H.H., Kelley, J.T., Belknap, D.F. and Dickson, S.M., 2004. The effects of storms and storm-generated currents on the sand beaches in southern Maine. *Marine Geology*, 210, 149– 168.

Hogben, N. and. Lumb, F.E., 1967. *Ocean Wave Statistics.* H.M. Stationary Office.

Horikawa, K., 1988. *Nearshore dynamics and coastal processes*. University of Tokyo Press, pp 522.

Hume, T.M., Bell, R.G., Black, K.P., Healy, T.R. and Nichol, S.L., 1999. Mangawhai-Pakiri Sand Study. Final Report, Sand Movement and Storage and Nearshore Sand Extraction in the Mangawhai-Pakiri Embayment, NIWA *Client Report* ARC 60201/10 prepared for The Working Party, Mangawhai-Pakiri Sand Study, ARC Environment, Auckland Regional Council, New Zealand.

Jayappa, K.S., 1996. Longshore sediment transport along the Mangalore coast, West coast of India. *Indian Journal of Marine Sciences,* 25, 157-159.

Jena, B.K. and Chandramohan, P., 1997. Sediment transport near the peninsular tip of India. *Proc.* Second Indian National conference on Harbour and Ocean Engineering, Trivandrum, 1054-1060.

Jena, B.K., Chandramohan, P and Sanil Kumar, V., 2001. Longshore transport based on directional waves along north Tamil Nadu coast. *Journal of Coastal Research*, 17, 322-327.

Jimenez, J.A., Sanchez-Arcilla, A., Garcia, M.A., van Overeem, J. and Maldonado, A., 1991. The Ebro Delta project: a first sediment budget. *Proc.* Coastal Sediments '91, 2323-2334.

John, J.E. and George, V., 1980. Shoreline changes on the Kerala coast. In: *Geology and geomorphology of Kerala*, Trivandrum.

John, V.C., Srivastava, P.S. and Malhotra, A.K., 1979. Oceanographic studies off Narara Bet, Gulf of Kutch. *Indian Journal of Marine Sciences*, 8, 20-26.

Jose, F. Kurian, N.P. and Prakash, T.N., 1997. Longshore sediment transport along the southwest coast of India. *Proc.* Indian National Conference in Harbour and Ocean Engineering, 1047-1053.

Jose, F., 2000. Coastal hydrodynamics and sediment transport along SW coast of India with special reference to heavy sand. *Unpublished Ph.D. thesis. Cochin University of Science and Technology*, 207p.

Joseph, E.S., 1962. Shore erosion and protection with special reference to Kerala coast, *M.Sc. Thesis, University of Kerala*, Trivandrum.

Kelley, J.T., Barberb, D.C., Belknap, D.F., FitzGerald, D.M., Heterenc, S.C. and Dicksond, S.M., 2005. Sand budgets at geological, historical and contemporary time scales for a developed beach system, Saco Bay, Maine, USA. *Marine Geology,* 214, 117–142.

Komar, P.D., 1976. *Beach Processes and sedimentation.* Prentice Hall, Inc., Englewood Cliffs, New Jersey, 429p.

Komar, P.D., 1989. Physical processes of waves and currents and the formation of marine placers. *CRC Critical Reviews in Aquatic Sciences*, Oregon Sea Grant, Publication No. ORESU-R-89-019, 1, 393-423.

Komar, P.D., 1998. *Beach Processes and Sedimentation* (second edition). Prentice Hall, Inc., Englewood Cliffs, New Jersey.

Kraus, N.C. and Rosati, J.D., 1999a. Estimation of Uncertainty in Coastal-Sediment Budgets at Inlets. Coastal Engineering Technical Note CETN IV-16, U.S. Army Engineer Research and Development Center, Coastal and Hydraulics Laboratory, Vicksburg.

Kurian, N. P., 1989. Shallow water wave transformation. In: *Ocean wave studies and applications* (Eds: Baba, M. and Hameed, T.S.S.), CESS, 15-32.

Kurian, N.P. and Baba, M., 1987. Wave attenuation due to bottom friction across the southwest Indian continental shelf. *Journal of Coastal Research*, 3, 485-490.

Kurian, N.P., 1987. Wave height and spectral transformation in the shallow waters of Kerala coast and their prediction. *Unpublished Ph.D Thesis, Cochin University of Science and Technology*, Cochin, India, 147p.

Kurian, N.P., 1988. Waves and littoral processes at Calicut. In: *Ocean waves and beach processes* (Eds: Baba, M. and Kurian, N. P.), CESS, 91-110.

Kurian, N.P., Baba, M. and Hameed, T.S.S., 1985. Prediction of nearshore wave heights using a refraction programme. *Coastal Engineering*, 9, 347-356.

Kurian, N.P., Prakash, T.N., Thomas, K.V., Hameed, T.S.S., Chattopadhyay, S. and Baba, M., 2002. Heavy mineral budgeting and management at Chavara. *Project Report,* CESS, Thiruvananthapuram. Vol 1 and 2, 513p.

List, J.H., Jaffe, B.E. and Sallenger, A.H., 1991. Large-scale coastal evolution of Louisiana's barrier islands. *Proc.* Coastal Sediments '91. Specialty Conference/WR, 1532– 1546.

Machado, T. and Baba. M, 1984. Movement of beach sand in Vizhinjam, West Coast of India. *Indian Journal of Marine Sciences*, 13,144-146.

Machado, T. and Vasudevan, V., 1984. Spatial bathymetric variation over the innershelf off Trivandrum. *Mahasagar,* 17, 55-58.

Madsen O. S. and Grant, W. D., 1975. The threshold of sediment movement under oscillatory water waves: A discussion. *Journal of Sedimentary Petrology*, 45, 2, 360-361.

Madsen O.S. and Grant, W.D., 1976. Sediment transport in the coastal environment. *Rep. 209*, Ralph M. Parsons Lab for Water Resources and Hydrodynamics, Dept. of Civil Engineering, Mass. Inst. Of Technology, Cambridge, 105p.

Madsen O.S. and Grant, W.D., 1977. Quantitative description of sediment transport by waves. *Proc.* 15th Coastal Engineering Conference, II, 1093-1112.

McCreary, J.P., Kundu, P.K. and Molinari, R.L., 1993. A numerical investigation of dynamic, thermodynamics and mixed-layer processes in the Indian Ocean. *Progress in Oceanography*, 31, 181-244.

Menon M.R.B., 1964. Beach erosion and defense. *M.Sc. Thesis, University of Kerala,* Trivandrum.

Mocke, G.P. and Smith, G.G., 1992. Wave breaker turbulence as a mechanism for sediment suspension. *Proc.* Coastal Engineering, 2, 2279-2292.

Mony, N.S. and Nambiar, A.K.N., 1965. Study of artificial nourishment at Purakad coastal area, Kerala. *Proc.* 35th Annual Research Session of CBIP, India.

Mony, N.S. and Nambiar, A.K.N., 1966. Study of seasonal variations in the beaches of the Kerala state. *Irrigation and Power Journal*, 24, 2-12.

Mukherjee, A.K. and Sivaramakrishnan, T.R., 1982a. Waves over Arabian sea during monsoon. *Mausam*, 33, 59-64.

Mukherjee, A.K. and Sivaramakrishnan, T.R., 1982b. Swells over Bay of Bengal around the time of onset of monsoon. *Mahasagar*, 16, 51-52.

Muraleedharan, G., Unnikrishnan Nair, N. and Kurup, P.G., 1989. A study of the average visual save statistics vis-à-vis recorded waves. *Proc.* National Conference on Coastal Zone Management, 1-8.

Murty, C.S. and Varadachari, V.V.R., 1980. Topographic changes of the beach Valiathura, Kerala. *Indian Journal of Marine Sciences*, 9, 31-34.

Murty, C.S., 1977. Studies on the physical aspects of the shoreline dynamics at some selected places along the west coast of India. *Unpublished Ph.D. Thesis, University of Kerala*, 149p.

Muty, C.S., Sastry, J.S. and Varadachary, V.V.R., 1980. Shoreline deformation in relation to shore protection strecture along Kerala coast. *Indian Journal of Marine Sciences*, 9, 77-81.

Narasimha Rao, T.V. and Prabhakara Rao, B., 1989. Alongshore velocity field off Visakhapatnam, east coast of India during pre monsoon season. *Indian Journal of Marine Sciences,* 18, 46-49.

Narasimha Rao, T.V., Prabhakara Rao, B., Subha Rao, V. and Sadhuram, Y., 1995. Variability of the flow field in the inner shelf along the central east coast of India during April, 1989. *Continental Shelf Research*, 15, 241-253.

Nerem, R.S., Schrama, E.J., Koblinsky, C.J. and Beckley, B.D., 1994. A preliminary evaluation of ocean topography from the TOPEX/POSEIDON mission. *Journal of Geophysical Research*, 99, 565-583.

Nielsen, P., 1986. Suspended sediment concentrations under waves. *Coastal Engineering*, 10, 23-31.

Nielsen, P., 1992. *Coastal Bottom Boundary Layers and Sediment Transport.* Advanced Series on Ocean Engineering Vol. 4, World Scientific, Singapore, 324p.

NIO 1982. Wave (Swell) Atlas for Arabian Sea and Bay of Bengal. National Institute of Oceanography, Goa, 385p.

NPOL 1978. Wave Statistics of the Arabian Sea. Naval Physical and Oceanographic Laboratory, Cochin, 204p.

Osborne, P.D. and Greenwood, B., 1992a. Frequency dependent cross-shore suspended sediment transport. 1. A non-barred shore face. *Marine Geology*, 106, 1-24.

Osborne, P.D. and Greenwood, B., 1992b. Frequency dependent cross-shore suspended sediment transport. 2. A barred shore face. *Marine Geology,* 106, 25-48.

Oxford, J.D., Carter, R.W.G., Jennings, S.C., 1996. Control domains and morphological phases in gravel-dominated coastal barriers. *Journal of Coastal Research*, 12, 589– 605.

Park, J.Y. and Wells, J.T., 2005. Longshore Transport at Cape Lookout, North Carolina: Shoal Evolution and the Regional Sediment Budget. *Journal of Coastal Research*, 21, 1–17.

Pilkey, O.H., Morton, R.A., Kelley, J.T. and Penland, S., 1989. Coastal land loss. 28th International Geological Congress, Short Course in Geology, 2. Geophysical Union. 73p.

Pilkey, O.P. and Dixon, K., 1996. The Shore and the Corps. Island Press, Washington, DC. 272p.

Pope, D.L., Penland, S., Suter, J.R. and McBride, R.A., 1991. Holocene geologic framework of the trinity shoal region, Louisiana continental shelf. Gulf Coast Society of SEPM.

Prasada Rao, C.V.K., Hareesh Kumar, P.V. and Mohan Kumar, N., 1996. Premonsoon current structure in the shelf water off Cochin. *Proc.* Second workshop scientific Results, ORV Sagar Sampada, 19-24.

Prasannakumar, S., 1985. Studies on sediment transport in the surf zone along certain beaches of Kerala. *Unpublished Ph.D. Thesis, Cochin University of Science and Technology*, 110p.

Prasannakumar, S., Shenoi, S.S.C. and Kurup, P.G., 1983. Littoral drift along shoreline between Munambam and Andhakaranazhi, Kerala coast. *Indian Journal of Marine Sciences*, 12, 209–212.

Rajesh, G., Jossia Joseph, K., Harikrishnan, M. and Premkumar, K., 2005. Observations on extreme meteorological and oceanographic parameters in Indian seas. *Current Science*, 88, 1279-1282.

Rama Raju, V.S., Ramesh Babu, V. and Anto, A.F., 1986. Oceanography of Wadge Bank current measurements over a tidal cycle off the southeast coast of India. *Indian Journal of Marine Sciences*, 15, 135-140

Ramanujam, N., Radhakrishnan, V., Sabeen, H.M., and Mukesh, M.V., 1996. Morphodynamic state of beaches between Vaipar and Tiruchendur, Tamil Nadu. *Journal of the Geological Society of India*, 47, 741-746.

Rao, D.P. and Murthy, V.S.N., 1992. Circulation and geostrophic transport in the Bay of Bengal. In: Physical Processes in the Indian seas. Indian Society for Physical Science and Oceanography, 79-85.

Ravindran, T. A., Khalid, M. M. and Moni, N.S. 1971. Study of shoreline changes of selected beaches of Kerala. *Proc.* Coastal Erosion and Protection, KERI, Peechi, 9.1-9.7.

Reddy, M.P.M., 1970. A systematic study of wave conditions and sediment transport near Murmugao Harbour. *Mahasagar*, 3, 28-44.

Riggs, S.R., Ambrose, W.G., Cook, J.W. and Snyder, S.W., 1998. Sediment production on sediment-starved continental margins: the interrelationship between hard bottoms, sedimentological and benthic community processes and storm dynamics. *Journal of Sedimentological Research,* 68, 155– 168.

Rosati, J. D., Gravens, M. B., and Smith, W. G., 1999. Regional sediment budget for Fire Island to Montauk Point, New York, USA. *Proc.* Coastal Sediments '99, A.S.C. E., 802-817.

Rosati, J.D., 2005. Concepts in sediment budgets. *Journal of Coastal Research*, 21, 2, 307-322.

Sahu, H.K., Hariharan, V. and Katti, R.J., 1991. Seasonal fluctuation in the coastal currents off Mangalore. *Environment and Ecology,* 9, 521-525.

Sajeev, R., Chandramohan, P., Josanto, V. and Sankaranarayanan, V.N., 1997. Studies on sediment transport along Kerala coast, south west coast of India. *Indian Journal of Marine Sciences*, 26, 11-15.

Sanil Kumar, V., Anand, N.M. and Gowthaman, R., 2002. Variations in nearshore processes along Nagapattinam coast, India. *Current Science*, 82, 1381-1389.

Sanil Kumar, V., Ashok Kumar, K and Raju, N.S.N., 2001. Nearshore Processes along Tikkavanipalem Beach, Visakhapatnam, India. *Journal of Coastal Research*, 17, 271–279.

Sanil Kumar, V., Chandramohan, P., Kumar, K. A., Gowthaman, R. and Pednekar, P., 2000. Longshore currents and sediment transport along Kannirajapuram coast, Tamil Nadu, India. *Journal of Coastal Research*, 16, 247–254.

Sanil Kumar, V., Pathak, K.C., Pednekar, P., Raju, N.S.N. and Gowthaman, R., 2006. Coastal processes along the Indian coastline. *Current Science*, 91, 530-536.

Sanil Kumar, V., Raju, N.S.N., Pathak, K.C., and Anand, N.M., 2001. Nearshore processes along north Karnataka coast. *Proc.* International Conference in Ocean Engineering 2001, Chennai (India), 2, 451-458.

Sanil Kumar, V., Sarma, K.D.K.M., Joseph, M.X., Viswambaram, N.K., 1989. Variability in current and thermohaline structure off Visakhapatnam during late June, 1986. *Indian Journal of Marine Sciences*, 18, 232-237.

Santhosh, K.M. and Reddy, H.R.V., 2002. Study of sediment movement and coastal processes along Mangalore coast using satellite imageries. *Indian Journal of Marine Sciences*, 31, 290-294.

Sarma, M.S.S. and Rao, L.V.G., 1986. Currents and temperature structure off Godavari (east coast of India) during September, 1980. *Indian Journal of Marine Sciences*, 15, 88-91.

Sathe, P.V., Somayajulu, Y.K. and Gopalakrishna, V.V., 1979. Wave characteristics in the western and northwestern Bay of Bengal during the SW monsoon of 1978. *Indian Journal of Marine Sciences*, 8, 263-265.

Schwab, W.C., Thieler, E.R., Allen, J.R., Foster, D.S., Swift, B.A. and Denny, J.F., 2000. Influence of inner continental shelf framework on the evolution and behavior of the barrier island system between Fire Island Inlet and Shinnecock Inlet, Long Island, New York. *Journal of Coastal Research*, 16, 396– 407.

Shankar, D. and Shetye, S.R., 1997. On the dynamics of the Lakshadweep high and low in the southeastern Arabian Sea. *Journal of Geophysical Research*, 102, 12551-12562.

Shankar, D., Vinayachandran, P.N. and Unnikrishnan, A.S., 2002. The monsoon currents in the north Indian Ocean. *Progress in Oceanography,* 52, 63-120.

Shenoi, S.C. and Antony, M.K., 1991. Current measurements over western continental shelf of India. *Continental Shelf Research*, 11, 81-93.

Shenoi, S.S.C. and Prasannakumar, S., 1982. Littoral processes along shoreline from Andhakaranazhi to Azhikode along Kerala coast. *Indian Journal of Marine Sciences*, 11, 201-207.

Shepard, F.P. and Inman, D.L. 1950. Nearshore Circulation Related to Bottom Topography and Wave Refraction. *Transactions of the American Geophysical Union*, 31, 555-556.

Shetye, S.R., 1988. West India coastal current and Lakshadweep high/low. *Sadhana*, 23, 637-651.

Shetye, S.R., Gouveia, A.D., Shenoi, S.S.C., Michael, G.S., Sundar, D., Almeida, A.M. and Santanam, K., 1991. The coastal current of western India during the northeast monsoon. *Deep Sea Research*, 38, 1517-1529.

Shetye, S.R., Gouveia, A.D., Shenoi, S.S.C., Sundar, D., Michael. G.S., Almeida, A.M. and Santanam, K., 1990. Hydrography and circulation off the west coast of India during the southwest monsoon 1987. *Journal of Marine Research*, 48, 359-378.

Smith, J.D., 1977. Modeling of sediment transport on continental shelves. In: *The Sea*, Vol. 6 (Eds: Goldberg, E.D., McCave, I.N., O'Brien, J.J. and Steele, J.H.), New York, Wiley Interscience, 539-576.

Sreekala, S.P., Baba, M. and Muraleekrishna, M., 1998. Shoreline changes of Kerala coast using IRS data and aerial photographs. *Indian Journal of Marine Sciences*, 27, 144-148.

Srivastava, P.S. and George, M.D., 1971. Wave Characteristics of the seas around India. *Proc.* Coastal Erosion and protection, Kerala Engineering Research Institute, Peechi, 1-9.

Srivastava, P.S., Nair, D.K. and Kartha, K.R.R., 1968. Monthly Wave Statistics of the Arabian Sea, *Indian Jour. Met. Geophy.*, 19, 329-330.

Stramma, L., Fischer. J. and Schott, F., 1996. The flow field off southwest India at 8°N during the southwest monsoon of August 1993. *Journal of Marine Research,* 54, 55–72.

Suryanarayan, A. and Rao, D.P., 1992. Coastal circulation and upwelling index along the east coast of India. In: *Physical processes in the Indian seas.* (Eds: Swamy, G.N., Das, V.K. and Antony, M.K.), Indian Society for Physical Science and Oceanography, 1992, 125-129.

Swamy and Suryanarayana, 1992. Nearshore circulation in relation to effluent disposal off Thal, Maharashtra, West coast of India. *Mahasagar,* 25, 31-38.

Swamy, G.N., Varma, P.V., Pylee, A., Raju, V.S.R. and Chandramohan, P., 1979. Wave climate off Trivandrum (Kerala). *Mahasagar*, 12, 127-134.

Swart, D.H., 1974. A schematisation of onshore-offshore transport. *Proc.* 14th International Conference in Coastal Engineering, ASCE, 884-900.

Thirupad, P.U.V., 1971. Wave refraction studies in relation to coastal erosion along a part of the Kerala coast, *M.Sc. Thesis, University of Kerala,* 94p.

Thiruvengadathan, A., 1984. Waves in the Arabian Sea and the Bay of Bengal during the monsoon season. *Mausam*, 35, 103-106.

Thomas, K.V. and Baba, M., 1983. Wave climate off Valiathura, Trivandrum. *Mahasagar,* 16, 415-421.

Thomas, K.V., 1988. Waves and nearshore processes in relation to beach development at Valiathura. In: *Ocean waves and Beach processes of the South-west coast of India and their prediction*, (Eds: Baba, M, and Kurian, N.P.), CESS, 47-66.

Thrivikramji, K.P., Anirudhan, S. and Nair, A.S.K. 1983. Shoreline fluctuation of Kerala-Retrospect, perfect and prospect. *Proc.* Management of environment Engineering.

U.S Army, Coastal Engineering Research Centre, 1984. Shore Protection Manual, U.S. Govt. Press, Washington, D.C.

U.S Army, Coastal Engineering Research Centre, 2002. Coastal Engineering Manuel, U.S. Govt. Press, Washington, D.C

Udayavarma, P.P., Ramaraju, V.S., Pylee, A. and Narayanaswamy, G., 1981. Sediment budget of a portion of Trivandrum beach (Kerala). *Mahasagar*, 14, 17-21.

van Rijn, L.C., 1993. *Principles of Sediment Transport in Rivers, Estuaries and Coastal Seas*, Aqua Publications, Amsterdam.

Varma, P.U. and Varadachari, V.V.R. 1977. Stability of the coastline from Manakodam to Thottappalli along the Kerala coast. *Proc.* Indian Academy of Science, 85p.

Williams, S.J., Reid, J.M. and Manheim, F.T., 2003. A bibliography of selected references to U.S.marine sand and gravel mineral resources. U.S. Geological Survey Open-File Report 03-300. 67p.

Yalin, M.S., 1977. *Mechanics of sediment Transport.* Pergamon–Oxford, 1st ed., 290p.